

UNCLASSIFIED

AD NUMBER

AD882109

LIMITATION CHANGES

TO:

Approved for public release; distribution is unlimited.

FROM:

Distribution: Further dissemination only as directed by Electromagnetic Compatability Analysis Center, Annapolis, MD, DEC 1970, or higher DoD authority.

AUTHORITY

ECAC ltr 20 Aug 1972

THIS PAGE IS UNCLASSIFIED

V
ESD-TR-70-207

AD882109

DEPARTMENT OF DEFENSE

ELECTROMAGNETIC COMPATIBILITY ANALYSIS CENTER

ANALYSIS OF PULSED INTERFERENCE TO AMPLITUDE MODULATED RECEIVERS, VOLUME I

Prepared by W. Hatch, R. Hinkle, R. Mayher
of the IIT Research Institute

December 1970



**Best
Available
Copy**

ESD-TR-70-207

When U.S. Government drawings, specifications, or other data are used for any purpose other than a definitely related government procurement operation, the government thereby incurs no responsibility nor any obligation whatsoever, and the fact that the government may have formulated, furnished, or in any way supplied the said drawings, specifications, or other data is not to be regarded by implication or otherwise, or in any manner licensing the holder or any other person or corporation, or conveying any rights or permission to manufacture, use or sell any patented invention that may in any way be related thereto.

Do not return this copy. When not needed, destroy.

ESD-TR-70-207

**ANALYSIS OF PULSED INTERFERENCE TO
AMPLITUDE MODULATED RECEIVERS,
VOLUME I**

Technical Report

No. ESD-TR-70-207

December 1970

**DEPARTMENT OF DEFENSE
Electromagnetic Compatibility Analysis Center**

**Prepared by W. Hatch, R. Hinkle, R. Mayher
of the IIT Research Institute**

DOD DISTRIBUTION STATEMENT

**This document may be further distributed by any holder
only with specific prior approval of ECAC.**

**Published by
Electromagnetic Compatibility Analysis Center
North Severn
Annapolis, Maryland 21402**

FOREWORD

The Electromagnetic Compatibility Analysis Center (ECAC) is a Department of Defense facility, established to provide advice and assistance on electromagnetic compatibility matters to the Secretary of Defense, the Joint Chiefs of Staff, the military departments and other DOD components. The Center, located at North Severn, Annapolis, Maryland 21402, is under executive control of the Director of Defense Research and Engineering and the Chairman, Joint Chiefs of Staff or their designees who jointly provide policy guidance, assign projects, and establish project priorities. ECAC functions under the direction of the Secretary of the Air Force and the management and technical direction of the Center are provided by military and civil service personnel. The technical operations function is provided through an Air Force sponsored contract with the IIT Research Institute (IITRI).

This report was prepared as part of AF Project 649E under Contract F-19628-70-C-0291 by the staff of the IIT Research Institute at the Department of Defense Electromagnetic Compatibility Analysis Center.

To the extent possible, all abbreviations and symbols used in this report are taken from American Standard Y10.19 (1967) "Units Used in Electrical Science and Electrical Engineering" issued by the United States of America Standards Institute.

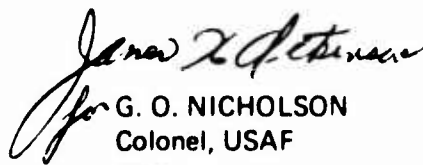
Users of this report are invited to submit comments which would be useful in revising or adding to this material to the Director, ECAC, North Severn, Annapolis, Maryland 21402, Attention ACX.

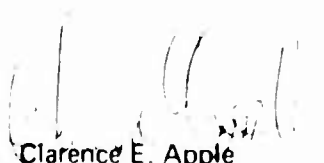
Reviewed by:


R. Mayher
Project Engineer


J. M. DETERDING
Director of Technical Operations

Approved:


G. O. NICHOLSON
Colonel, USAF
Director


Clarence E. Apple
Lieutenant Colonel, USA
Deputy Director

ABSTRACT

This report documents two general methods for evaluating the performance degradation of amplitude modulated (AM) receivers subjected to pulsed interference. The first method involves a time waveform receiver simulation model that provides detailed theoretical solutions for a range of pulse parameters. The second method uses a combination of measured data and engineering trends which cover a reasonably complete range of pulse parameters.

The predominant cause of performance degradation to AM receivers is the energy of the pulse spectrum within the receivers' bandpass. For rectangular pulses with duty cycles less than 8%, the pulsed interference does not appreciably lower the average voice intelligibility in terms of Articulation Score (AS). The performance degradation is, in general, proportional to the log of the pulse repetition frequency (PRF) and is independent of the pulse width for on-tune pulses wider than the inverse of twice the baseband bandwidth.

KEY WORDS

**AMPLITUDE MODULATION (AM)
COMMUNICATION
INTERFERENCE
PULSE
SIMULATION
RECEIVER**

ACKNOWLEDGEMENT

The completion of this general investigation required the contribution of many individuals. In particular, without the measurements provided by the Army through the USAEPG (Fort Huachuca, Arizona) and the SAFEGUARD Program Office, this investigation would not have been feasible. The completion of the measurement program was also due to the coordination efforts of Mr. R. Seach (USAEPG-ECAC Liaison) in solving the numerous problems that came about in the course of this program. In addition, Mr. R. Meyers (IITRI) contributed extensively to the completion of this investigation by programming the receiver simulation model that was developed as part of this analysis.

TABLE OF CONTENTS

Subsection	Page
SECTION 1	
INTRODUCTION	
BACKGROUND	1- 1
OBJECTIVE	1- 2
APPROACH	1- 2
SECTION 2	
RESULTS	
DISCUSSION	2- 1
CONCLUSIONS	2- 1
SECTION 3	
ANALYSIS BACKGROUND	
GENERAL	3- 1
RECEIVER DESCRIPTION	3- 1
SECTION 4	
AM RECEIVER ANALYSIS	
GENERAL	4- 1
IF FILTER ANALYSIS	4- 1
DETECTOR ANALYSIS	4-20
BASEBAND FILTER ANALYSIS	4-23
AGC - AMPLIFIER SATURATION EFFECT	4-24
RECEIVER SIMULATION MODEL	4-34

TABLE OF CONTENTS
(continued)

Subsection Page

SECTION 5

DESCRIPTION OF MEASUREMENTS

GENERAL	5 1
AM RECEIVER TEST PROCEDURE	5 2
AUDIO THRESHOLD TEST	5 18

SECTION 6

MODELING OF PULSED INTERFERENCE EFFECTS

INTRODUCTION	6 1
VOICE INTELLIGIBILITY	6 8
DEGRADATION WITH PULSE RATE	6-15
DEGRADATION WITH PULSE WIDTH	6-20
DEGRADATION WITH CHIRPED AND NON-CHIRPED PULSES	6-28
DEGRADATION WITH OFF-TUNING	6-41
DEGRADATION WITH OUTPUT SIGNAL-TO-NOISE RATIO	6-50
BASEBAND POWER RATIOS	6-58
MINIMUM INTERFERENCE THRESHOLD DEGRADATION EFFECTS	6-71
Introduction	6-71
Receiver Threshold Measurements	6-71
Audio Threshold Measurements	6-72
AUDIO LIMITING	6-74
AGC AND AMPLIFIER SATURATION EFFECTS	6-79

TABLE OF CONTENTS

LIST OF ILLUSTRATIONS

Figure		Page
3- 1	Typical Basic Receiver Structure	3- 2
3- 2	Receiver Simulation Structure	3- 4
4- 1	Equivalent Circuit for a Double Tuned, Transformer Coupled Amplifier	4- 3
4- 2	IF Filter Transfer Function	4- 5
4- 3	IF Output Time Waveform	4- 8
4- 4	IF Output Time Waveform	4- 9
4- 5	IF Output Time Waveform	4-10
4- 6	IF Output Time Waveform	4-12
4- 7	IF Output Time Waveform	4-13
4- 8	IF Output Time Waveform	4-14
4- 9	IF Output Time Waveform	4-15
4-10a	IF Output Time Waveform	4-16
4-10b	IF Output Time Waveform	4-17
4-11	IF Output Time Waveform	4-18
4-12	Typical IF Output Time Waveform Responses for On Tune and Off Tune Pulses	4-19
4-13	Detector and Audio Output Time Waveforms	4-25
4-14	Power Transfer Curve and AGC Level for Pulsed Interference to an AM Receiver	4-27
4-15	Articulation Index for Pulsed Interference to an AM Receiver	4-28
4-16	Power Transfer Curve and AGC Level for Pulsed Interference to an AM Receiver	4-29
4-17	AGC Effects for Pulsed Interference to an AM Receiver	4-30
4-18	AGC Level as a Function of PRF	4-32
4-19	AGC Level as a Function of PRF	4-33
4-20	Computer Simulation Model	4-35
4-21a	Simulated Audio Output Time Waveform	4-38
4-21b	Measured Audio Output Time Waveform	4-39

TABLE OF CONTENTS

LIST OF ILLUSTRATIONS

(continued)

Figure		Page
4-22a	Simulated Audio Output Time Waveform	4-40
4-22b	Measured Audio Output Time Waveform	4-41
4-23	Articulation Index for Pulsed Interference to an AM Receiver	4-42
4-24	Articulation Index for Pulsed Interference to an AM Receiver	4-43
4-25	Articulation Index for Pulsed Interference to an AM Receiver	4-44
4-26	Articulation Index for Pulsed Interference to an AM Receiver	4-45
4-27	Articulation Index for Pulsed Interference to an AM Receiver	4-46
4-28	Articulation Index for Pulsed Interference to an AM Receiver	4-47
4-29	Articulation Index for Pulsed Interference to an AM Receiver	4-48
4-30	Articulation Index for Pulsed Interference to an AM Receiver	4-49
4-31	Articulation Index for Pulsed Interference to an AM Receiver	4-50
4-32	Articulation Index for Pulsed Interference to an AM Receiver	4-51
4-33	Articulation Index for Pulsed Interference to an AM Receiver	4-52
4-34	Input Signal to Peak Interference as a Function of Δf	4-53
4-35	Input Signal to Peak Interference as a Function of Δf	4-54
4-36	Input Signal to Peak Interference as a Function of Δf	4-55
5- 1	Functional Block Diagram of AM Receiver No. 1	5- 3
5- 2	Functional Block Diagram of AM Receiver No. 2	5- 4
5- 3	RF Selectivity of AM Receiver No. 1	5- 5

TABLE OF CONTENTS

LIST OF ILLUSTRATIONS

(continued)

Figure		Page
5- 4	IF Selectivity of AM Receiver No. 1	5- 6
5- 5	Audio Selectivity of AM Receiver No. 1	5- 7
5- 6	RF Selectivity of AM Receiver No. 2	5- 8
5- 7	IF Selectivity of AM Receiver No. 2	5- 9
5- 8	Dynamic Range of Receivers No. 1 and No. 2	5-10
5- 9	Instrumentation Diagram - AM Test Link Receiver Setup	5-11
5-10	Instrumentation Diagram - AM Desired Signal Test Link Transmitter	5-12
5-11	Instrumentation Diagram - AM Interferer with a Rectangular Non-Chirped Pulse	5-13
5-12	Instrumentation Diagram - AM Interferer Pulse With Chirp Setup	5-14
5-13	Threshold Measurement Block Diagram	5-20
6- 1	Average Articulation Score for a Duty Cycle δ ($\delta \leq 8\%$)	6- 9
6- 2	Average Articulation Score for a Duty Cycle δ ($8\% < \delta \leq 25\%$)	6-10
6- 3	Average Articulation Score for a Duty Cycle δ ($\delta > 25\%$)	6-11
6- 4	Speech Masked by Periods of Silence with Speech Time Fraction as the Parameter	6-13
6- 5	Articulation Score for Speech Masked by White Noise	6-14
6- 6	Articulation Score Versus Articulation Index for an AM Receiver	6-16
6- 7	Input Signal to Peak Interference as a Function of PRF	6-19
6- 8	Articulation Index as a Function of PRF	6-21
6- 9	Articulation Score as a Function of PRF	6-22
6-10	Average Articulation Score (AS) as a Function of PRF	6-23
6-11	Input Signal to Peak Interference as a Function of Pulse Width	6-24
6-12	IF Filter Power Loss Transfer Function	6-25
6-13	Articulation Index as a Function of Pulse Width	6-27

TABLE OF CONTENTS

LIST OF ILLUSTRATIONS
(continued)

Figure		Page
6-14	Input Signal to Peak Interference as a Function of Δf	6-30
6-15	Input Signal to Peak Interference as a Function of Δf	6-31
6-16	Input Signal to Peak Interference as a Function of Δf	6-32
6-17	Input Signal to Peak Interference as a Function of Δf	6-33
6-18	Envelope of Idealized Chirped Spectrum	6-34
6-19	Input Signal to Peak Interference as a Function of Δf	6-35
6-20	Input Signal to Peak Interference as a Function of Δf	6-36
6-21	Input Signal to Peak Interference as a Function of Δf	6-37
6-22	IF Filter Power Loss Transfer Function	6-38
6-23	IF Filter Power Loss Transfer Function	6-39
6-24	Input Signal to Peak Interference as a Function of Δf	6-42
6-25	Input Signal to Peak Interference as a Function of Δf	6-43
6-26	Input Signal to Peak Interference as a Function of Δf	6-44
6-27	Input Signal to Peak Interference as a Function of Δf	6-45
6-28	Input Signal to Peak Interference as a Function of Δf	6-46
6-29	Input Signal to Peak Interference as a Function of Δf	6-47
6-30	Input Signal to Peak Interference as a Function of Δf	6-48
6-31	Input Signal to Peak Interference as a Function of Δf	6-49

TABLE OF CONTENTS

LIST OF ILLUSTRATIONS
(continued)

Figure		Page
6-32	Input Signal to Peak Interference as a Function of Δf	6-51
6-33	Input Signal to Peak Interference as a Function of Δf	6-52
6-34	Input Signal to Peak Interference as a Function of Δf	6-53
6-35	Input Signal to Peak Interference as a Function of Δf	6-54
6-36	Input Signal to Peak Interference as a Function of Δf	6-55
6-37	Articulation Index Versus Input Signal Level	6-59
6-38	Average Audio Threshold as a Function of Signal-to-Noise	6-61
6-39	Mean Power Transfer Curves for Pulsed Interference to an AM Receiver	6-64
6-40	Mean Power Transfer Curves for Pulsed Interference to an AM Receiver	6-65
6-41	Synthesized Performance Degradation Procedure	6-67
6-42	Power Transfer Curves for an AM Receiver	6-68
6-43	Power Transfer Curves for an AM Receiver	6-69
6-44	Power Transfer Curves for an AM Receiver	6-70
6-45	Average Threshold Input Signal to Peak Interference as a Function of Δf	6-73
6-46	Power Transfer Loss to an AM Receiver	6-75
6-47	Audio Output with Limiter On	6-76
6-48	Audio Output with Limiter Off	6-76
6-49	Articulation Index for Pulse Interference to an AM Receiver	6-77
6-50	Articulation Index for RCVR 1 Versus Articulation Index for RCVR 2	6-78
6-51	Articulation Score Versus Articulation Index for an AM Receiver	6-80

TABLE OF CONTENTS

LIST OF ILLUSTRATIONS
(continued)

Figure		Page
6-52	Input Signal to Peak Interference as a Function of Δf	6-82
6-53	Input Signal to Peak Interference as a Function of Δf	6-83

TABLE OF CONTENTS

LIST OF TABLES

Table		Page
5- 1	INTERFERENCE MEASUREMENT CONDITIONS FOR AM RADIO RECEIVER NO. 1	5-16
5- 2	INTERFERENCE MEASUREMENT CONDITIONS FOR AM RADIO RECEIVER NO. 2	5-17
5- 3	AUDIO THRESHOLD TEST PARAMETERS	5-19
6- 1	BASIC AM PULSED PERFORMANCE DEGRADATION DATA SUMMARY	6- 2 thru 6- 7
6- 2	ARTICULATION INDEX VERSUS ARTICULATION SCORE FOR DIFFERENT TYPES OF INTERFERENCE	6-17
6- 3	COMPARISON OF INBAND POWER FOR CHIRPED AND NON CHIRPED PULSES	6-40
6- 4	DIFFERENCE IN INPUT (S/I) FOR RECEIVER NO. 1 AND NO. 2	6-57
6- 5	AVERAGE DIFFERENCE FOR THE INPUT SIGNAL-TO-PEAK INTERFERENCE RATIO FOR TWO SIGNALS	6-60
6- 6	COMMON OUTPUT BASEBAND POWER MEASURES	6-63
6- 7	SATURATION BREAKPOINTS FOR AM RECEIVER NO. 1	6-84

TABLE OF CONTENTS

LIST OF APPENDIXES

Appendix

- | | |
|-----|-------------------------------------|
| I | EQUIVALENT LOW PASS FILTER ANALYSIS |
| II | DETECTOR ANALYSIS FOR AM RECEIVER |
| III | BASIC AM PULSED DEGRADATION DATA |
| IV | DEGRADATION MEASURES |

REFERENCES

GLOSSARY

α'	=	The probability of false alarm
A	=	The amplitude of the pulse at IF input
AGC	=	Automatic gain control
AI	=	Articulation Index
$A_{S(U)}$	=	The amplitude of the desired (undesired) signal at the IF output
AM	=	Amplitude Modulation
$A(t)$	=	The undesired signal amplitude modulation after IF filtering
AS	=	Articulation Score
β'	=	The probability of false dismissal
B	=	3 dB bandwidth of a single stage filter in radians
B_{AUDIO}	=	Baseband (audio) filter
B_{IF}	=	IF bandwidth
B_n	=	3 dB bandwidth of a filter of n stages in radians
B_t	=	The total frequency deviation
BW	=	Bandwidth
CORODIM	=	Correlation of the recognition of degradation with intelligibility measurements
δ	=	Duty cycle of pulse
δ	=	$\frac{\omega}{\omega - \omega_0}$ for a filter function

GLOSSARY (continued)

- Δf = Off-tuned frequency difference between the carriers of the desired and undesired signal
- Δf_c = Off tuning for chirped pulse
- Δf_{nc} = Off tuning for non chirped pulse
- $\Delta \omega$ = The frequency difference between the carriers of the desired and undesired signal in radians
- FFT = Fast Fourier Transform
- t_m = $1/\pi$ for $\pi B_{IF} \leq 64$
 $B_{IF}/2$ for $\pi B_{IF} > 64$
- q_{ls} = Lowpass equivalent of $q_s(t)$ or $q(t)$
- $q_{l1}(t)$ = Lowpass equivalent of $q_1(t)$
- $q_{l2}(t)$ = Lowpass equivalent of $q_2(t)$
- $G_{l1}(\omega)$ = Lowpass equivalent of $G_1(\omega)$
- $G_{l2}(\omega)$ = Lowpass equivalent of $G_2(\omega)$
- $G(\omega)$ = Any system function or narrowband spectrum of a real signal
- $G^+ \text{ or } ^-(\omega)$ = Positive or negative frequency portion of $G(\omega)$
- $G_s^+ \text{ or } ^-(\omega)$ = Positive or negative frequency portion of $G_s(\omega)$
- $G_s(\omega)$ = Symmetrical system function
- $g_s(t)$ = Impulse response of a symmetrical filter
- $g(t)$ = Narrowband time waveform whose Fourier Transform is $G(\omega)$

GLOSSARY (continued)

$g_1(t)$	=	Fourier transform of $G_1(\omega)$
$g_2(t)$	=	Fourier transform of $G_2(\omega)$
$G_1(\omega)$	=	Even portion of $G(\omega)$
$G_2(\omega)$	=	Odd portion of $G(\omega)$
$G_1^+ \text{ or }^- (\omega)$	=	Positive or negative frequency portion of $G_1(\omega)$
$G_2^+ \text{ or }^- (\omega)$	=	Positive or negative frequency portion of $G_2(\omega)$
IF	=	Intermediate frequency
$(I/N)_0$	=	The peak interference to noise power ratio at the audio output
$(I_{pp}/N)_0$	=	Peak to peak interference to RMS noise power ratio at the audio output
K'	=	Decision threshold level
m_s	=	The desired modulation index after IF filtering
n	=	Number of double tuned stages in cascade
N	=	Integer 1, 2, 3,
ω	=	Angular frequency
ω_1	=	$.64 \omega_L$
ω_2	=	$.64 \omega_H$
ω_H	=	High frequency 3 dB cutoff
ω_c	=	The carrier frequency of the pulsed CW, in radians

GLOSSARY (continued)

ω_L	=	Low frequency 3 dB cutoff
ω_0	=	Center frequency of the IF amplifier, in radians
ω_s	=	The frequency of the desired modulating tone in radians
PB	=	Phonetically balanced
PCI	=	Pattern correspondence index
PRF	=	Pulse repetition frequency
$PRF_{1,2}$	=	PRF at rate 1, 2
PW	=	Pulse width
$p(t)$	=	The amplitude modulation of the pulsed interfering signal plus the amplitude transients caused by the IF filter
P_i	=	Input power
$P_n(x)$	=	Output signal plus noise density
P_o	=	Output power
$\phi_i(t)$	=	The undesired signal phase modulation after IF filtering
$\phi(t)$	=	Phase modulation of detector output signal
ψ	=	The phase shift of the information after IF filtering
Q	=	The Q factor of a filter
Q_n	=	Q factor of n-cascaded filters

GLOSSARY (continued)

$Q_n(x)$	=	Output noise density
RF	=	Radio frequency
RMS	=	Root mean square
R_I	=	A_I/A_S = the ratio of the undesired signal amplitude to the desired signal amplitude at the IF output
R_I	=	Means take the real part
R_S	=	A_S/A_I = the ratio of the desired signal amplitude to the undesired signal amplitude at the IF output
S	=	Desired signal power in dBm
SCIM	=	Speech communication index meter
SINAD	=	Signal plus noise plus distortion to noise plus distortion power ratio
S/N	=	RMS signal to noise power ratio
(S/I)	=	The RMS signal to RMS interference power ratio
(S/\hat{I})	=	The RMS signal to peak interference power ratio
(\hat{S}/\hat{I})	=	The peak desired signal to peak interfering signal power ratio
$(S/\hat{I})_{1,2}$	=	The (S/\hat{I}) in dB at PRF 1 or 2
$(S/I)_D$	=	The RMS signal-to-RMS interference power ratio at the detector output

GLOSSARY (continued)

$(S/I)_i$	=	The RMS signal to peak interference power ratio at the detector input
$(S/I)_{if}$	=	The RMS signal to peak interference power ratio at the IF input
$(S/I)_o$	=	The RMS signal to RMS interference power ratio at the audio output
$(\hat{S}/\hat{I})_{if}$	=	The peak signal to peak interference power ratio at the IF output
$(S/I)_{rf}$	=	The RMS signal to peak interference power ratio at the RF input
$(S/I_{z,p})_o$	=	The RMS signal to zero to peak interference power ratio at the audio output
$(S/I_{p,p})_o$	=	The RMS signal to peak to peak interference power ratio at the audio output
$[S/(N+D+I)]_o$	=	The RMS signal to RMS (noise plus distortion plus interference) power ratio at the audio output
$[S/(N+D+I)_{p-p}]_o$	=	The RMS signal to peak to peak noise plus distortion plus interference power ratio at the audio output
σ	=	Standard deviation
T	=	The pulse period
τ	=	The pulse width
τ_b	=	The transmitted pulse width
θ_o	=	The phase difference between the desired and undesired carriers after IF filtering (phase angle of desired carrier = 0°)

GLOSSARY (continued)

UPL	=	Upper performance level
VIAS	=	Voice interference analysis system
$V_d(t \text{ or } \omega)$	=	The detector output signal in time or frequency
$V'_{I+N}(t \text{ or } \omega)$	=	The IF input interference plus noise signal in time or frequency
$V_o(t \text{ or } \omega)$	=	The lowpass filter output signal in time or frequency
$V'_{S \text{ or } I+N}(t \text{ or } \omega)$	=	The IF output desired or interference plus noise signal in time or frequency
$V'_{S \text{ or } I \text{ or } N}(t \text{ or } \omega)$	=	The IF input desired, interference, or noise signal in time or frequency
$V(t)$	=	The detector input desired plus undesired signal
$X(t)$	=	IF filter input time waveform
$X(\omega)$	=	Spectrum for periodic rectangular pulse
$X_I(t)$	=	Quadrature component of desired signal
$X_R(t)$	=	Quadrature component of desired signal
$X_S(t)$	=	Complex envelope of desired signal
$Y_I(t)$	=	Quadrature component of undesired signal
$Y_{I+N}(t)$	=	Complex envelope of undesired signal
$Y_R(t)$	=	Quadrature component of undesired signal
*	=	Denotes the complex conjugate

SECTION 1**INTRODUCTION****BACKGROUND**

The Electromagnetic Compatibility Analysis Center (ECAC) is engaged in a continuing study of the relationship of various desired and undesired signals to the performance of receiving systems. This investigation is part of the Center's effort to formulate methods to analyze equipment electromagnetic compatibility. Some of this performance evaluation effort has been previously reported (References 1 - 5).

A general investigation of pulsed interference effects was initiated because of the increasing use of pulsed communication and radar systems. Information concerning a wide range of pulse parameters and different types of desired modulation was of interest. An initial literature review (References 6 through 9) revealed that insufficient information was available to cover a full range of pulsed interference effects. Therefore, a general investigation of the effects of pulsed interference in the following receiver types was undertaken:

1. Amplitude Modulation (AM)
 - a. Voice (Narrow and Wideband (High Fidelity))
 - b. Analog
 - c. Digital
2. Frequency Modulation (FM)
 - a. Voice (Narrow and Wideband (High Fidelity))
 - b. Analog
 - c. Digital
3. Television (TV)
4. Frequency Division Multiplex (FDM)
 - a. Voice
 - b. Analog
 - c. Digital
5. TACAN
6. Radar

This report, which is the first in a series concerning pulsed interference, analyzes the performance of amplitude modulated (AM) receivers. The effects of pulsed interference on other receiver types will be reported in subsequent documents, and a summary of the overall analysis results is planned.

OBJECTIVE

The objective of this effort was to develop the capability to solve the general problem of pulsed interference to AM receivers. In particular, to

1. Obtain, through measurements and analysis, curves and/or relationships that describe the performance degradation of AM receivers interfered with by a range of "typical" pulsed interference.
2. Develop a model which provides detailed simulation of an AM receiver to evaluate performance degradation in the presence of pulsed interference, and which has the capability of accommodating a full range of pulse parameters.

APPROACH

It was originally desired to model voice modulated AM as well as digital and analog modulated AM. Since measurements were not available in sufficient detail for all types of AM receivers, the study concentrated on the predominant case, voice modulated AM. All AM receivers involve the same basic functions (only the baseband output signal processing differs). Consequently, although the output signal processing of digital and analog modulated systems was not modeled, the solution to these problems can be obtained from the baseband output solutions of this investigation. The application to a digital system is outlined in Appendix IV.

The program began with a literature search and a preliminary investigation to determine an "hypothesized" degradation mechanism and analysis. This was followed by the preparation of a test plan and subsequent measurements to investigate pulsed interference for a general range of pulse widths, pulse rates, frequency sweeping (chirping) and interference off tuning. The output performance degradation was measured in terms of the basic voice degradation measurements of articulation score (AS), articulation index (AI), minimum interference thresholds and signal to interference ratios.

The measurement program was divided into two phases in order to expedite solutions to the pulsed interference problem. The results of MIL-STD 449 () (reference 10) type

measurements and simple output degradation measures were obtained under Phase I. Those measurements that required detailed subjective evaluation (i.e., articulation scoring for voice systems) were reported in Phase II.

Two detailed investigations were undertaken. The first consisted of analyzing the basic receiver signal processing structure and the Phase I measurements to determine if the hypothesized pulsed degradation mechanism was correct. The second was to develop a *time waveform* receiver simulation model, based upon the pulsed degradation mechanism, capable of generalization to any type of pulsed interference problem. The simulation model was developed to obtain quantitative solutions to an interference problem that is generally untractable using truncated series approximations (reference 5).

After the conclusion of the Phase II measurements, a comparison was made between the outputs of the simulated receiver and the measured receiver to validate the simulation procedure. Engineering models were then constructed from a combination of the measured and simulated receiver outputs.

SECTION 2

RESULTS

DISCUSSION

The results of this analysis have evolved from a combination of two different, but simultaneous, approaches to the problem. The first approach was to develop and use a receiver simulation model which provides detailed, theoretical solutions for a general range of pulse parameters.

In the second approach, an extensive set of data (summarized in TABLE 6-1 and presented in Appendix III) was examined to determine the dependence of receiver performance on variations in signal-to-peak interference power, pulse width, pulse repetition frequency, off tuning, chirp rate, AGC effects, linear filtering, and any special non-linear characteristics of the victim receiver. Engineering trends were revealed which generalize the basic data to include a reasonably complete range of pulse parameters.

A discussion of the signal processing in the receiver simulation model referred to frequently in this report is contained in Section 4. The model transforms a desired signal, along with a pulsed interfering signal and narrowband gaussian noise, through an IF filter, the second detector, and a baseband filter. Voice modulated desired signals are further processed through an articulation index (AI) decision mechanism. The model has been validated through comparison with measured data.

CONCLUSIONS

The results of the theoretical and empirical approaches to predicting the effects of pulsed interference on AM systems were analyzed extensively. This analysis led to the formulation of the following conclusions, which are discussed in detail in Section 6:

1. The predominant cause of receiver degradation for a periodic pulse train is the power of the pulse spectrum contained within the receiver bandpass. Degradation from the RF nonlinear effect of cross modulation, due to the presence of pulsed signals, was not observed in this investigation for peak interference power levels up to 24 dBm. It is difficult to eliminate the adjacent channel (non-spurious) effects of pulsed interference in a receiver because band stop filters, centered at the undesired carrier frequency, will not remove in band power.

2. Pulsed degradation to AM receivers can be evaluated by analyzing the processing of desired and undesired signals through the intermediate frequency (IF) bandpass filter, the envelope detector, the baseband filter, and an appropriate decision mechanism.

3. The far off-tune response of receivers whose IF bandwidth is greater than the reciprocal of the interfering pulse width follows the fall-off rate (envelope) of the pulse spectrum (20 dB per decade for a rectangular pulse). Measured data showing the typical receiver response to off-tune rectangular pulses is presented in Figure 2-1. The figure presents the type of information required for the prediction of degradation to AM systems due to pulsed interference, given transmitted power and propagation loss. Solutions for a range of pulse parameters may be obtained from similar curves in this report.

4. Performance degradation is a function of the input signal-to-peak interference power ratio for desired input signal levels much greater than the noise. For low or "sensitivity type" input signal levels, degradation is a function of both interference and noise.

5. Rectangular pulsed interference, averaged over all pulse widths and pulse repetition frequencies, does not appreciably lower voice intelligibility in terms of articulation score (AS) until the duty cycle approaches 50%. For duty cycles less than 8% (radars are typically less than 1%) rectangular pulses do not lower intelligibility even for input signal-to-peak interference ratios as low as -70 dB.

6. Performance degradation increases linearly with the log of the interference pulse repetition frequency (PRF) up to approximately 1,000 PPS. In particular:

a. The input signal-to-peak interference ratio (S/\hat{I}) required for a constant articulation index (AI) value increases linearly with log PRF.

b. The input (S/\hat{I}) required for a "just perceptible" threshold interference condition increases linearly with log PRF.

7. The input signal-to-peak interfering ratio (S/\hat{I}) required for a constant AI value increases linearly with log of the PW up to the inverse of twice the baseband bandwidth. Degradation is not a function of interference pulse width for on-tune pulses longer than the inverse of twice the baseband bandwidth.

8. Approximately 2 dB more interference power within the receiver IF bandwidth is required for non-chirped pulses than for equivalent (pulse shape, PRF, PW)

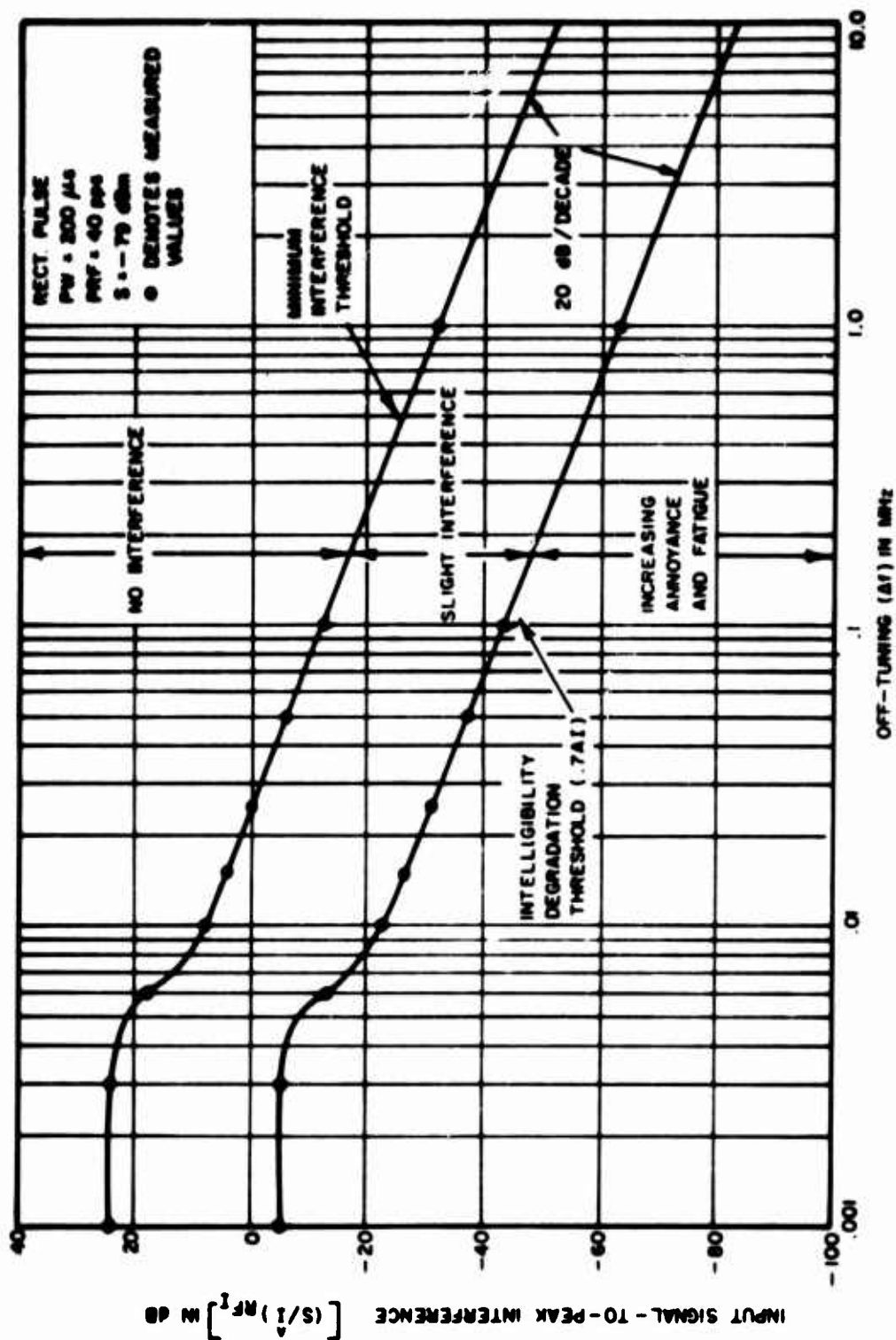


Figure 2-1. Typical AM Off-Tune Pulse Degradation Response

chirped pulses for the same AI performance level. The degradation effect of chirped pulses is primarily a function of the interference power in the IF bandwidth and of the interference PRF.

9. Performance specifications in terms of articulation score (AS) or articulation index (AI) for pulsed interference can be determined by measuring, in the baseband, either the signal-to-peak interference power or the signal-to-average interference power ratios.

10. The minimum interference threshold level is a function of the input signal-to-peak interference ratio and the baseband signal-to-noise ratio. (It is also proportional to the log of the PRF as stated in conclusion 7.)

11. Audio limiting improves the performance in terms of AI for narrowband AM systems that can tolerate some clipping distortion. Systems that require a minimum interference threshold level will not benefit through audio limiting. The intelligibility in terms of AS was approximately the same with and without limiting.

SECTION 3

ANALYSIS BACKGROUND

GENERAL

The approach to the AM receiver degradation investigation was to combine detailed measurements and analyses. The analytic portion consisted of a theoretical study, a computer receiver simulation and an investigation of the measured and simulated degradation trends.

Section 4 contains a discussion of the analytic investigation and an outline of the computer simulation model. Section 5 contains a description of the measurement procedure. Section 6 contains the analysis of the measured and simulated data and the subsequent models obtained for pulsed interference to AM receivers.

RECEIVER DESCRIPTION

In order to consider receiver degradation effects an initial investigation of the "typical complete" receiver structure shown in Figure 3.1 is required. This figure shows RF, IF and baseband signal processing elements that must be considered.*

The modeling of strong adjacent channel peak interference levels should include the nonlinear receiver effects of cross modulation (or intermodulation), saturation, desensitization and spurious responses. These effects are generally difficult to analyze because superposition does not apply.

The measurements that were analyzed did not indicate the presence of cross modulation (or intermodulation) due to RF nonlinear effects for interference levels up to 24 dBm. This type of response was, therefore, either a secondary effect or non-existent and was not considered in the modeling.

* Throughout this report degradation is described in terms of the signal to interference (S/I) ratio. The symbolism used to describe this quantity for the various locations within the receiver are basically defined in Figures 3.1 and 3.2. In these figures, the input ratio of the RF (or IF) signal to peak interference was symbolized as $(S/I)_{RF}$. The average power of a signal is symbolized by a letter. The peak power has been symbolized with the A symbol. This symbolism has been used on the various figures contained within this report and where it was appropriate within the text. However, the input power ratio term was used so extensively that an equivalent form has also been used. That is, the phrase "input (S/I) ratio" has been used to replace $(S/I)_{RF}$.

$(S/I)^{\hat{A}}$: THE SIGNAL - TO - PEAK INTERFERENCE POWER RATIO
 (S/I) : THE SIGNAL - TO - AVERAGE - INTERFERENCE POWER RATIO

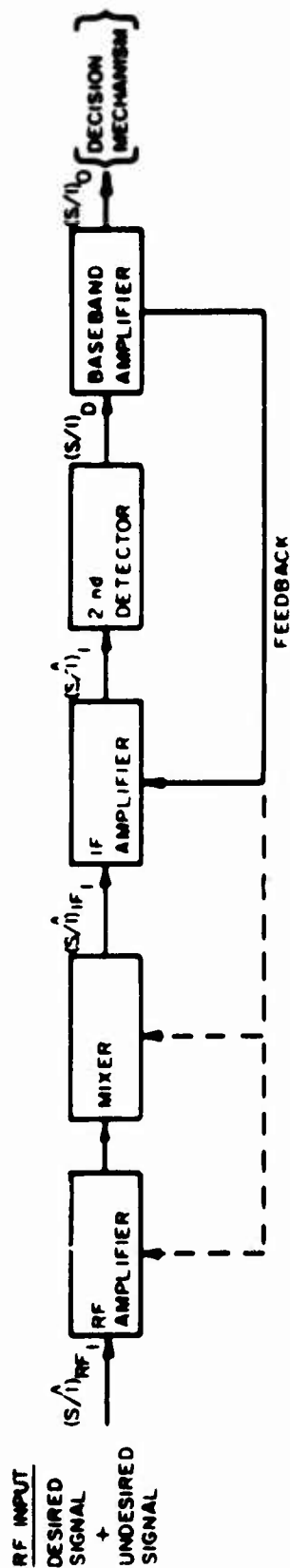


Figure 3-1. Typical Basic Receiver Structure

Spurious responses can be eliminated from consideration by noting that receiver performance degradation from pulsed interference located exactly at a spurious response frequency involves the same mechanism (i.e., the power transfer due to the nonlinearity) as the case when the interference source is a continuous (non pulsed) source. The investigation of these spurious response frequency locations has been extensively analyzed in the literature (references 11 and 12). They are primarily a statistical problem associated with a particular nomenclatured equipment and will not add to the understanding of the general AM pulsed interference phenomena. Consequently, the spurious response area will not be further considered in this investigation. All that is required to extend the solutions in this report is a knowledge of the spurious response frequencies, the rejection levels, and the spurious response selectivity of the particular receiver being investigated. This can be obtained from spectrum signature data (References 12, 13 and 14)

The related problems of saturation and AGC desensitization should be addressed in order to properly process high power pulsed interference. This area will be treated in Section 4.

The reduced receiver structure to be specifically analyzed in this report is given in Figure 3-2. This analysis concentrates on the receiver mechanisms that determine the transformation of both the desired signal and pulse interference between the IF input and the baseband filter output. It was assumed that saturation will not occur up to some specified level, to be determined separately, and that the RF amplifier section has a bandwidth sufficiently wide to pass the undesired pulse without modification within the limits of the IF bandwidth. The analytic investigation involved the analysis of the IF filter, second detector, baseband filter, AGC circuitry and the output decision mechanism. The investigation resulted in

- a. An understanding of the signal processing of the individual receiver sub-structures (i.e., IF, detector, baseband filter, decision mechanism) and the overall combination of these elements to form the basic receiver.
- b. Asymptotic signal-to-peak interference (S/\hat{I}) solutions (i.e., solutions valid when $S \gg \hat{I}$ or $\hat{I} \gg S$), which are limited in application but are sometimes simple solutions to the problem. For a general discussion of this approach, see references 1 and 5.
- c. Formulation of the general equations and procedures used in the receiver time waveform simulation process.

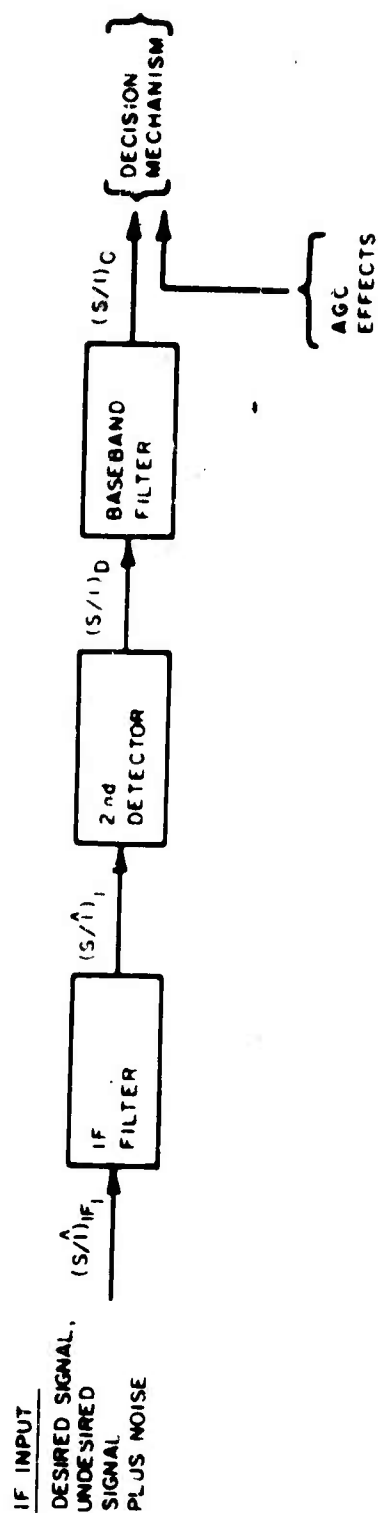


Figure 3-2. Receiver Simulation Structure

The receiver simulation is the heart of a family of detailed receiver models that ECAC is developing. These models are different from many others in that the time waveform (amplitude, phase) characteristics are processed through the receiver structures in a manner analogous to the processing of the voltage (or current) in a real receiver. This is a digital computer simulation of an analog model of a complete receiver. This kind of processing is in contrast with the power filtering models employed in most analysis techniques. The power models are generally adequate only when it has been shown that power is an appropriate degradation measure.

The simulation approach is presently feasible because of the Fast Fourier Transform technique (reference 15) which allows efficient transformations between the time and frequency domains as required for the linear and nonlinear receiver signal processing.

The AM receiver simulation procedure which is a part of this program will be outlined in Section 4. A full description of the details of this simulation process will be written in the future as a separate report of this series.

Section 6 discusses the modeling of the interference effects, based upon a combination of measured and simulated data. It is the purpose of that section to develop models that can be used to extend the measured performance degradation data to other cases of interest. The most accurate results will be obtained by running the receiver simulation model for a particular case of interest. However, this solution may not be available to all investigators.

The overall goals of this program are to investigate pulsed interference to AM, FM, TV, FDM, TACAN and Radar systems. The results of this investigation are also applicable to PM, SSB, TDM and other pulse modulation techniques which are not specifically investigated in this report. The solution to latter modulation types involves the signal processing of the narrowband amplitude (envelope) or phase angle of the signal or (in some special cases) a combination of both. In both sets of modulation types, the output decision mechanisms involve only voice, digital or analog modulated signals. The general solution to the latter set of problems will be covered in this investigation.

If PM, SSB or TDM systems are examined in detail, the following minor changes are required. The general PM solution requires a determination of the narrowband phase angle. Since the FM solution required a derivative of this phase angle (Appendix I of reference 1), it is only necessary to turn off this function in the simulation model to solve this type of problem. The SSB systems typically employ product detectors. This linear operation simply removes the second detector operation and reduces the simulation model to filter and decision mechanism processing elements. All the other modulation methods typically employ some form of amplitude or phase angle modulation and can be readily adapted from the general purpose simulation model.

SECTION 4

AM RECEIVER ANALYSIS

GENERAL

This section discusses the analysis of the AM receiver signal processing elements shown in Figures 3-2 and 4-20. This includes the analysis of the IF filter, second detector, baseband filter, AGC circuitry, the output decision mechanism (see Appendix IV) and the receiver simulation model. The purpose of this section is to define the equations used in the simulation process and to discuss the mechanisms that are involved in pulsed interference.

IF FILTER ANALYSIS

The following analysis primarily considers the transformation of pulsed signals through an effective linear IF filter. This topic has been previously investigated in references 16 and 17. A discussion of the implications of particular examples applicable to this investigation follows.

Since superposition applies and the IF has been designed to pass the desired signal, only the transformation of the pulsed interfering signal need be covered in detail. For the purpose of this analysis it is assumed that the effective IF filter takes into account the combined effects of RF and IF filtering for those cases in which the mixer is acting as an ideal mixer (or frequency translator).

In general, the IF amplifier output for a pulsed input signal can be expressed as the sum of a steady state term plus a transient term. The transient term represents a distortion term and includes the amplitude and phase modulation produced in the IF amplifier. The transient term arises because the system response is unable to build up and decay as fast as the input signal.

It is necessary to have an IF filter model to predict these transient and steady state terms. One method of modeling the IF filter function is in terms of cascaded tuned amplifiers. Both single-tuned and double-tuned amplifiers are used in communication receivers. The double-tuned, transformer coupled amplifier is commonly used in the IF of AM receivers. It produces a more constant amplification over a band of frequencies and the gain falls more sharply outside this band of frequencies than in the case of the single-tuned stage. The double-tuned amplifier was used to model the effective IF filter for this study.

The equivalent circuit for a double-tuned amplifier is shown in Figure 4-1. The transfer function for a critically coupled double-tuned amplifier with equal primary and secondary values of Q (reference 18), is given by

$$H(\omega) = \frac{1}{1 - 2\delta^2 Q^2 + j2\delta Q} \quad (4-1)$$

where

$$\delta = \frac{\omega - \omega_o}{\omega_o}$$

$$Q = \frac{\omega_o}{\sqrt{2}\pi B}$$

$$B = \text{3 dB bandwidth of a single stage in radians}$$

$$\omega_o = \text{Center frequency of amplifier in radians}$$

When the effective IF incorporates more than one stage of amplification the transfer function is given by

$$H_n(\omega) = \frac{1}{[1 - 2\delta_n^2 Q_n^2 + j2\delta_n Q_n]^n} \quad (4-2)$$

where

$$n = \text{Number of double-tuned stages in cascade}$$

$$\delta_n = \frac{\omega - \omega_o}{\omega_o}$$

$$Q_n = \left(\sqrt{\frac{2^{1/n} - 1}{4}} \right) \frac{\omega_o}{B_n \pi}$$

$$B_n = \text{3 dB bandwidth of the } n \text{ stages in radians}$$

$$B_n = \frac{B}{\sqrt{2^{1/n} - 1}}$$

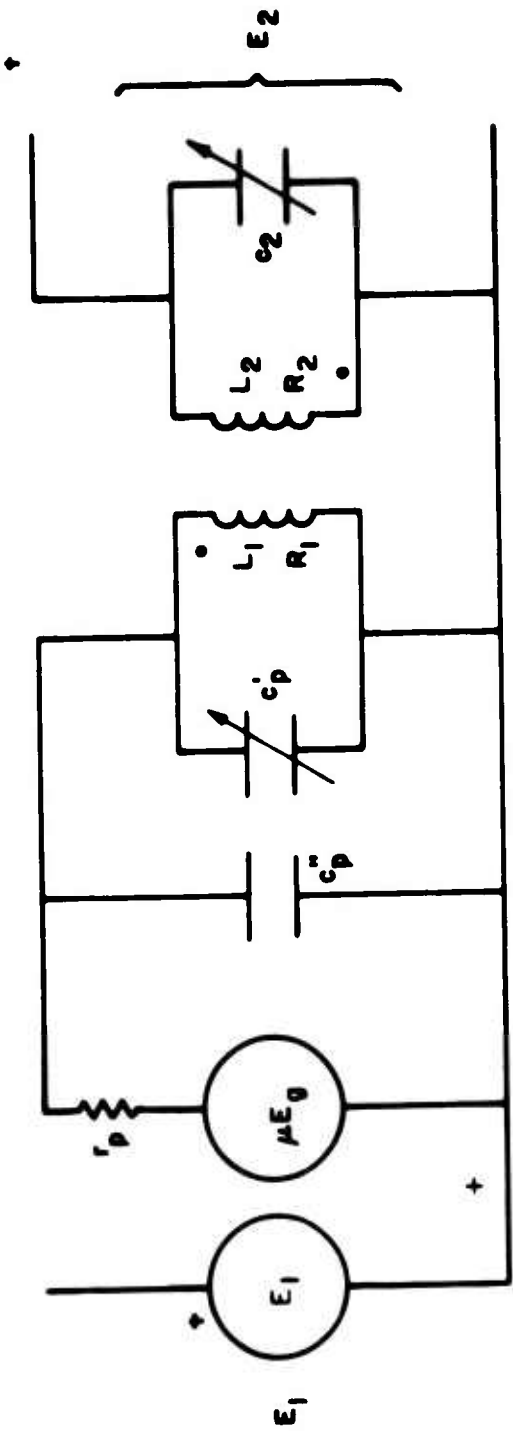


Figure 4-1. Equivalent Circuit for a Double-Tuned, Transformer Coupled Amplifier

In order to simulate the IF selectivity of a typical AM receiver, a representative number of IF stages must be chosen. From a preliminary investigation, it was found that three cascaded, double-tuned stages represented a number of narrowband AM receivers. This configuration was used in all the simulated runs and reasonably represents both of the investigated receivers under pulsed interference conditions. Although the second receiver had a much sharper selectivity curve (both selectivity curves are discussed in Section 5), it was subsequently found that this resulted in only a fractional dB change. This small difference is because the interference is pulsed. The difference would not be negligible if off-tune continuous (CW) interference were being investigated.

The transfer function for three cascaded amplifiers is given by

$$H_1(\omega) = \frac{1}{[1 - 2\delta_1^2 Q_1^2 + j2\delta_1 Q_1]^3} \quad (4.3a)$$

$$= \frac{1}{1 - 18\delta_1^2 Q_1^2 + 36\delta_1^4 Q_1^4 + 8\delta_1^6 Q_1^6 + j6\delta_1 Q_1 - j32\delta_1^3 Q_1^3 + j24\delta_1^5 Q_1^5} \quad (4.3b)$$

where

$$\delta_1 = \frac{\omega - \omega_0}{\omega_0}$$

$$Q_1 = \frac{1.009 \omega_0}{2\pi B_1} = 1.26 \times 10^{-4} f_0$$

A plot of this transfer function for $B_1 = 8$ kHz is shown in Figure 4.2.

The input signal, $x(t)$, to the IF filter will consist of a pulse that may contain both amplitude and frequency modulation. If the IF filter has the impulse response $h(t)$, the output signal, $g(t)$, is given by the convolution integral

$$g(t) = \int_{-\infty}^{\infty} x(\tau)h(t-\tau)d\tau \quad (4.4)$$

Since convolution in the time domain is equivalent to multiplication in the frequency domain, it will be more convenient to use the frequency domain expressions. If the input signal, $x(t)$, has a Fourier transform, $X(\omega)$, and the transfer function of the IF filter is $H(\omega)$, then the output spectrum is given by

$$G(\omega) = H(\omega) X(\omega) \quad (4.5)$$

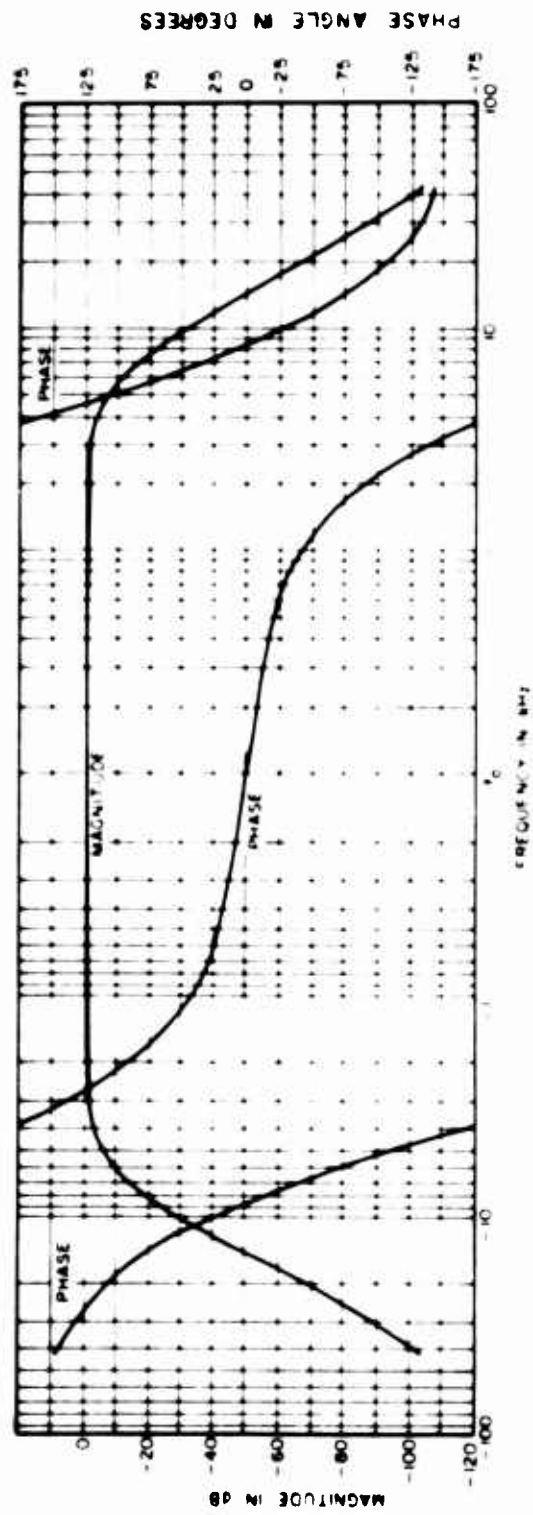


Figure 4.2. IF Filter Transfer Function

When the interference is modeled as a periodic rectangular pulse with zero rise and fall time, the spectrum is given by

$$X(\omega) = \frac{A\pi\tau}{T} \sum_{n=-\infty}^{\infty} \frac{\sin \pi n\tau/T}{\pi n/T} \left\{ \delta\left(\omega - \omega_1 - \frac{2\pi n}{T}\right) + \delta\left(\omega + \omega_1 - \frac{2\pi n}{T}\right) \right\} \quad (4-6)$$

where

A	=	The amplitude of the pulse
τ	=	The pulse width
T	=	The pulse period
ω_1	=	The carrier frequency in radians
n	=	Integer 1, 2, 3, ...
δ	=	Dirac delta function

The output spectrum, $G(\omega)$, is the product of the filter transfer function and the pulse spectrum. The general shape of the output spectrum, $G(\omega)$, will be a function of the filter characteristic, pulse characteristics and off tuning. The inverse Fourier transform of $G(\omega)$ will then be the output time waveform $g(t)$. The time waveform for a symmetrical spectrum will contain amplitude modulation but no phase modulation and is given in Appendix I by Equation (I-25) as:

$$g(t) = 2g_{\ell S}(t) \cos \omega_0 t \quad (4-7)$$

where

$$g_{\ell S}(t) = \text{Lowpass equivalent of } g(t)$$

The time waveform for an unsymmetrical spectrum will contain both amplitude and phase modulation and is given by Equation (I-53) as:

$$g(t) = A(t) \cos [\omega_0 t + \theta_0 + \phi_1(t)] \quad (4-8)$$

where

$A(t)$	=	The undesired signal amplitude modulation after IF filtering
θ_o	=	The undesired signal carrier phase angle
$\phi_i(t)$	=	The undesired signal phase modulation after IF filtering

The three basic cases of interest are pulses whose bandwidth is much greater than, approximately equal to, or much narrower than, the effective bandwidth of the IF filter.

When the pulse bandwidth is much greater than the bandwidth of the IF filter, $rB_{IF} \ll 1$, the spectrum of the pulse within the IF passband for the on tune, $\Delta f = 0$, case is approximately flat and has even symmetry about the carrier frequency. The Fourier transform of the resulting spectrum will approximate the impulse response of the network with some ringing on the trailing edge. The output time waveform will be much longer than the input pulse time waveform with the peak amplitude of the output pulse reduced approximately by the ratio of the pulse bandwidth to the filter bandwidth. Since the bandwidth of the pulse is much greater than the IF bandwidth, the shape of the spectrum within the IF passband as the pulse is off tuned will be approximately the same except near the nulls of the input spectrum. Therefore, as the pulse spectrum is off tuned the IF output time waveform will remain approximately the same as the on tune case with the inband power determining the peak level of the output pulse. In the vicinity of the null point the spectrum will no longer be flat and it will approach odd symmetry when centered about the null point. The Fourier transform of an unsymmetrical spectrum will produce both amplitude and phase modulation as shown in Equation (4.8). Typical simulated output time waveforms (the time waveform simulation process is discussed later in this section) for an IF bandwidth of 8 kHz and a 5 μ sec pulse for $\Delta f = 0$, 800 kHz and 1.5 MHz off-tune are shown in Figures 4-3, 4-4 and 4-5. The input pulse of width τ and unity amplitude is assumed to be symmetrical about time $t = 0$. This is true for all pulses discussed in this section.

When the pulse bandwidth is approximately equal to the IF bandwidth, the spectrum of the pulse within the IF passband for the on tune, $\Delta f = 0$, case will be symmetrical and even. The sidelobes will be attenuated by the filter function causing a more rapid fall-off of the pulse spectrum. The Fourier transform of the resulting spectrum will approximate the impulse response, with the amount of energy within the passband again determining the peak level of the output pulse. As the pulse is off tuned the pulse spectrum out of the IF filter will be unsymmetrical, thereby producing both amplitude and phase modulation as

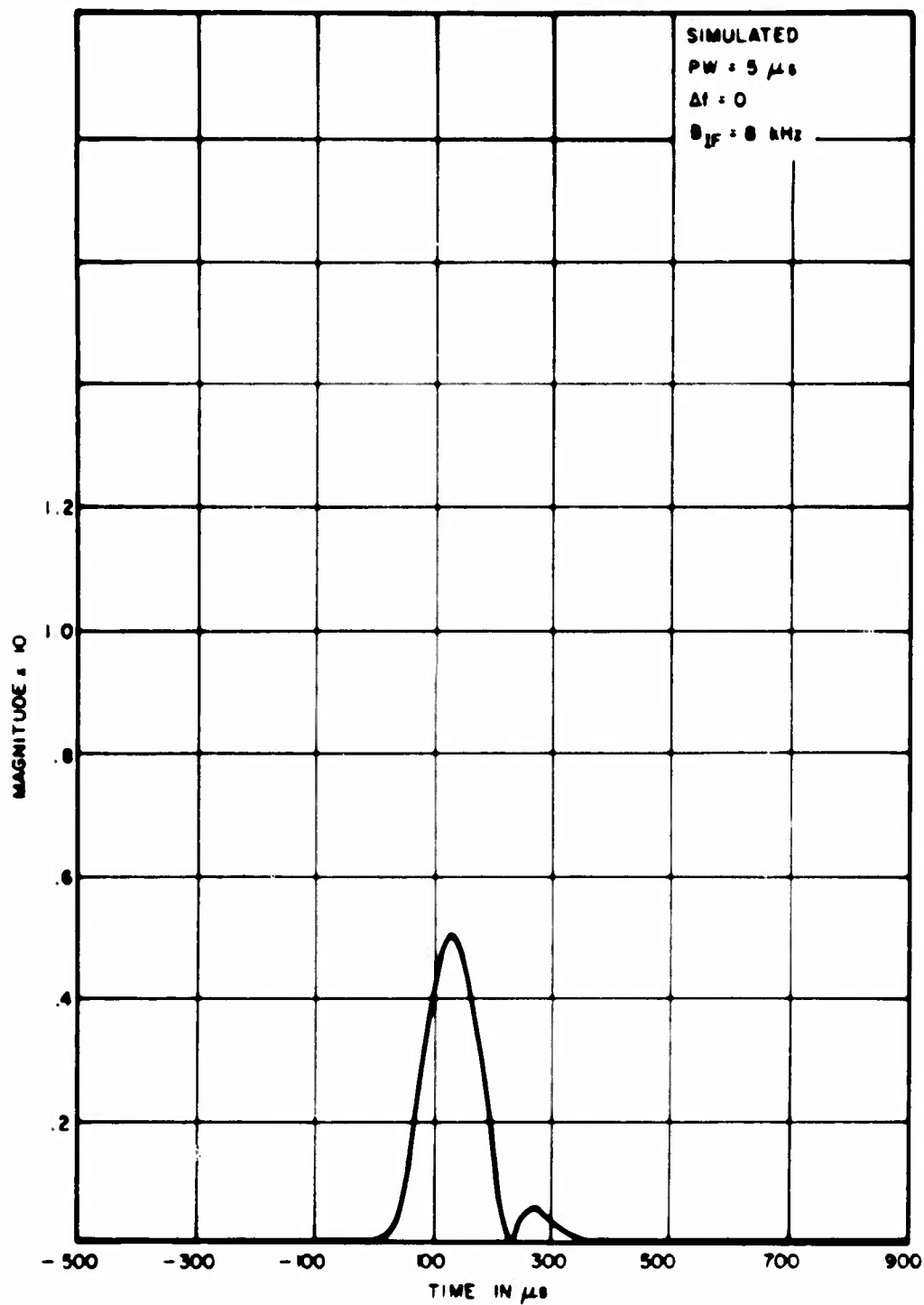


Figure 4-3. IF Output Time Waveform

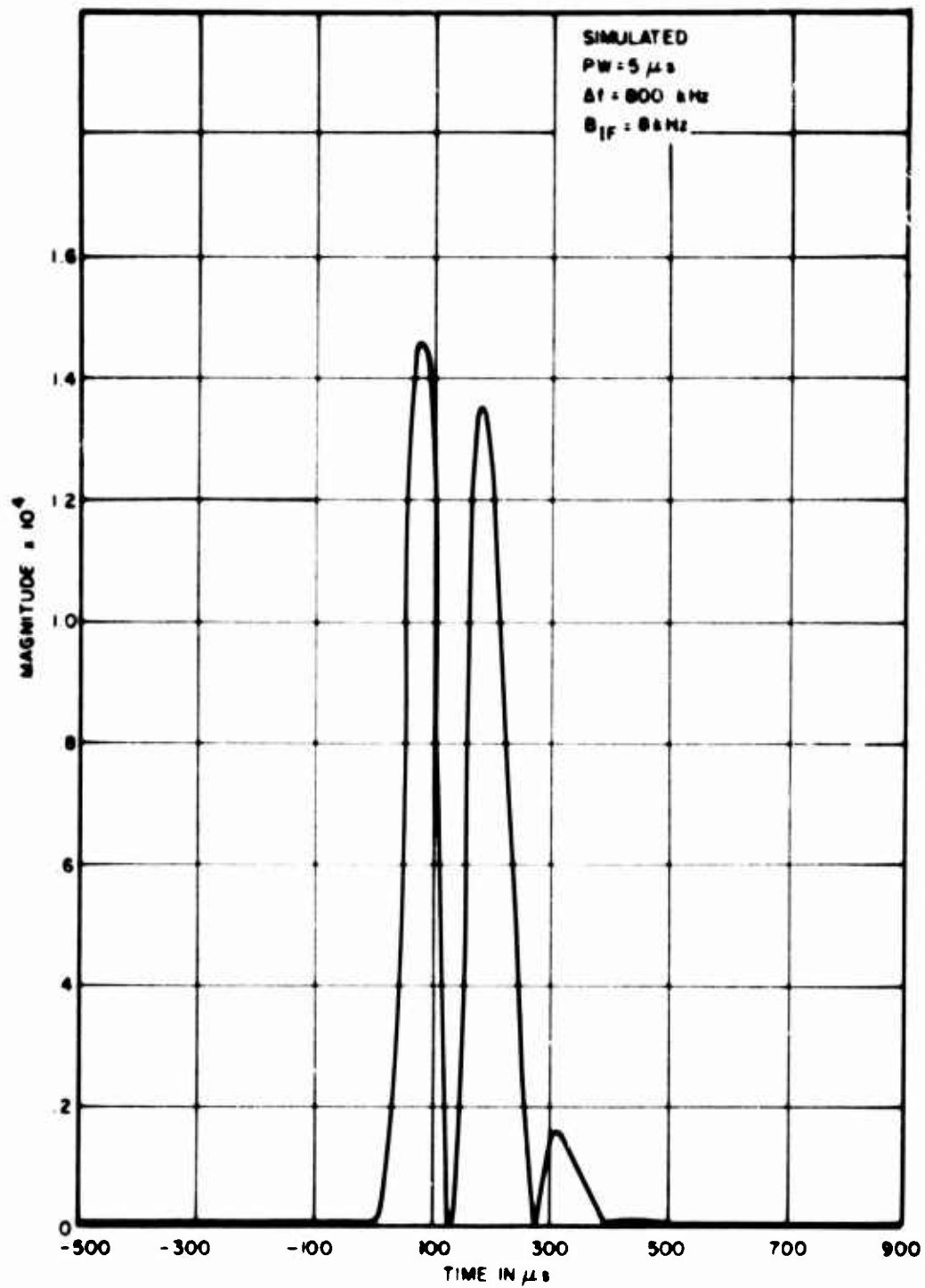


Figure 4-4. IF Output Time Waveform

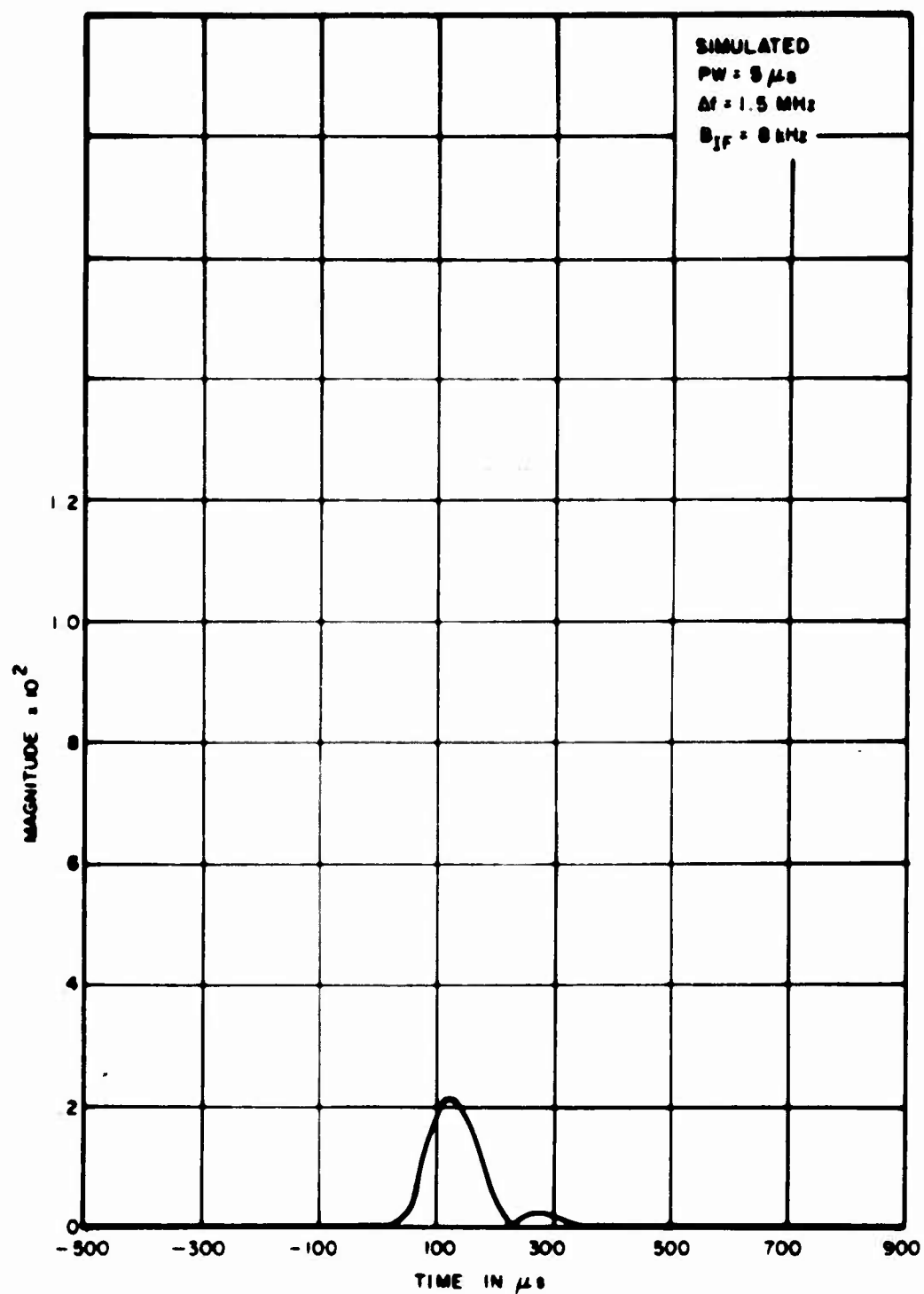


Figure 4-5. IF Output Time Waveform

shown in Equation (4-8). The Fourier transform of the output pulse spectrum produces time waveforms that appear to contain a separate response from the leading and trailing edge of the pulse. As the off-tuning is increased the double response becomes more pronounced due to the attenuation of the steady state portion of the pulse by the filter characteristics. Typical output time waveform for an IF bandwidth of 8 kHz and a 200 μ sec pulse for $\Delta f = 0, 62.5$ kHz and 100 kHz are shown in Figures 4-6, 4-7 and 4-8.

When the pulse bandwidth is much narrower than the IF filter bandwidth and $\Delta f < \text{one half the IF bandwidth}$, the input time characteristics are produced at the filter output along with some ringing or overshoot on the leading and trailing edges. As the pulse is off tuned the pulse spectrum out of the filter will be unsymmetrical, thereby producing amplitude and phase modulation similar to the case of the 200 μ sec pulse mentioned above. The steady state of the pulse will again be attenuated by the off tuned characteristics of the filter and therefore the shape and magnitude of the output pulses will be determined by the power and shape of the spectrum within the filter passband.

A plot of the phase angle for $\Delta f = 10$ kHz shows the phase modulation produced by the leading and trailing edges of the pulse and the 10 kHz beat tone with respect to the tuned frequency during the steady state portion of the pulse. Thus, during the steady state portion, the interference carrier, $\omega_i = \omega_o + \Delta\omega$, is present but is greatly attenuated. Typical output time waveforms for an IF bandwidth of 8 kHz and a 1 msec pulse for $\Delta f = 0, 10$ kHz and 64 kHz are shown in Figures 4-9, 4-10a and 4-11. A plot of the phase angle relative to the IF center frequency f_o for $\Delta f = 10$ kHz is also shown in Figure 4-10b.

In summary, the transformation of pulsed signals through a linear IF filter have been discussed. Particular examples of outputs from a simulated IF were given. These outputs can be conveniently summarized in terms of τB categories as shown in Figure 4-12. IF output waveforms in these categories have been discussed in some detail because they are the pulses that interfere with the desired signal. In particular, these IF output pulses compete with the desired signal in the detector (the next processing element) with the result that the larger signal captures the receiver output.

This result is similar to the capture phenomenon that would take place with continuous interference except for the duty cycle of the pulse signal. This is shown in Figure 4-12, in which a capture level has been symbolically drawn (the capture level actually consists of a region) to represent the amplitude of the desired signal. The region of the pulses above the capture level (i.e., the level in which $I > S$) varies with the τB_{IF} product and the off-tuning. In general, the shape of the pulse in this region is complex and difficult to determine by a simple model. It is for this reason that these details will not be solved deterministically in advance. Instead, the problem will be generally simulated so the actual

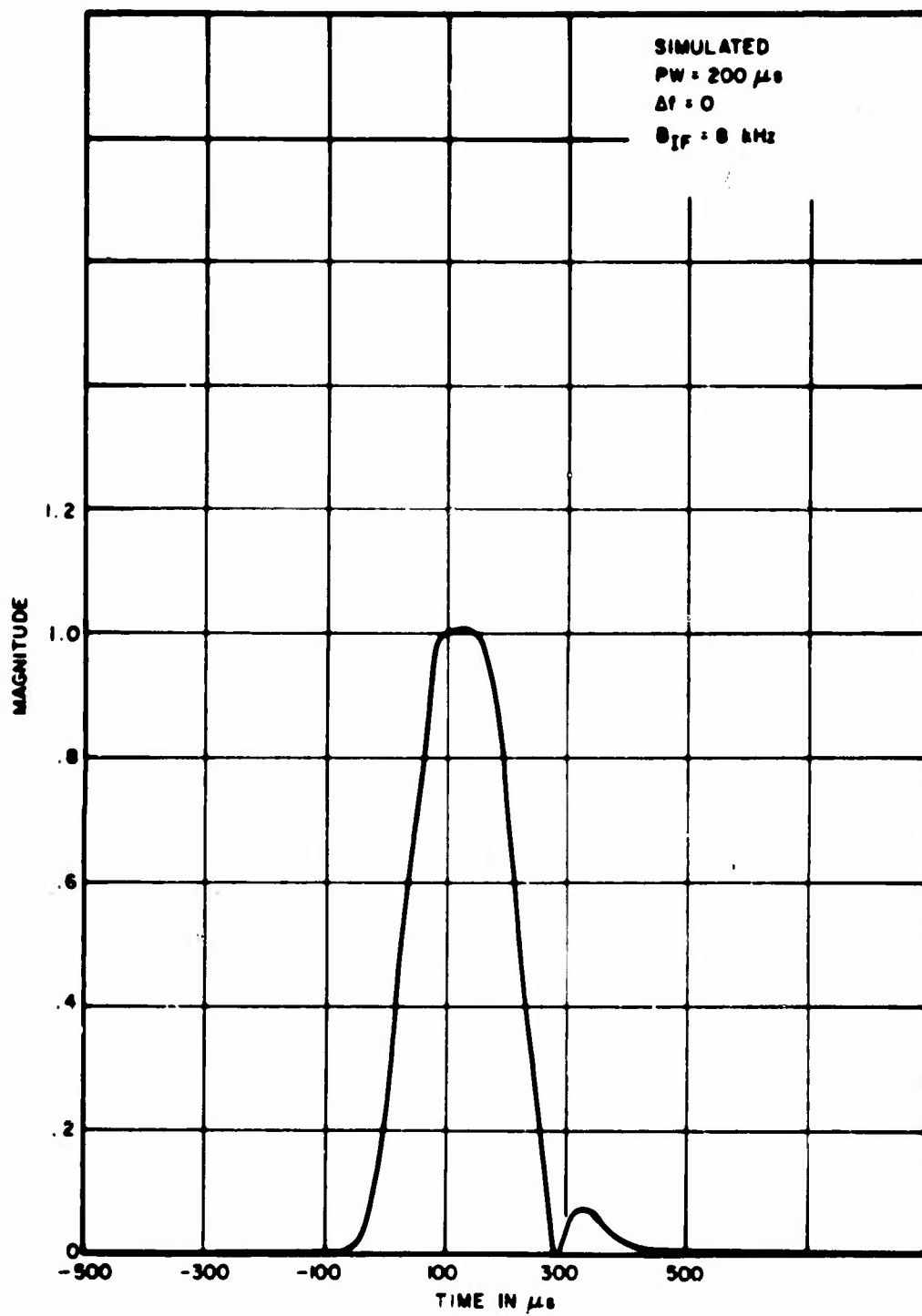


Figure 4-6. IF Output Time Waveform

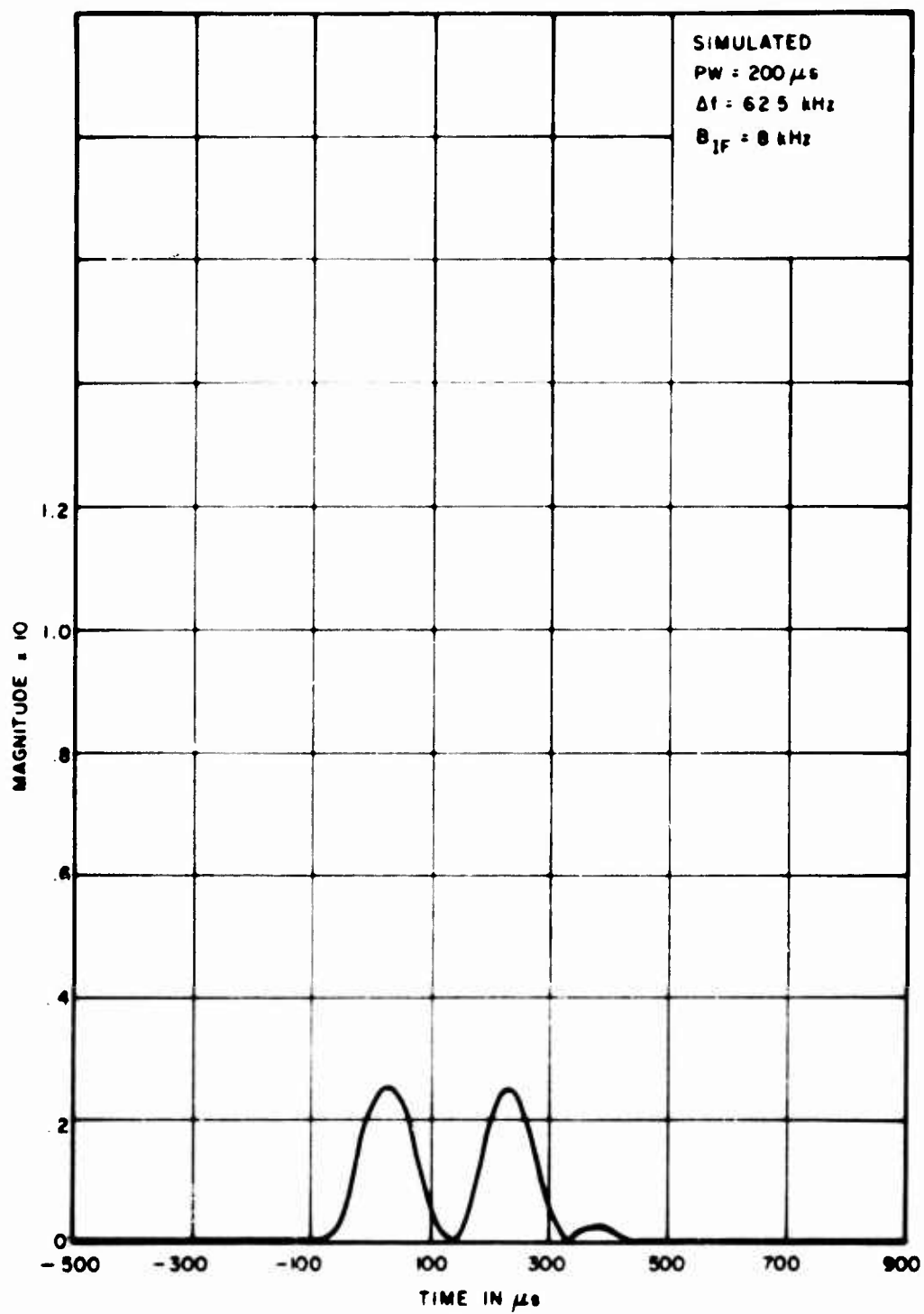


Figure 4 7. IF Output Time Waveform

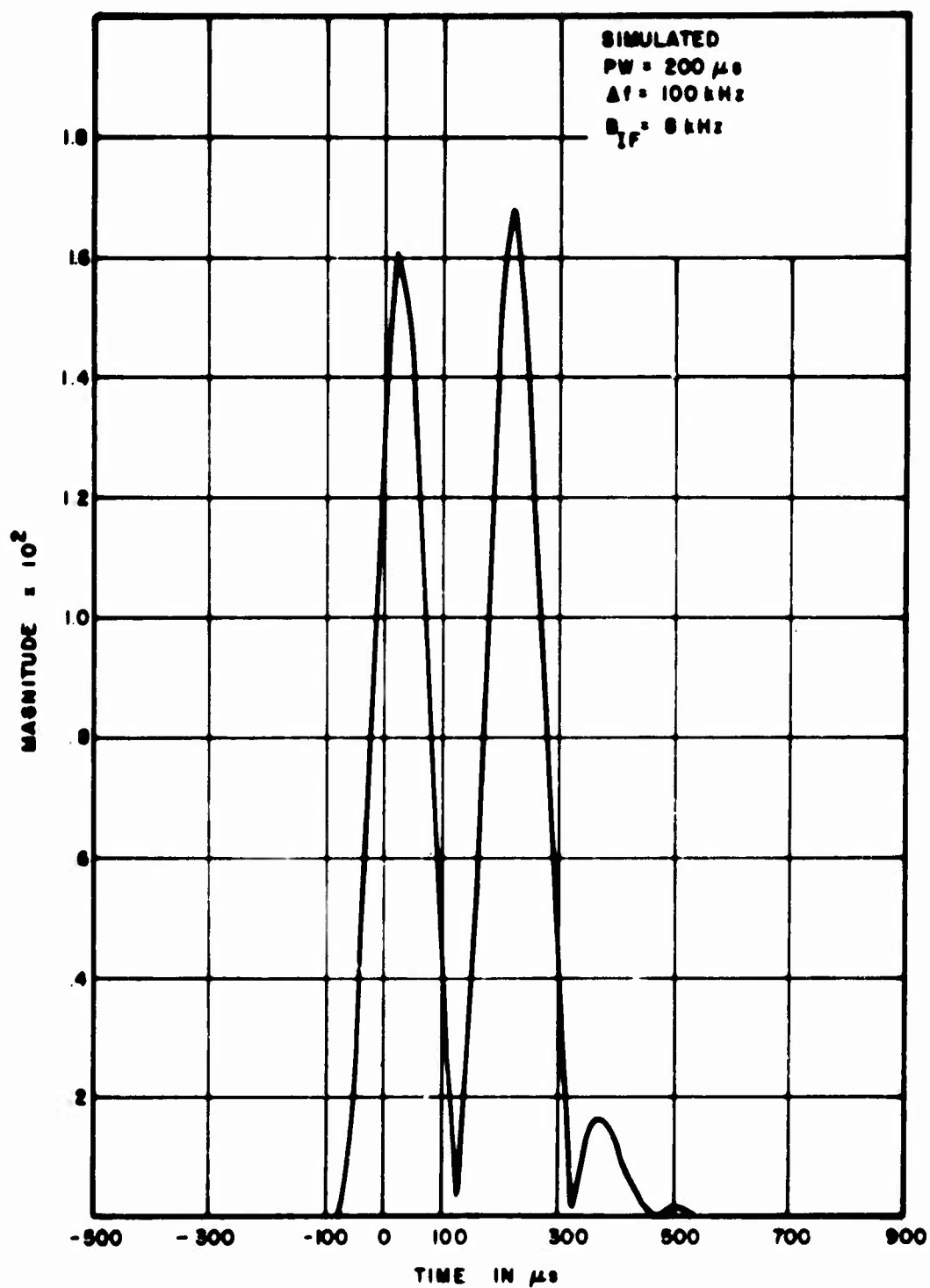


Figure 4-8. IF Output Time Waveform

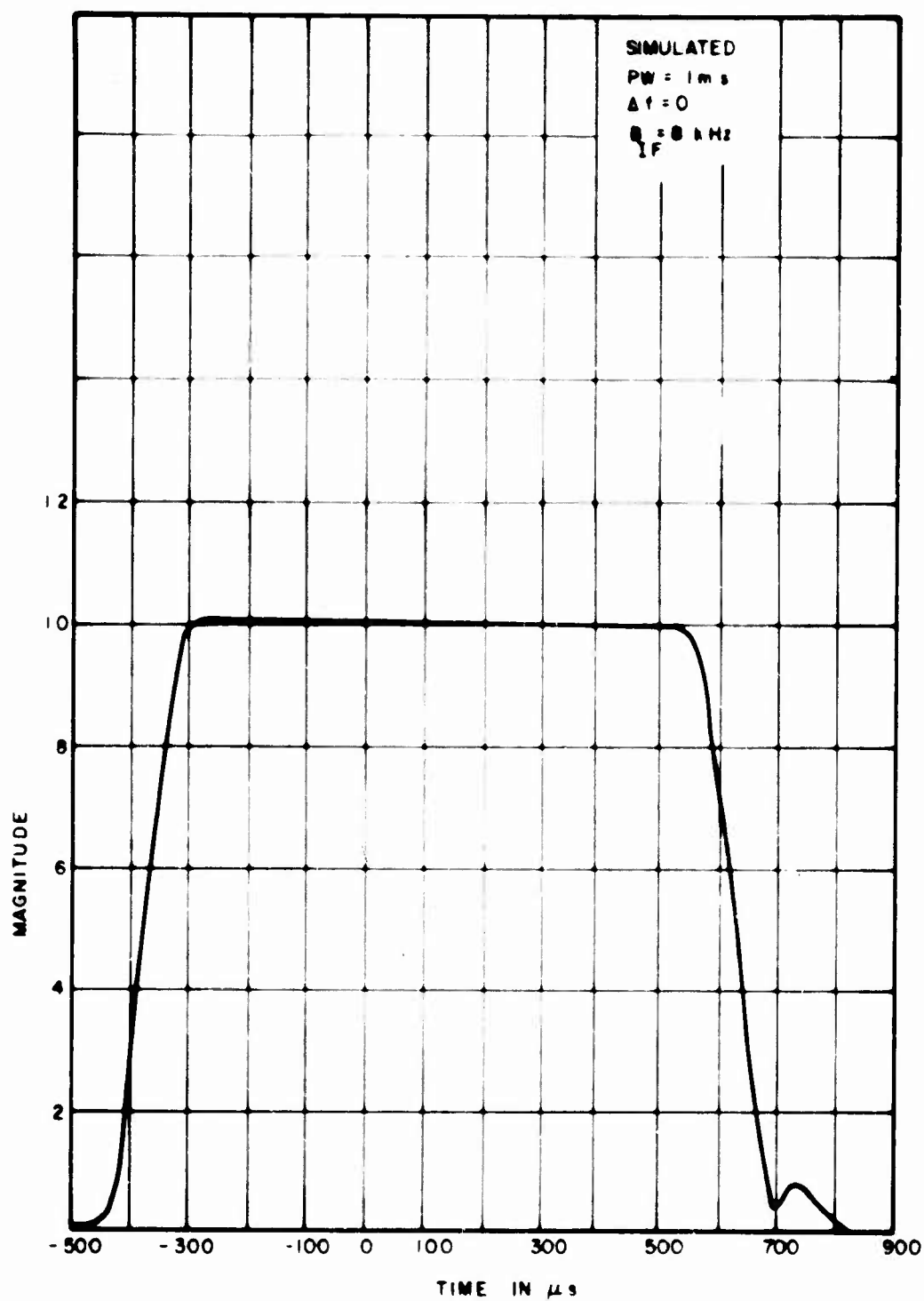


Figure 4 9 IF Output Time Waveform

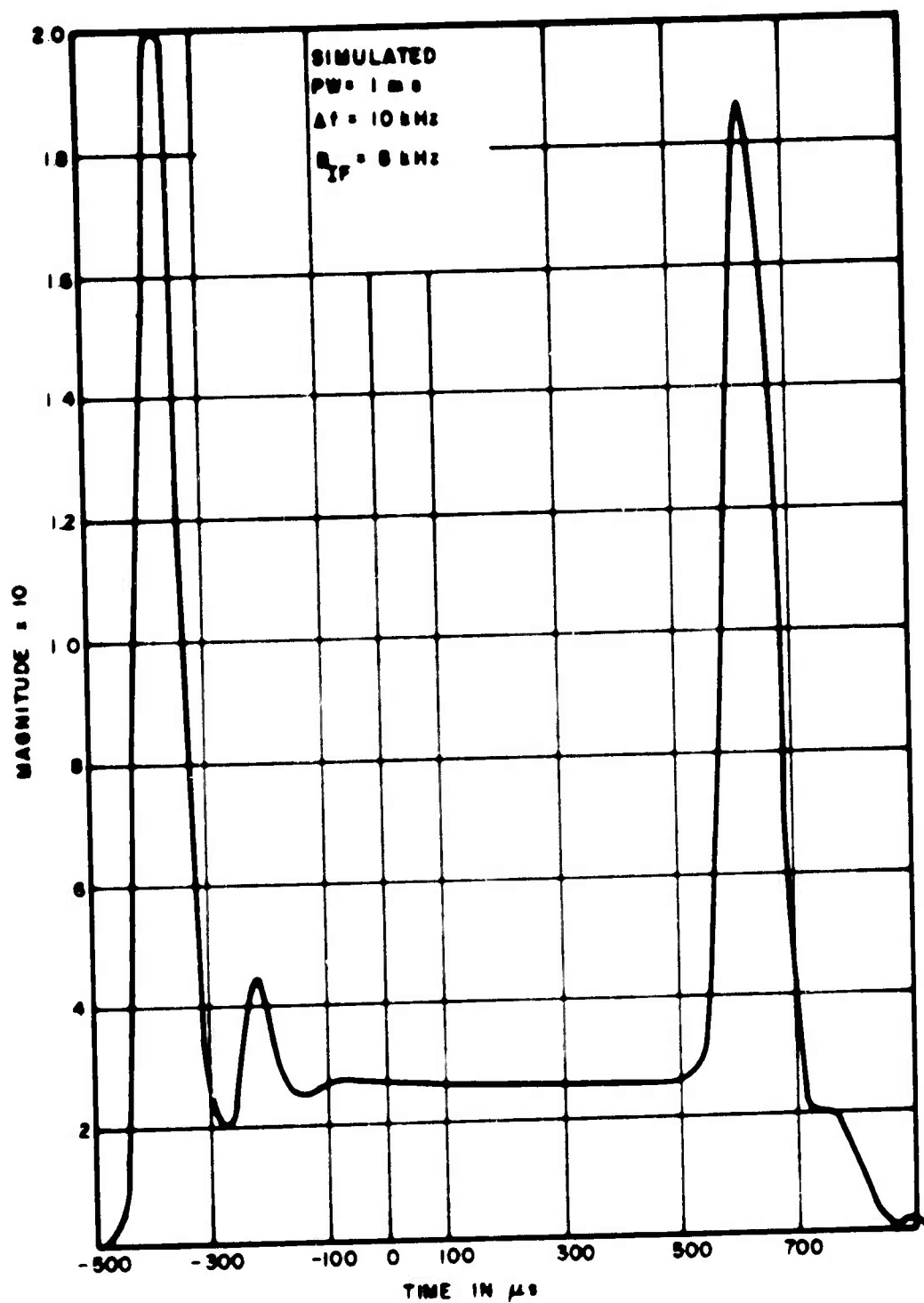


Figure 4-10a. IF Output Time Waveform

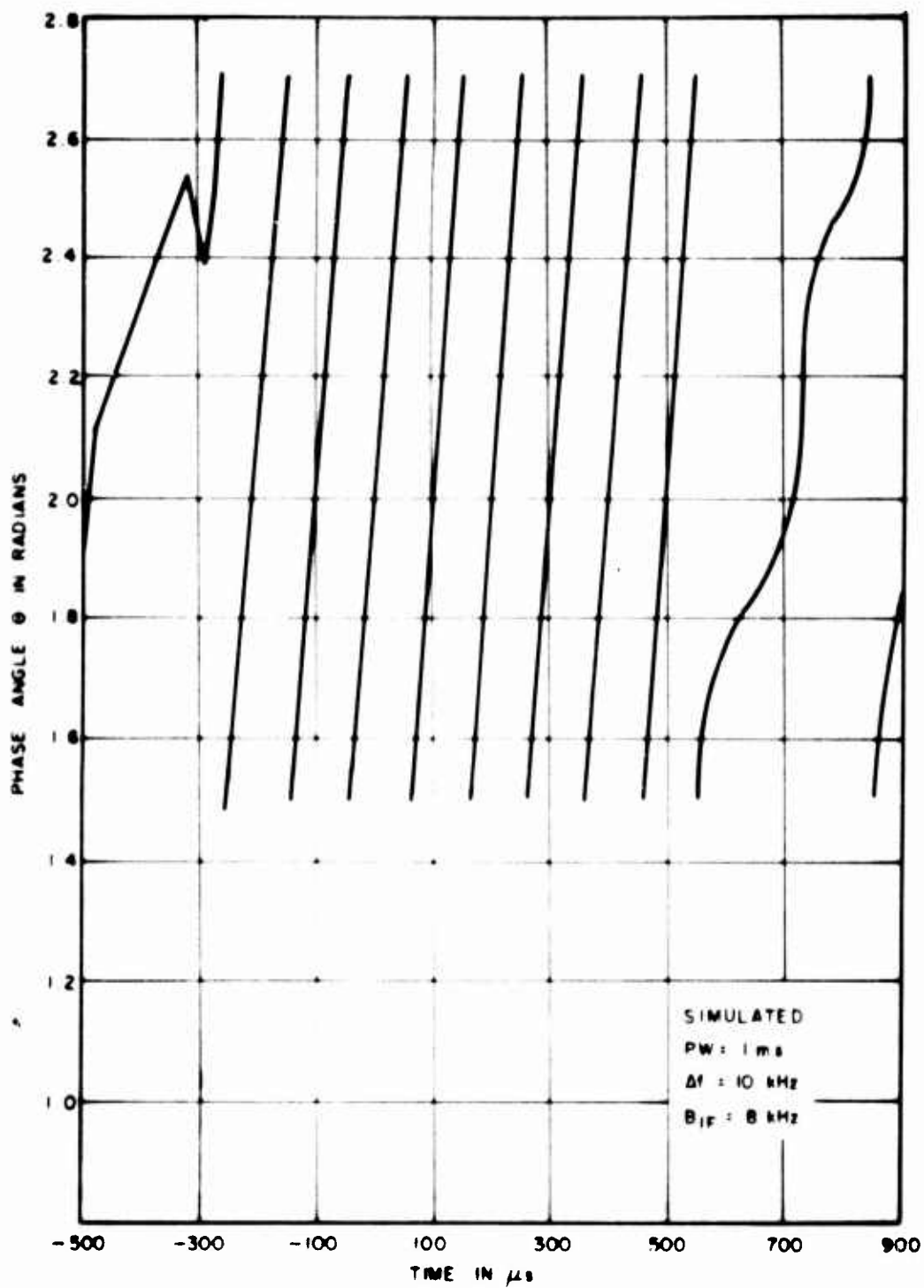


Figure 4-10b. IF Output Phase Function

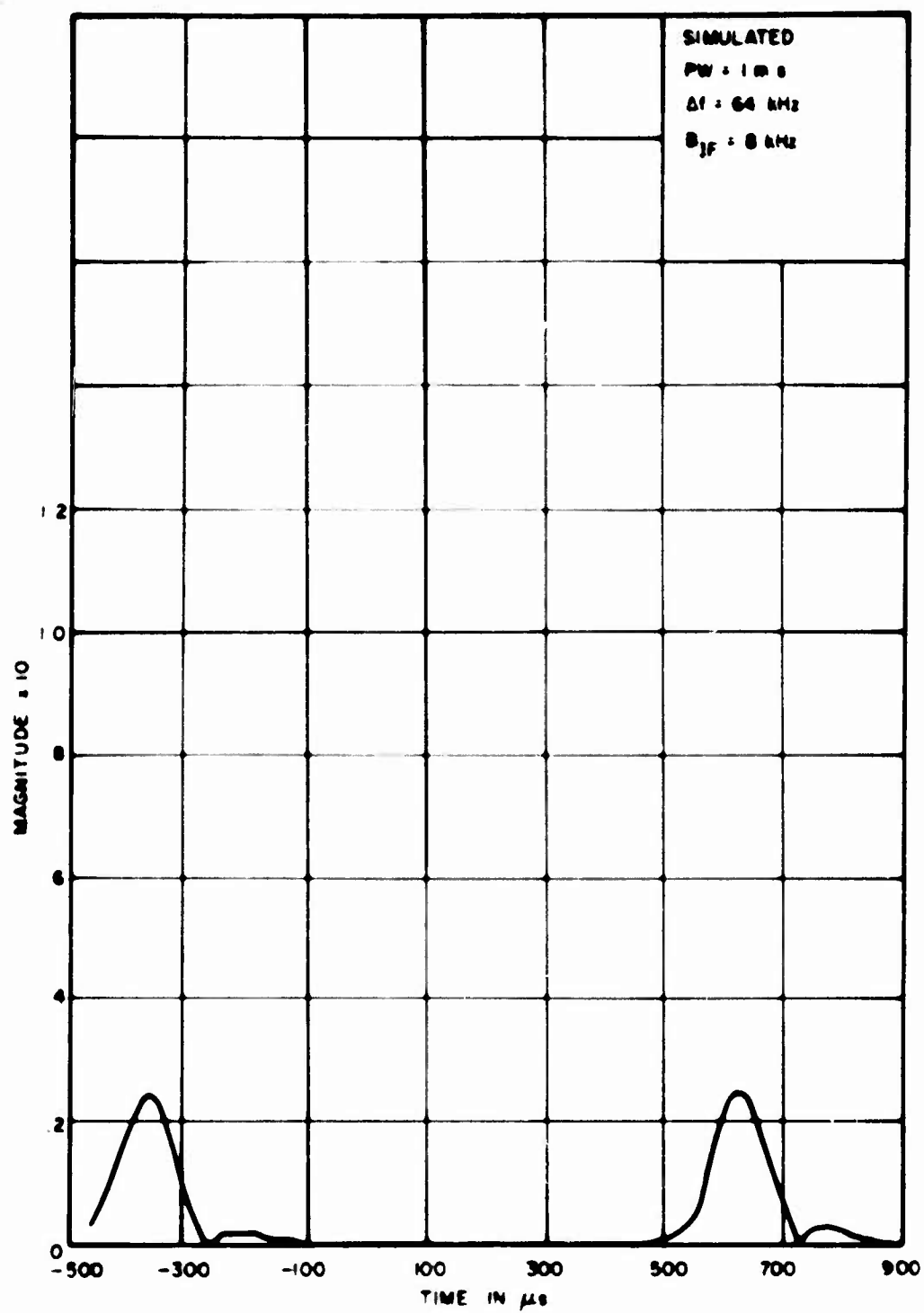


Figure 4-11. IF Output Time Waveform

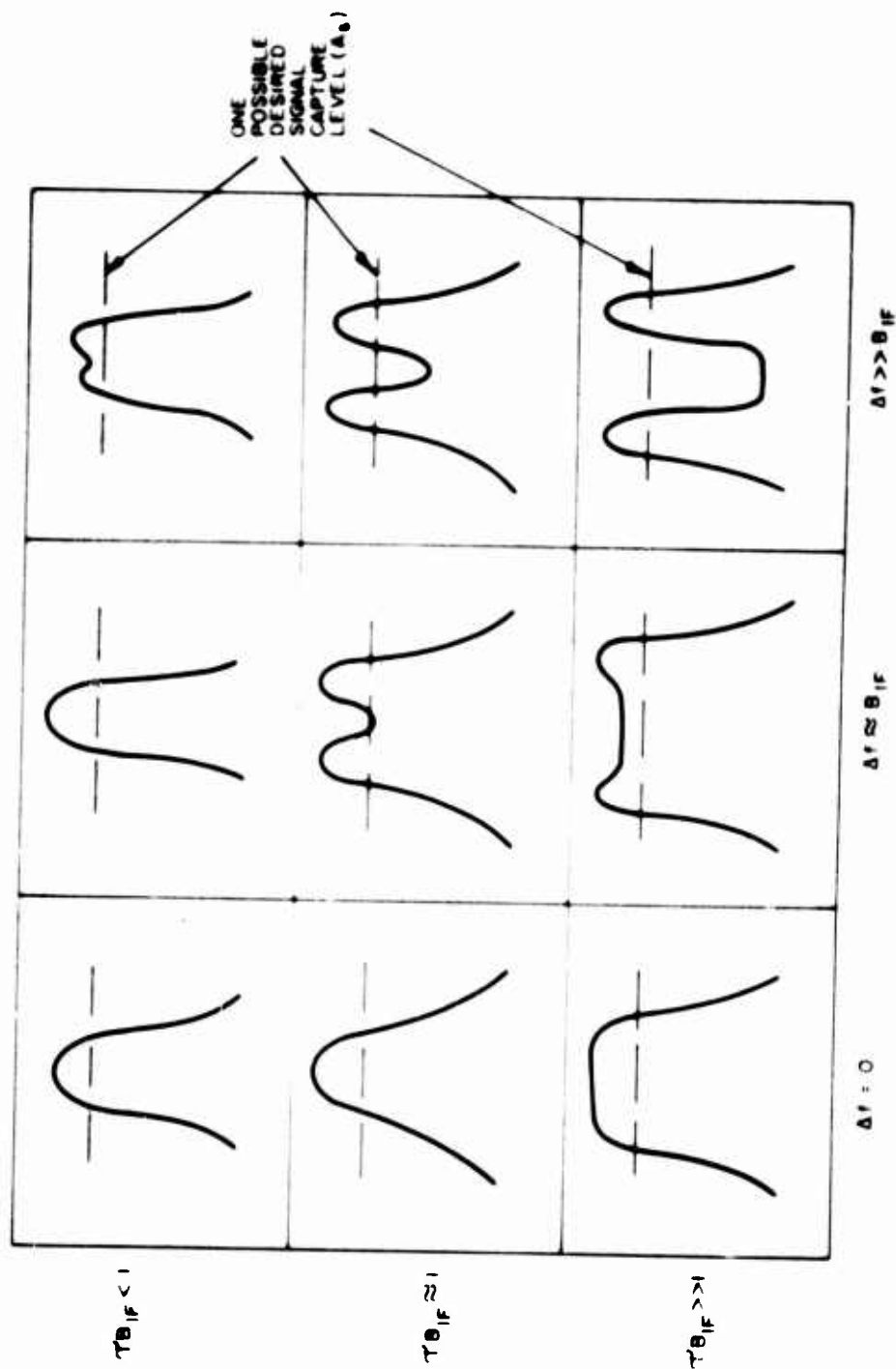


Figure 4-12 Typical IF Output Time Waveform Responses for On-Tune and Off-Tune Pulses

time waveform out of the IF will be obtained, and the details will be left to the simulated receiver processing elements.

DETECTOR ANALYSIS

The detector analysis considers how the transformed pulse interference, band limited Gaussian noise, and the desired signal from the IF filter are simultaneously processed by the envelope detector. The analysis assumes the detector is a linear envelope (zero memory) detector which is sensitive only to the slow amplitude variations of the input signal.

The disturbance caused by the pulsed carrier will be a function of the relative magnitude, frequency separation between the desired and undesired signals, pulse width, pulse shape, and pulse repetition frequency of the particular pulse train, as well as the receiver selectivity and detector characteristics. Considering only amplitude variation in the IF output time waveform, it is shown in Appendix II, Equation (II 11), that the detector output can be generally written as

$$V_D(t) = \left\{ \left[A_s [1 + M_s \cos(\omega_s t + \psi)] + A(t) \cos \phi(t) \right]^2 + \left[A(t) \sin \phi(t) \right]^2 \right\}^{1/2} \quad (4.9)$$

where

$\phi(t)$	=	$\Delta\omega t + \theta_0 + \phi'_i(t)$
$\phi'_i(t)$	=	$\phi_i(t) - \Delta\omega t$
A_s	=	Amplitude of the desired signal at the IF output
M_s	=	The desired modulation index after IF filtering
ω_s	=	The frequency of the desired modulating tone in radians
$\Delta\omega$	=	The frequency difference between the carrier of the desired and undesired signal in radians
ψ	=	The phase shift of the desired information after IF filtering

θ_0 = The phase difference between the desired and undesired carriers after IF filtering (phase angle of desired carrier = 0°)

In order to obtain a better understanding of the degradation caused by the pulsed interference, the equation describing the detector output should be in a form that separates the pulsed interference components from the desired signal components. This can be accomplished by considering a large interfering carrier to noise ratio (so that noise may be neglected) and expanding the detector output equation in a series for $A_s > A_i$ and $A_i > A_s$. Neglecting the higher order terms of the series, it is shown in Appendix II, Equations (II 19) and (II 31), that the detector output signal is of the form

For $A_s > A_i$

$$\begin{aligned} \frac{V_d(t)}{A_s} = & \quad 1 + M_s \cos(\omega_s t + \psi) & \left. \begin{array}{l} \\ \\ \end{array} \right\} & \text{Desired Signal} \\ & + R_i P(t) \cos(\phi(t) + \psi) & \left. \begin{array}{l} \\ \\ \end{array} \right\} & \text{Interfering Signal} \\ & + R_i^2 P^2(t) \cdot (1 + M_s^2 / 2) & \\ & + \text{Higher Order Terms} & \end{aligned} \quad (4.10a)$$

For $A_i > A_s$

$$\begin{aligned} \frac{V_d(t)}{A_i} = & \quad \left[\frac{R_s^2}{2P(t)} \right] M_s \cos(\omega_s t + \psi) & \left. \begin{array}{l} \\ \\ \end{array} \right\} & \text{Desired Signal} \\ & + P(t) & \\ & + R_s \cos(\phi(t) + \psi) & \left. \begin{array}{l} \\ \\ \end{array} \right\} & \text{Interfering Signal} \\ & + \frac{R_s}{2} M_s \cos[(\omega_s t + \psi) \pm \phi(t)] & \\ & + \text{Highest Order Terms} & \end{aligned} \quad (4.10b)$$

where

A_i = The amplitude of the interfering signal at IF output

$p(t)$ = The amplitude modulation of the pulsed interfering signal at the IF filter output

R_s = A_s/A_i

R_i = A_i/A_s

For the case in which $A_s > A_i$, the desired output signal consists of a DC term plus the modulated voice signal. The first order interfering signal component at the detector output is a pulse spectrum centered about the beat frequency difference ($\Delta\omega$) between the desired and undesired signal carriers. Additional interfering signal components consist of a pulse squared spectrum centered about zero (DC) and higher order pulse terms. When the beat frequency difference ($\Delta\omega$) is too low or too high to be in the audio passband the first order interference component is attenuated by the audio filter. Therefore, when the off tuning ($\Delta\omega$) is in the audio passband the pulsed interference causes more degradation than when the interference is on-tune ($\Delta\omega = 0$). This effect is more pronounced for long pulses (pulse spectrum bandwidth much narrower than the audio bandwidth). The most important interfering component when the beat frequency is greater than the audio passband is the pulse squared term centered about zero.

For the case in which $A_i > A_s$, the main interfering term is a pulsed term centered about zero with secondary terms consisting of the beat note and the modulating frequency plus and minus the beat note. The desired modulated signal is also present. However, the DC term proportional to the desired carrier level which is present when $A_s > A_i$ is missing. The unnormalized signal amplitude is given approximately by

$$\frac{A_s R_s}{2p(t)} M_s \cos(\omega_s t + \phi) \quad (4.11)$$

In the absence of the strong interfering carrier, this term becomes approximately

$$A_s M_s \cos(\omega_s t + \phi) \quad (4.12)$$

Therefore, the strong interfering carrier has reduced the desired signal approximately by a factor of

$$\frac{R_s}{2p(t)} \quad (4.13)$$

over the normal signal level. This corresponds to a dB value of:

$$20 \log \frac{R_s}{2p(t)} \quad (4.14)$$

which, for a representative value of $R_s/2p(t) = .05$ equals a 26 dB reduction in the normal signal level and essentially eliminates the desired signal during the on-time of the pulse.

BASEBAND FILTER ANALYSIS

The transformation of the pulsed detector output signal by the baseband (audio) filter, and the difference in this effect for a minimum and wide IF bandwidth, will be discussed.

The baseband (audio) filter is assumed to consist of a two stage high and low pass filter which represent typical audio filtering stages. The high pass filter transfer function is given by

$$H_{HP}(\omega) = \frac{1}{1 - \left(\frac{\omega_1}{\omega}\right)^2 + j2\left(\frac{\omega_1}{\omega}\right)} \quad (4.15)$$

where

$$\begin{aligned} \omega_1 &= 64 \omega_L \\ \omega_L &= \text{Low frequency 3 dB cutoff} \end{aligned}$$

The low pass filter transfer function is given by

$$H_{LP}(\omega) = \frac{1}{1 - \left(\frac{\omega}{\omega_2}\right)^2 + j2\left(\frac{\omega}{\omega_2}\right)} \quad (4.16)$$

where

$$\begin{aligned} \omega_2 &= \omega_H / 64 \\ \omega_H &= \text{High frequency 3 dB cutoff} \end{aligned}$$

These transfer functions are incorporated in the receiver simulation model that will be subsequently summarized.

The change in the characteristics and level of pulsed interference will be negligible between the input and output of these filters for AM systems with minimum IF bandwidths (i.e., systems in which the IF bandwidth equals twice the baseband bandwidth). There may,

however, be a significant difference between the optimum IF bandwidth case and one in which the IF bandwidth is much greater than the minimum IF bandwidth.

In the first case the IF bandwidth is approximately twice the baseband bandwidth and consequently the baseband only allows the transfer of the same pulse spectral components as the IF. The time waveform characteristics between the input and output of the filter should, therefore, be similar. The pulsed IF output signals were previously discussed in the IF filter section with the overall responses summarized in Figure 4-12. These on-tune and off-tune IF output pulses essentially pass through the system with modifications from the addition of the desired signal and the transformation of the envelope detector. The resulting pulses at the output of the baseband filter appear similar to the IF output pulses except for the addition of overshoot responses primarily due to the envelope detector action. Typical pulses with this type of response are shown in Figure 4-13.

When the bandwidth of the IF is much greater than twice the baseband bandwidth, the detector output pulses may contain higher frequencies than will be passed by the baseband filter. The result is that the detector output pulses will resemble input pulses of bandwidth equal to or less than the IF bandwidth. The audio filter then removes the high frequency components of the pulses and again limits the effective IF input frequency components that pass through the overall system to twice the baseband bandwidth.

The baseband filter output pulse shape is approximately the same for both cases. However, the level may be different due to the difference in IF bandwidth. In particular, for the wide IF bandwidth case and a pulse spectrum equal to twice the baseband bandwidth the output pulse level remains constant as the pulse is off tuned until one half the IF bandwidth is reached. If the same result were compared with the minimum IF bandwidth case, the level would have been reduced at a 20 dB per decade rate from one half the minimum bandwidth.

The result is that for $rB_{IF} \geq 1$ the effective interference level begins to decrease (for a constant input interference level) at approximately one half the IF bandwidth for both the minimum bandwidth IF (approximately 6 kHz) and a wider IF bandwidth. (This is discussed further in Section 6 under Off-Tuning Effects.)

AGC -- AMPLIFIER SATURATION EFFECT

This discussion concerns the effect the AGC circuit has on the modeling of pulsed interference in an AM receiver. In general, AGC circuits are designed to maintain a constant output level over a large range of input signal levels. The circuits that accomplish this function usually act upon the DC level of the detector output or the RMS level of the IF

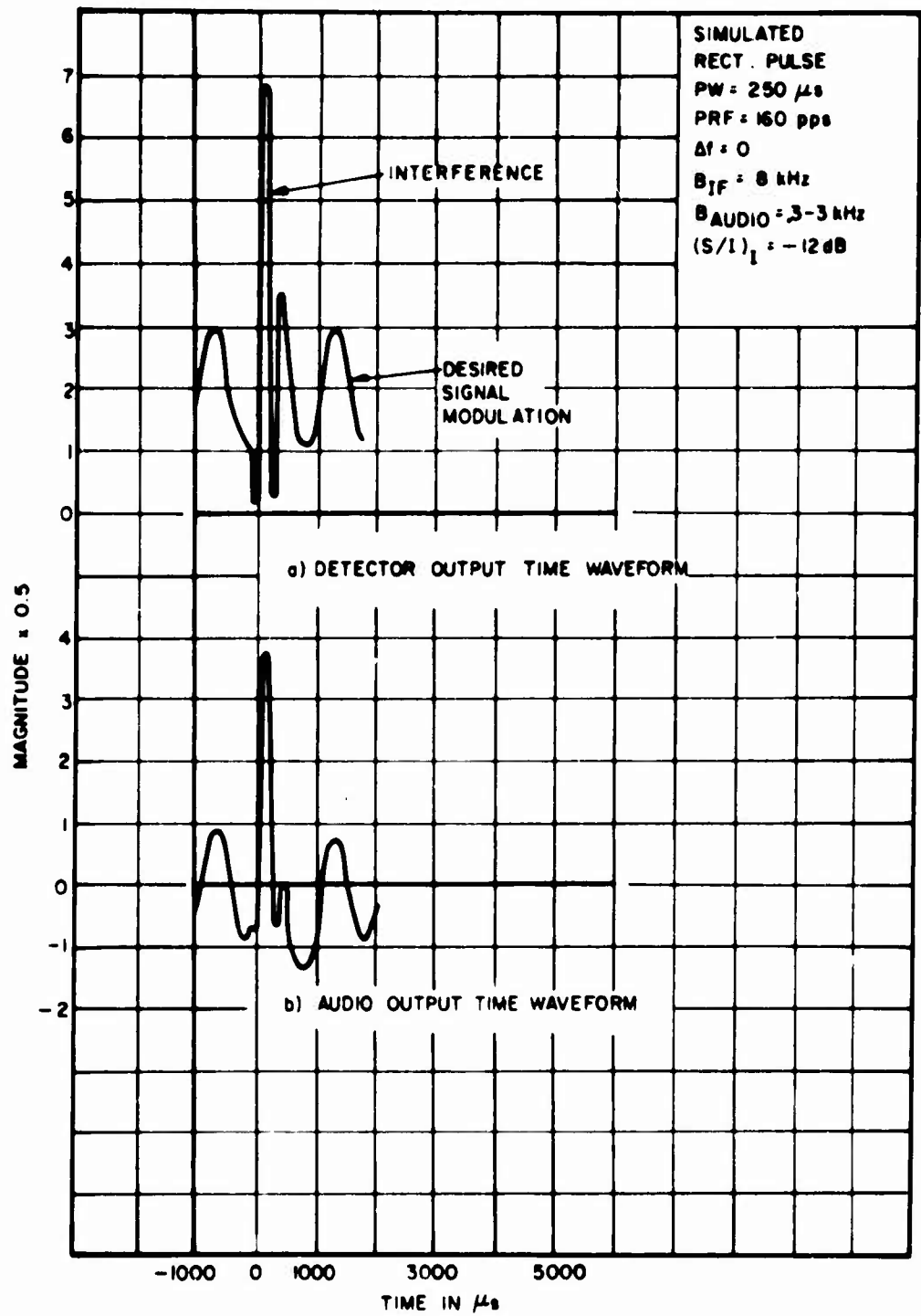


Figure 4-13. Detector and Audio Output Time Waveforms

output. If a large interfering signal is introduced into the receiver, the AGC may respond to the interfering signal depending upon the interfering signal parameters and the AGC time constants. The amount of degradation caused by a particular interfering pulse signal depends on the effect the interfering signal has on the DC level of the AGC bias line. The receiver simulation model does not include the effects of AGC and it is the purpose of this discussion to outline what does happen with pulsed interference and the limitations of the present model without AGC.

If the interfering pulse signal does not affect the DC level of the AGC bias line, the interfering signal can saturate a particular amplifier stage or stages of the receiver causing the interfering signal pulse amplitude to be clipped. When the interfering signal pulse amplitude is clipped, the $(\hat{S}/\hat{I})_{IF}$ power ratio at the IF output is limited. Therefore, the amount of degradation caused by the interference is limited. Measured data plotted in Figures 4-14 and 4-15 shows what happens when the DC level of the AGC bias line is not affected by the interfering signal. Figure 4-14 shows AGC voltage level and IF output power ratios, $(\hat{S}/\hat{I})_{IF}$, versus RF input power ratio, $(S/I)_{RF}$, for an interfering signal with a 400 μ sec pulse width and a PRF of 10.* The figure indicates that the receiver becomes saturated at $(S/I)_{RF}$ equal to -18 dB. The $(\hat{S}/\hat{I})_{IF}$ level decreases by only 2 dB as the $(S/I)_{RF}$ level is decreased from -18 dB to -63 dB. The curves also show that the AGC voltage level is relatively unaffected until the (S/I) level at the RF input reaches -63 dB. As the $(S/I)_{RF}$ power ratio is decreased below -63 dB the AGC voltage level changes rapidly, causing the $(\hat{S}/\hat{I})_{IF}$ power ratio to decrease rapidly. Figure 4-15 shows degradation in terms of Articulation Index (AI) as a function of the RF input power ratio, $(S/I)_{RF}$, for the same interfering signal. The curve shows that for $(S/I)_{RF}$ values between -18 dB and -63 dB the degradation levels off, indicating that the receiver is saturated. For $(S/I)_{RF}$ values more negative than -63 dB, the AGC voltage level was affected causing the degradation to increase. Since the present receiver simulation model does not consider receiver saturation effects, the simulation model would show the degradation increasing instead of leveling off as the $(S/I)_{RF}$ ratio is decreased between -18 dB and -63 dB. Therefore, the present receiver simulation model will give a pessimistic AI level when the receiver becomes saturated.

If the DC level of the AGC bias line is controlled by the interfering signal level, the receiver gain will decrease causing the desired signal level to decrease as the interfering signal level increases. This causes the receiver to become desensitized to the desired signal and also allows more negative $(\hat{S}/\hat{I})_{IF}$ power levels. Therefore, the receiver degradation is greater if the interfering signal affects the AGC. Measured data are plotted in Figures 4-16 and 4-17 to

* (\hat{S}/\hat{I}) means peak desired signal to peak interfering signal. (S/I) means RMS desired signal to peak interfering signal.

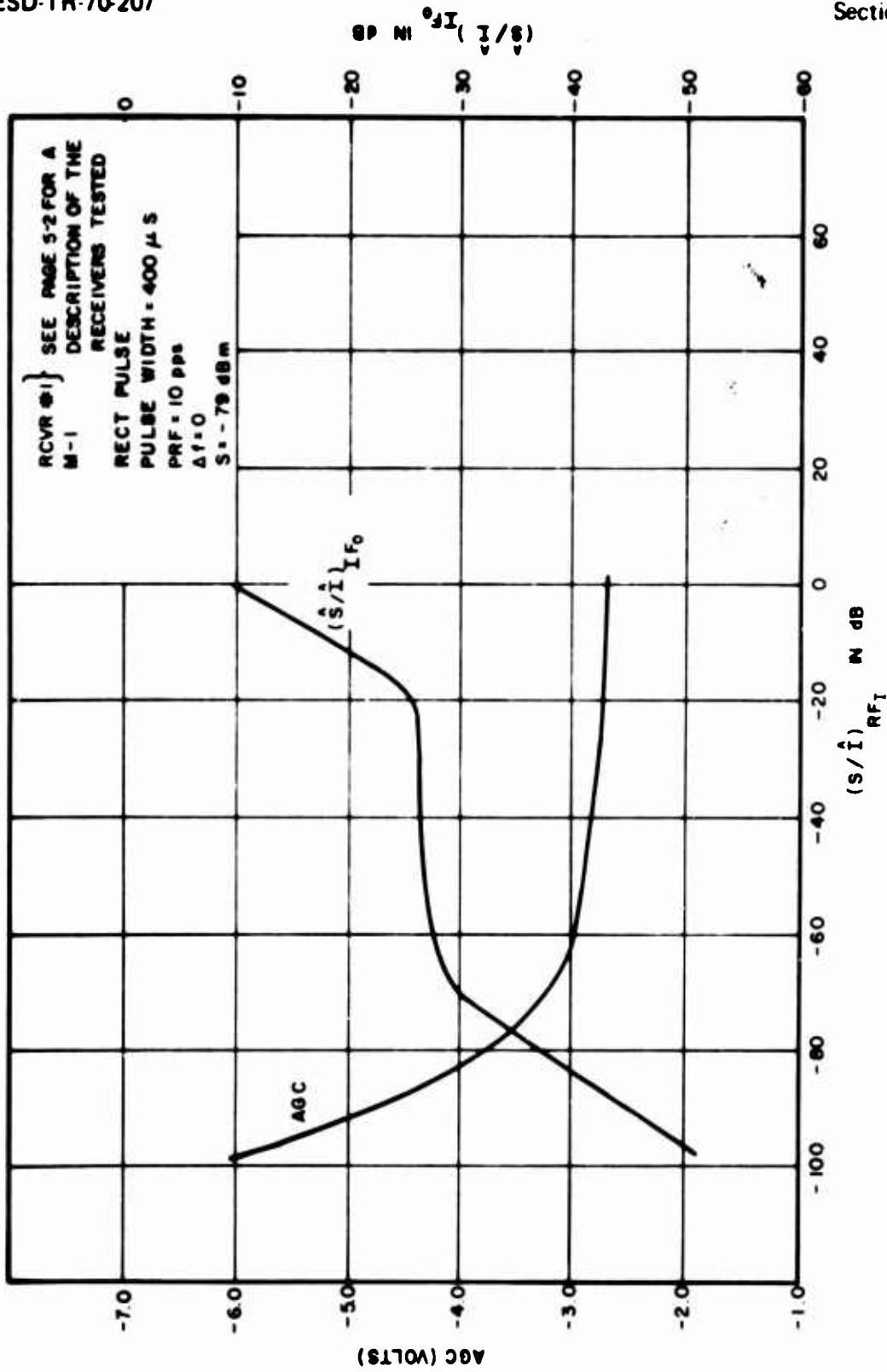


Figure 4.14. Power Transfer Curve and AGC Level for Pulsed Interference to an AM Receiver

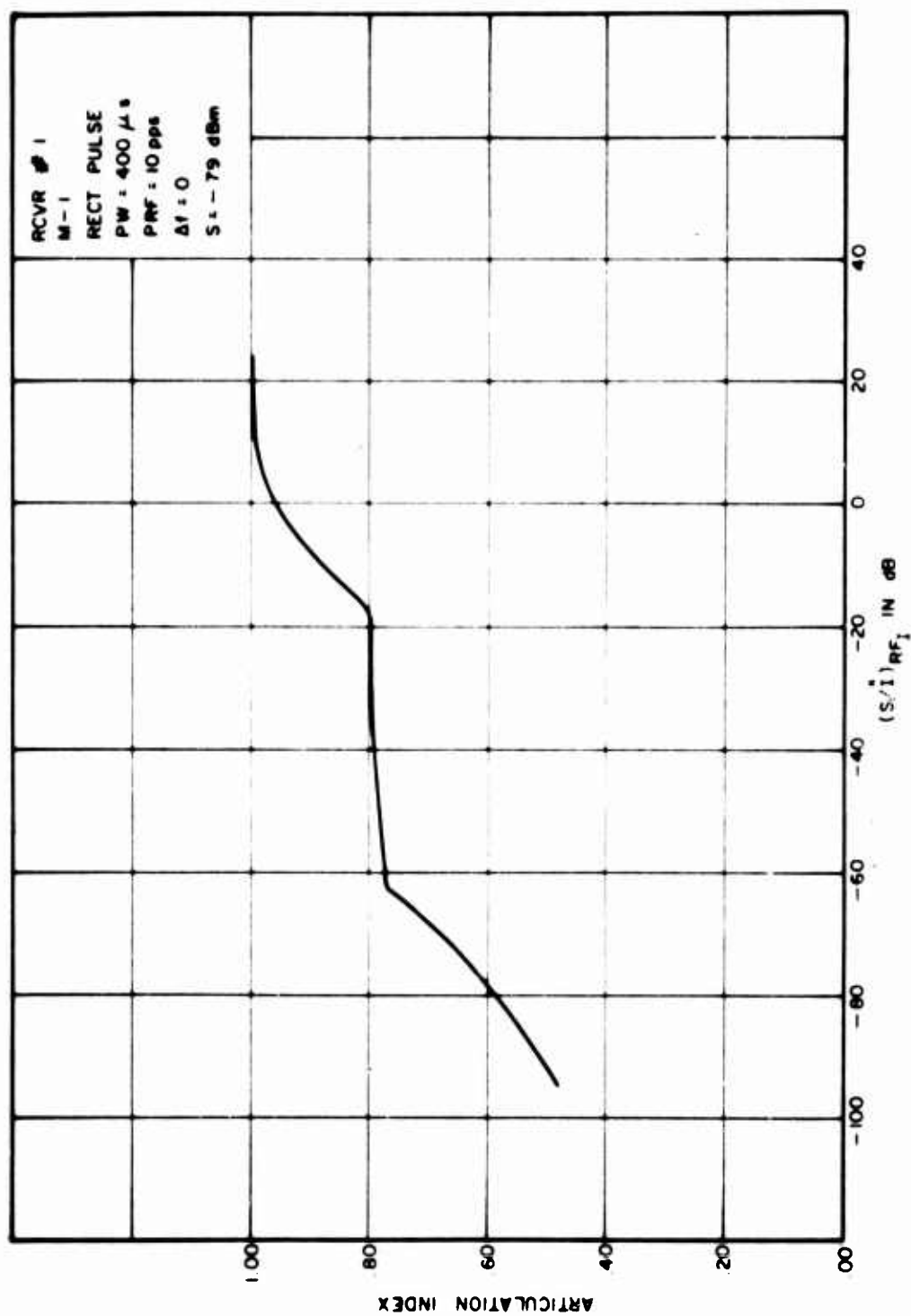


Figure 4-15. Articulation Index for Pulsed Interference to an AM Receiver

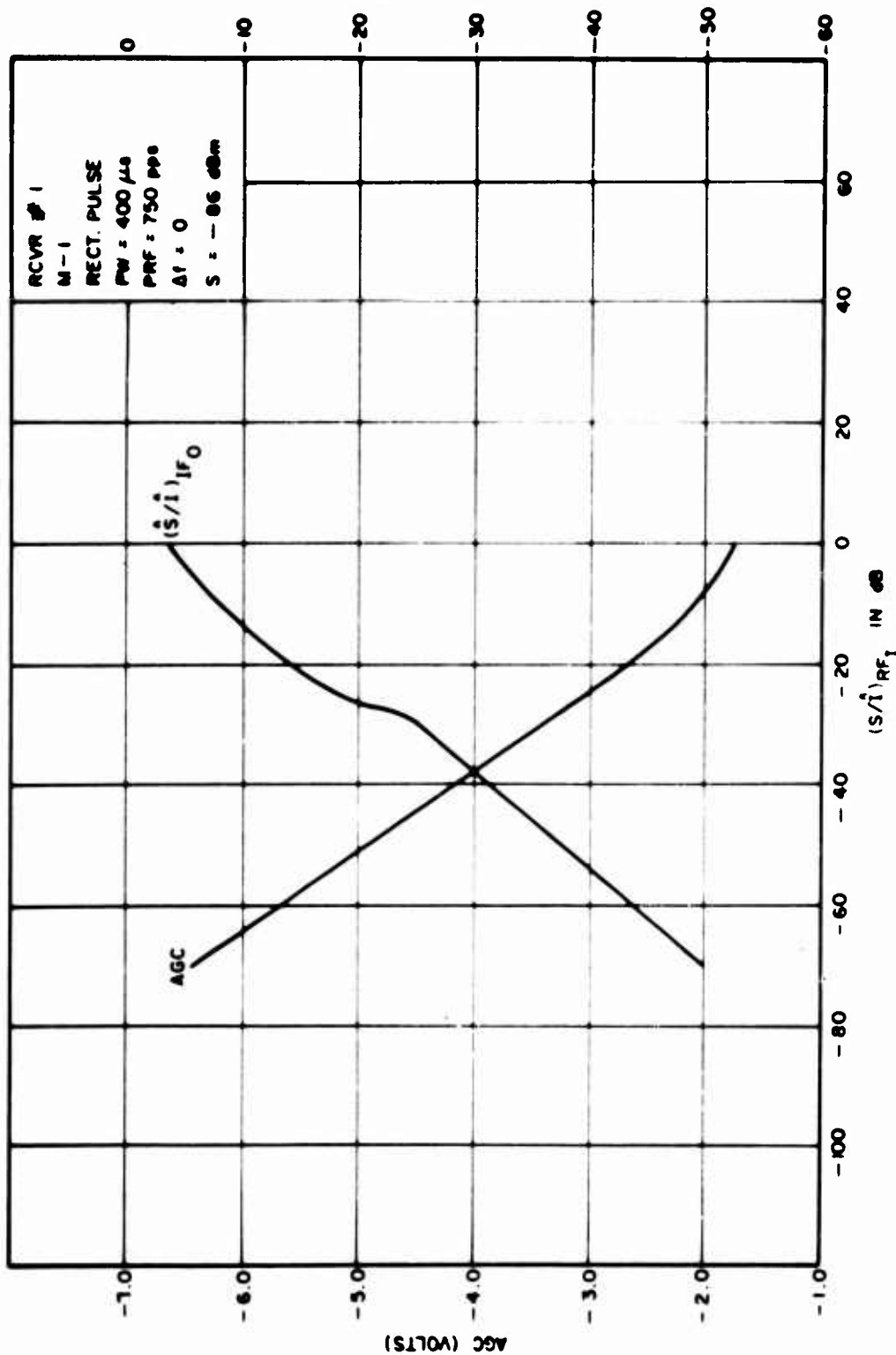


Figure 4-16. Power Transfer Curve and AGC Level for Pulsed Interference to an AM Receiver

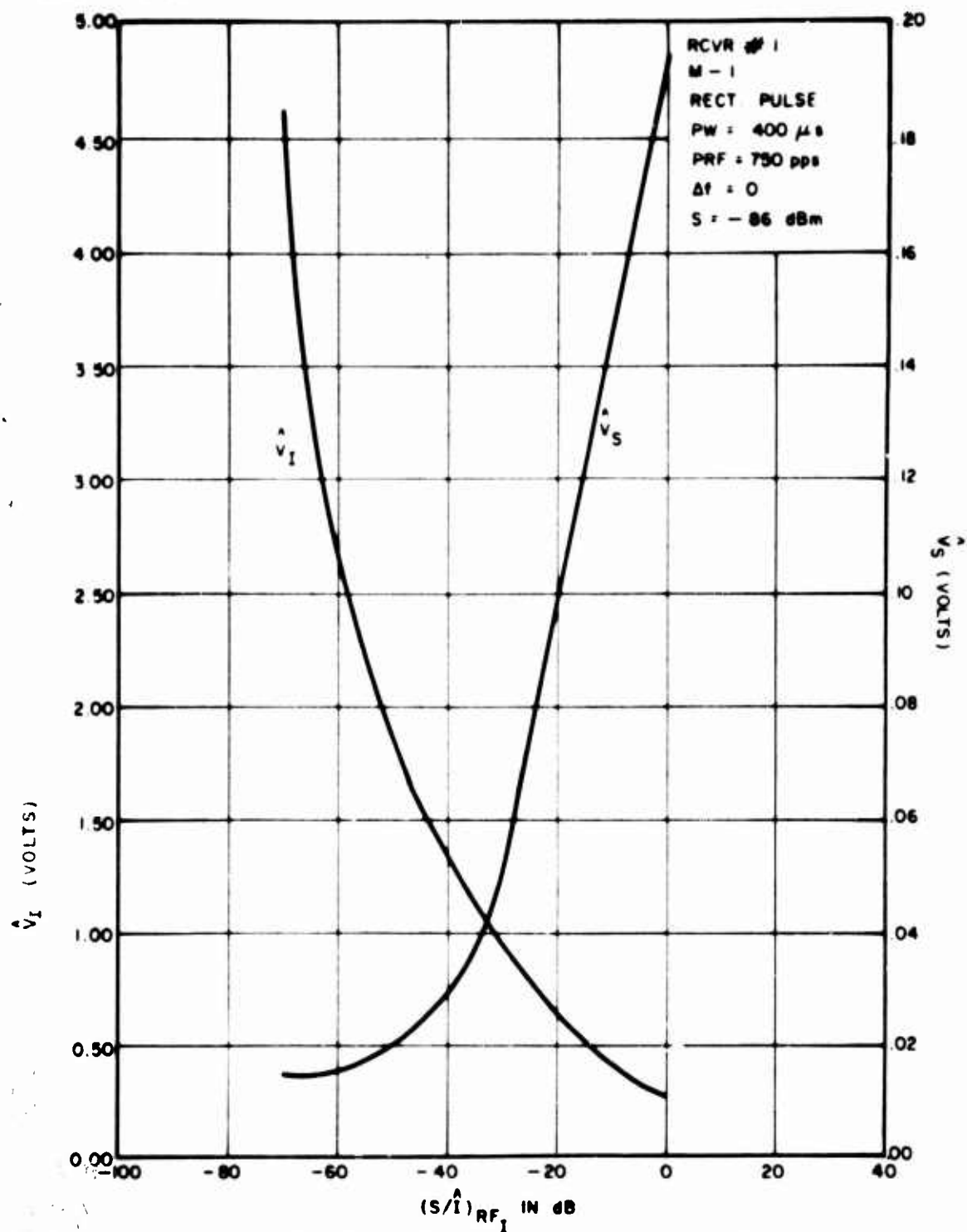


Figure 4-17. AGC Effects for Pulsed Interference to an AM Receiver

show what happens when the DC level of the AGC bias line is affected by the interfering signal. Figure 4-16 shows the AGC voltage level and IF output power ratio, $(\hat{S}/\hat{I})_{IF}$, versus RF input power ratio, $(S/\hat{I})_{RF}$, for an interfering signal with a 400 μ sec pulse width and a PRF of 750. The figure indicates that the interfering signal affects the DC level of the AGC bias line, allowing the $(\hat{S}/\hat{I})_{IF}$ level to become more negative as the $(S/\hat{I})_{RF}$ level is decreased. Therefore, the receiver does not become saturated. If the interfering signal does not cause receiver saturation, the present receiver simulation model will give an accurate degradation level in terms of AI as a function of the $(S/\hat{I})_{RF}$ level.

Figure 4-17 shows peak interference voltage (\hat{V}_I) and peak desired voltage (\hat{V}_S) at the IF output versus RF input power ratio, $(S/\hat{I})_{RF}$, for an interfering signal with a 400 μ sec pulsewidth and a PRF of 750 pps. The desired signal voltage decreases linearly for approximately 20 dB and levels off as the $(S/\hat{I})_{RF}$ is made more negative. The desired signal voltage levels off as it approaches the receiver noise level. The figure also shows the peak interfering voltage increasing from 37 to 5 volts (approximately 23 dB) as the $(S/\hat{I})_{RF}$ level is made more negative.

Measurements were also made to show how the AGC voltage level is a function of the pulse width and PRF of the interfering signal. Figure 4-18 shows AGC voltage level versus PRF for pulse widths of 250 and 400 μ sec. The $(S/\hat{I})_{RF}$ level was held constant at -10 dB. There is very little difference in the AGC voltage level for the two pulse widths. Figure 4-19 shows AGC voltage level versus PRF for various $(S/\hat{I})_{RF}$ levels. The pulse width is held constant at 400 μ sec. At low PRF's the AGC voltage level is relatively unaffected as the $(S/\hat{I})_{RF}$ level is made more negative. Therefore, at low PRF's the receiver will become saturated. At high PRF's there is a larger change in the AGC voltage level as the $(S/\hat{I})_{RF}$ level is made more negative. Therefore, for this condition, the receiver will not become saturated.

It is concluded from the measured data that the effect the interfering signal has on the AGC voltage level is a function of pulse width, PRF, $(S/\hat{I})_{RF}$ level and the characteristics of the AGC circuit. These conclusions are based upon the measurements made on receiver No. 1 which has SLOW, MEDIUM and FAST time constant settings of 0.015, 0.3 and 5.0 seconds, respectively. The measurements indicated that the DC level of the AGC bias line was the same for both the SLOW and FAST switch settings for interfering signals with a duty cycle greater than 1.25 percent. The measured degradation data showed that for high PRF's the receiver did not become saturated. The average saturation levels encountered in this test are discussed in Section 6.

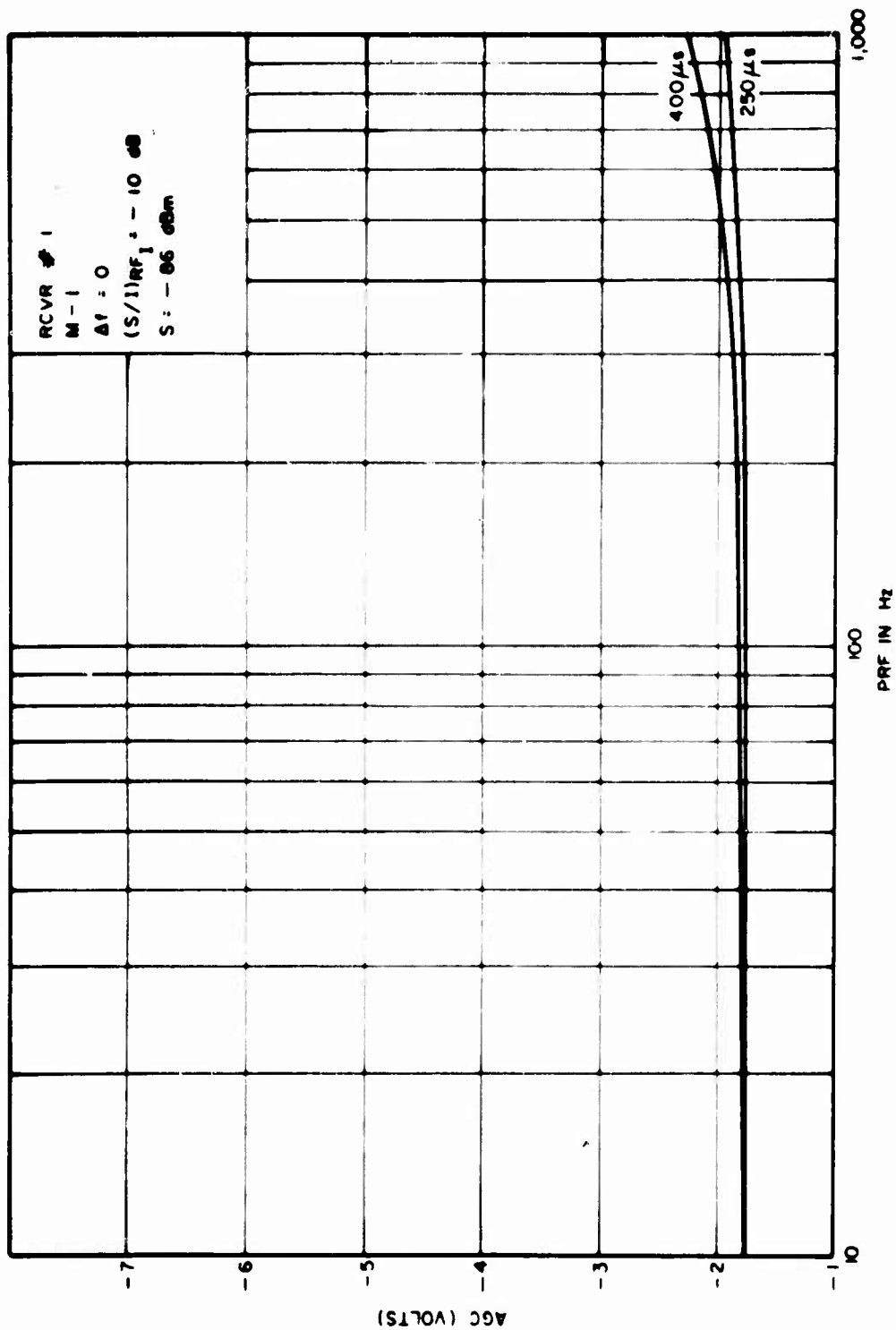


Figure 4-18. AGC Level as a Function of PRF

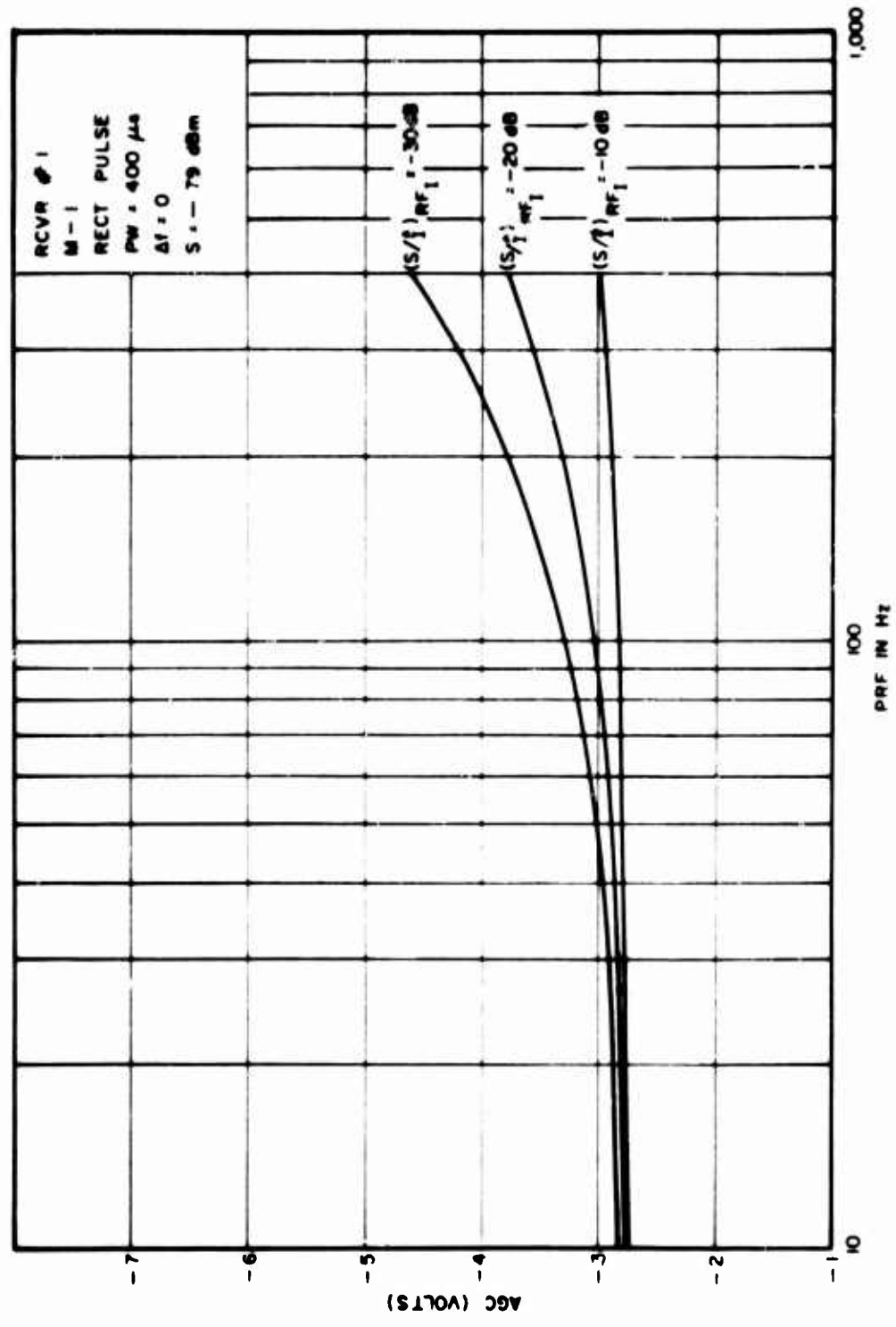


Figure 4 19. AGC Level as a Function of PRF

RECEIVER SIMULATION MODEL

The previously mentioned equations for the effective IF filter, detector and low pass filter were combined in a computer program to simulate the processing of signals through an AM receiver. A block diagram of the computer simulation is shown in Figure 4-20. This receiver simulation model will be fully documented in a future report. The following discussion summarizes the model and indicates the basis of the theoretical investigation of pulsed interference effects upon AM receivers.

The interfering signal or signals are generated in either the time or frequency domain. If they are generated in the time domain, the Fast Fourier Transform (FFT) technique is used to obtain the frequency spectra. Since the IF filter is linear, the response to the desired signal plus undesired signal is the sum of the response of each individual signal. Therefore, the desired and interfering signals can be processed separately. The interfering signals and noise are combined before the IF filter (in the frequency domain) in order to reduce the complexity of the computer program. The resultant signal is then multiplied by the IF filter function to produce an output spectrum, $V_{I+N}(\omega)$.

The inverse Fast Fourier Transform of $V_{I+N}(\omega)$ is then performed. The resulting time waveform is given by Equation (I-53), APPENDIX I, as:

$$V_{I+N}(t) = A(t) \cos [\omega_0 t + \phi_0 + \phi_i(t)] \quad (4-17)$$

$V_{I+N}(t)$ may contain both amplitude and phase modulation.

The desired signal, being amplitude modulated by a single tone, is easily converted analytically to either the time or frequency domains. The desired signal is then processed by the IF filter, either analytically or using the computer, and the output spectrum is obtained. The inverse Fourier transform of $V_S(\omega)$ is then performed and the resulting output time waveform is given by Equation (II-3d), APPENDIX II, as

$$V_S(t) = A_S [1 + M_S \cos(\omega_S t + \psi)] \cos \omega_0 t \quad (4-18)$$

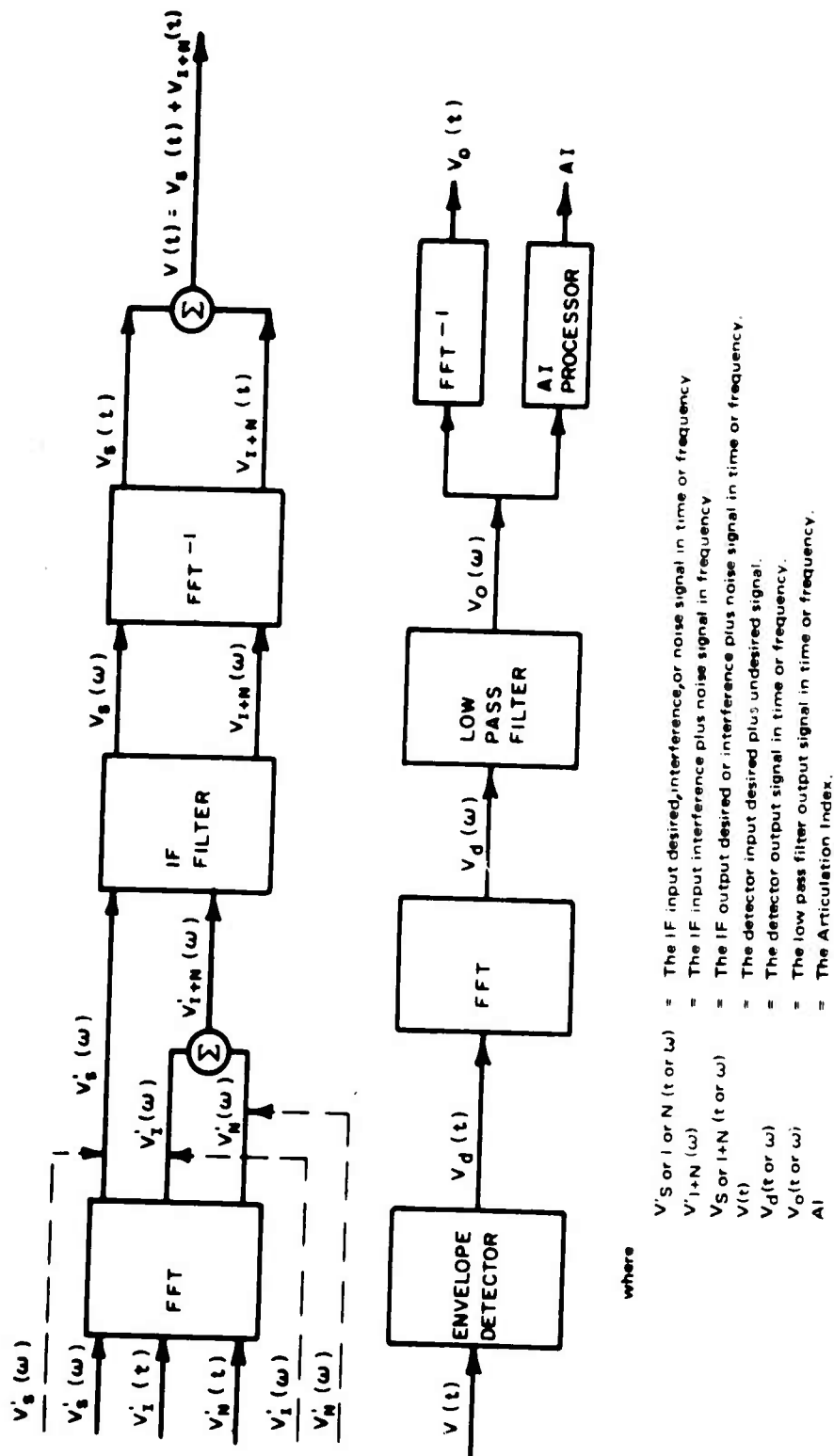


Figure 4-20. Computer Simulation Model

The desired and undesired signals are then combined at the input to the detector to produce a composite time signal,

$$V(t) = V_S(t) + V_{I+N}(t) \quad (4-19a)$$

$$= [A_S(1 + M_S \cos(\omega_S t + \psi)) + A(t) \cos \phi(t)] \cos \omega_0 t - A(t) \sin \phi(t) \sin \omega_0 t \quad (4-19b)$$

This combined signal is then processed by the envelope detector to produce the output time signal given by Equation (II-11) in APPENDIX II as:

$$V_D(t) = \left\{ [A_S(1 + M_S \cos(\omega_S t + \psi)) + A(t) \cos \phi(t)]^2 + [A(t) \sin \phi(t)]^2 \right\}^{1/2} \quad (4-20)$$

Again using the Fast Fourier Transform technique, the spectrum of the detector output, $V_D(t)$, is obtained and passed through the audio filter. The corresponding output spectrum is then used in several ways: (a) to obtain the output signal-to-interference power ratio, (b) as the input to a program designed to calculate articulation index, (c) or Fast Fourier Transformed to produce a composite output time waveform containing the desired and interference signals.

The time waveform is useful in determining the shape of the interference at the audio output and can be used as a comparison between the simulated and measured output time waveforms.

Plots of the simulated time waveforms are shown in Figures 4-21a and 4-22a. The interfering pulse in Figure 4-21a is a 250 μ sec rectangular pulse with a pulse repetition frequency of 40 pps. The desired carrier was modulated by a 1 kHz tone with a 50% modulation index. The IF and audio bandwidth were specified as 8 kHz and 3 kHz respectively with an input (S/\hat{I}) of -15 dB. The interfering pulse in Figure 4-22a is a 400 μ sec rectangular pulse with a pulse repetition frequency of 80 pps. The modulation on the desired carrier was set equal to zero for this simulation. The IF and audio bandwidths were specified as 8 kHz and 3 kHz respectively with an input (S/\hat{I}) of -25 dB.

The measured output time waveform for the same set of conditions using a typical AM receiver are shown in Figures 4-21b and 4-22b. Since the desired modulation was zero in Figures 4-22a and 4-22b, only the relative shape of the output time waveforms can be compared. The magnitude cannot be compared directly because a reference level was not established for the measured results. These waveforms illustrate the agreement between measured and analytical results.

The time waveform shows that although the peak level of the pulse has been attenuated it is still larger than the desired signal. The interfering pulse will, therefore, mask the desired signal during its on-time (this was also concluded in the Detector Section).

The output signal-to-interference power ratio, $(S/I)_O$, and the input signal-to-interference power ratio, $(S/I)_{RF}$, define the power transfer function between the receiver input and baseband output. This enables the intelligibility function, as specified at the baseband output, to be transferred to an input signal-to-interference criterion. This is further discussed in Section 6 and is symbolically shown in Figure 6-40.

In order to calculate AI using the simulation model, a single tone is used to modulate the desired carrier. The level of the desired tone at the audio output is then used to reconstruct the long term average speech spectrum as shown in Figure IV-2. This speech spectrum then determines the representative speech levels in the 14 bands. Using the audio spectrum thus obtained, and a program developed to calculate AI, the AI can be determined for each set of interference conditions. The AI can then be referenced to the RF input through the power transfer curve.

Selected runs from the computer model were compared with the measured data. The results of these comparisons are depicted in Figures 4-23 through 4-36.

Figures 4-23 through 4-29 and 4-30 through 4-33 show the AM degradation curves, AI versus $(S/I)_{RF}$, for non chirped and chirped rectangular pulse interference, respectively. The curves compare quite favorably for both the chirped and non-chirped pulses with an average difference less than 3 dB in the linear region of the curve.

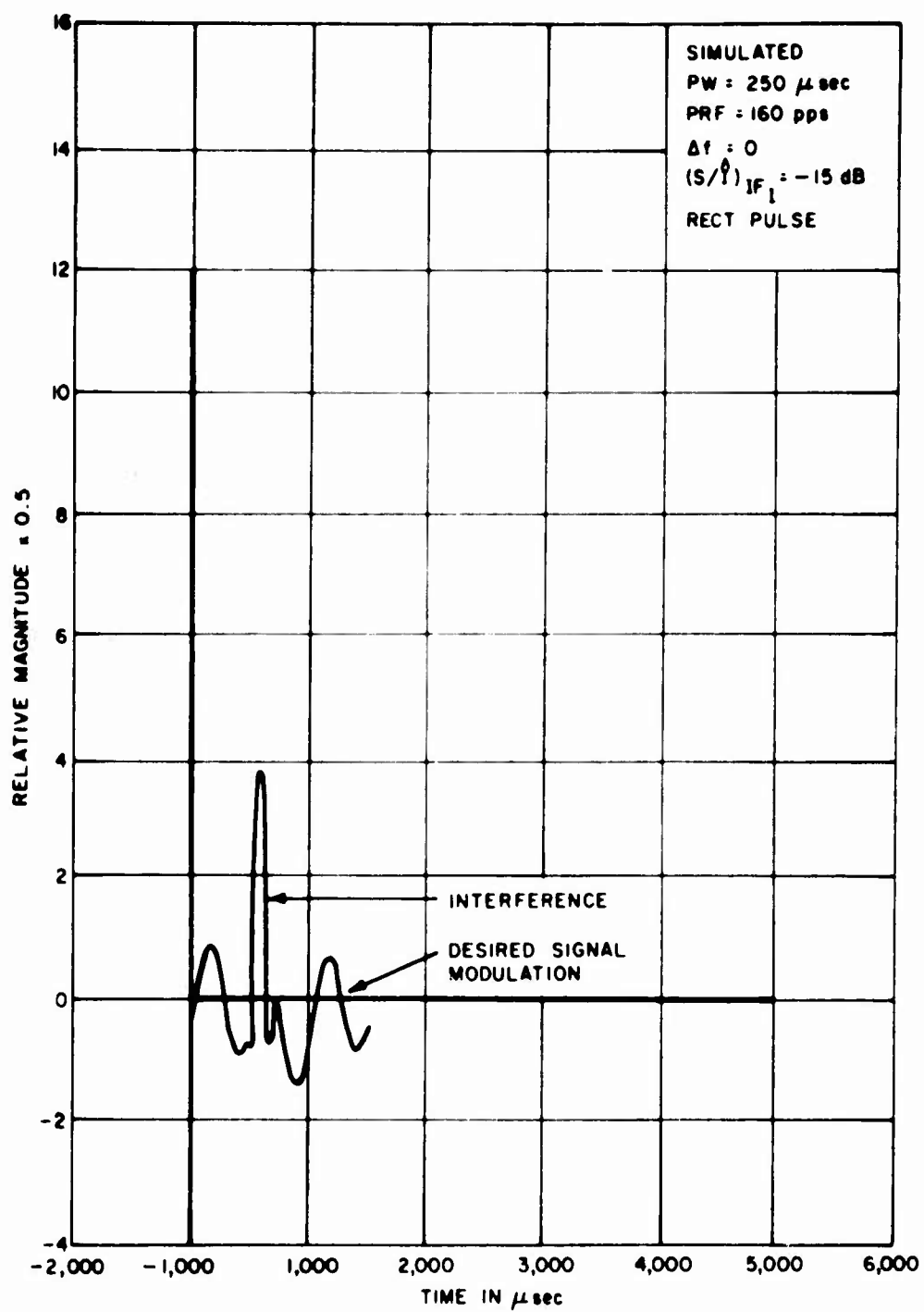


Figure 4-21a. Simulated Audio Output Time Waveform

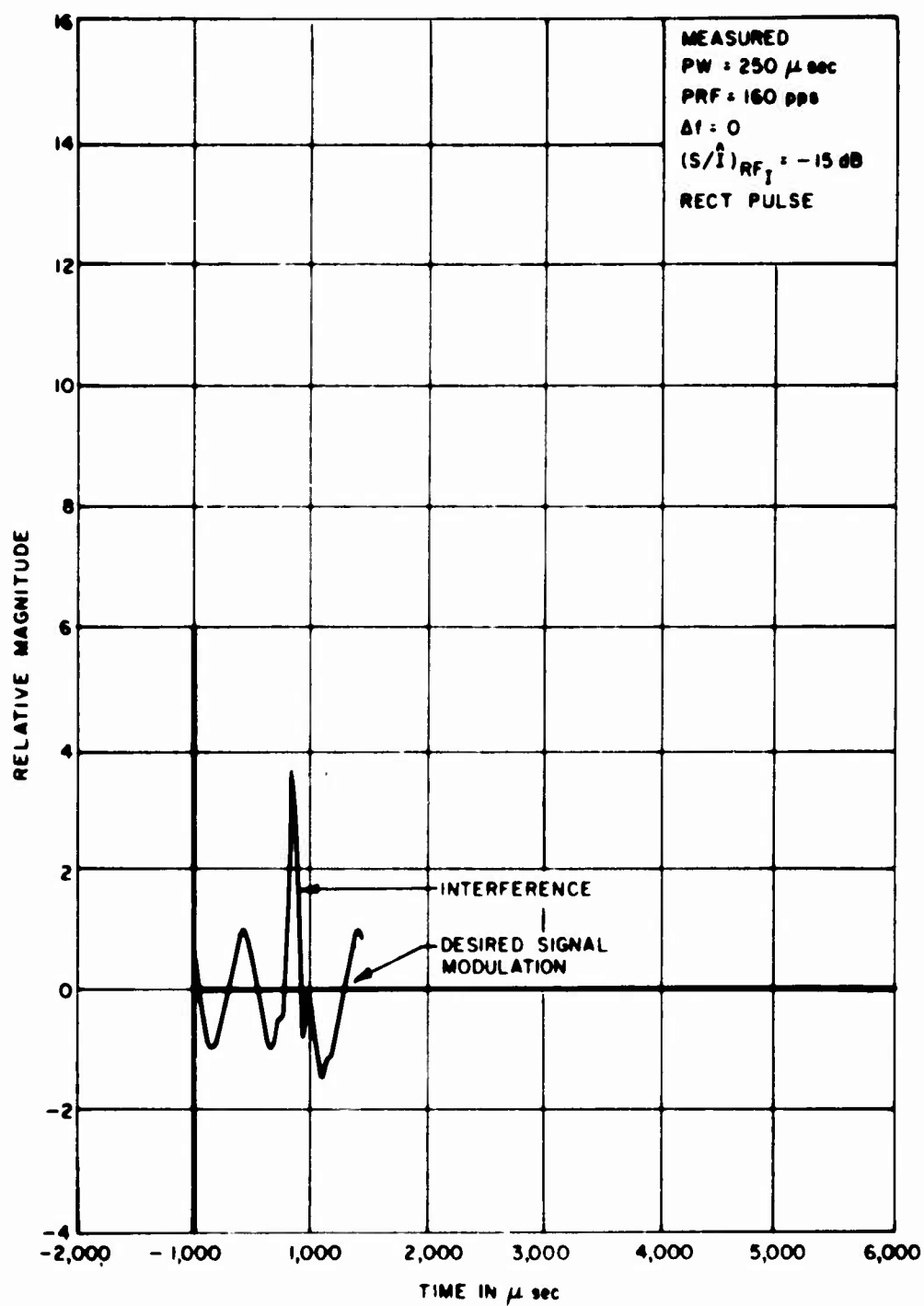


Figure 4-21b. Measured Audio Output Time Waveform

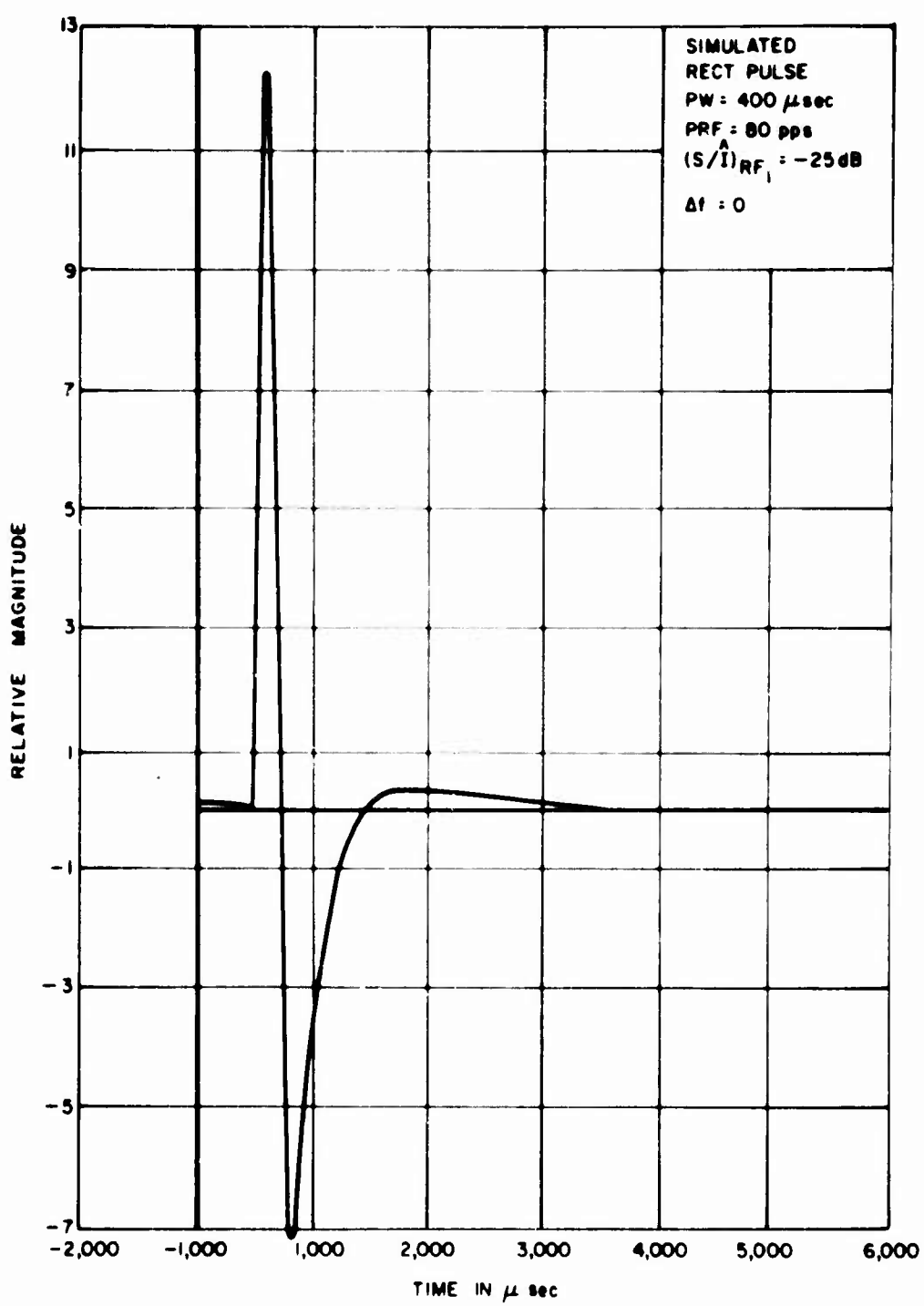


Figure 4-22a. Simulated Audio Output Time Waveform

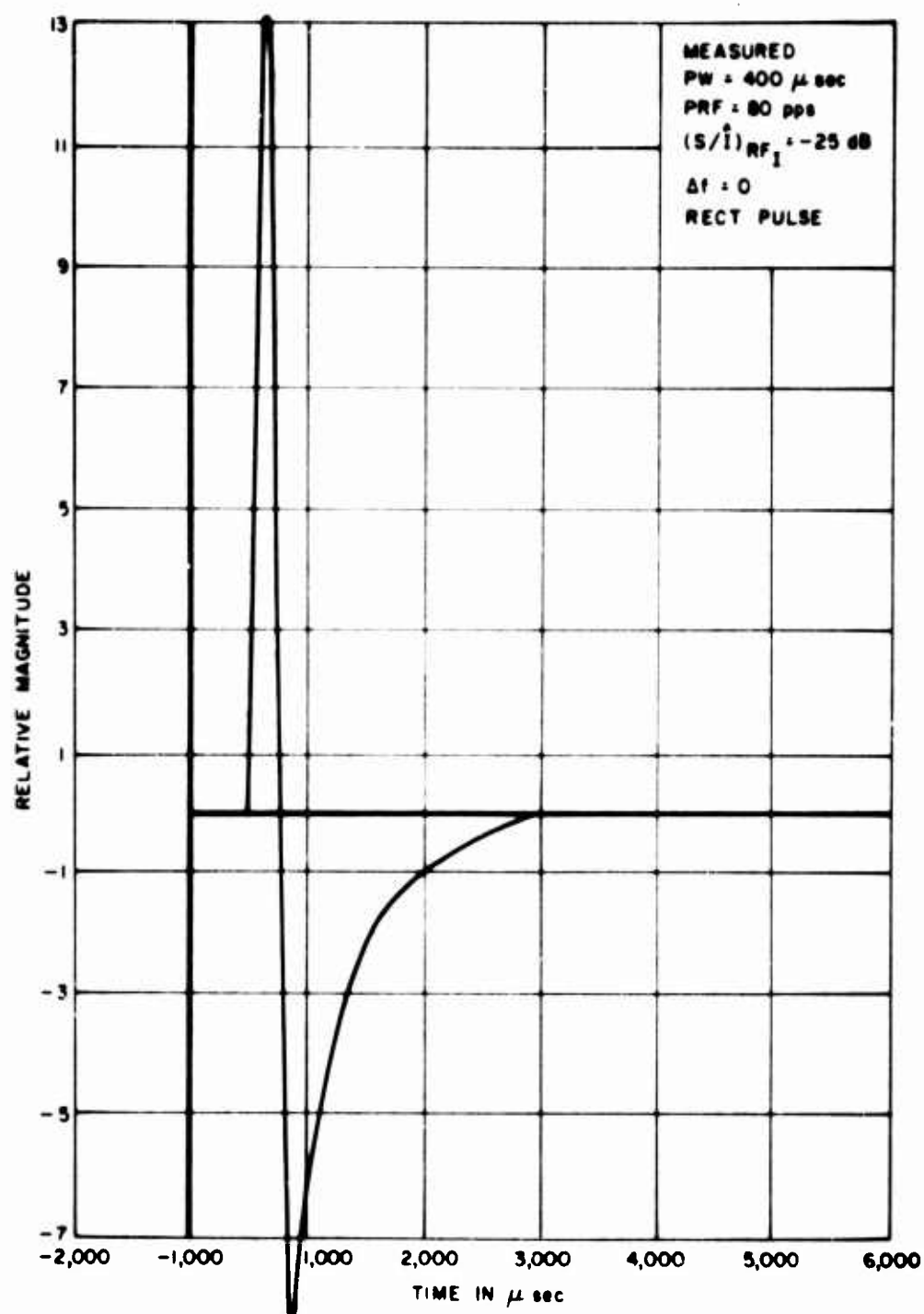


Figure 4-22b. Measured Audio Output Time Waveform

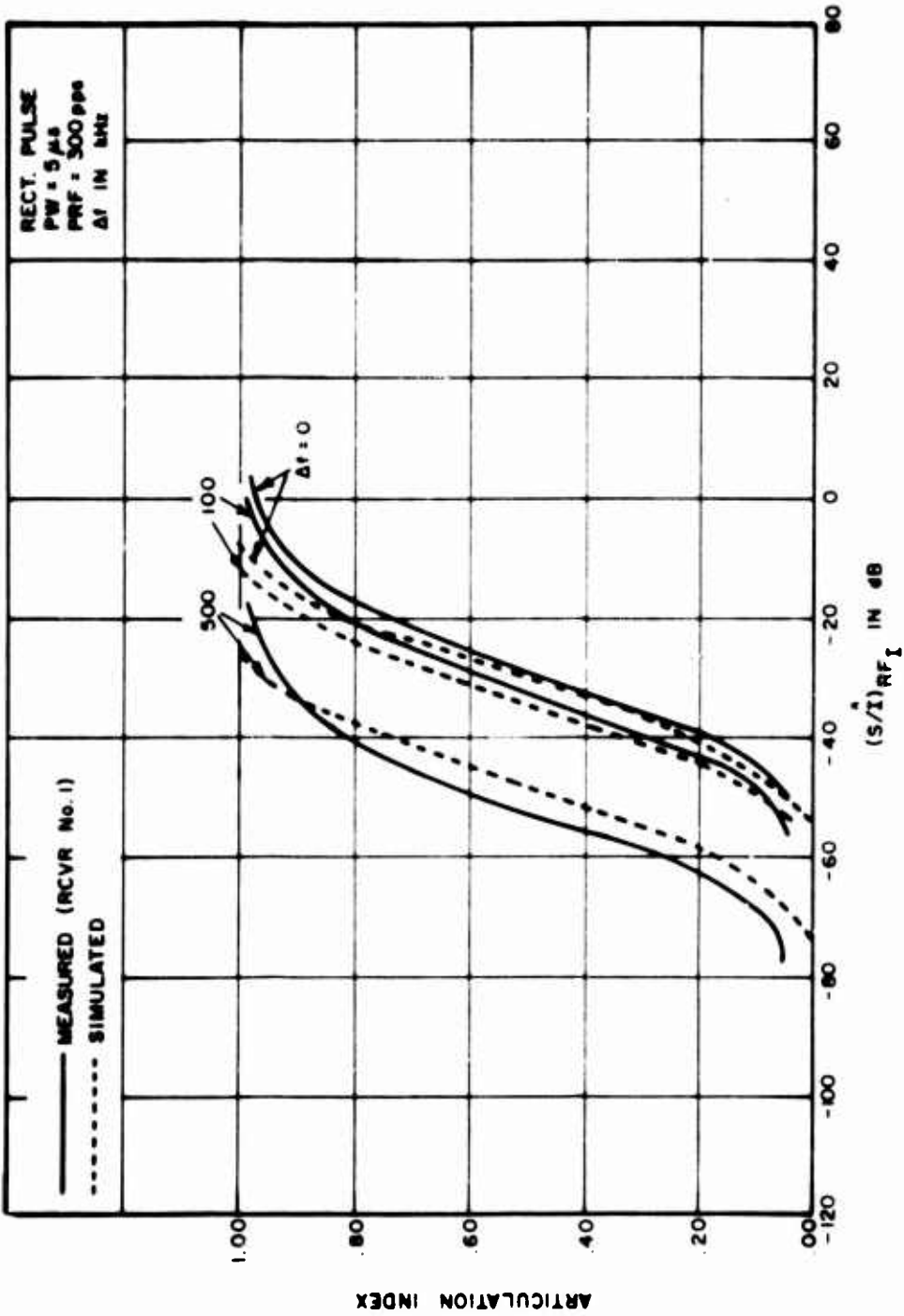


Figure 4-23. Articulation Index for Pulsed Interference to an AM Receiver

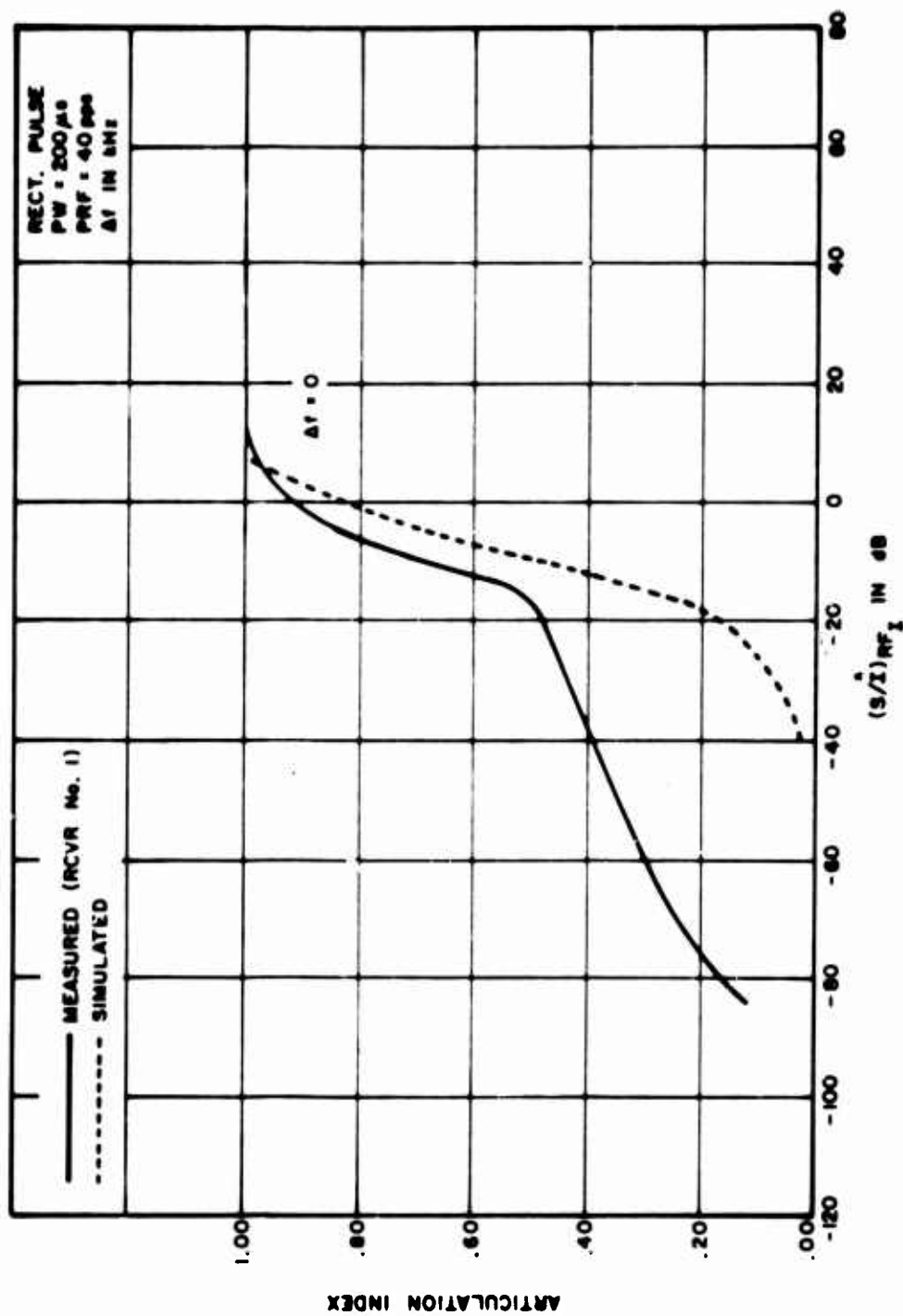


Figure 4 24. Articulation Index for Pulsed Interference to an AM Receiver

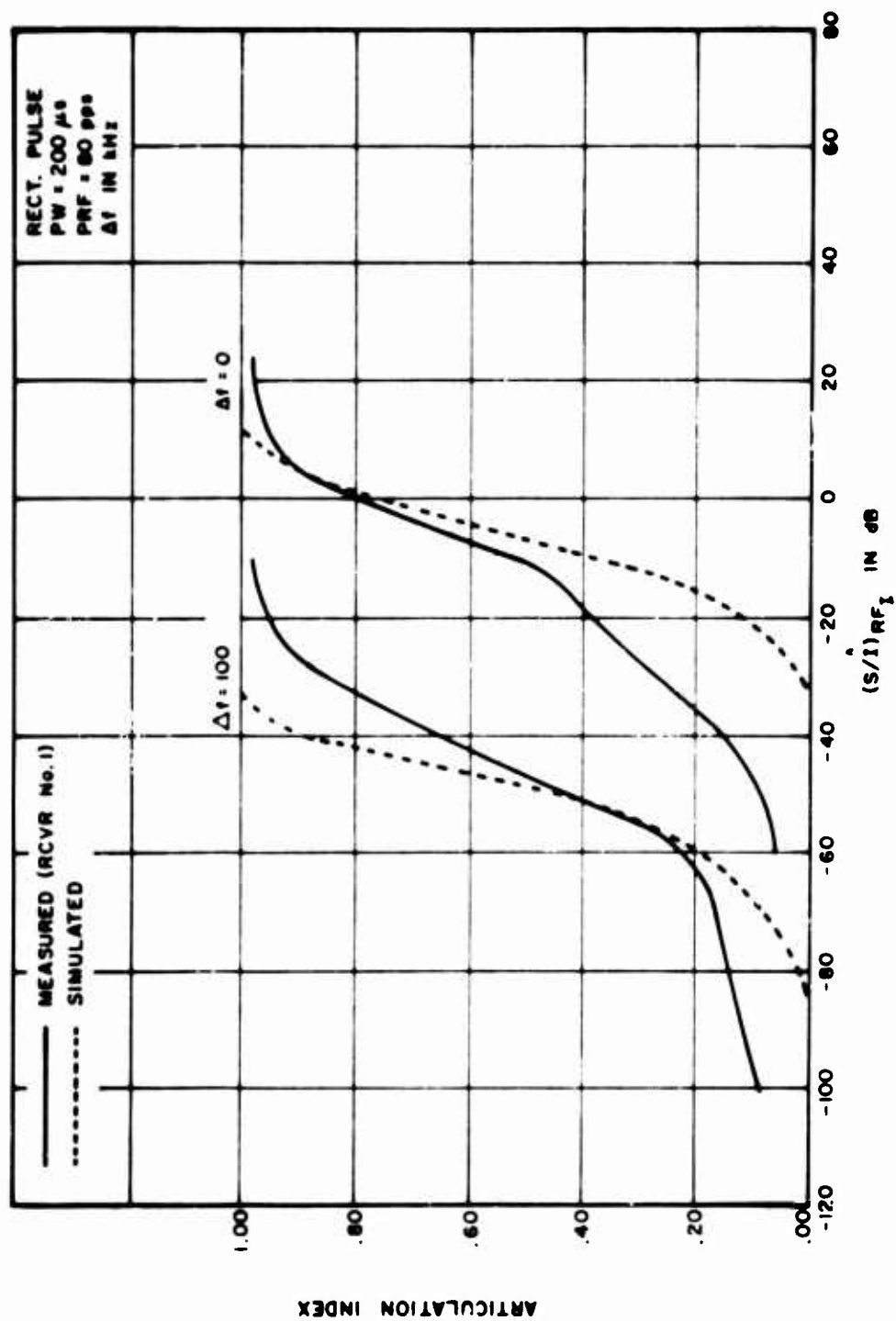


Figure 4-25. Articulation Index for Pulsed Interference to an AM Receiver

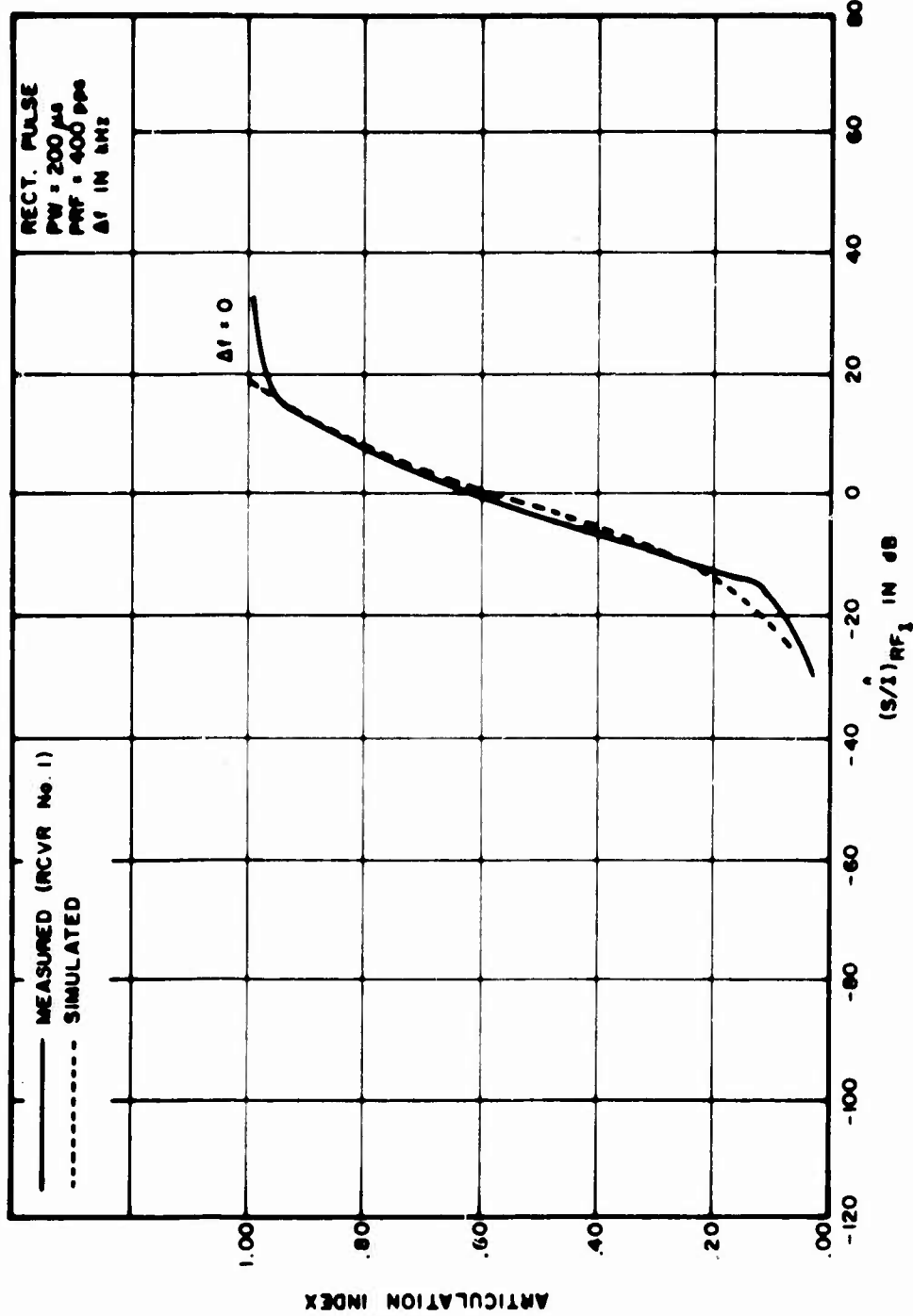


Figure 4.26. Articulation Index for Pulsed Interference to an AM Receiver

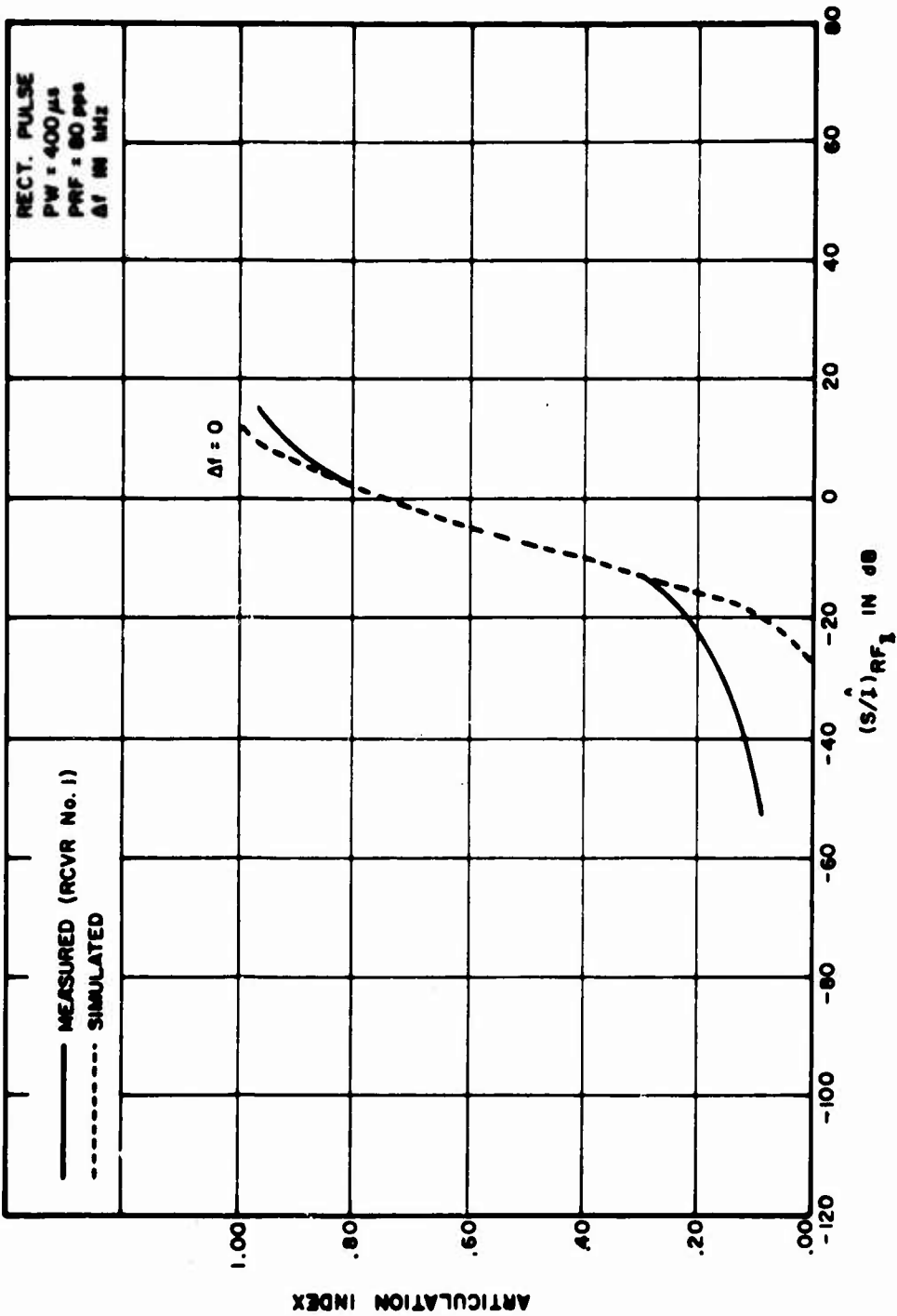


Figure 4-27. Articulation Index for Pulsed Interference to an AM Receiver

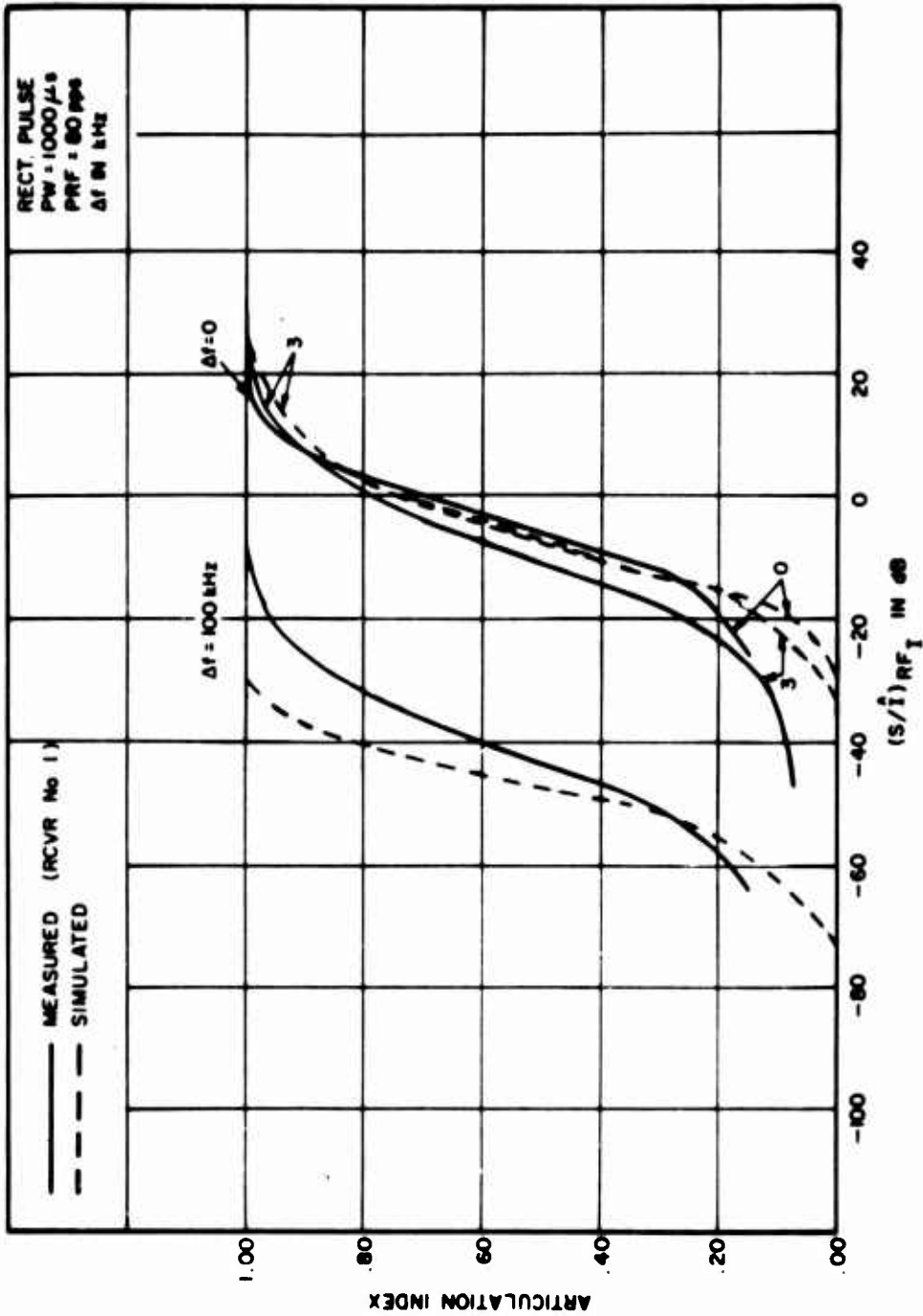


Figure 4-28. Articulation Index for Pulsed Interference to an AM Receiver

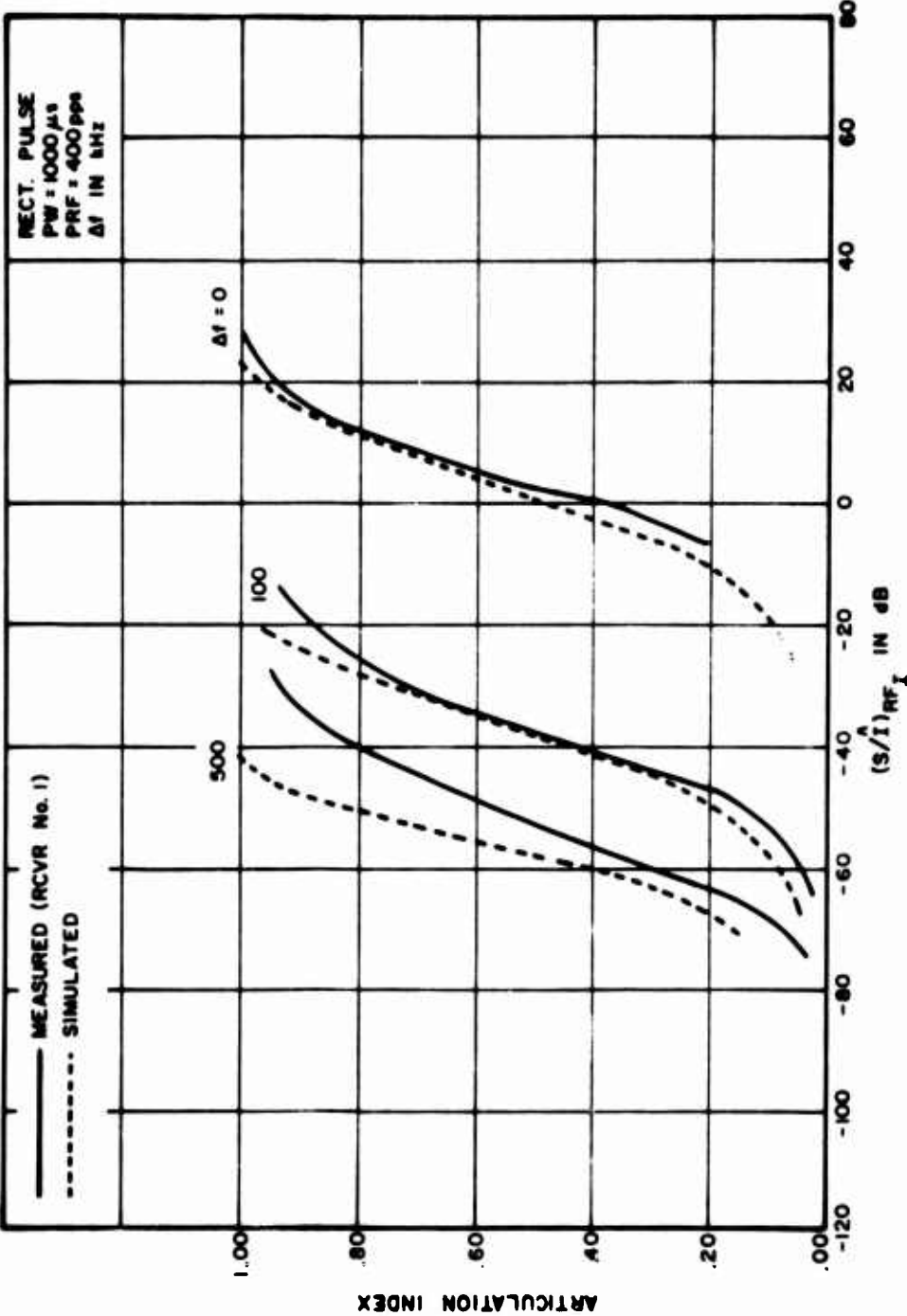


Figure 4-29. Articulation Index for Pulsed Interference to an AM Receiver

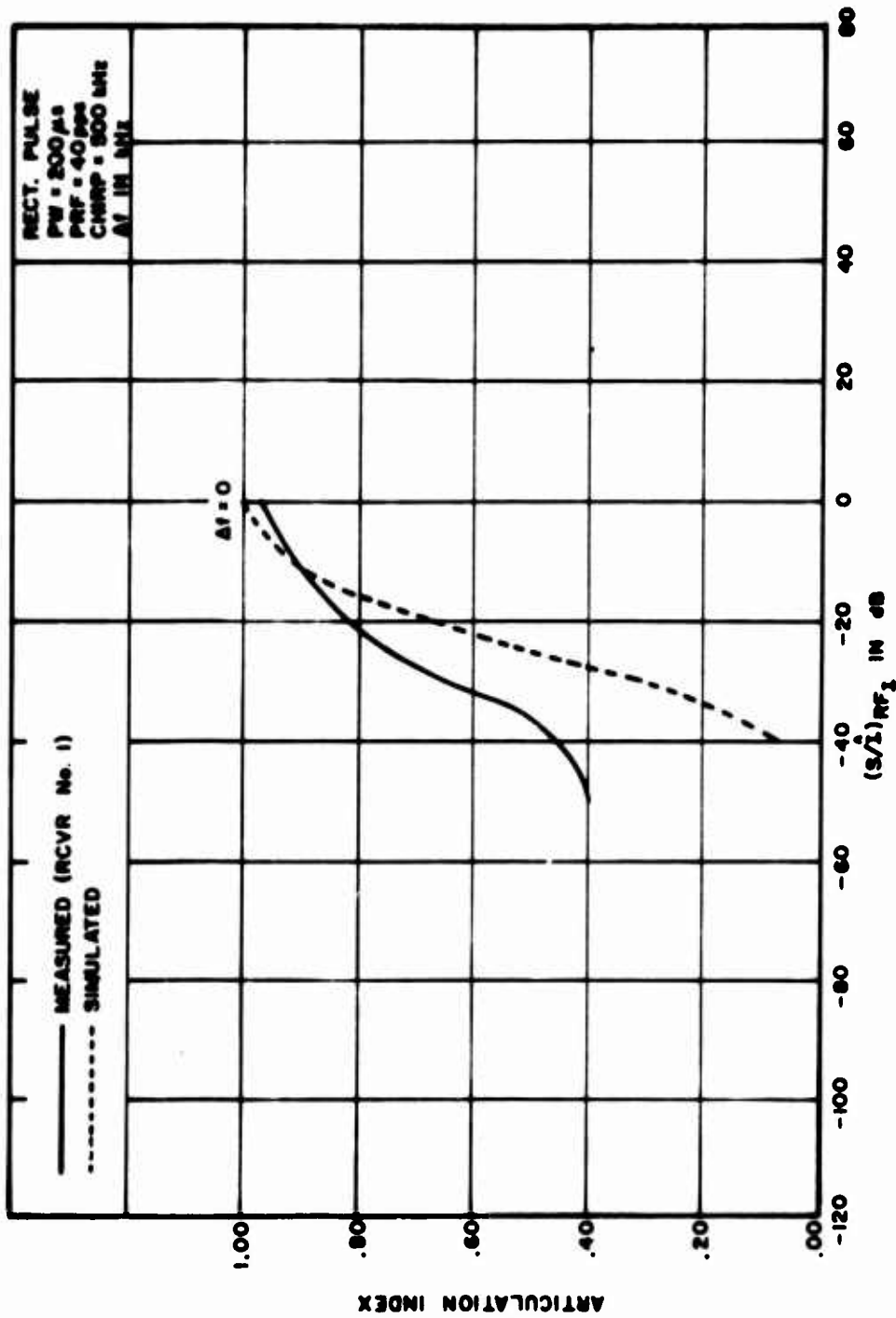


Figure 4-30. Articulation Index for Pulsed interference to an AM Receiver

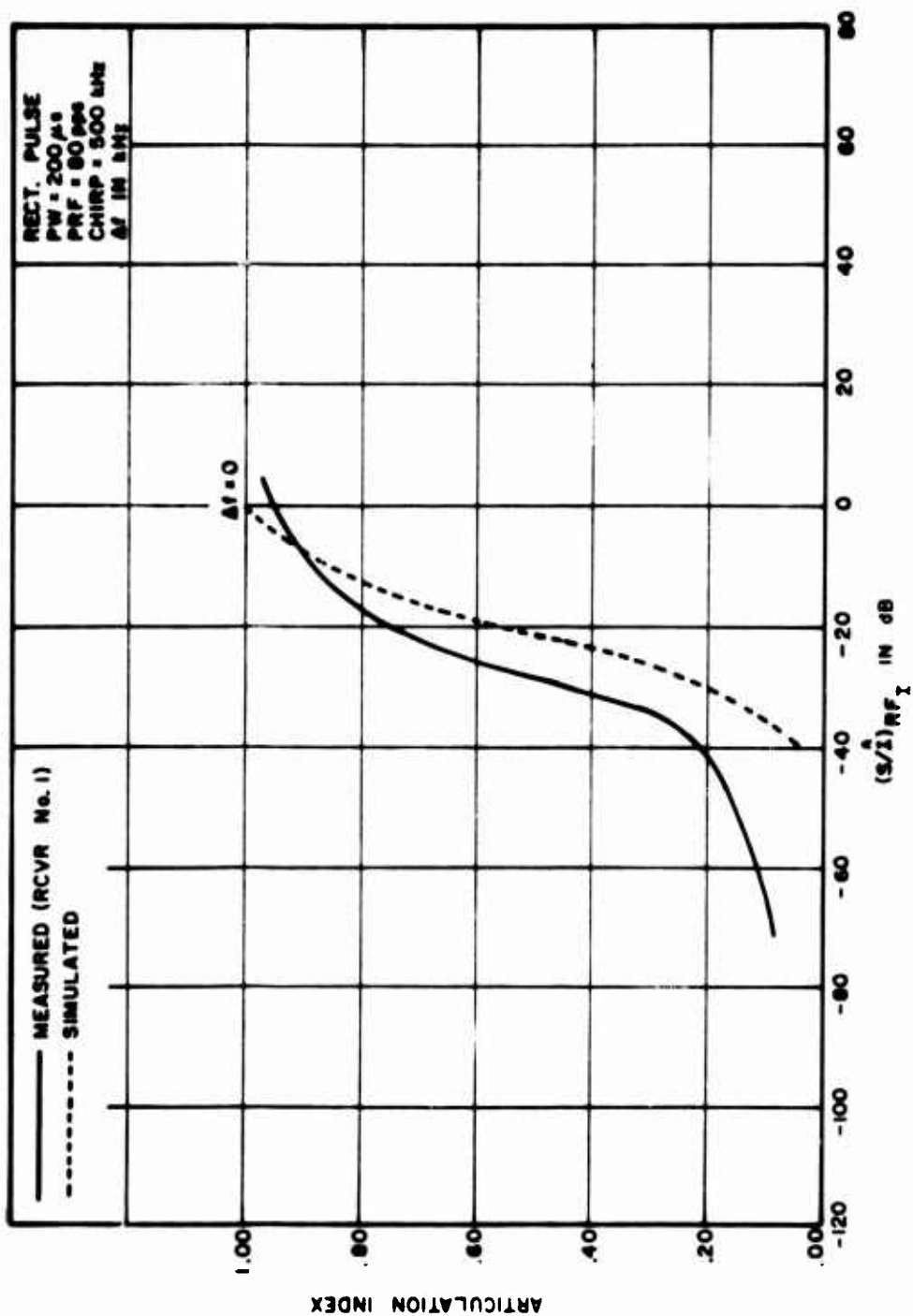


Figure 4-31. Articulation Index for Pulsed Interference to an AM Receiver

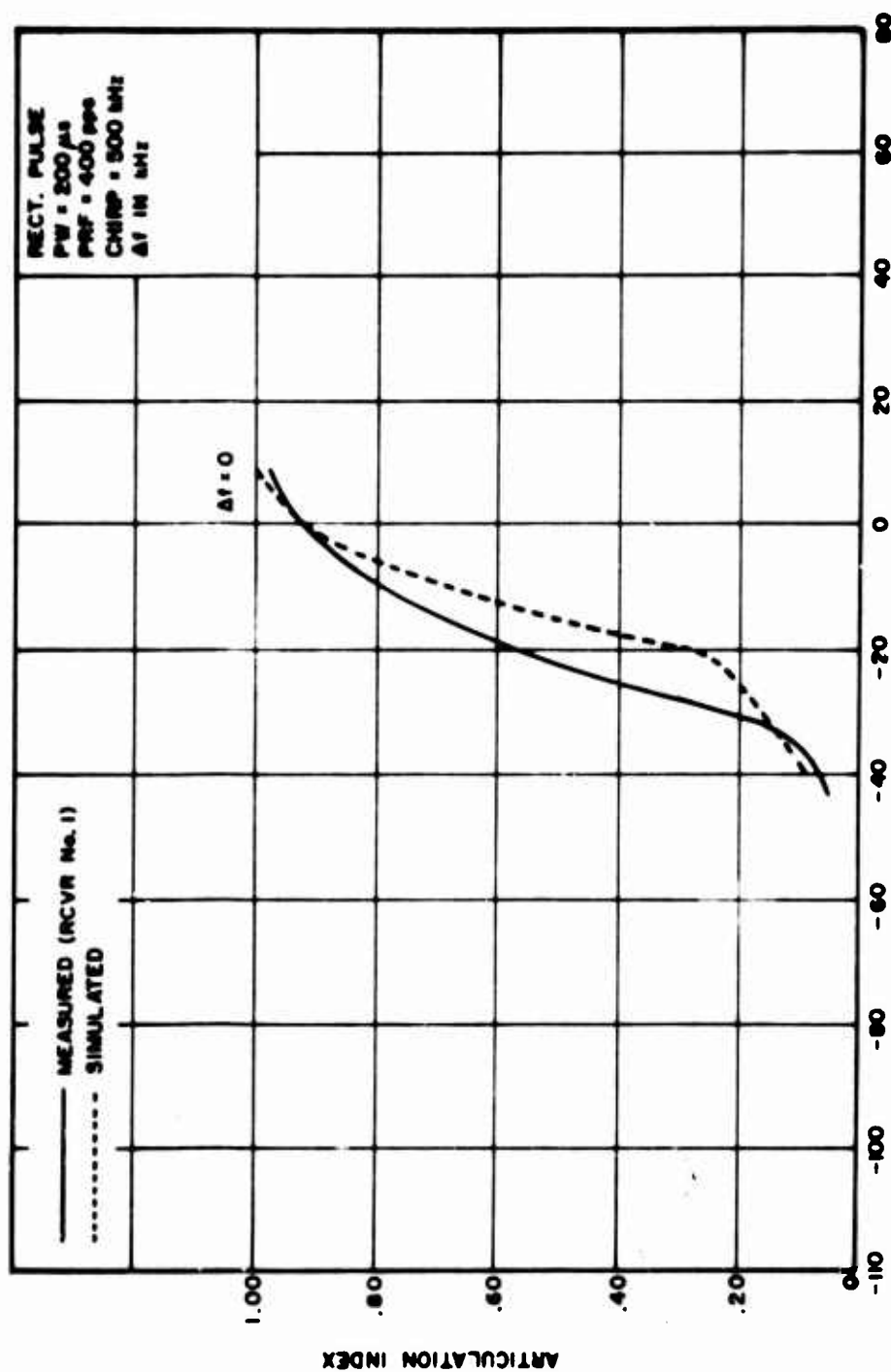


Figure 4-32. Articulation Index for Pulsed Interference to an AM Receiver

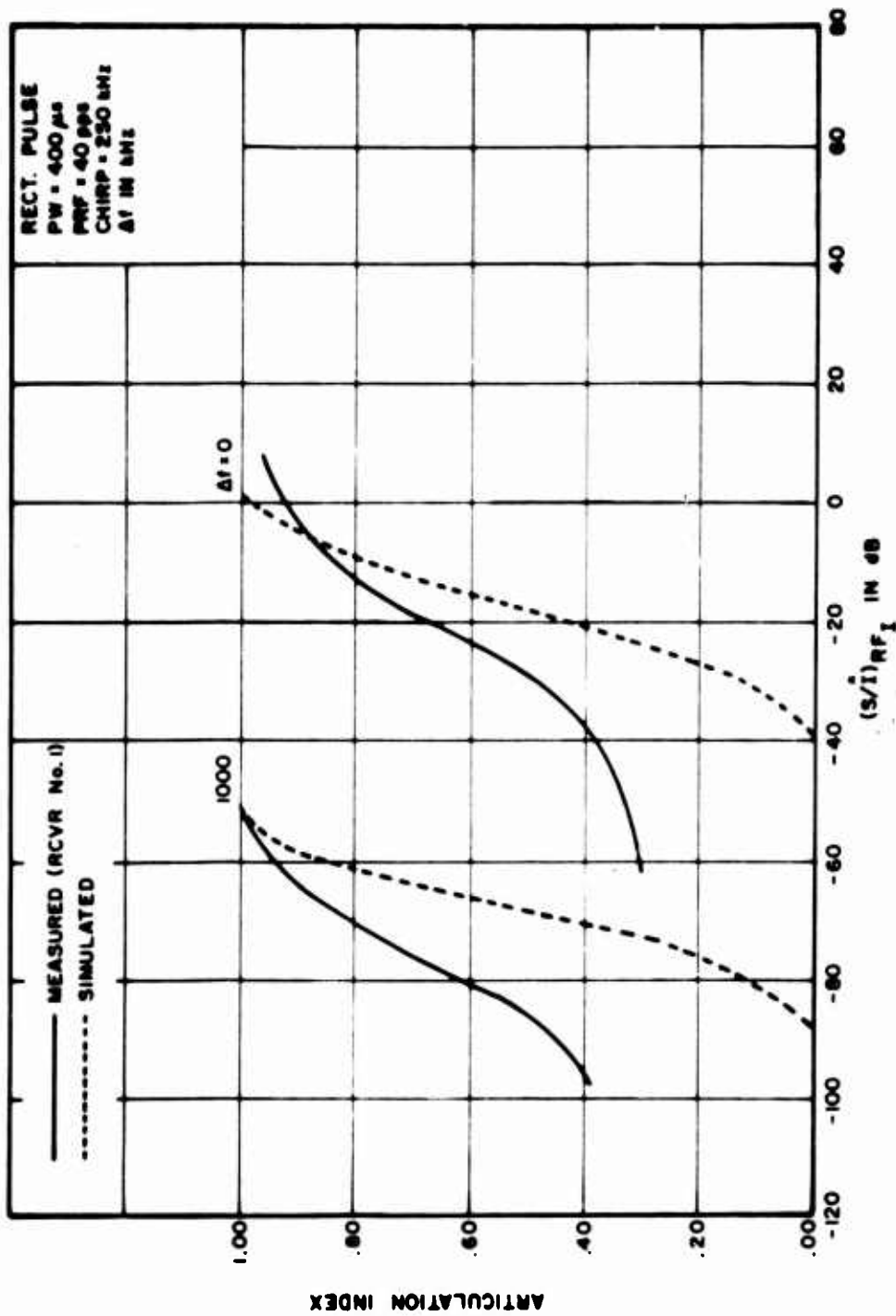


Figure 4.33. Articulation Index for Pulsed Interference to an AM Receiver

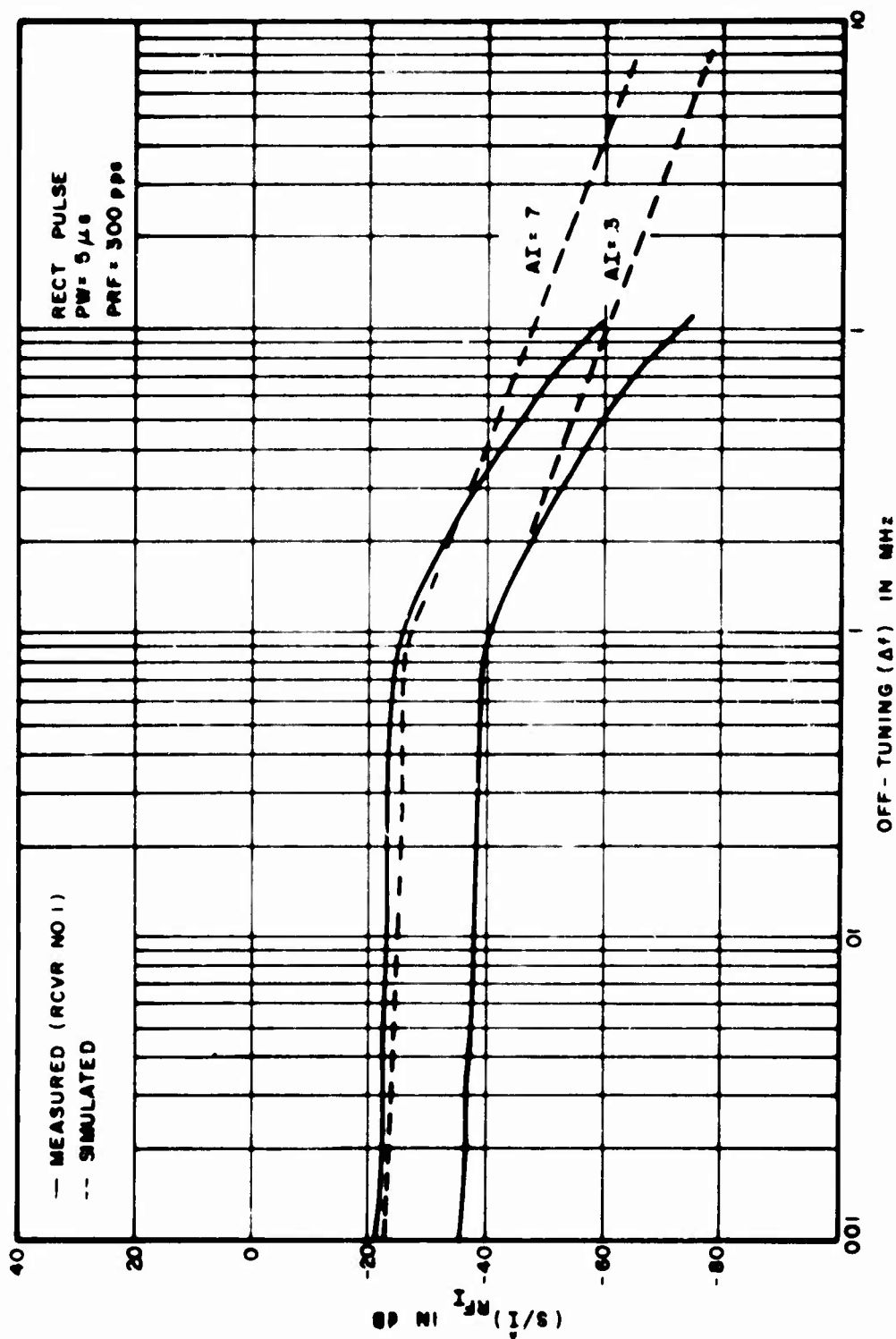


Figure 4-34. Input Signal to Peak Interference as a Function of Δf

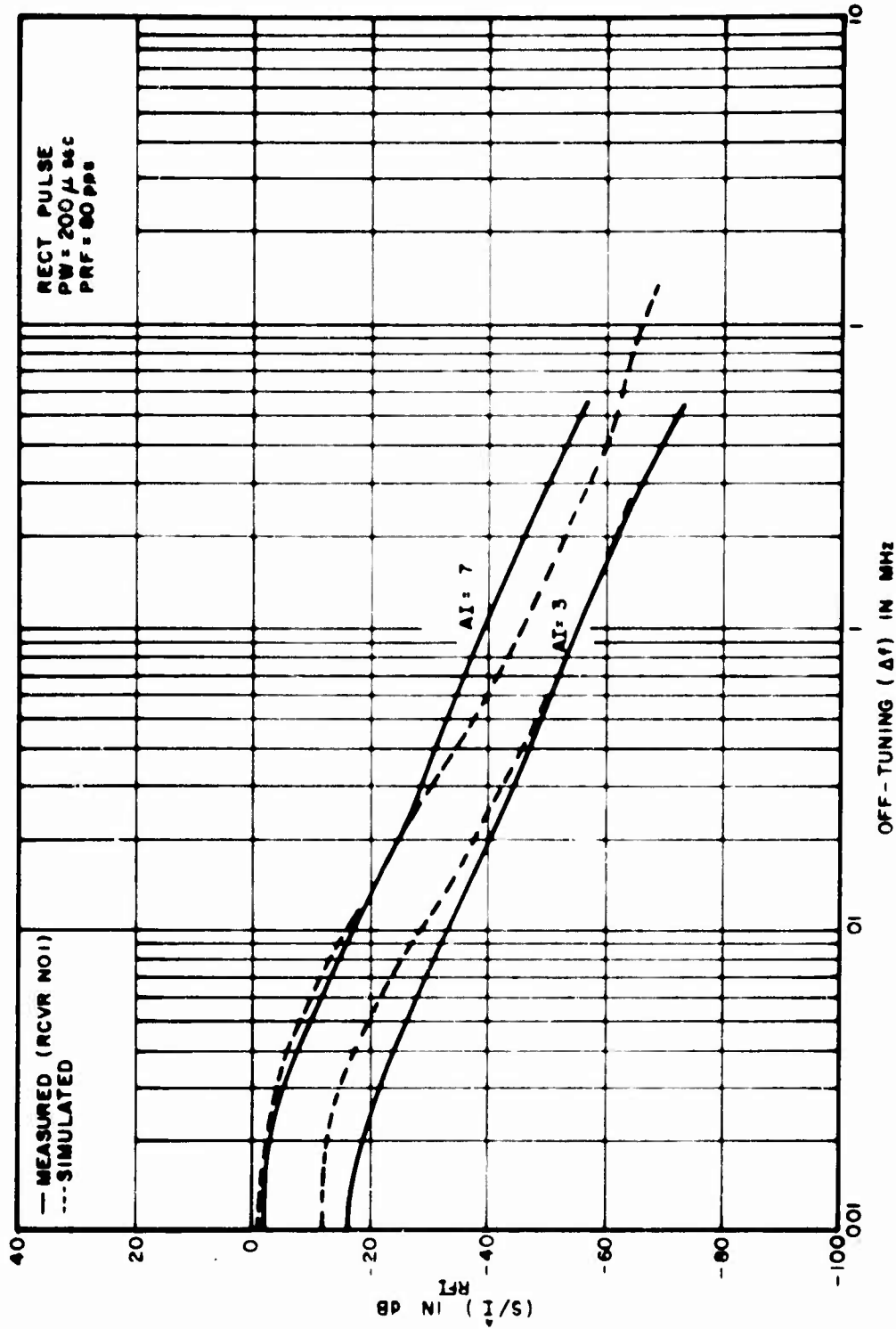


Figure 4.35. Input Signal to Peak Interference as a Function of Δf

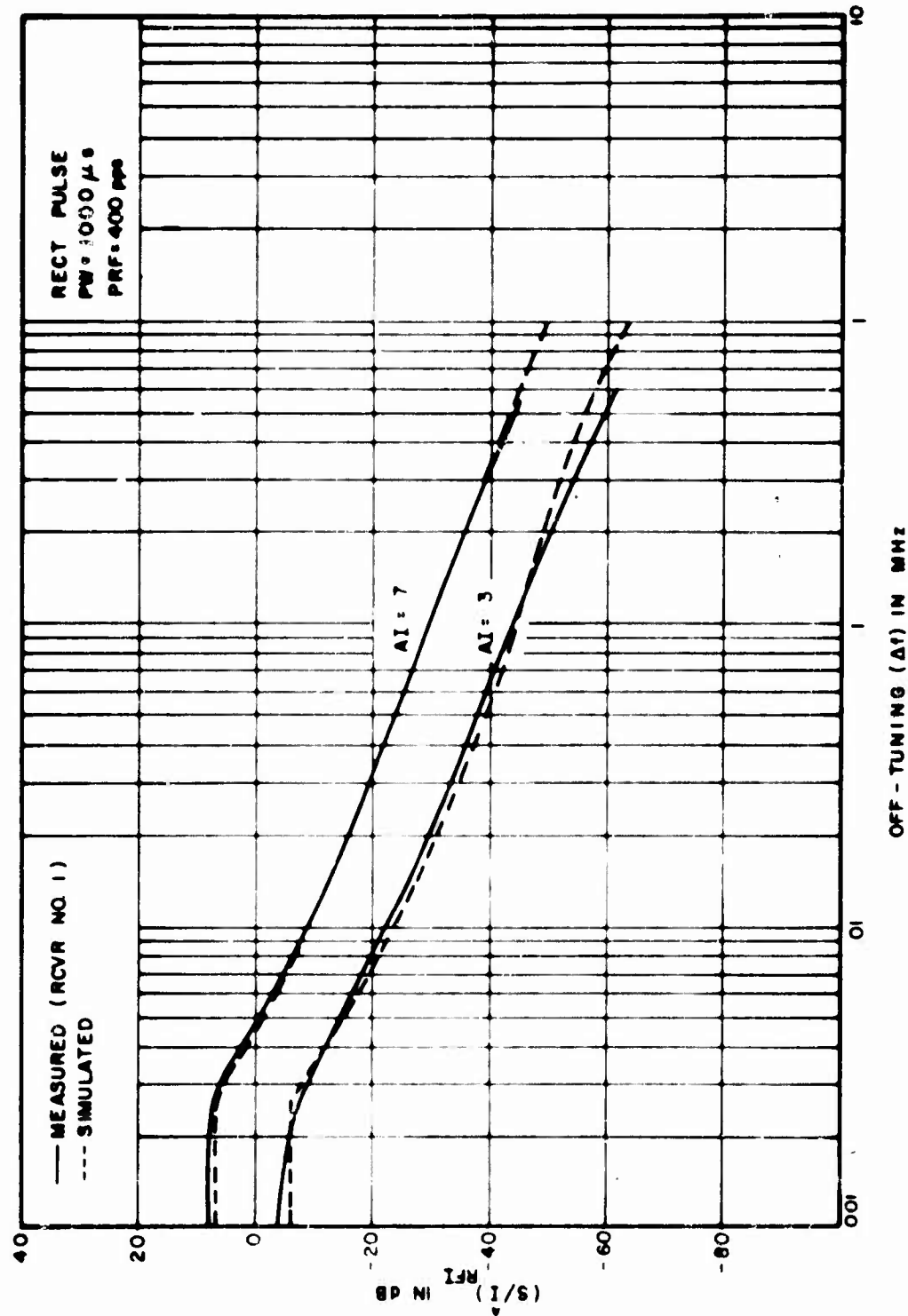


Figure 4-36. Input Signal to Peak Interference as a Function of Δf

The largest discrepancies occur for low PRF's, less than 80 pps, and an input (S/I) ratio in the receiver passband of -15 dB or less. As previously explained, the low PRF's do not affect the DC level of the AGC, thus causing the receiver to saturate. The computer program is unable to account for this nonlinearity and therefore discrepancies can be expected when this phenomenon occurs. This is further discussed in Section 6 under AGC effects.

A further comparison was made between the measured and computed data as shown in Figures 4-34 through 4-36. The curves are plots of the input (S/I) ratio versus off-tuning (Δf) for constant AI values of .7 and .3. The computed and measured data again compare quite favorably.

The general conclusion that can be drawn from the above comparison is that, within the linear operating region of the receiver, the computer model calculates the performance of an AM voice system subjected to pulsed interference from the on-tune case to the far adjacent channel case. The pulse simulation model will currently generate rectangular, trapezoidal, and chirped pulses for a wide range of pulse widths and pulse repetition frequencies. The model can be modified to handle any pulsed interference that can be expressed mathematically in either the time or frequency domain, providing the storage capacity of the computer is not exceeded.

The model will calculate output performance measures for any level of input interference or input signal-to-peak interference ratios. However, the results must generally be limited to approximately $+30$ dBm of peak interfering power or signal-to-peak interference ratios of approximately -100 dB. For all but a few special cosine type problems, this is not a limitation as the complete range required for interference analysis has been covered. For those cases in which a higher interference level is desired, tables of burn out levels should be considered and not degradation criteria.

SECTION 5

DESCRIPTION OF MEASUREMENTS

GENERAL

A number of closed system degradation tests were made in order to acquire the performance degradation data necessary for the AM receiver analysis investigation.

AM degradation measurements for chirped and nonchirped rectangular pulsed interference of various pulse widths, PRF's and off tuning (Δf) were obtained. Articulation Index (AI) and Articulation Score (AS) were used as the primary receiver output degradation measures. The AI was obtained using the Voice Interference Analysis System (VIAS) (APPENDIX IV). The AS was obtained by subjecting a group of listeners to a preselected group of words corrupted by a specific type of interference. The result of this test, expressed as the percentage of words heard correctly, is referred to as the Articulation Score. The word groups used in the tests were the Harvard phonetically balanced (PB) words as recommended by the American Standards Association for Articulation testing (reference 19). The master PB word tapes used as modulation sources in the tests were prepared by Bell Aerosystems Company and are used at their system scoring facility in Tucson, Arizona (reference 20).

The minimum interference threshold (i.e., the level at which interference is first heard), the maximum interference threshold (i.e., the level at which the desired signal could no longer be detected), and various AI and AS levels between these thresholds were obtained as a function of the following

1. RF input signal to peak interference power ratio, $(S/I)_{RF}$.
2. Audio output RMS signal to-RMS noise plus distortion plus interference power ratio, $[S/(N+D+I)]_O$.
3. Audio output RMS signal to-noise plus distortion plus interference peak-to-peak power ratio, $[S/(N+D+I)_{p-p}]_O$.

The $(S/I)_{RF}$ values were calculated from the RMS power level of the desired signal and the RMS peak power level of the interfering pulse.

In addition to the degradation data, MIL-STD-449 () (reference 10) type measurements of receiver RF, IF, and audio selectivity, and dynamic range were obtained. Photographs were also taken showing the audio interference output time waveform of the victim receiver.

The MIL-STD-449 () (reference 10) measurements along with the AI scores were reported as Phase I measurements. The AS scoring and additional data were reported as Phase II measurements due to the additional time required to subjectively obtain the AS scores.

The AM degradation tests were conducted on two typical narrowband AM voice receivers. These are designated RCVR NO. 1 and RCVR NO. 2. Measurements were also made on two different serial numbers of Receiver No. 1. These measurements are designated by M-1 and M-2. Figures 5-1 and 5-2 show the block diagrams of these two receivers. The main difference between the two test receivers is the IF bandwidth. The No. 1 receiver has an IF bandwidth of 8 kHz while the No. 2 receiver has an 85 kHz bandwidth. These bandwidths are typical of those encountered in AM receivers. Both receivers have an audio limiter and an audio bandwidth of approximately 3 kHz. The measurements on the No. 2 receiver were made with the limiter on, while the measurements on the No. 1 receiver were made with the limiter off. A plot of the RF, IF and audio selectivity for the No. 1 receiver obtained from the Phase I measurements is shown in Figures 5-3, 5-4 and 5-5, respectively. A plot of the RF and IF selectivity for the No. 2 receiver is shown in Figures 5-6 and 5-7, respectively. The dynamic range curves for both receivers are shown in Figure 5-8.

These measurements were obtained in order to model the functions required in the simulation model. Sections 4 and 6 discuss the overall effect of these elements on receiver performance.

AM RECEIVER TEST PROCEDURE

The set-up used for the AM receiver test link degradation measurements is shown in Figure 5-9. The set-up used for the desired AM transmitter test link is shown in Figure 5-10. The set-ups used for the undesired transmitter test links for non-chirped and chirped rectangular pulsed interference are shown respectively in Figures 5-11 and 5-12.

Balanced mixers were used in the generation of the pulsed signals to ensure the residual carrier was attenuated by 60 dB or more. This was necessary since $(S/I)_{RF}$ levels used in the tests were at least -60 dB with the desired signal level typically being held constant at -79 dBm. If the carrier is not adequately suppressed, the system will be interfered with by the residual carrier level rather than the pulse being tested.

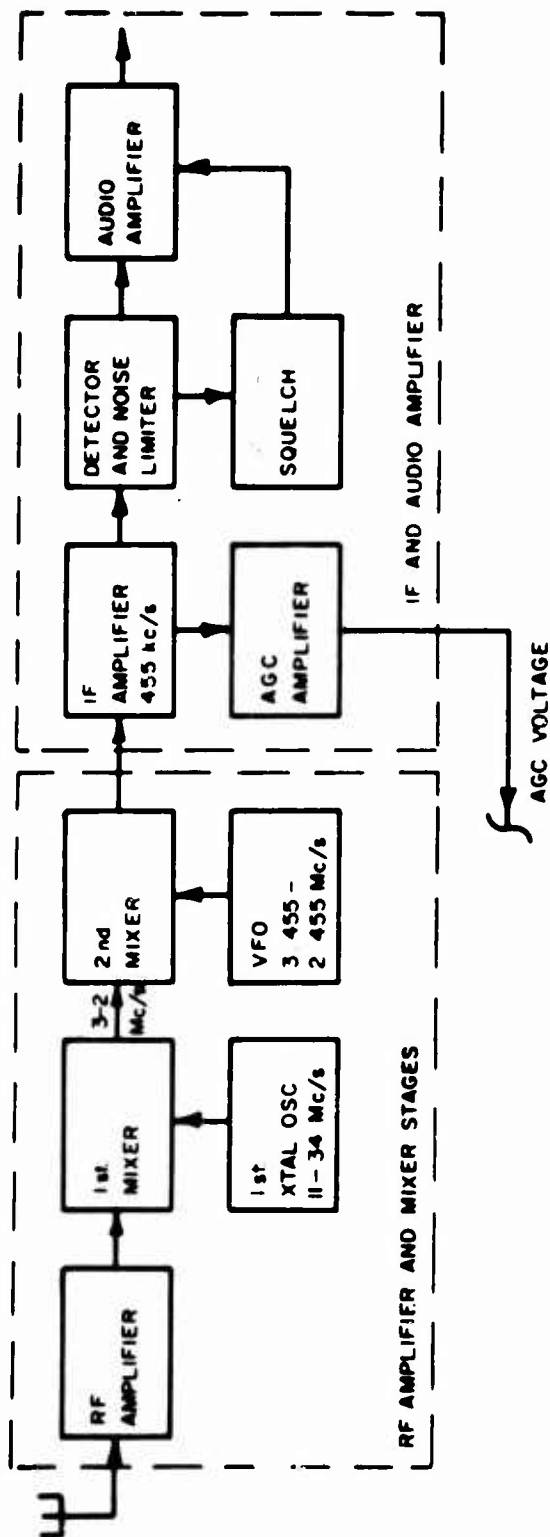


Figure 5-1. Functional Block Diagram of AM Receiver No. 1

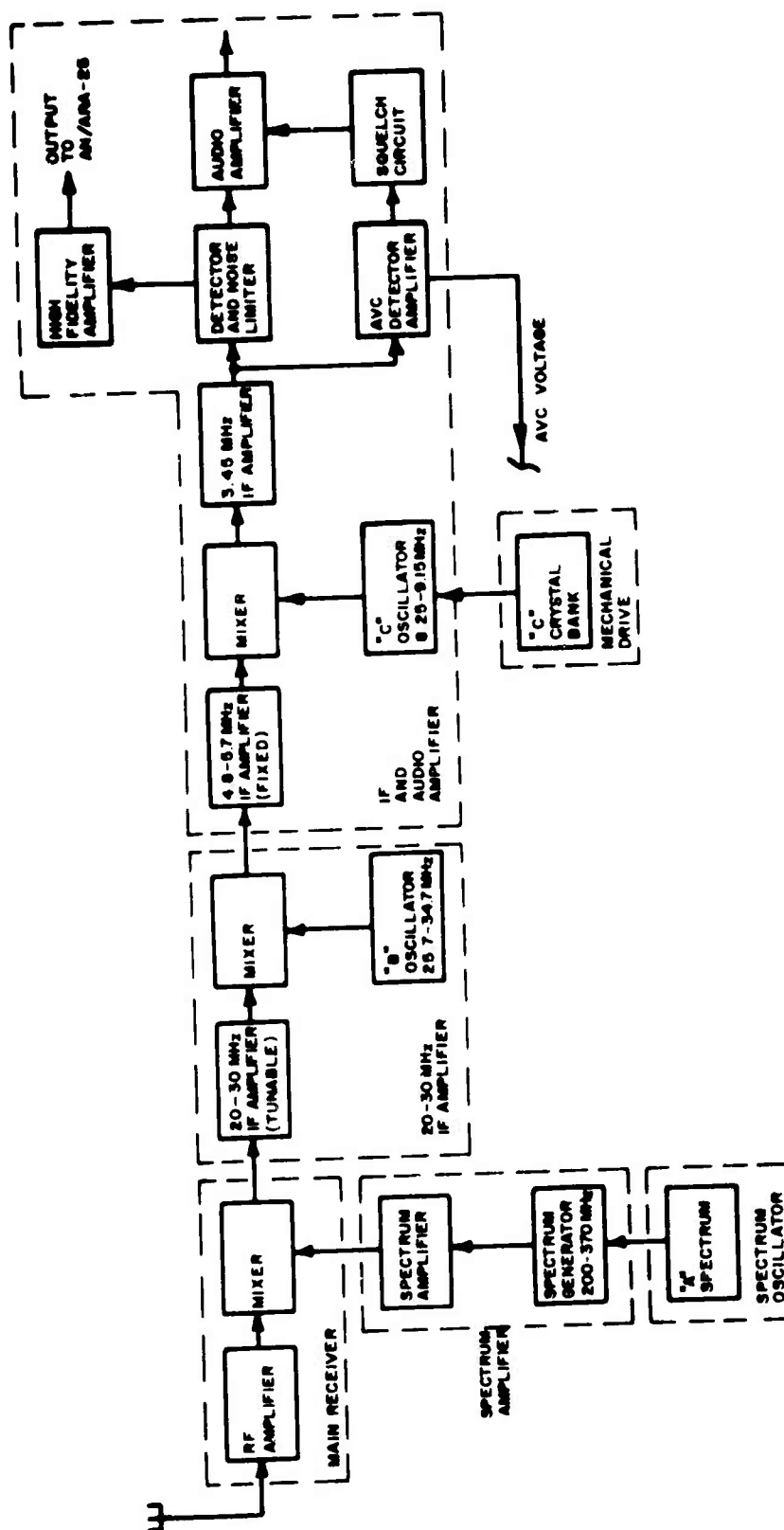


Figure 5-2. Functional Block Diagram of AM Receiver No. 2

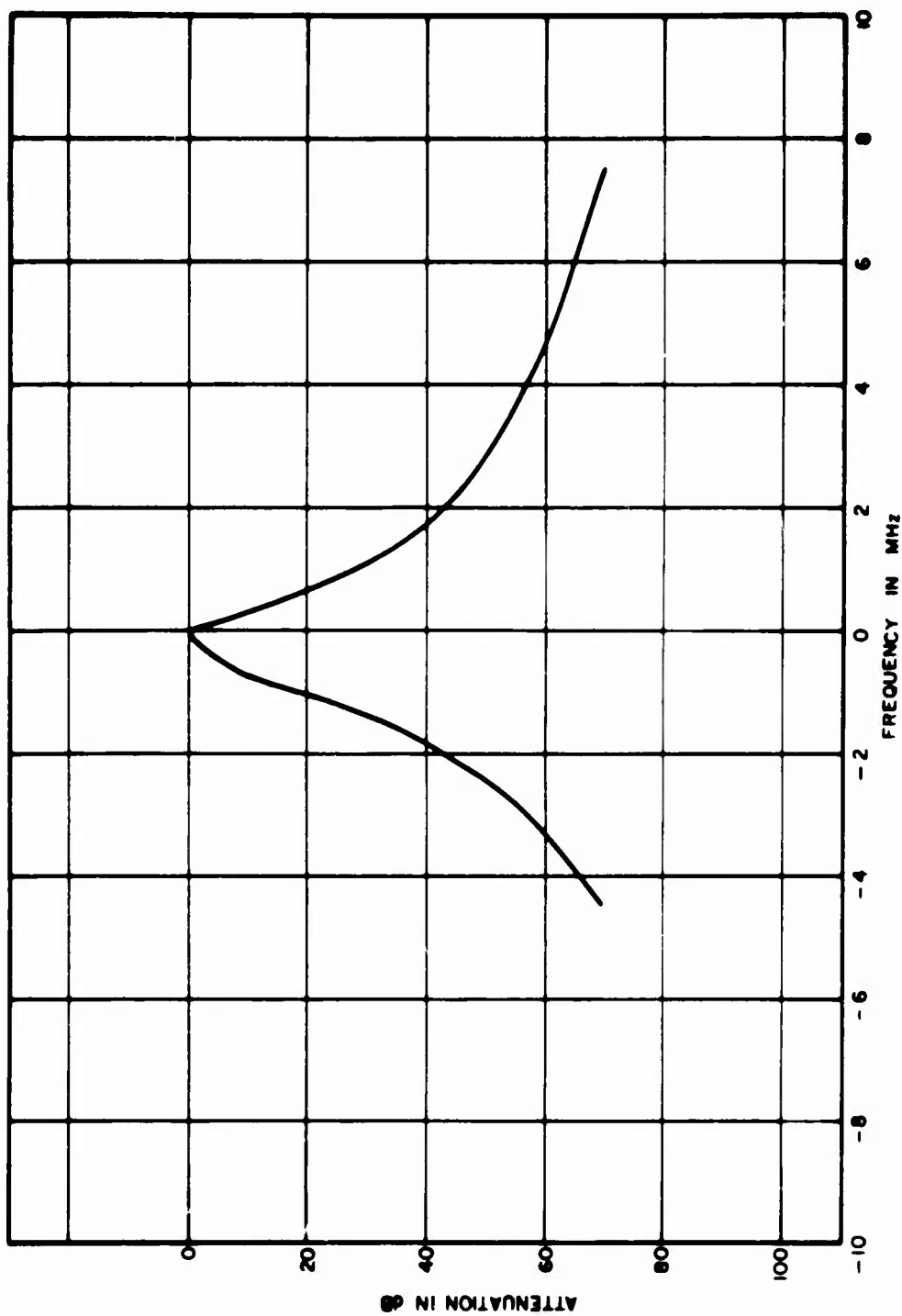


Figure 5-3. RF Selectivity of AM Receiver No. 1

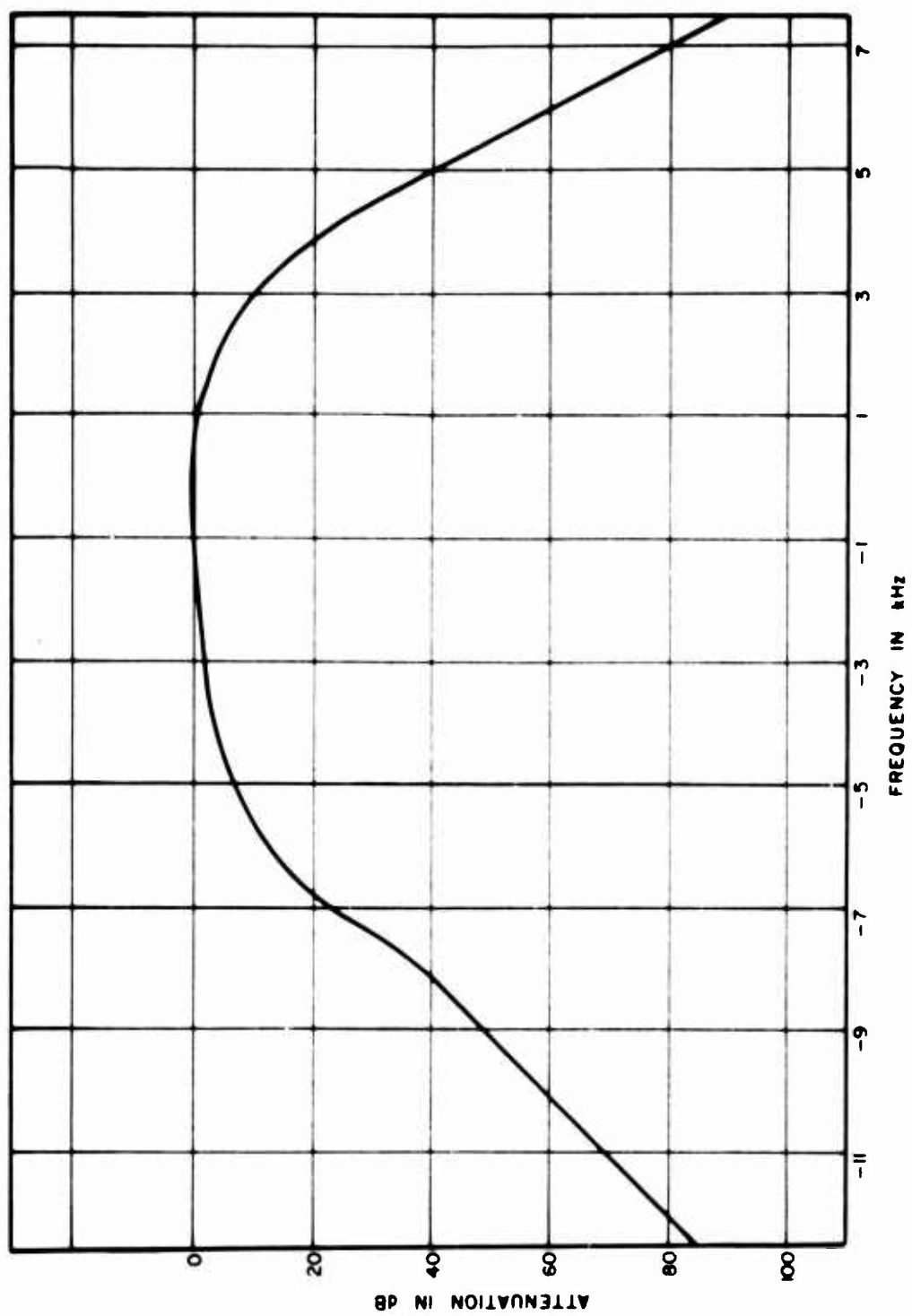


Figure 5-4. IF Selectivity of AM Receiver No. 1

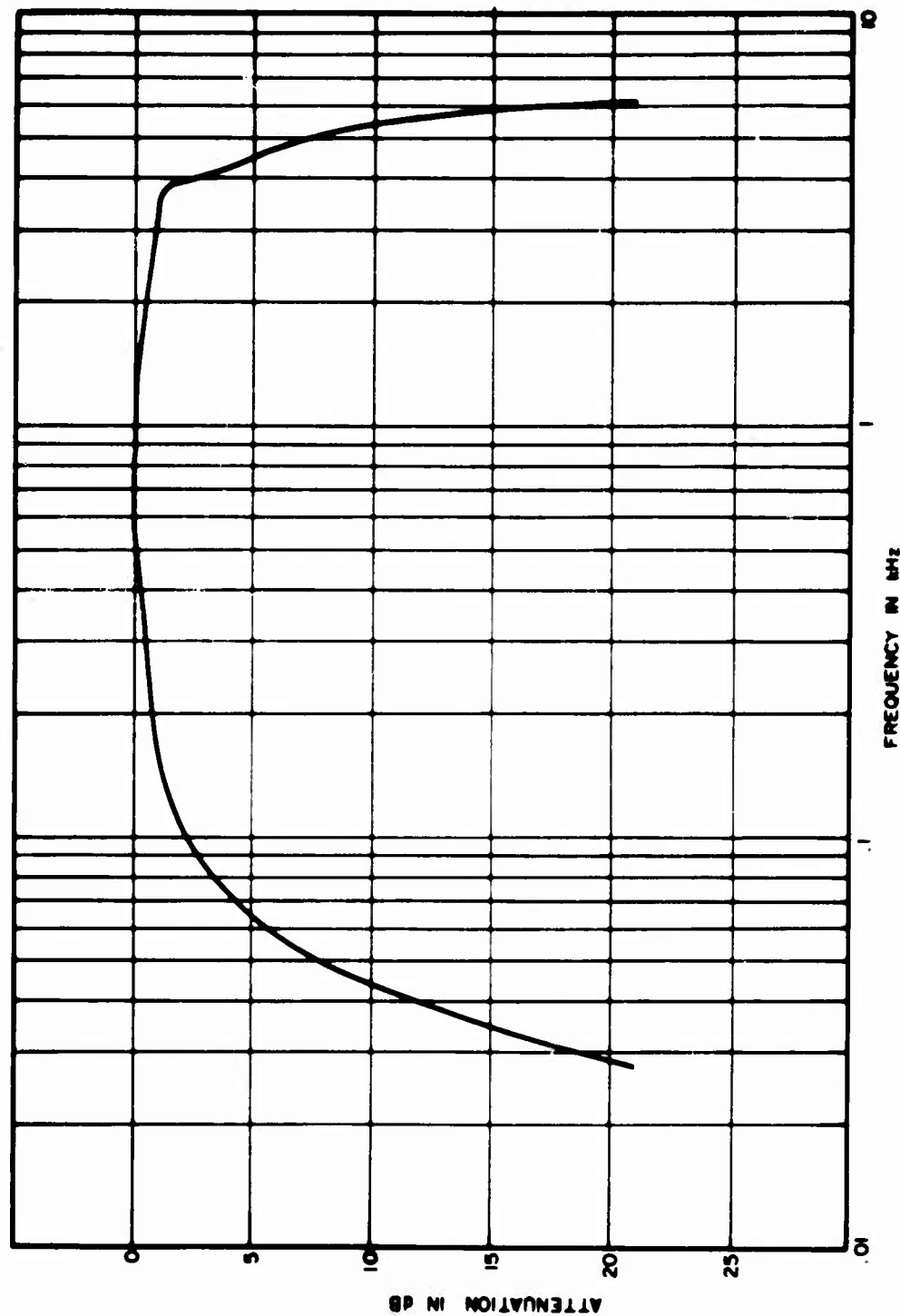


Figure 5-5. Audio Selectivity of AM Receiver No. 1

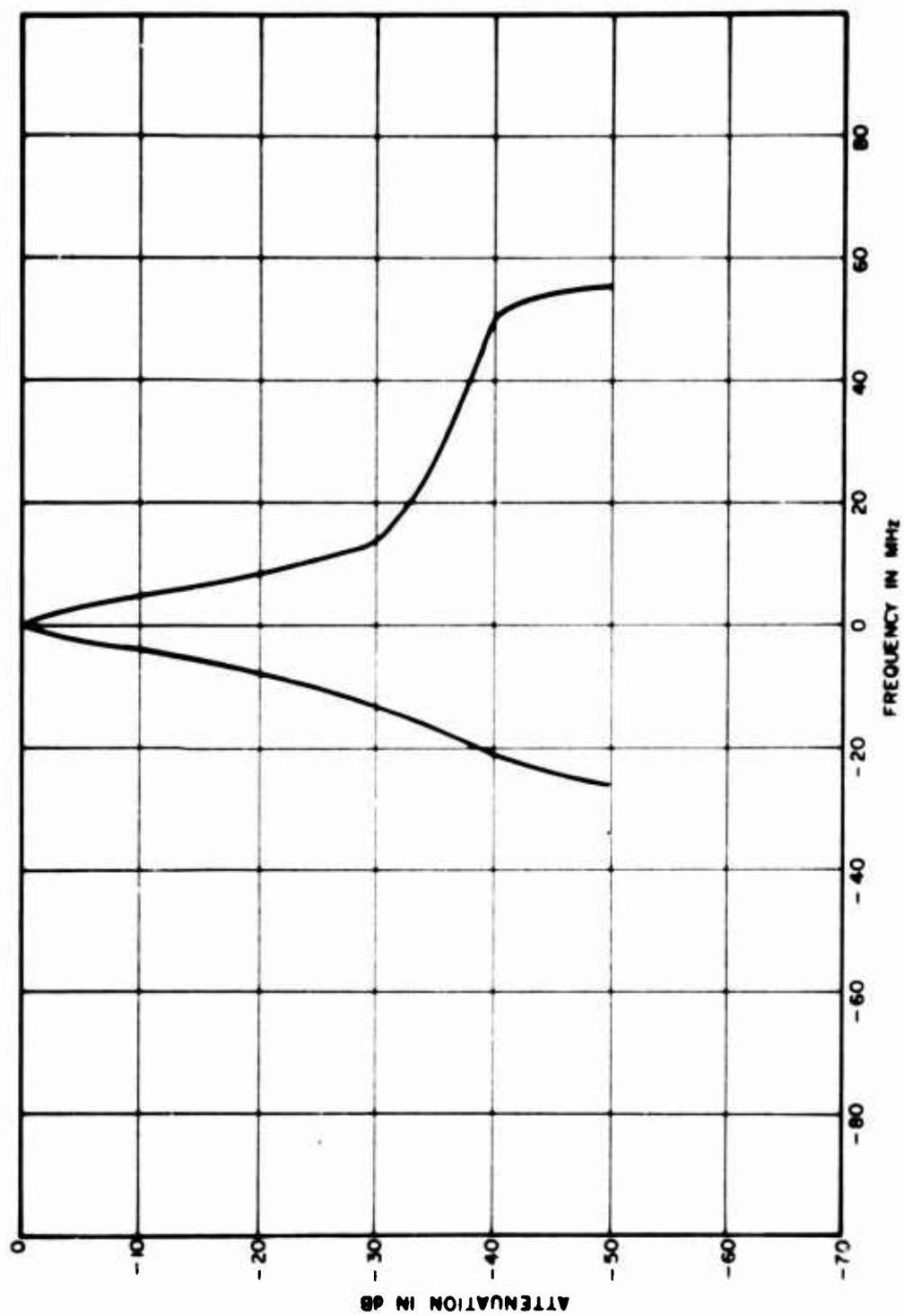


Figure 5.6. RF Selectivity of AM Receiver No. 2

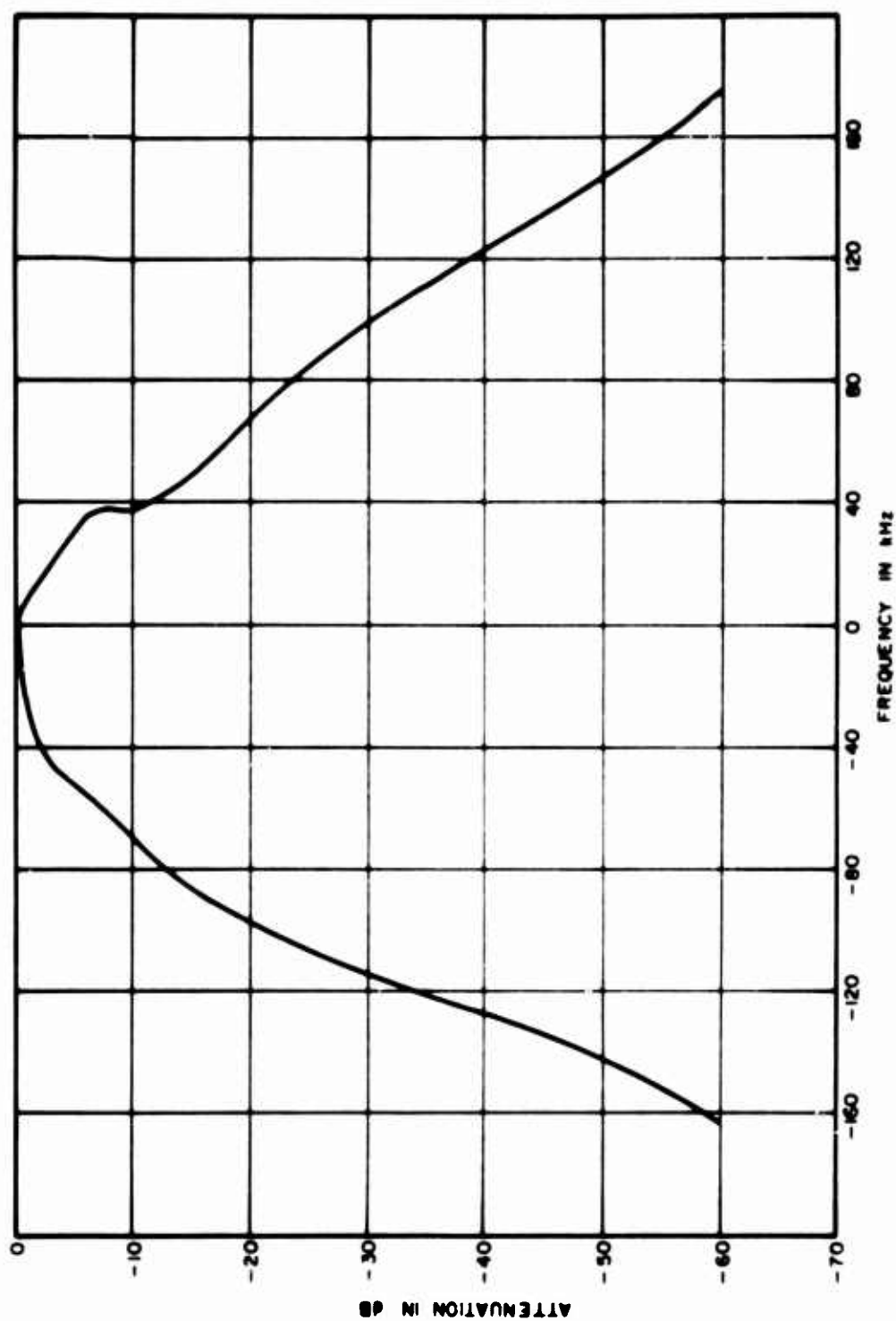


Figure 5.7. IF Selectivity of AM Receiver No. 2

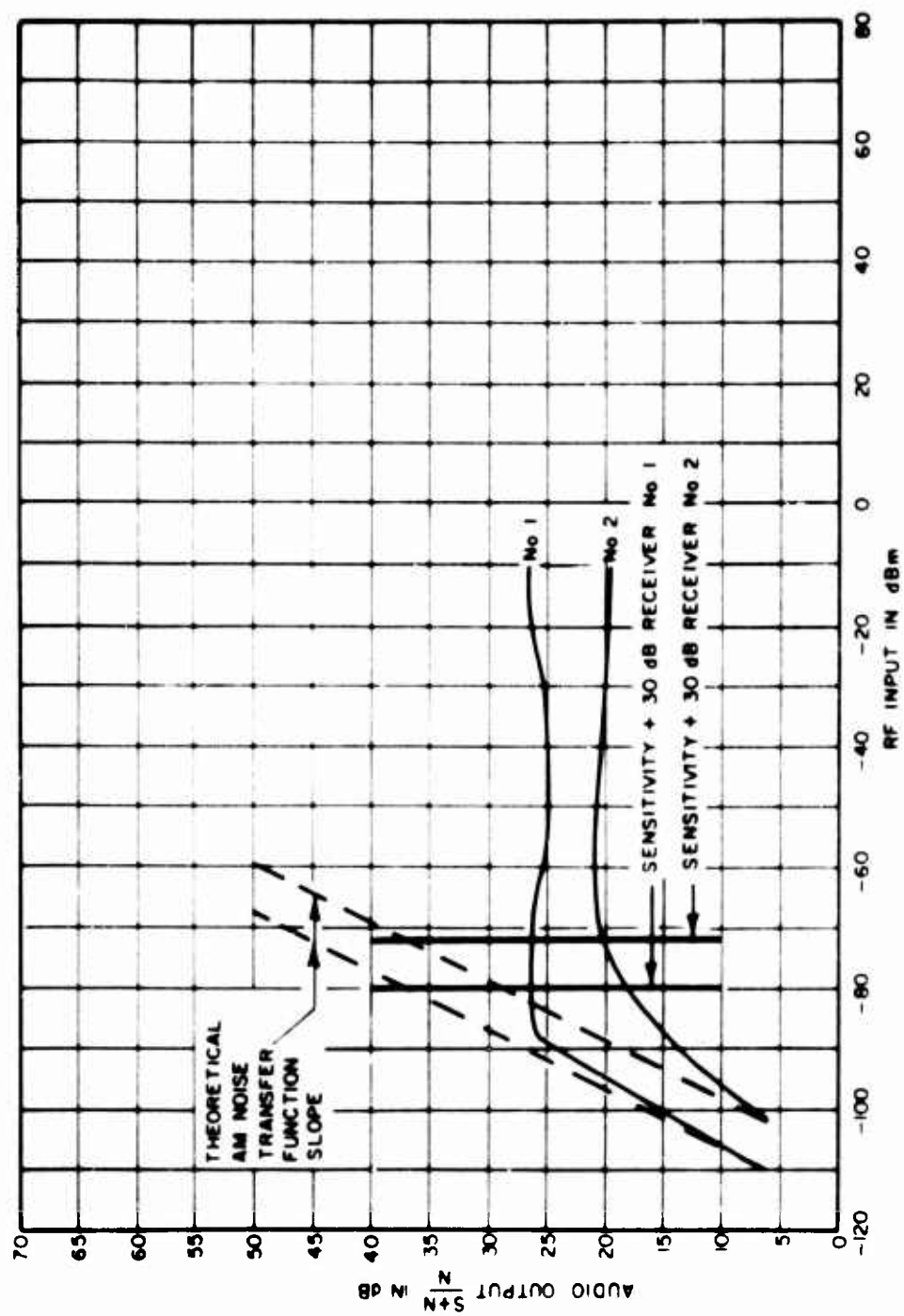


Figure 5-8 Dynamic Range of Receivers No. 1 and No. 2

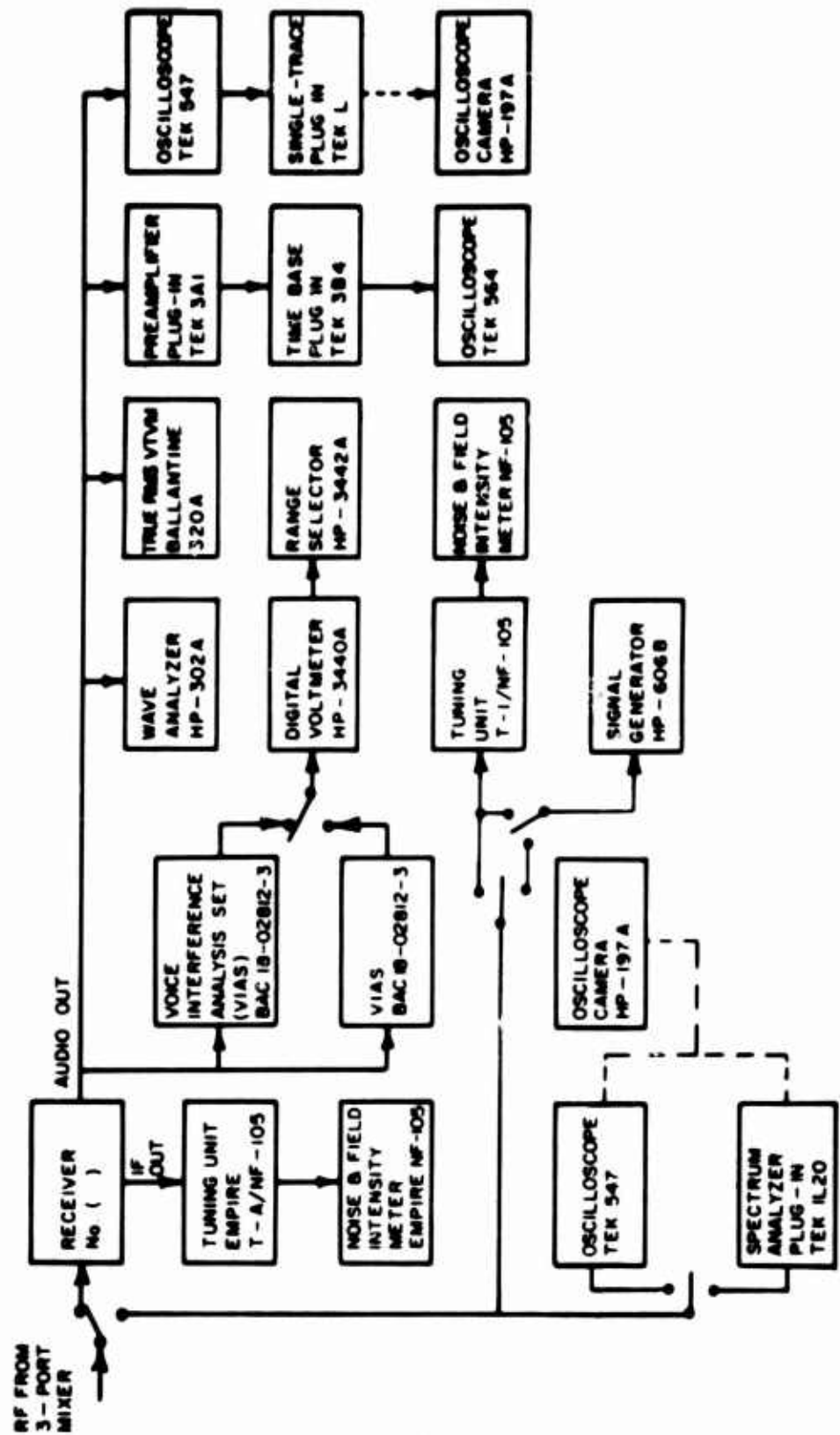


Figure 5-9. Instrumentation Diagram - AM Test Link Receiver Setup

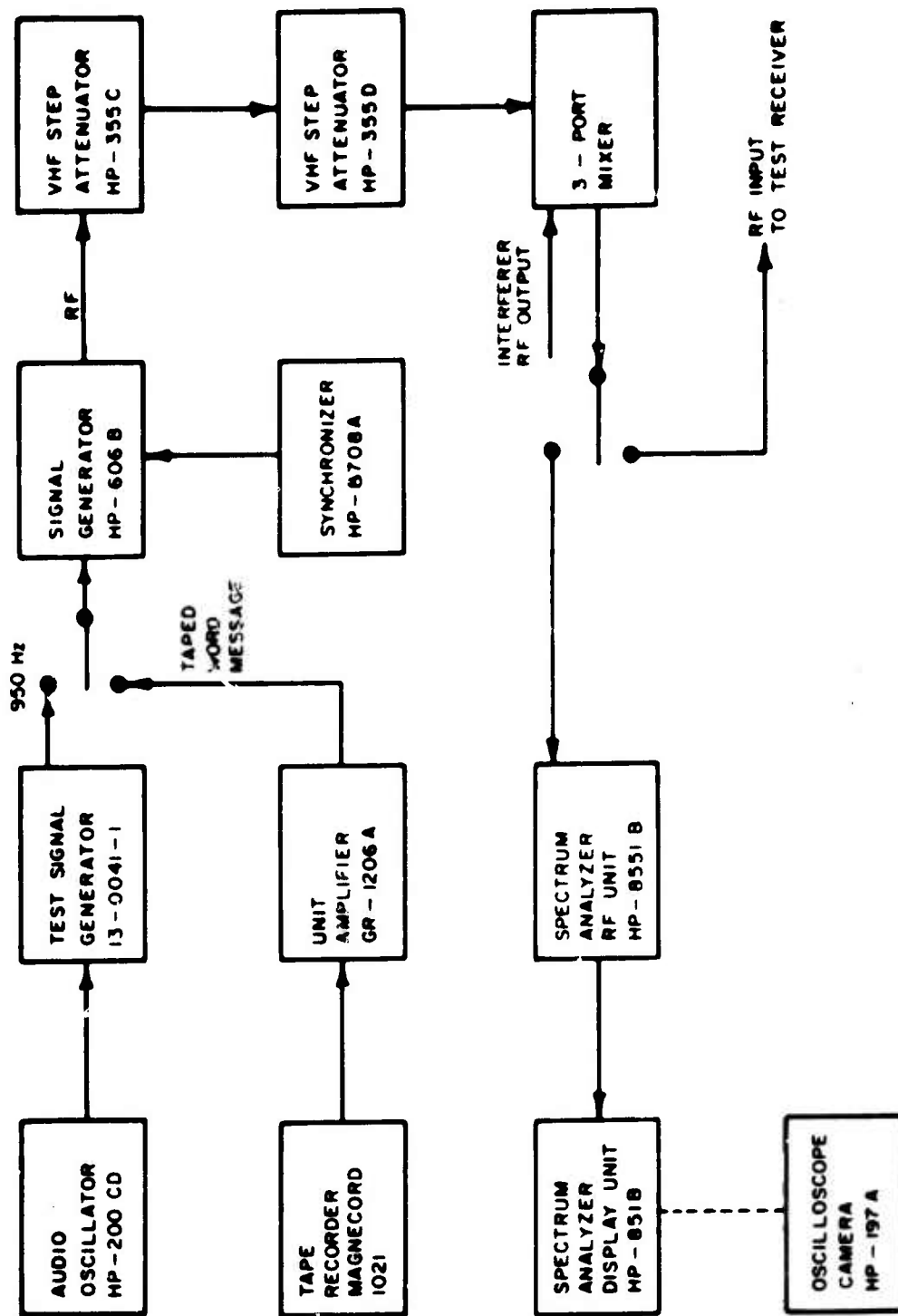


Figure 5-10. Instrumentation Diagram - AM Desired Signal Test Link Transmitter

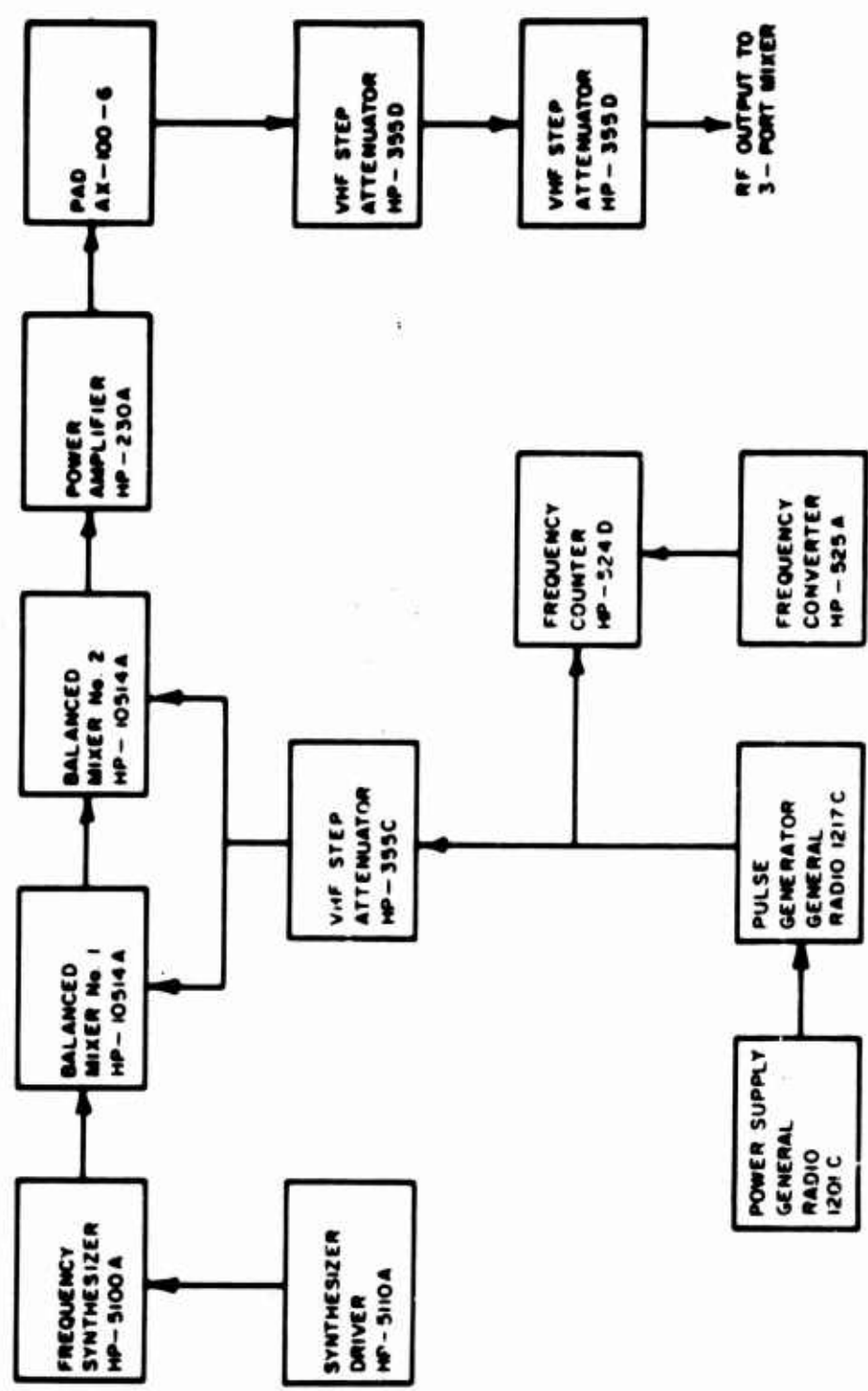


Figure 5-11. Instrumentation Diagram - AM Interferer with a Rectangular Non-Chirped Pulse

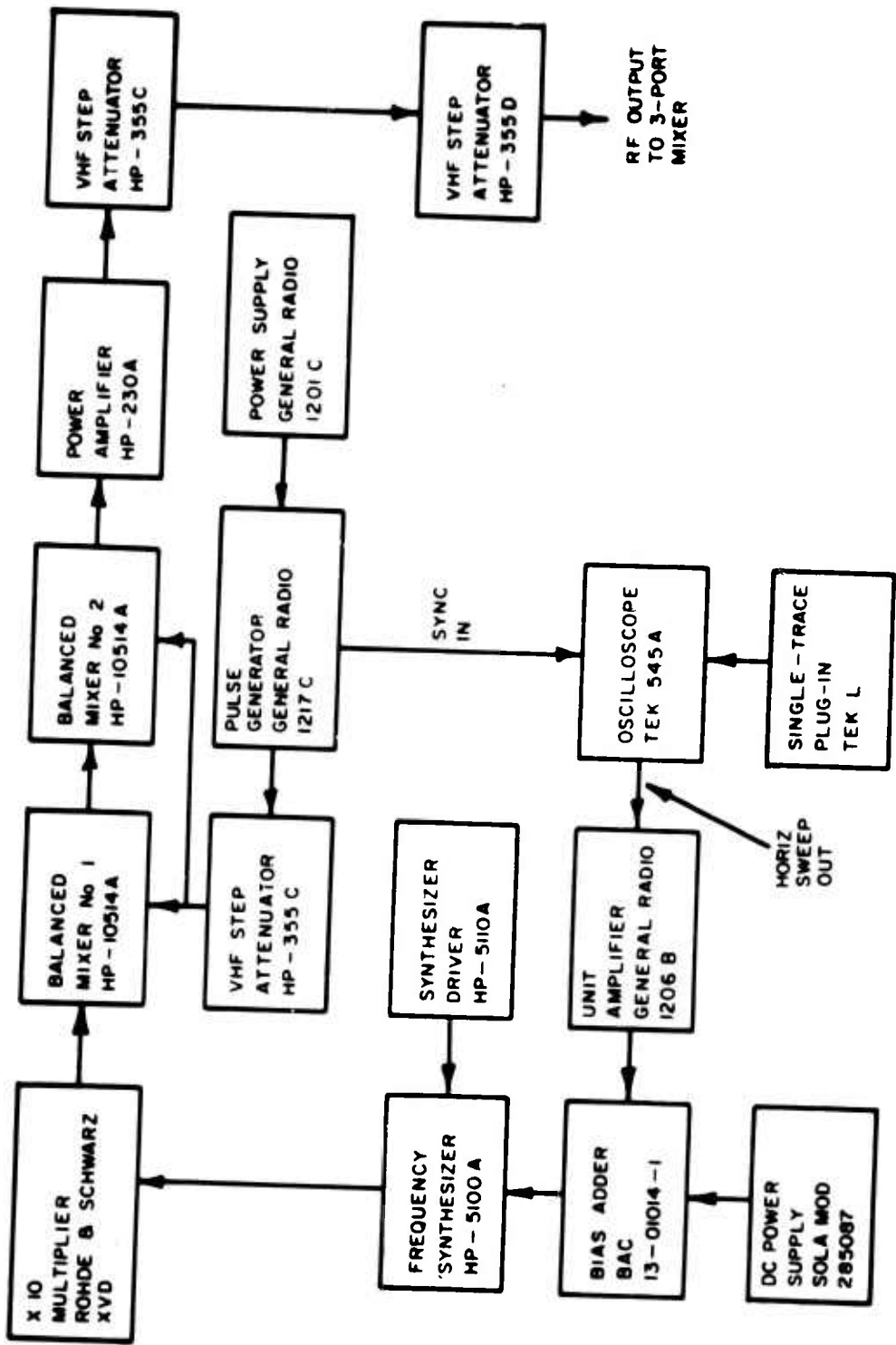


Figure 5-12. Instrumentation Diagram - AM Interferer Pulse With Chirp Setup

Tables 5-1 and 5-2 show the interference measurement conditions for which degradation data were obtained on receivers No. 1 and No. 2, respectively. The following method was used to obtain the degradation data:

1. The desired AM test link transmitter frequency was set to the selected channel frequency.
2. The output of the Hewlett-Packard Model 606B signal generator (the test transmitter) was coupled through an appropriate attenuator to the input of the receiver. The attenuator was adjusted so that the signal level at the receiver input was 30 dB greater than receiver sensitivity. (This ensures that the output signal-to-noise ratio is high and consequently the noise is not greatly affecting the pulsed degradation investigation.)
3. The test transmitter was modulated with the standard VIAS test signal and a clear channel upper performance limit (UPL) AI was obtained and recorded. (The UPL is governed by the input signal level and the noise characteristics of the receiver. This value is not a function of the interference since this has been set equal to zero.)
4. The interference was set up in the measurement configuration shown in Figure 5-11 (or 5-12) and the interfering generator was set up for one of the test conditions in Tables 5-1 and 5-2.
5. The test transmitter carrier was then modulated with phonetically balanced (PB) words. The modulation index was set to 50%.
6. Two observers listened to the audio output of the receiver. The interference signal power output was increased to a level where interference was just perceptible to either of the observers. This was defined as the minimum interference threshold. The $(S/I)_{RF}$ level was measured and recorded. The interference signal level was then increased to the point where the listener could no longer detect the presence of the desired signal modulation. The interference signal was then reduced in increments until the desired signal modulation was just perceptible to either of the listeners. This was the maximum interference threshold. The $(S/I)_{RF}$ level was again measured and recorded.

TABLE 5-1
INTERFERENCE MEASUREMENT CONDITIONS
FOR AM RADIO RECEIVER NO. 1

Pulse Width (μ s)	Pulse Repetition Frequency (p/s)	Δf (interference carrier frequency minus transmitter frequency)
Desired Signal Level: 30 dB > Sensitivity		
1	300, 1,000	0 kHz, 4.5 MHz
5	300, 1,000	0 kHz, 3 kHz, 25 kHz, 100 kHz, 500 kHz, 1 MHz
10	300, 1,000	0 kHz, 100 kHz, 750 kHz
100	40, 80, 160, 400	0 kHz, 3 kHz, 15 kHz, 25 kHz, 38.5 kHz, 100 kHz, 500 kHz
100	300	0 kHz
200	40, 80, 400	0 kHz, 3 kHz, 25 kHz, 100 kHz, 500 kHz
250	10, 40, 80, 160 500, 1,000, 1,600	0 kHz, 6 kHz, 14 kHz, 30 kHz, 60 kHz
400	10, 40, 80, 400	0 kHz, 3 kHz, 25 kHz, 100 kHz, 500 kHz, 1 MHz, 10 MHz
500	40, 60, 80, 160	0 kHz, 3.75 kHz, 30 kHz
1,000	10, 40, 80, 400	0 kHz, 3 kHz, 5 kHz, 25 kHz, 100 kHz, 500 kHz
High Desired Signal Level: 40 dBm		
100	10, 40, 400	0 kHz, 3 kHz, 100 kHz, 1 MHz
400	10, 40, 400	0 kHz, 3 kHz, 100 kHz, 1 MHz
1,000	10, 40, 400	0 kHz, 3 kHz, 100 kHz, 1 MHz
Desired Signal Level: 30 dB > Sensitivity Rectangular Pulses with Frequency Modulation (Chirp)		
100	40, 80, 400	0 kHz, 3 kHz, 100 kHz, 1 MHz (Chirp 0.5 MHz)
200	40, 80, 400	0 kHz, 3 kHz, 100 kHz, 1 MHz (Chirp 0.5 MHz)
400	10, 40, 80	0 kHz, 3 kHz, 100 kHz, 1 MHz (Chirp 250 kHz)

TABLE 5-2
INTERFERENCE MEASUREMENT CONDITIONS
FOR AM RADIO RECEIVER NO. 2

Pulse Width (μ s)	Pulse Repetition Frequency (pps)	Δf (interference carrier frequency minus transmitter frequency)
Desired Signal Level 30 dB > Sensitivity		
5	300, 1,000	0 kHz, 100 kHz, 750 kHz, 1 MHz, 10 MHz, 20 MHz
100	40, 80, 400	0 kHz, 100 kHz, 1 MHz, 10 MHz, 20 MHz
100	300	0 kHz
200	40, 80, 400	0 kHz, 100 kHz, 1 MHz, 10 MHz, 20 MHz
400	10, 40, 80, 400	0 kHz, 3 kHz, 15 kHz, 100 kHz, 1 MHz, 10 MHz, 20 MHz
1,000	10, 40, 80, 400	0 kHz, 3 kHz, 1 MHz, 10 MHz, 20 MHz
High Desired Signal Level - 36 dBm		
100	10, 40, 400	0 kHz, 1 MHz, 10 MHz, 20 MHz
400	10, 40, 400	0 kHz, 1 MHz, 10 MHz, 20 MHz
1,000	10, 40, 400	0 kHz, 1 MHz, 10 MHz, 20 MHz
Desired Signal Level 30 dB > Sensitivity Rectangular Pulses with Frequency Modulation (Chirp)		
100	40, 80, 400	0 kHz, 1 MHz, 10 MHz, 20 MHz (Chirp 1 MHz)
200	40, 80, 400	0 kHz, 100 kHz, 10 MHz, 20 MHz (Chirp 1 MHz)
400	10, 40, 80	0 kHz, 100 kHz, 10 MHz, 20 MHz (Chirp 250 kHz)

7. Articulation score (AS) recordings at the minimum and maximum interference threshold and at $(S/I)_{RF}$ levels between the thresholds were obtained for later scoring at the System Scoring Facility.
8. The transmitter was then modulated with the standard VIAS test signal (950 Hz tone). At the S and \hat{I} levels determined for the minimum and maximum degradation thresholds and the region between the two thresholds the $(S/I)_{RF}$ and the following audio data were recorded: AI , $Sp-p$, S_{RMS} , $(N+D+I)_{p-p}$, $(S+N+D+I)_{p-p}$ and $(S+N+D+I)_{RMS}$.
9. Steps 5 through 8 were repeated for all test conditions in Tables 5-1 and 5-2 where the desired signal was set at $30 \text{ dB} > \text{sensitivity}$.
10. The transmitter was modulated with phonetically balanced (PB) words, and the attenuators were then adjusted for the high desired signal level. This was the highest signal level compatible with the output test equipment power capability that would permit a $(S/I)_{RF}$ of at least -60 dB .
11. The transmitter was then modulated with the standard VIAS test signal, and a clear channel UPL AI was obtained.
12. Steps 5 through 8 were repeated for all measurement conditions listed under "High Desired Signal Level", in Tables 5-1 and 5-2.
13. The desired signal level was reset to 30 dB greater than receiver sensitivity.
14. The interference source measurement configuration was set up as shown in Figure 5-12, and the interfering generator was set to provide the "Rectangular Pulses with Frequency Modulation (Chirp)" as shown in Tables 5-1 and 5-2.
15. Steps 5 through 8 were repeated for all measurement conditions listed under "Frequency Modulation (Chirp)" pulses.

The measured data are documented in Appendix III. A summary listing of the location in Appendix III of the various measured data is contained in Table 6-1.

AUDIO THRESHOLD TEST

This is a description of an audio threshold test that was performed in addition to the

overall receiver minimum threshold test previously described. This test was run using the average responses of three subjects trained to respond to a minimum audio interference threshold. The measurement block diagram and the test parameters are given in Figure 5-13 and Table 5-3, respectively.

The following method was used to obtain the minimum audio threshold:

1. Set PB word group to normal comfort hearing level (600 mv).
2. Set bandwidth limited noise to the S/N levels required at Headset input.
3. Set desired PW and PRF in pulse generator. increase output until pulse is noted, back-off until threshold is obtained.
4. Record:
 - a. Signal level (voltage) at input to adder and Headset input.
 - b. Interference level (voltage) peak-to-peak at adder input and Headset input.
 - c. S/N levels at Headset input
 - d. Photographs of all pulses at adder and Headset input with signal and noise turned off.

The results of this test are described in Section 6 under Threshold Degradation Effects.

TABLE 5-3
AUDIO THRESHOLD TEST PARAMETERS

PW	200,	400,	800,	1000			μ sec
PRF	40,	80,	400,	800			pps
S/N LEVELS	5,	10,	15,	20,	30,	40	dB

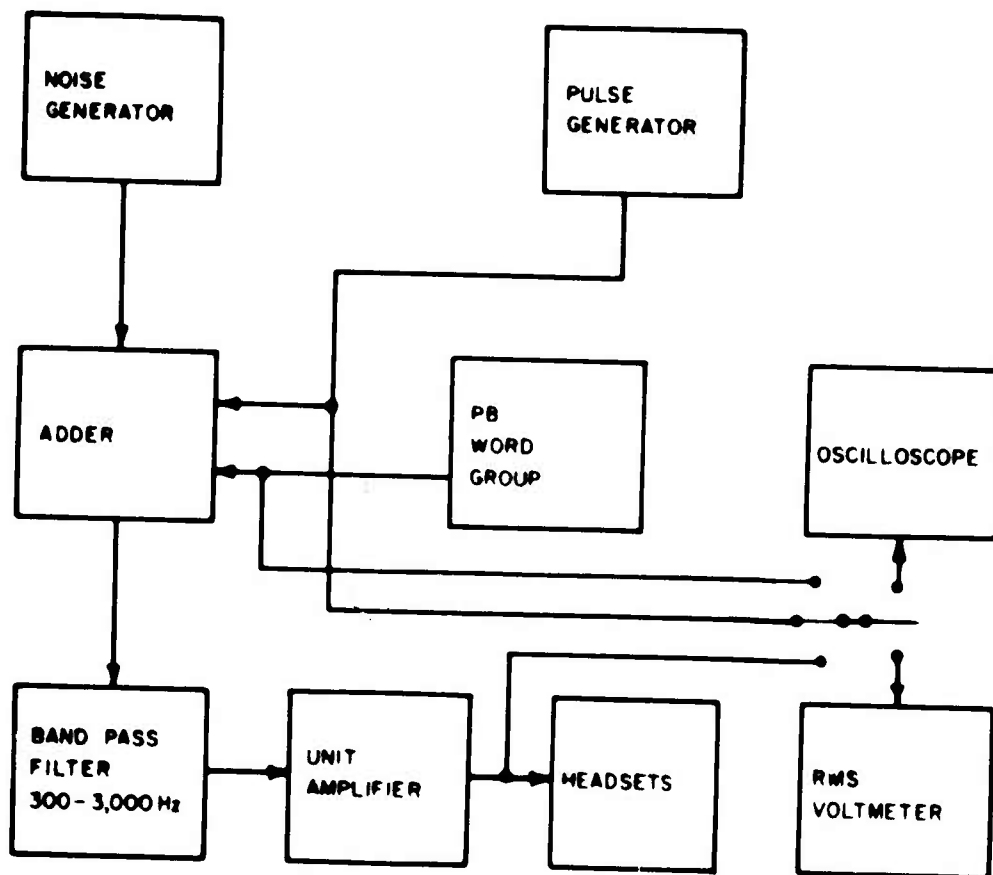


Figure 5-13. Threshold Measurement Block Diagram

SECTION 6

MODELING OF PULSED INTERFERENCE EFFECTS

INTRODUCTION

This section discusses the modeling of pulsed interference effects or trends. These results are based upon a combination of measured and simulated data. The measured data (Section 5 contains a description of the measurement procedure) are documented in Appendix III as the data base for this and possibly other AM pulsed interference investigations. The data are presented in Appendix III as a series of graphs. The simulated data are discussed in Section 4.

The data presented in Appendix III show the relationship of:

1. Articulation Score (AS) versus the receiver input signal to peak interference ratio $[(S/\hat{I})_{RF}]$
2. Articulation Index (AI) versus the receiver input signal to peak interference ratio
3. Degradation Threshold versus receiver input signal to peak interference ratio
4. The receiver input signal to peak interference versus the baseband output signal-to-interference (average) and signal to peak-to-peak interference ratio.

Table 6-1 lists a summary of the page numbers of these figures according to their interference parameters.

The measured and computer simulated data were specifically examined for trends relating pulsed interference to:

1. Voice Intelligibility
2. Degradation with Pulse Rate
3. Degradation with Pulse Width
4. Degradation with Chirped and Non-Chirped Pulses
5. Degradation with Off-Tuning
6. Degradation with Output Signal-to-Noise Ratio
7. Baseband Power Ratios

TABLE 6-1
BASIC AM PULSED PERFORMANCE DEGRADATION DATA SUMMARY

Type of Basic Data Presentation	Parameter Description				Receiver Number	Figure Number	Page Number
	Pw (μs)	PRF	Chirp (MHz)	S (dBm)			
As vs. (S/I) RF	1	300		- 83	1	III 1	III 6
As vs. (S/I) RF	1	1000		- 83	1	III 2	III 7
As vs. (S/I) RF	10	300		- 83	1	III 3	III 8
As vs. (S/I) RF	10	1000		- 83	1	III 4	III 9
As vs. (S/I) RF	100	40		83	1	III 5	III 10
As vs. (S/I) RF	100	80		83	1	III 6	III 11
As vs. (S/I) RF	100	160		83	1	III 7	III 12
As vs. (S/I) RF	100	300		83	1	III 8	III 13
As vs. (S/I) RF	280	10		- 83	1	III 9	III 14
As vs. (S/I) RF	250	40		83	1	III 10	III 15
As vs. (S/I) RF	250	80		83	1	III 11	III 16
As vs. (S/I) RF	250	160		83	1	III 12	III 17
As vs. (S/I) RF	250	500		83	1	III 13	III 18
As vs. (S/I) RF	280	1000		83	1	III 14	III 19
As vs. (S/I) RF	250	1600		83	1	III 15	III 20
As vs. (S/I) RF	500	40		83	1	III 16	III 21
As vs. (S/I) RF	500	60		83	1	III 17	III 22
As vs. (S/I) RF	500	80		83	1	III 18	III 23
As vs. (S/I) RF	500	160		83	1	III 19	III 24
As vs. (S/I) RF	1000	40		- 83	1	III 20	III 25
As vs. (S/I) RF	1000	80		- 83	1	III 21	III 26
As vs. (S/I) RF	1000	160		- 83	1	III 22	III 27
As vs. (S/I) RF	10000	40		- 83	1	III 23	III 28
As vs. (S/I) RF	10000	80		- 83	1	III 24	III 29
As vs. (S/I) RF	5	300		- 72	2	III 25	III 30
As vs. (S/I) RF	5	1000		- 72	2	III 26	III 31
As vs. (S/I) RF	100	40		- 72	2	III 27	III 32

TABLE 6-1 (Sheet 2 of 6)

Type of Basic Data Presentation	Parameter Description				Receiver Number	Figure Number	Page Number
	P _w (μs)	PRF	Chirp (MHz)	S (dBm)			
As vs. (S/I) ^A RF	100	80		- 72	2	III-28	III-33
As vs. (S/I) ^A RF	100	300		- 72	2	III-29	III-34
As vs. (S/I) ^A RF	100	400		- 72	2	III-30	III-35
As vs. (S/I) ^A RF	200	40		- 72	2	III-31	III-36
As vs. (S/I) ^A RF	200	80		- 72	2	III-32	III-37
As vs. (S/I) ^A RF	200	400		- 72	2	III-33	III-38
As vs. (S/I) ^A RF	400	10		- 72	2	III-34	III-39
As vs. (S/I) ^A RF	400	40		- 72	2	III-35	III-40
As vs. (S/I) ^A RF	400	80		- 72	2	III-36	III-41
As vs. (S/I) ^A RF	400	400		- 72	2	III-37	III-42
As vs. (S/I) ^A RF	1000	10		- 72	2	III-38	III-43
As vs. (S/I) ^A RF	1000	40		- 72	2	III-39	III-44
As vs. (S/I) ^A RF	1000	80		- 72	2	III-40	III-45
As vs. (S/I) ^A RF	1000	400		- 72	2	III-41	III-46
As vs. (S/I) ^A RF	100	80	1 0	- 72	2	III-42	III-47
As vs. (S/I) ^A RF	100	400	1 0	- 72	2	III-43	III-48
As vs. (S/I) ^A RF	200	40	1 0	- 72	2	III-44	III-49
As vs. (S/I) ^A RF	200	80	1 0	- 72	2	III-45	III-50
As vs. (S/I) ^A RF	200	400	1 0	- 72	2	III-46	III-51
As vs. (S/I) ^A RF	400	10	0 25	- 72	2	III-47	III-52
As vs. (S/I) ^A RF	400	40	0 25	- 72	2	III-48	III-53
As vs. (S/I) ^A RF	400	80	0 25	- 72	2	III-49	III-54
AI vs. (S/I) ^A RF	5	300		- 79	1	III-50	III-55
AI vs. (S/I) ^A RF	5	1000		- 79	1	III-51	III-56
AI vs. (S/I) ^A RF	100	40		- 79	1	III-52	III-57
AI vs. (S/I) ^A RF	100	80		- 79	1	III-53	III-58
AI vs. (S/I) ^A RF	100	300		- 79	1	III-54	III-59
AI vs. (S/I) ^A RF	100	400		- 79	1	III-55	III-60

TABLE 6-1 (Sheet 3 of 6)

Type of Basic Data Presentation	Parameter Description				Receiver Number	Figure Number	Page Number
	Pwr(μ)	PRF	Chirp (MHz)	S(dBm)			
As vs. (S/I) RF	200	60		-79	1	III-58	III-61
As vs. (S/I) RF	200	80		-79	1	III-59	III-62
As vs. (S/I) RF	200	400		-79	1	III-58	III-63
As vs. (S/I) RF	400	10		-79	1	III-59	III-64
As vs. (S/I) RF	400	40		-79	1	III-60	III-65
As vs. (S/I) RF	400	80		-79	1	III-61	III-66
As vs. (S/I) RF	400	400		-79	1	III-62	III-67
As vs. (S/I) RF	1000	10		-79	1	III-63	III-68
As vs. (S/I) RF	1000	40		-79	1	III-64	III-69
As vs. (S/I) RF	1000	80		-79	1	III-65	III-70
As vs. (S/I) RF	1000	400		-79	1	III-66	III-71
As vs. (S/I) RF	100	10		40	1	III-67	III-72
As vs. (S/I) RF	100	40		40	1	III-68	III-73
As vs. (S/I) RF	100	400		40	1	III-69	III-74
As vs. (S/I) RF	400	10		40	1	III-70	III-75
As vs. (S/I) RF	400	40		40	1	III-71	III-76
As vs. (S/I) RF	400	400		40	1	III-72	III-77
As vs. (S/I) RF	1000	10		40	1	III-73	III-78
As vs. (S/I) RF	1000	40		40	1	III-74	III-79
As vs. (S/I) RF	1000	400		40	1	III-75	III-80
As vs. (S/I) RF	100	40	5	-79	1	III-76	III-81
As vs. (S/I) RF	100	80	5	-79	1	III-77	III-82
As vs. (S/I) RF	100	400	5	-79	1	III-78	III-83
As vs. (S/I) RF	200	40	5	-79	1	III-79	III-84
As vs. (S/I) RF	200	80	5	-79	1	III-80	III-85
As vs. (S/I) RF	200	400	5	-79	1	III-81	III-86
As vs. (S/I) RF	400	10	0.25	-79	1	III-82	III-87
As vs. (S/I) RF	400	40	0.25	-79	1	III-83	III-88
As vs. (S/I) RF	400	80	0.25	-79	1	III-84	III-89

TABLE 6-1 (Sheet 4 of 6)

Type of Basic Data Presentation	Parameter Description				Receiver Number	Figure Number	Page Number
	P_{av} (μ W)	PRF	Chirp (MHz)	S (dBm)			
As vs. (S/I) $_{RF}$	5	300		-72	2	III-85	III-90
As vs. (S/I) $_{RF}$	5	1000		-72	2	III-86	III-91
As vs. (S/I) $_{RF}$	100	40		-72	2	III-87	III-92
As vs. (S/I) $_{RF}$	100	80		-72	2	III-88	III-93
As vs. (S/I) $_{RF}$	100	300		-72	2	III-89	III-94
As vs. (S/I) $_{RF}$	100	400		-72	2	III-90	III-95
As vs. (S/I) $_{RF}$	200	40		-72	2	III-91	III-96
As vs. (S/I) $_{RF}$	200	80		-72	2	III-92	III-97
As vs. (S/I) $_{RF}$	200	400		-72	2	III-93	III-98
As vs. (S/I) $_{RF}$	400	10		-72	2	III-94	III-99
As vs. (S/I) $_{RF}$	400	40		-72	2	III-95	III-100
As vs. (S/I) $_{RF}$	400	80		-72	2	III-96	III-101
As vs. (S/I) $_{RF}$	400	400		-72	2	III-97	III-102
As vs. (S/I) $_{RF}$	1000	40		-72	2	III-98	III-103
As vs. (S/I) $_{RF}$	1000	80		-72	2	III-99	III-104
As vs. (S/I) $_{RF}$	1000	400		-72	2	III-100	III-105
As vs. (S/I) $_{RF}$	100	40		-36	2	III-101	III-106
As vs. (S/I) $_{RF}$	100	400		-36	2	III-102	III-107
As vs. (S/I) $_{RF}$	400	40		-36	2	III-103	III-108
As vs. (S/I) $_{RF}$	400	400		-36	2	III-104	III-109
As vs. (S/I) $_{RF}$	1000	40		-36	2	III-105	III-110
As vs. (S/I) $_{RF}$	1000	400		-36	2	III-106	III-111
(S/I) $_{RF}$ VS $\left[\frac{S}{N+D+I} \right]_{dB}$	5	300		-79	1	III-107	III-112
"	5	1000		-79	1	III-108	III-113
"	100	40		-79	1	III-109	III-114
"	100	80		-79	1	III-110	III-115
"	100	300		-79	1	III-111	III-116
"	100	400		-79	1	III-112	III-117

TABLE 6-1 (Sheet 5 of 6)

Type of Basic Data Presentation	Parameter Description				Receiver Number	Figure Number	Page Number
	Pw (μs)	PRF	Chirp (MHz)	S (dBm)			
$(S/I)_{RF} \text{ vs } \left[\frac{S}{N+D+I} \right]_{PD_O}$	200	40		-79	1	III-113	III-118
"	200	80		-79	1	III-114	III-119
"	200	400		-79	1	III-115	III-120
"	1000	10		-79	1	III-116	III-121
"	1000	40		-79	1	III-117	III-122
"	1000	80		-79	1	III-118	III-123
"	1000	400		-79	1	III-119	III-124
"	100	40	.5	-79	1	III-120	III-125
"	100	80	.5	-79	1	III-121	III-126
"	100	400	.5	-79	1	III-122	III-127
"	200	40	.5	-79	1	III-123	III-128
"	200	80	.5	-79	1	III-124	III-129
"	200	400	.5	-79	1	III-125	III-130
"	400	10	0.25	-79	1	III-126	III-131
"	400	40	0.25	-79	1	III-127	III-132
"	400	80	0.25	-79	1	III-128	III-133
"	100	10		-40	1	III-129	III-134
"	100	40		-40	1	III-130	III-135
"	100	400		-40	1	III-131	III-136
"	400	10		-40	1	III-132	III-137
"	400	40		-40	1	III-133	III-138
"	400	400		-40	1	III-134	III-139
"	1000	10		-40	1	III-135	III-140
"	1000	40		-40	1	III-136	III-141
"	1000	400		-40	1	III-137	III-142
$(S/I)_{RF} \text{ vs } (S/I)_O$	5	300		-79	1	III-138	III-143
"	5	1000		-79	1	III-139	III-144
"	100	40		-79	1	III-140	III-145
"	100	80		-79	1	III-141	III-146

TABLE 6-1 (Sheet 6 of 6)

Type of Basic Data Presentation	Parameter Description				Receiver Number	Figure Number	Page Number
	Pw (μs)	PRF	Chirp (MHz)	S (dBm)			
(S/I) _{RF} VS (S/I) ₀	100	300		-70	1	III-142	III-147
"	100	400		-70	1	III-143	III-148
"	200	40		-70	1	III-144	III-149
"	200	80		-70	1	III-145	III-150
"	200	400		-70	1	III-146	III-151
"	400	10		-70	1	III-147	III-152
"	400	40		-70	1	III-148	III-153
"	400	80		-70	1	III-149	III-154
"	400	400		-70	1	III-150	III-155
"	1000	10		-70	1	III-151	III-156
"	1000	40		-70	1	III-152	III-157
"	1000	80		-70	1	III-153	III-158
"	1000	400		-70	1	III-154	III-159
"	100	40	.5	-70	1	III-155	III-160
"	100	80	.5	-70	1	III-156	III-161
"	200	40	.5	-70	1	III-157	III-162
"	200	80	.5	-70	1	III-158	III-163
"	400	10	0.25	-70	1	III-159	III-164
"	400	40	0.25	-70	1	III-160	III-165
"	400	80	0.25	-70	1	III-161	III-166
THRESHOLDS TABLES	ALL	ALL	-	-63	1	III-1	III-2
"	ALL	ALL	ALL	ALL	1	III-2	III-3
"	ALL	ALL	-	-	2	III-3	III-4
"	ALL	ALL	ALL	ALL	2	III-4	III-5

8. Minimum Threshold Degradation Effects
9. Audio Limiting
10. AGC and Amplifier Saturation Effects

The resulting models or effects are useful in representing the dependence of AM receiver performance upon various pulse parameters.

VOICE INTELLIGIBILITY

The following is a discussion of how the intelligibility of a voice signal at the receiver output is degraded by pulsed interference. Voice intelligibility was measured by subjecting a group of listeners to a preselected group of words corrupted by specific types of pulsed interference. The results of this type of test are expressed as the percentage of words heard correctly and is defined as the Articulation Score (AS). The basic data obtained for this test are given in Appendix III (Figures III 1 to III 49).

Figures 6-1, 6-2 and 6-3 are plots of the average articulation score as a function of the input (S/I) ratio for various duty cycles (δ). The on tuned data (interference and desired signal carrier frequencies equal) were averaged since this does not require an additional off tune filter power correction factor. The pulse widths were from 1 μ sec to 10,000 μ sec. The results show that for a duty cycle $\delta \leq 8\%$ (radars are typically less than 1%) the pulsed interference cannot effectively block intelligibility in an AM receiver. The articulation score remains higher than 90% even for large interference levels as shown by Figure 6-1. The rectangular pulse is detected as a loud "pop" at the pulse repetition frequency (PRF) rate or as a "buzz" at the audio output depending on the PRF and pulse level. The pulsed interference is on for only a fraction of time compared to a word length and therefore only a small portion or portions of the word is interrupted. It is therefore reasonable to expect the intelligibility to be high.

When the duty cycle is between 8% and 25%, the pulsed interference causes minimal degradation for (S/I) levels above -15 dB. For (S/I) levels below -15 dB there is a rapid decrease in system performances as shown in Figure 6-2. For this case, the pulsed interference is on for longer periods of time, thereby interrupting larger portions of the speech waveform. The upward spread of masking (masking of frequencies higher than the audio interfering frequency, see Reference 21) due to large interference levels also aids in reducing the intelligibility of the system.

Figure 6-3 is shown for a duty cycle greater than 25% and indicates that for negative (S/I) ratios the system performance falls off very rapidly. The pulsed interference is on for a long enough period of time to mask complete words or sentences. This causes a

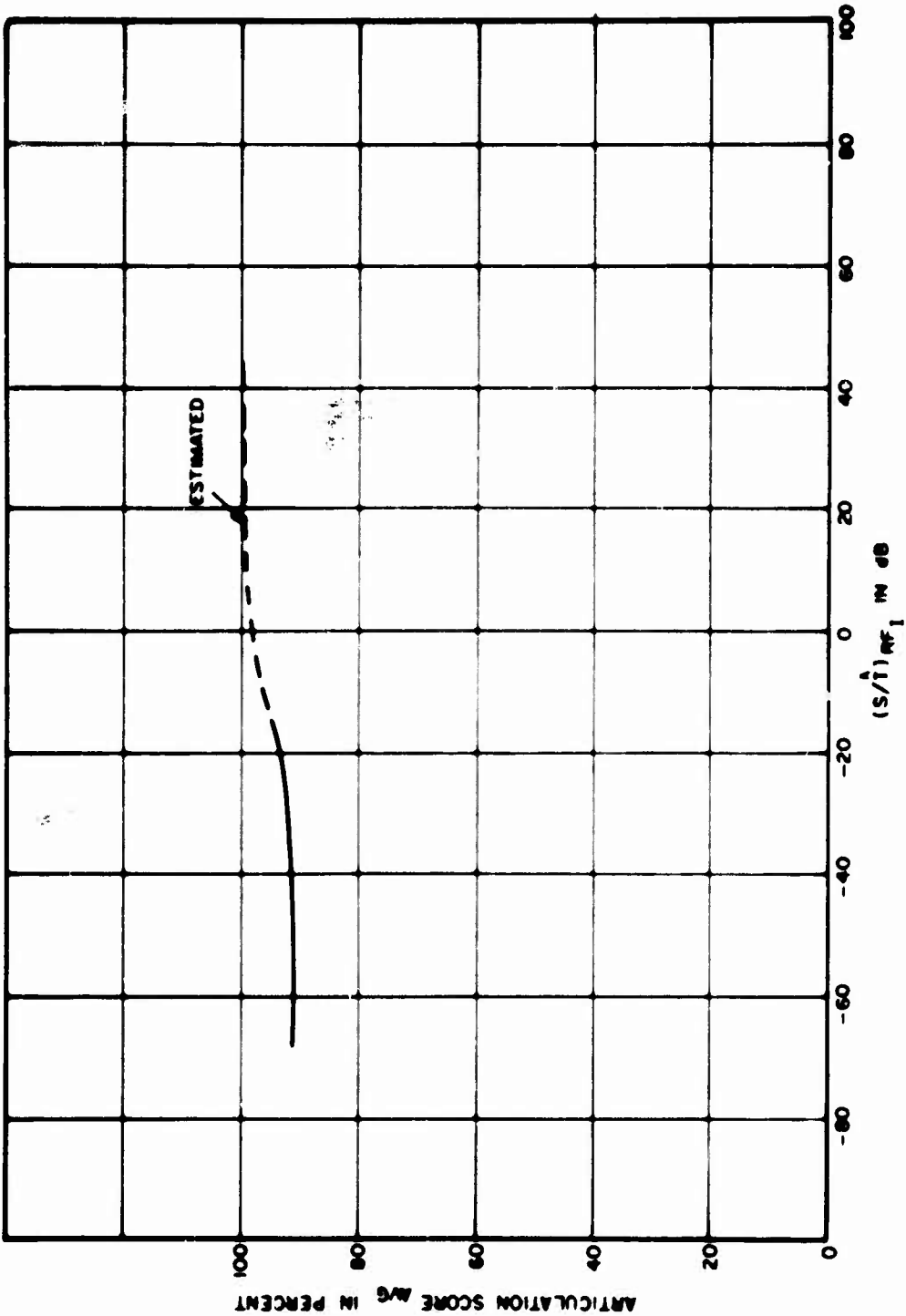


Figure 6-1. Average Articulation Score for a Duty Cycle δ ($\delta \leq 8\%$)

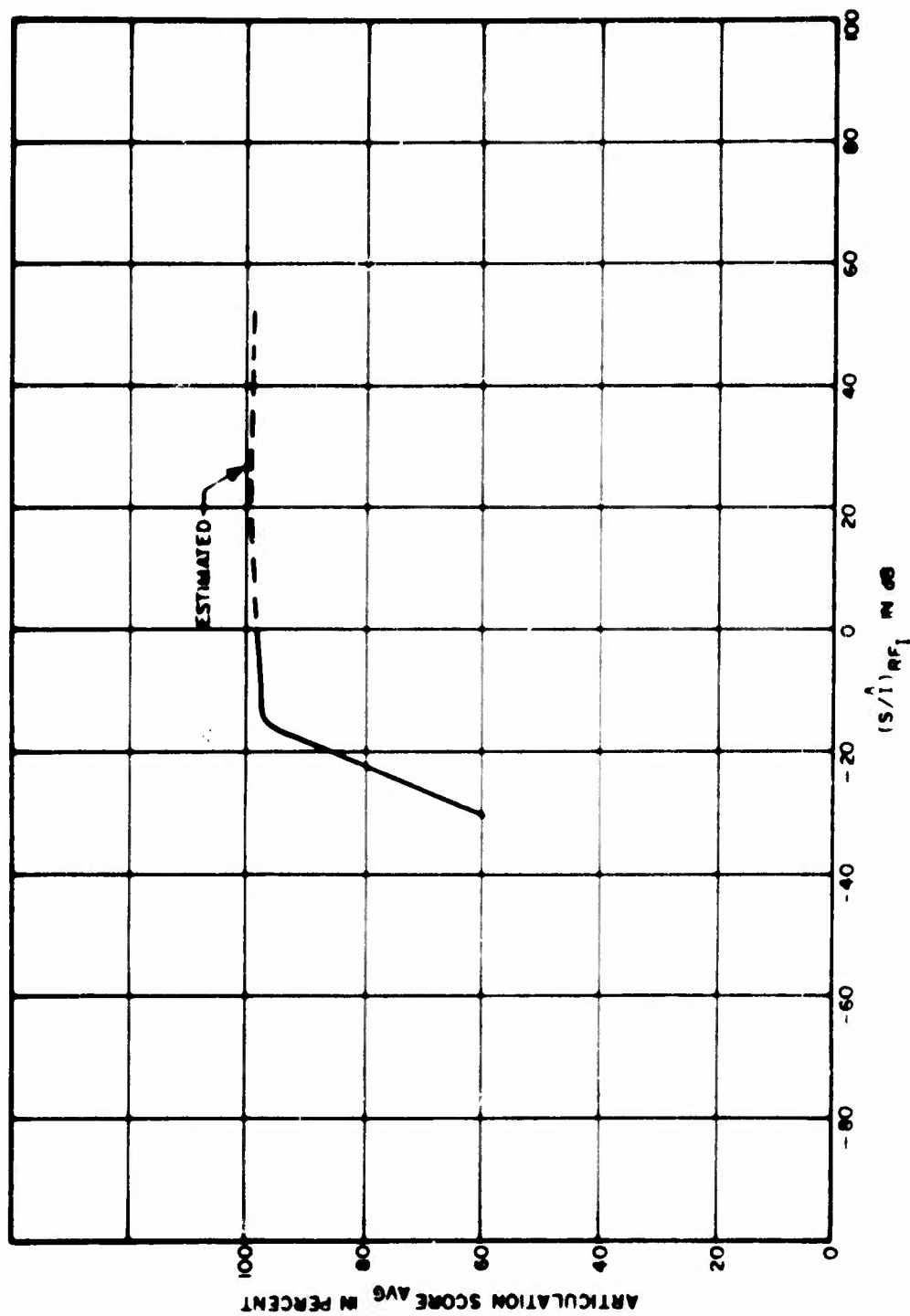
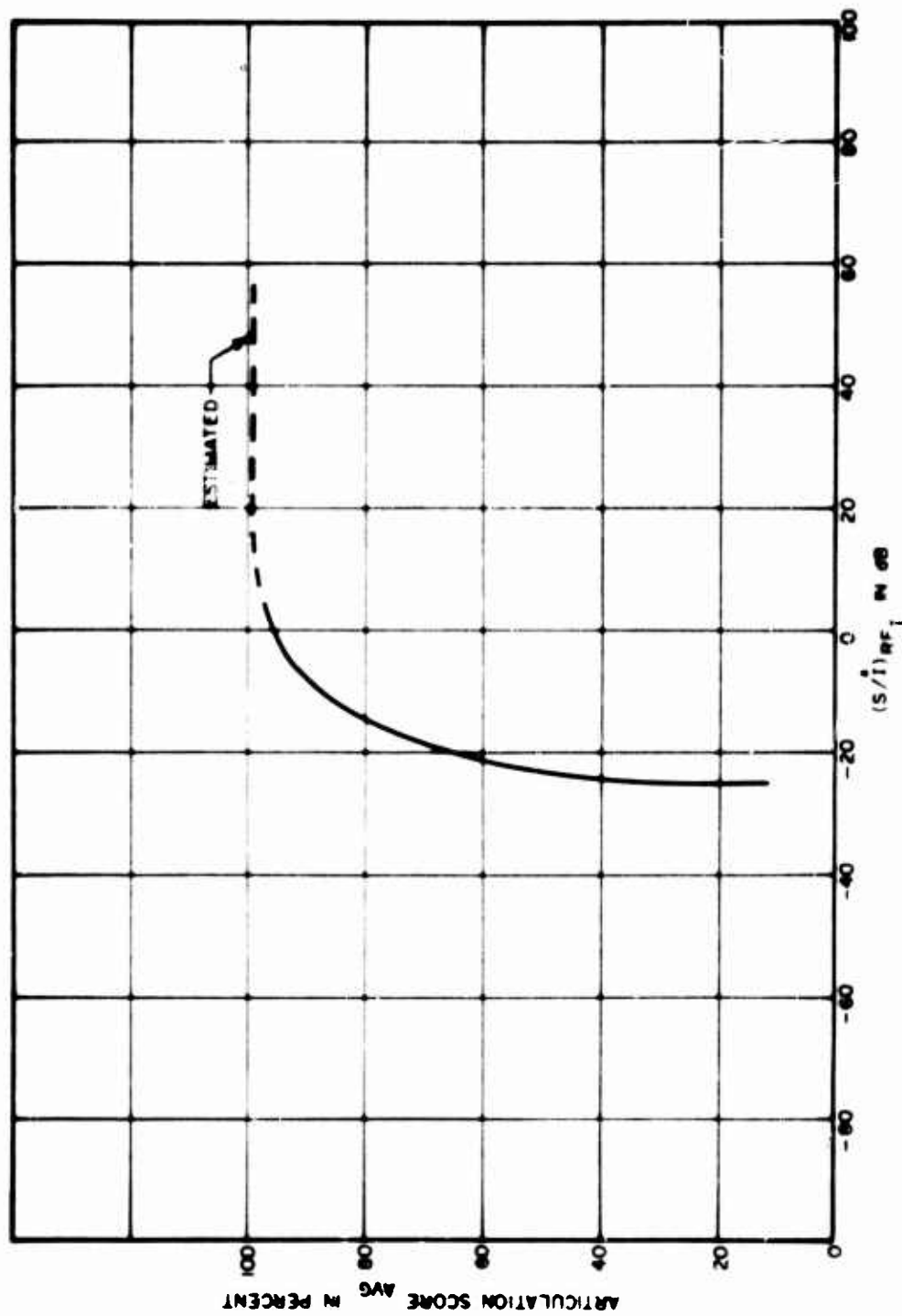


Figure 6-2. Average Articulation Score for a Duty Cycle δ ($8\% < \delta \leq 25\%$)

Figure 6-3. Average Articulation Score for a Duty Cycle δ ($\delta > 25\%$)

correspondingly large change in articulation score when the pulsed interference is stronger than the desired signal. A review of the literature showed that a similar trend was demonstrated in a test conducted by Miller and Licklider (reference 22). In that test, undistorted speech was turned off at various intervals and the resulting articulation score was obtained. The proportion of time that speech is on is called the speech time fraction. The results of their tests are shown in Figure 6-4. In this figure, the articulation score is plotted as a function of the frequency of interruption with the speech time fraction as the variable parameter.

Since undistorted speech was turned off at audio, the results do not include the masking effect of the pulsed interference. However, even with these differences, there is considerable similarity between the two sets of data. Both sets of data show that for low interference duty cycle and high speech time fraction, the degradation to speech is minimal and increases steadily for an increase in interference duty cycle or a decrease in the speech time fraction.

The intelligibility (AS) trends of the data discussed in this section were obtained for a narrowband AM system with approximately a 3 kHz audio or information bandwidth. Commercial and high fidelity systems employ bandwidths up to 15 kHz. It is, therefore, desirable that the results of this investigation be extended to wideband systems. The basic information that can be used for this transformation is the relationship of AS scores to bandwidth and audio signal-to-noise ratios. Figure 6-5 shows this relationship which was obtained using the basic AS versus signal-to-noise ratio curves found in Reference 23 and the bandwidth correction curves found in Reference 24. Figure 6-5 shows that, for an AS of 80% or less, increasing the bandwidth of the system to 6 kHz or larger decreases the required $(S/N)_0$ ratio by up to 3 dB. For higher values of AS the decrease in required $(S/N)_0$ ratio is even greater and is approximately 12 dB for an AS of 95%. If instead the (S/N) ratio is held constant at 5 dB and the bandwidth is increased to 6 kHz or larger there is a 10% increase in AS and for a (S/N) ratio of 25 dB there is an increase in AS of only about 6%. In general, increasing the audio bandwidth will increase the system performance for the same (S/N) ratio. This increase will be greater for lower values of AS and will decrease as the AS value approaches 100%. Although bandwidth correction curves are not available specifically for pulsed interference, the corrections in Figure 6-5 can be applied to the pulsed interference curves, as a worst case (noise) transformation.

The high fidelity systems that cannot tolerate the presence of pulsed interference at the audio output regardless of the articulation score should not use the AS data discussed here. The data on pulsed interference threshold, reported later in this section, should be used in those cases where the very presence of pulsed interference at the audio output cannot be accepted.

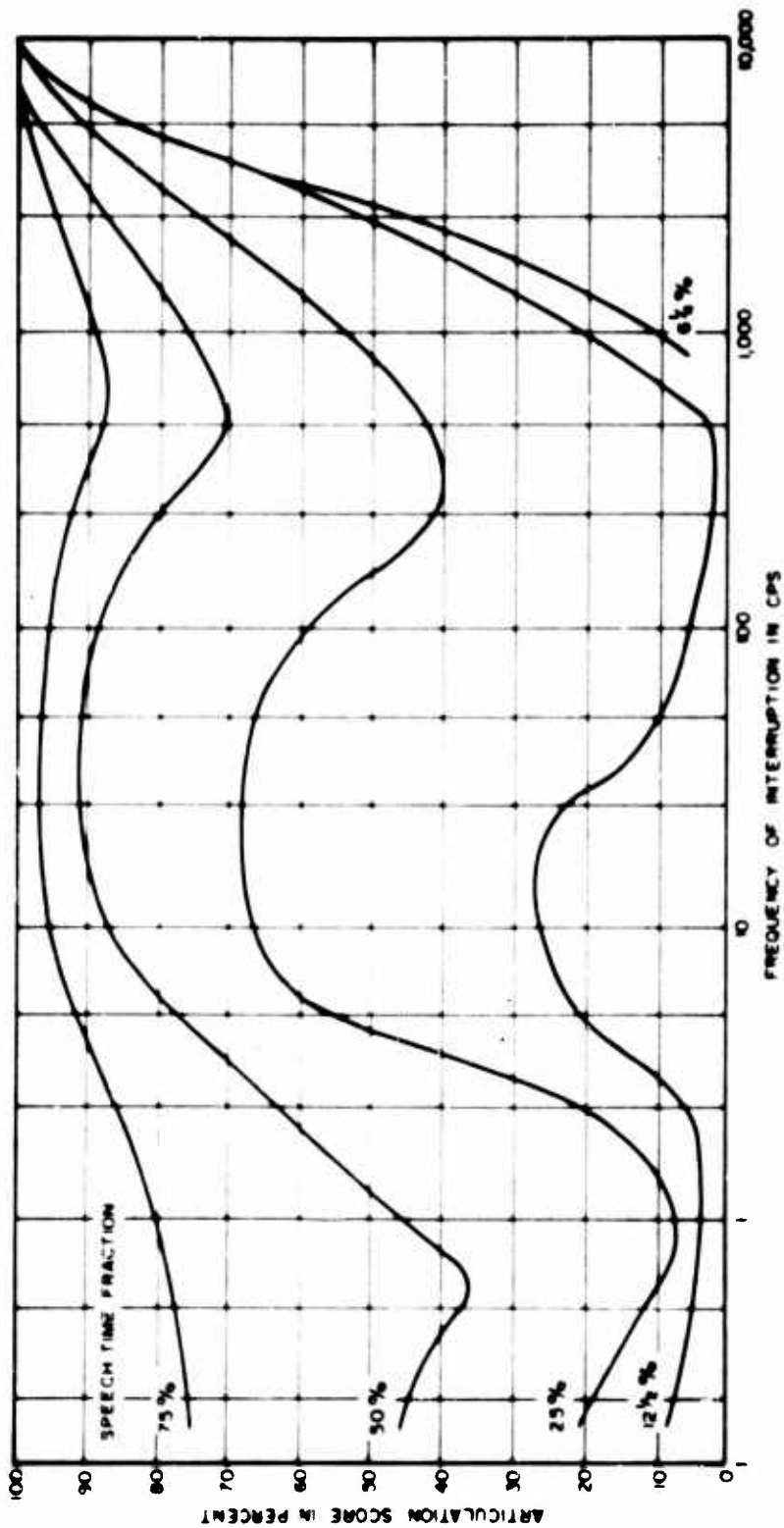


Figure 6-4. Speech Masked by Periods of Silence with Speech Time Fraction as the Parameter

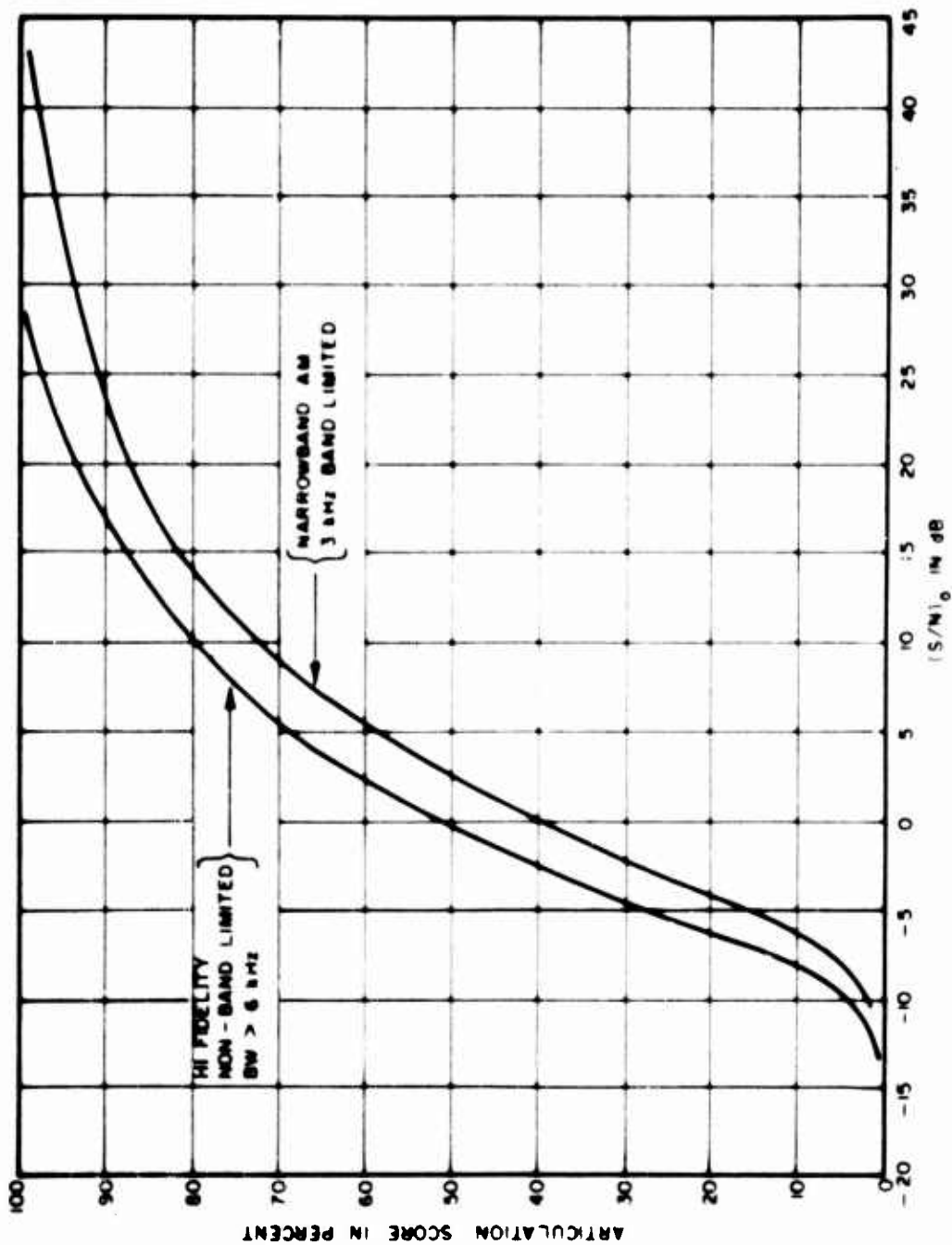


Figure 6-5. Articulation Score for Speech Masked by White Noise

This section has discussed voice intelligibility in terms of AS scores. The articulation index (AI) was also used in this investigation to measure the relative performance degradation of voice systems (AI is discussed in Appendix IV). The relationship between AS and AI is therefore desired and is shown in Figure 6-6 for the average of the pulse width and pulse rates considered in this investigation. This figure shows that the AI score does not correspond directly to intelligibility in terms of AS (a 45° line would indicate an ideal correspondence). This also indicates that the AI values used to indicate performance levels must generally be interpreted according to Figure 6-6. AI scores of .7 and .3 have generally been used in the literature to specify the point at which intelligibility is starting to decrease and the point at which voice communication is unacceptable. These criteria are used because they are good indicators for noise interference and because they are reasonably good indicators for continuous modulated interference. Table 6-2 compares the .3 and .7 AI values for noise, continuous modulated interference and pulsed interference. The values for the non-pulsed interference were obtained from Reference 25. This table shows that the .7 and .3 AI values cannot be specifically related to the same level of intelligibility in terms of AS unless the type of interference is specified. The table does, however, show that the difference in AS for the .7 AI criterion and different types of undesired signals is small (12%). This criterion, therefore, results in a reasonable constant standard in terms of AS intelligibility scores. The .3 AI criterion, however, can result in AS scores that vary between 11 and 97%. Therefore, the type of interference needs to be specified in order to reasonably determine a lower acceptability threshold.

Since the AS score is 97% for pulsed interference and a .3 AI criteria, it appears that another AI criteria could be used for the lower acceptability threshold. In particular, an AI criteria of .1 still results in an AS score of 86% and appears to be a reasonable choice for a lower threshold. However, it was observed in the course of this investigation that, although the AS score for a .1 AI criteria is acceptable in terms of intelligibility, the interference was extremely annoying or fatiguing. Therefore, an AI criteria lower than .3 should not be used unless the fatigue or annoyance factor is not considered to be important.

In general, it was concluded that for pulsed interference only the .7 AI threshold level should be used as a general indicator of an acceptability threshold. This level denotes the point at which intelligibility is starting to decrease. AI scores lower than this value still denote high intelligibility levels and do not conveniently define the lower acceptability threshold.

DEGRADATION WITH PULSE RATE

The following is a discussion of how degradation is related to the pulse repetition frequency (PRF) of the interfering signal and how this trend can be conveniently modeled.

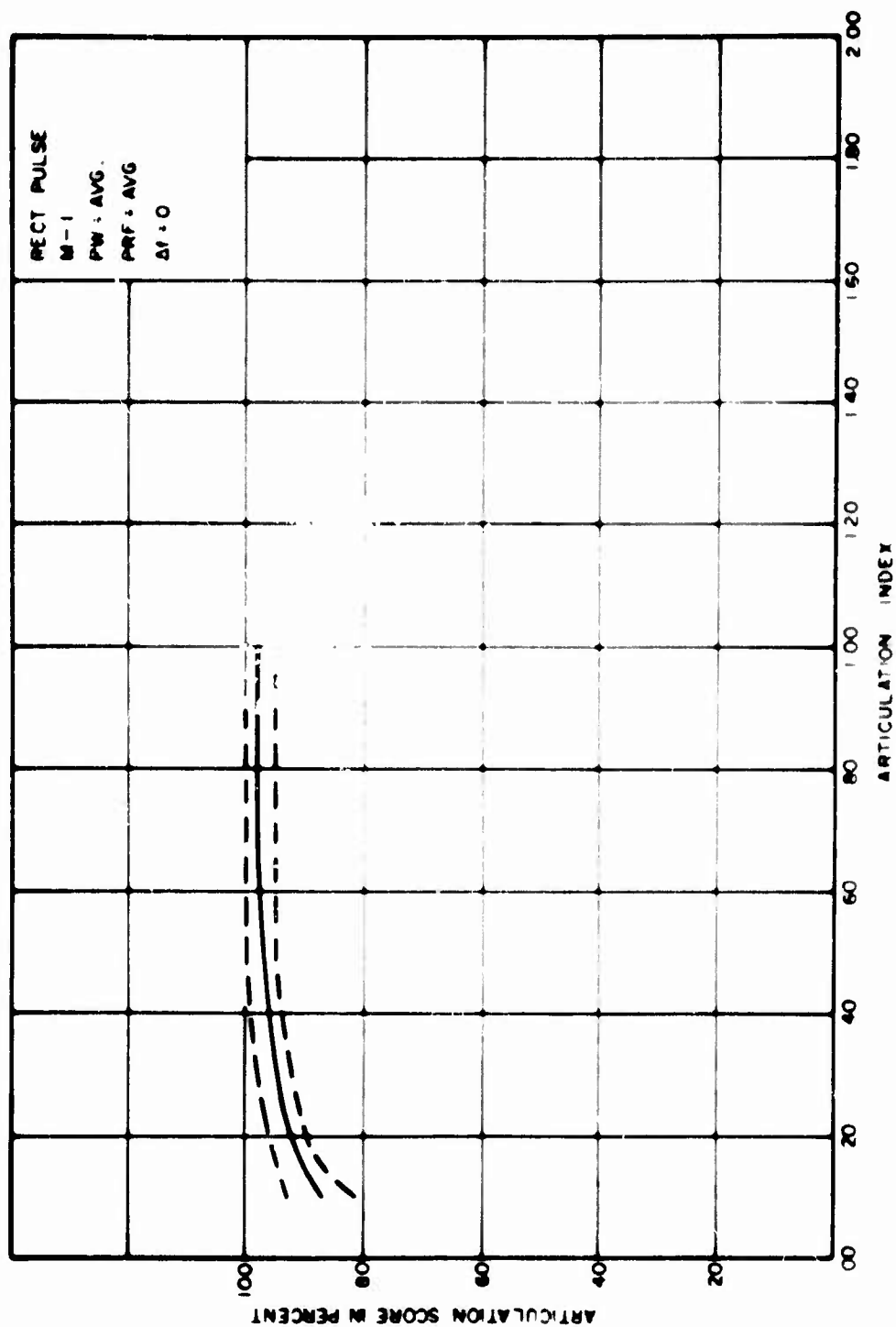


Figure 6-6. Articulation Score Versus Articulation Index for an AM Receiver

TABLE 6-2
ARTICULATION INDEX VERSUS ARTICULATION
SCORE FOR DIFFERENT TYPES OF INTERFERENCE

	Theoretical Noise Interference	VIAS Noise Interference	VIAS Continuous Modulated Interference	VIAS - Pulsed Interference
.7 AI	96% AS	87% AS	(86 94)% AS	98% AS
.3 AI	73% AS	47% AS	(11 38)% AS	97% AS

Figure 6-7 shows the input (S/I) ratio for a constant degradation criteria as a function of the PRF for non-chirped, rectangular pulse interference. These curves were plotted using on-tune data for pulse-widths of 5, 100, 200 and 1,000 μsec . An AI score of .8 was used as the degradation criterion and represents a median level of voice intelligibility. The on-tune data was analyzed since it does not require an additional off-tune filter power correction factor. The receiver simulation process described in Section 4 was used to obtain the data since the measurements did not cover a sufficiently wide range of pulse parameters.

Figure 6-7 indicates that for PRF's between 10 and 400 pps the required input signal-to-peak interference is increasing at the rate of

$$(S/I)_2 = 10 \log \left(\frac{\text{PRF}_2}{\text{PRF}_1} \right) + (S/I)_1 \quad (6.1)$$

where

$$(S/I)_{1,2} = \text{the } (S/I) \text{ in dB at PRF 1 and 2}$$

$$\text{PRF}_1 = \text{the lower value of PRF}$$

$$\text{PRF}_2 = \text{the higher value of PRF}$$

The range in which this equation is valid covers the PRF range encountered in most radars from the newer low PRF, chirped radars to the higher PRF, conventional search radars.

The increase in the (S/I) ratio is directly proportional to the increase in the average interference power. A doubling of the PRF will decrease the number of line spectra by one half and increase their respective (voltage) amplitudes by a factor of two thereby causing the average power to double. This increase in average interference power necessitates an equal increase in the desired signal power in order to maintain a constant level of AI. The increase is linear up to a PRF of 400 pps and could be extended to a PRF of 1,000 pps with less than 2 dB error. The reason for this can be readily explained with the aid of Figure IV-2 which shows the cut-off frequencies for the 14 frequency bands used in calculating AI. For low PRF's the pulsed interference line spectra are present in all 14 of the frequency bands used to calculate AI. As the PRF increases fewer line components of the pulse spectra are contained in the frequency bands. For PRF's above 400 pps a number of frequency bands do not contain any line spectra. This results in a decrease in the effective interference power and a corresponding decrease in the (S/I) ratio necessary to maintain a constant level of AI.

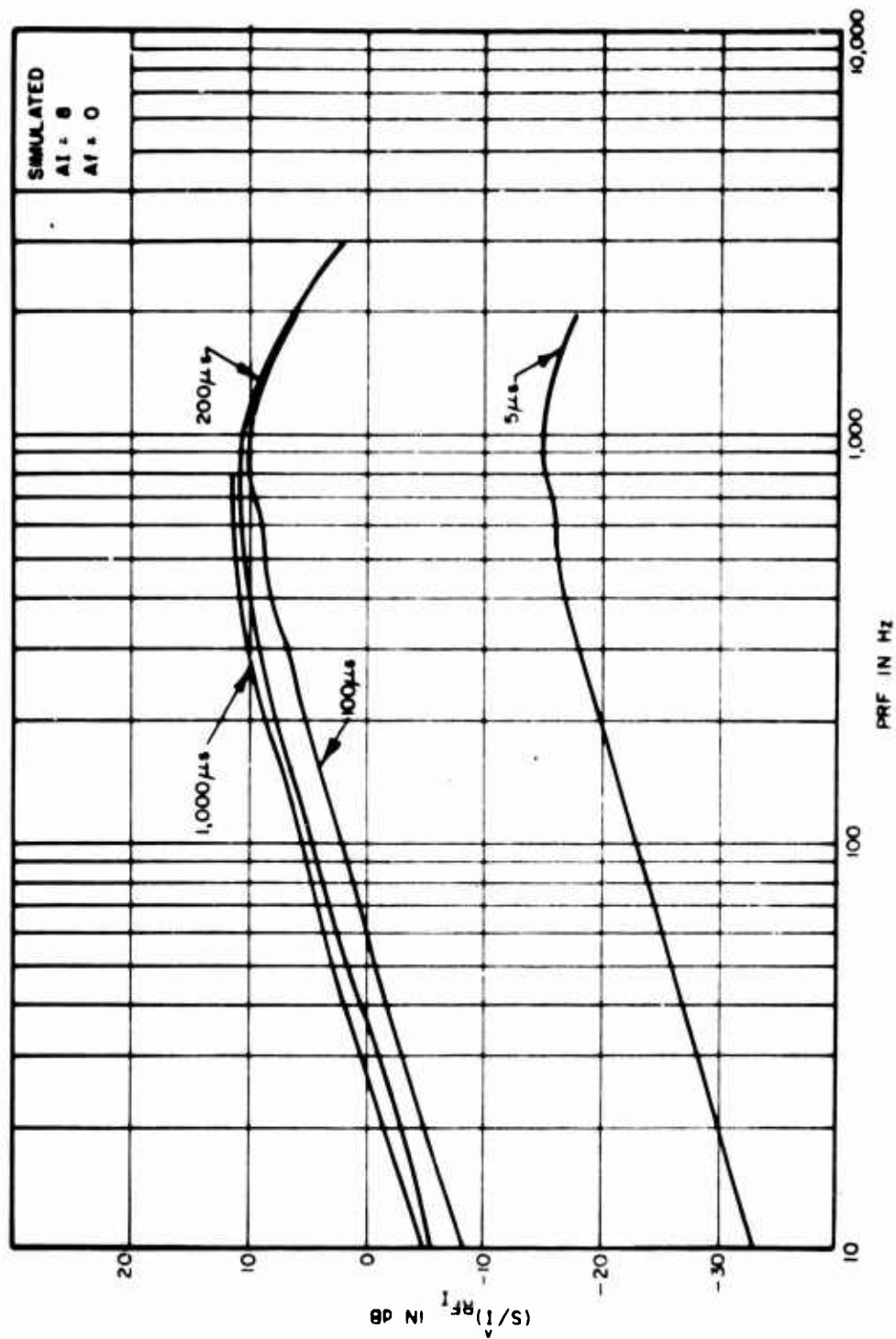


Figure 6-7. Input Signal to Peak Interference as a Function of PRF

Figure 6-7 also indicates that all pulse widths greater than $200 \mu\text{sec}$ create approximately the same performance degradation. Pulse width parameter variations are discussed later in this section.

Figure 6-8 shows how the AI score varies as a function of the PRF, PW and input (S/\hat{I}). The curves show that for a given (S/\hat{I}) ratio, there is a linear decrease in the value of AI up to approximately 400 pps and then a linear increase in AI as the PRF is increased above 400 pps. This is as expected since Figure 6-7 shows that the effective level of interference increases with an increase in PRF up to approximately 400 pps and then decreases as the PRF increases above 400 pps. The curves also show that for the higher (S/\hat{I}) levels ($> 10 \text{ dB}$) the maximum interference occurs at approximately 400 pps and at lower (S/\hat{I}) levels ($< 0 \text{ dB}$) the maximum interference occurs at approximately 300 pps. This effect appears to be caused by the upward spread of masking as the intensity of the interference is increased.

The AS data as a function of PRF for receiver number two is shown in Figures 6-9 and 6-10. Figures 6-9 and 6-10 indicate that the voice intelligibility in terms of AS, which is related to the AI score as previously discussed, is also degraded proportional to the PRF. This is due to the approximate uniform masking of the voice by the PRF lines across the baseband spectrum. The AS data was limited to extremely high AS scores (approximately 99%) and therefore was difficult to use in accurately indicating this trend. The first figure shows AS as a function of PRF for individual PW's and the second for an average of all the PW's. The data generally indicated a decrease in AS as the PRF increases. The change was, however, small enough (5%) that the effect of PW on AS can be neglected for most practical voice problems.

In summary, for fixed AI scores the input (S/\hat{I}) ratio is proportional to the log of the PRF from 10 to 400 pps and is approximately proportional up to 1,000 pps. The AI and the AS voice degradation measures also are proportional to the log of the PRF although the variation in AS is negligible for most problems.

DEGRADATION WITH PULSE WIDTH

The following is a discussion of how degradation is related to the interference pulse width (PW) and how this trend can be divided into different modeling categories.

Figures 6-11 and 6-13 show how AM degradation, caused by non-chirped rectangular pulse interference, is a function of the pulse width of the interfering signal. The data used in these figures was obtained from the receiver simulation process described in Section 4. Figure 6-11 is a plot of input (S/\hat{I}) versus PW for a constant PFR, Δf and AI. This shows an increase in the required input (S/\hat{I}) as the PW is increased. This trend is due to IF and baseband filter effects and is discussed in Section 4.

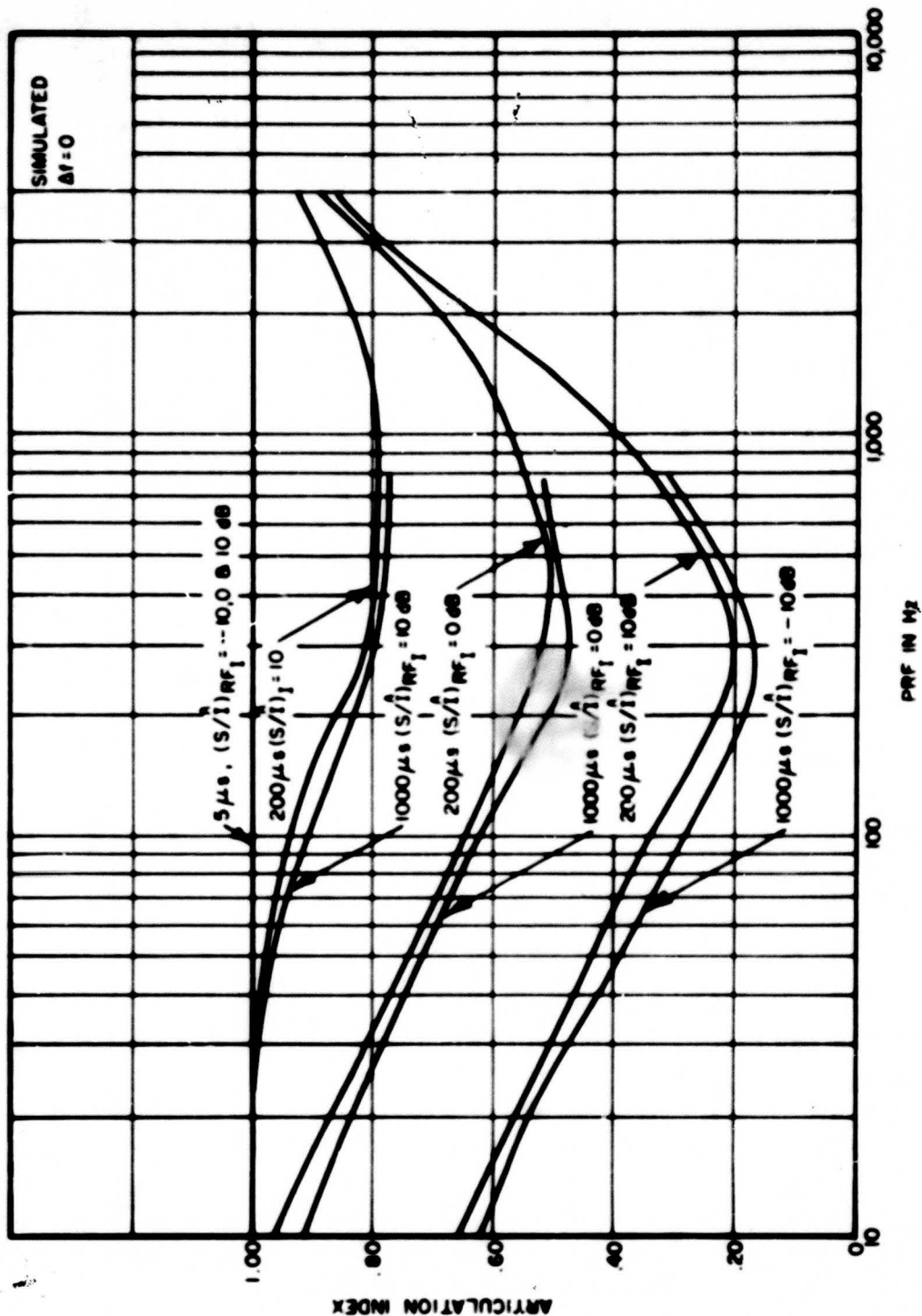


Figure 6-8. Articulation Index as a Function of PRF

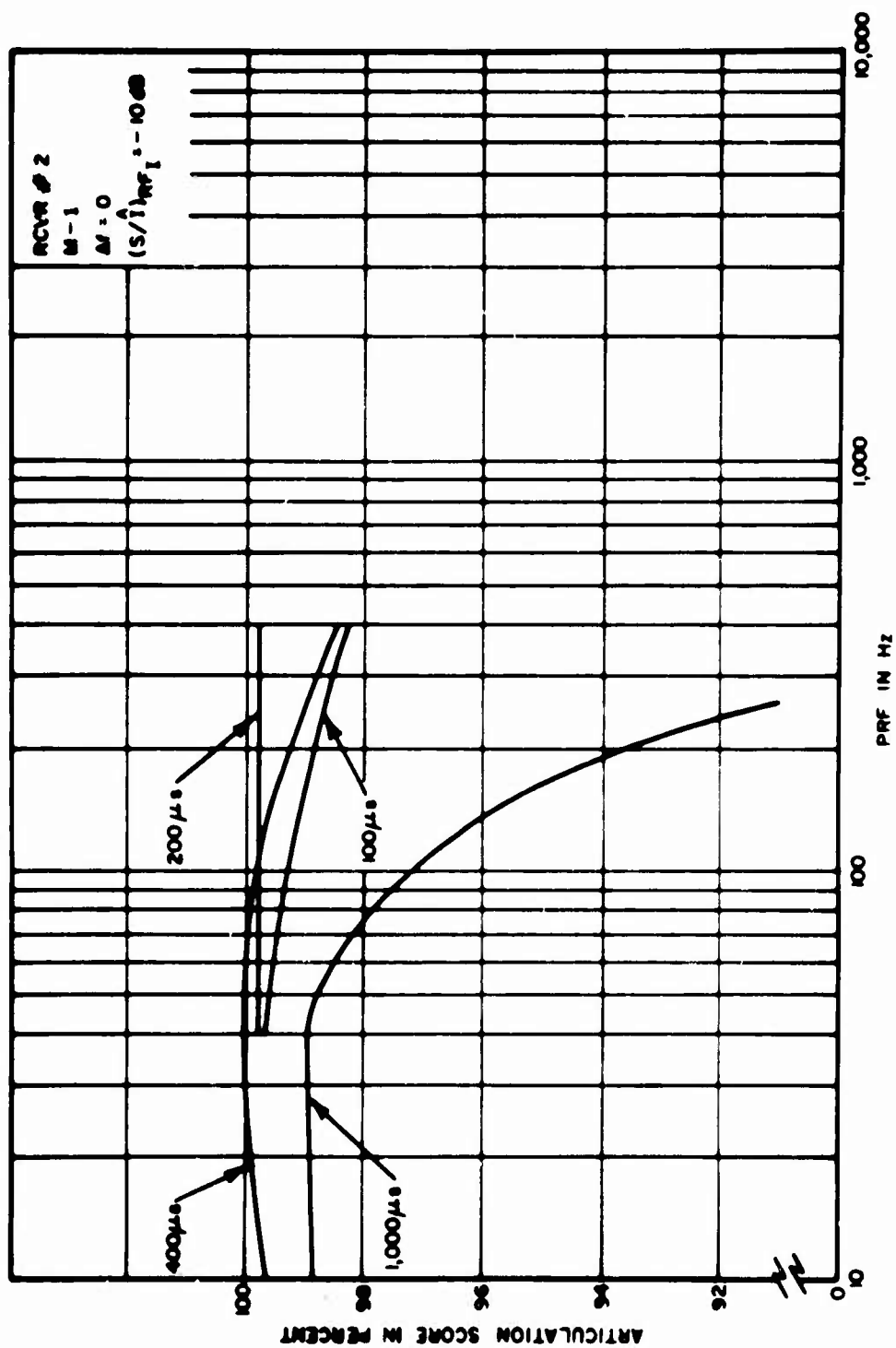


Figure 6-9. Articulation Score as a Function of PRF

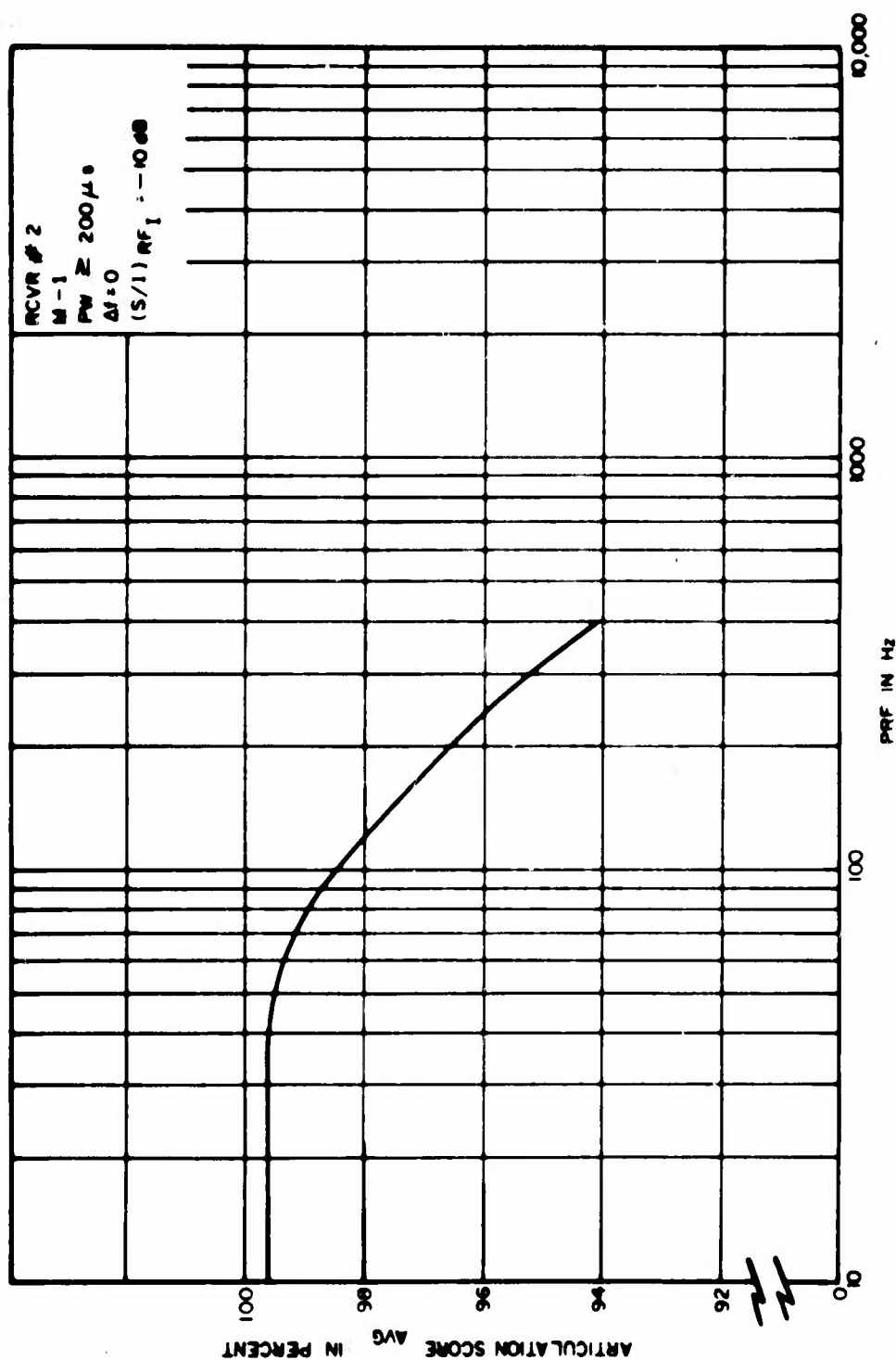


Figure 6-10. Average Articulation Score (AS) as a Function of PRF

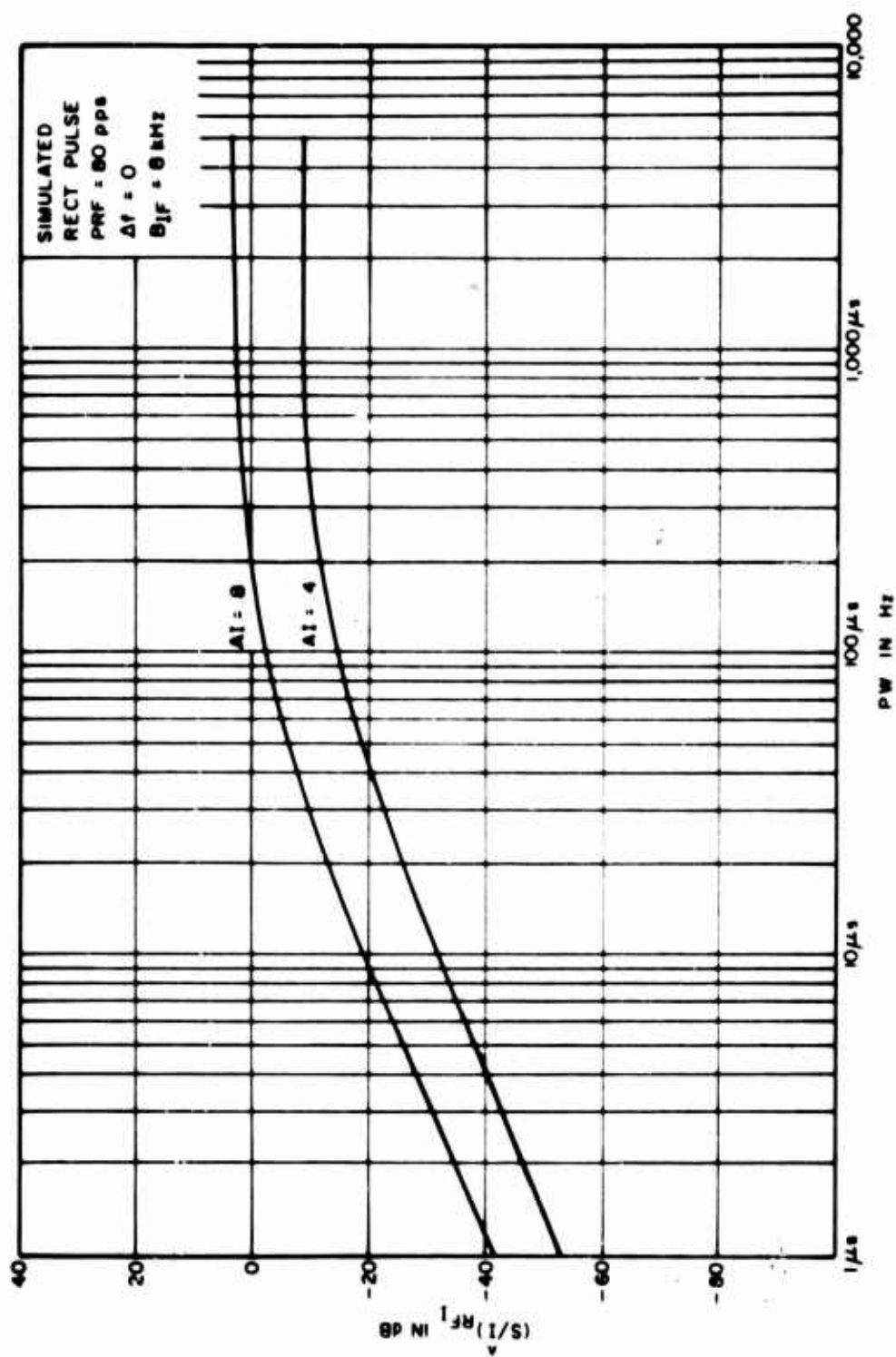


Figure 6-11. Input Signal to Peak Interference as a Function of Pulse Width

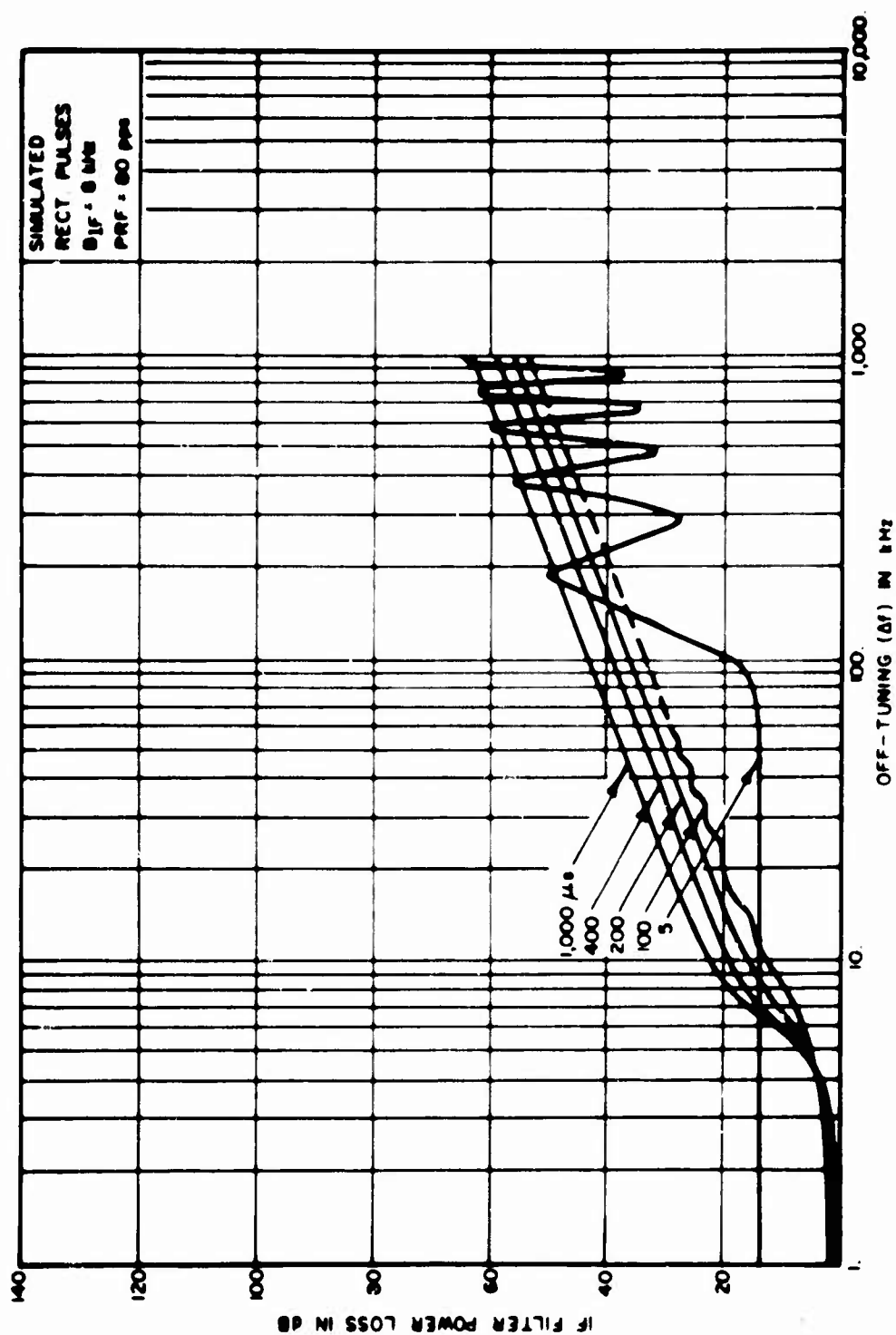


Figure 6-12. IF Filter Power Loss Transfer Function

When the input pulse has a spectrum wider than the IF bandwidth, a portion of this energy is lost at the IF output. This effect is shown in Figure 6-12 for an IF bandwidth of 8 kHz. The difference between the input and output energy is plotted as a function of off-tuning for various pulse widths. This figure shows that for on-tune PW's narrower than about 100 μ sec (the inverse of the IF bandwidth) the power loss is approximately,

$$\frac{P_o}{P_i} = 10 \log (B_{IF} \tau) \quad (6-2)$$

where

τ = The input pulse width

B_{IF} = The IF bandwidth

This figure also shows the characteristic spectrum envelope fall-off of 20 dB per decade. The 5 μ sec pulse also shows this spectrum fall-off for the upper or lower envelope although in general the response follows the peaks and nulls. This means the results from the narrow pulse case must be carefully specified to insure that off-tuning values are not on peaks and nulls of the spectrum or inconsistent off-tuning patterns will result.

The amount of power or energy passed through the various filtering sections is primarily a function of the IF and audio bandwidths. Since the case being considered has an IF bandwidth approximately twice the audio bandwidth (the IF BW = 8 kHz; the audio BW = 3 kHz) only slight additional filtering should be obtained from the audio filter (see Section 4). For the on-tune case in which the IF bandwidth is much greater than twice the audio bandwidth, most of the filtering is introduced by the audio bandwidth for pulse bandwidths equal to or less than the IF bandwidth. For the present problem, pulse widths greater than 100 μ sec do not completely pass the audio filter. Figure 6-13 shows that, in terms of AI, the score gradually decreases until about a 300 μ sec pulse width is reached.

In summary, the input (S/I) ratio required for a constant AI value increases linearly with the log of the PW up to the inverse of twice the baseband bandwidth. Pulses wider than this pass through the system and act similarly in their degradation effect. This is illustrated in Figure 6-13, which shows degradation in terms of AI as a function of PW. These curves go asymptotically to AI values of .36 and .20 independent of the larger pulse widths.

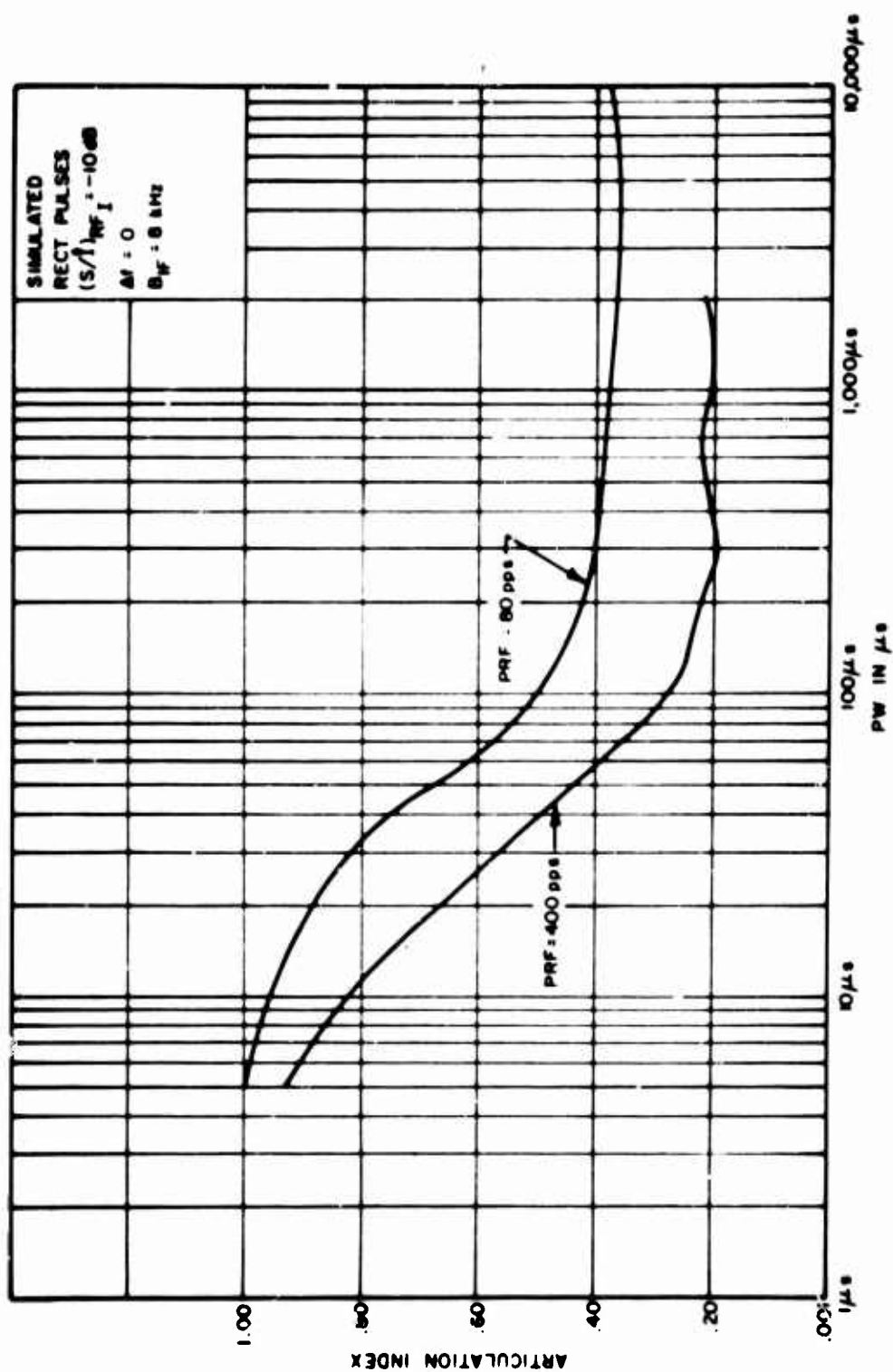


Figure 6-13. Articulation Index as a Function of Pulse Width

DEGRADATION WITH CHIRPED AND NON-CHIRPED PULSES

The following is a discussion of how degradation is related to the chirp rate of the rectangular pulse and how this trend can be conveniently modeled. Curves of input (S/\hat{I}) versus Δf for constant values of A_I and different chirp rates are shown in Figures 6-14 through 6-17. Figures 6-14 and 6-15 were plotted for pulse widths of 100 and 200 μsec and a chirp rate of 0.5 MHz. Figures 6-16 and 6-17 were plotted for pulse widths of 200 and 400 μsec and a chirp rate of 250 kHz. The PRF was 400 pps for the 100 and 200 μsec pulses and 40 pps for the 400 μsec pulse. The data used in these figures was obtained from the receiver simulation process described in Section 4 since the measurements did not cover a sufficiently wide range of pulse parameters. The limited measured data compares favorably with the simulated data and therefore no appreciable errors are expected from introduction of the simulated data. The curves of Figures 6-14 through 6-17 show that for a given value of A_I the input (S/\hat{I}) ratio is constant out to a given frequency Δf_1 . There is a sharp fall-off between Δf_1 and a second frequency Δf_2 . The fall-off above Δf_2 is at a rate of approximately 20 dB/decade.

At this point it is interesting to compare the off-tuned degradation trend with the chirped spectrum. A typical rectangular, chirped pulse spectrum was constructed using the procedures outlined in References 26 and 27 and is shown in Figure 6-18. The shape of the spectrum appears to follow very closely the shape of the degradation curves. It is shown in these references that the critical frequencies, Δf_1 and Δf_2 , are a function of the chirp rate and pulse width. The initial critical frequency, Δf_1 , is approximately

$$\Delta f_1 = \frac{B_t}{2} - \left(\frac{B_t}{2\tau_b} \right)^{1/2} \quad (6-3)$$

where

B_t = the total frequency deviation

τ_b = the transmitted pulse width

The second critical frequency (where the 20 db/decade fall-off begins) is approximately equal to the total frequency deviation and is given by:

$$\Delta f_2 = B_t \quad (6-4)$$

The critical frequencies, Δf_1 and Δf_2 , and fall-off's for the degradation curves correspond to the critical frequencies and fall-off's for the chirped pulse spectrum. These critical

frequencies and fall-off's indicate the degradation caused by chirped pulses is proportional to the *interference power within the receiver passband* since the contour curves fall off at the same rate as the pulse spectrum.

A convenient method for modeling the effects of chirped pulses would be to determine the amount of inband pulse power for a given chirped pulse and then relate this to an equivalent amount of power for the same pulse without chirp. To accomplish this, the equivalent curves for Figures 6-14 through 6-17 for non-chirped pulses were obtained and are shown in Figures 6-19 through 6-21. In order to determine the inband pulse power, the power loss in the IF filter was determined using the computer simulation model for both the chirped and non-chirped pulses. The non-chirped power loss transfer function was previously given in Figure 6-12. The 250 and 500 kHz chirp power loss transfer functions are given in Figures 6-22 and 6-23, respectively.

Using the curves of Figures 6-14 through 6-23, the inband power was obtained for the *on-tune* chirped and non-chirped pulses. The data is tabulated in Table 6-3 and shows there is an average of 3 dB more inband interference power for non-chirped pulses than for chirped pulses for a given AI performance level. This also shows that the chirped pulse requires an average of 3 dB inband higher signal-to-interference power ratio than the non-chirped pulse for the same system performance.

In order to calculate the equivalent inband power for various off-tuned values, it is necessary to normalize the off-tune values for chirped and non-chirped pulses so they are equivalent. The breakpoint frequency for rectangular non-chirped pulses that have a τB_{IF} product less than 0.64 is approximately $1/\pi\tau$ (reference 28). When the τB_{IF} product is equal to or greater than 0.64 the breakpoint frequency is approximately one half the IF bandwidth. The equivalent breakpoint frequency for the chirped pulse is equal to the maximum chirp frequency. It is, therefore, necessary to normalize the chirped off-tune frequency, for Δf values greater than the maximum chirp frequency, by the ratio of the non-chirped breakpoint frequency to the maximum chirp frequency. That is,

$$\Delta f_{NC} = \frac{f_m \Delta f_c}{\beta_t} \quad (6-5)$$

where

$$\Delta f_{NC} = \text{off-tuning for non-chirped pulse}$$

$$f_m = 1/\pi\tau \text{ or } B_{IF}/2$$

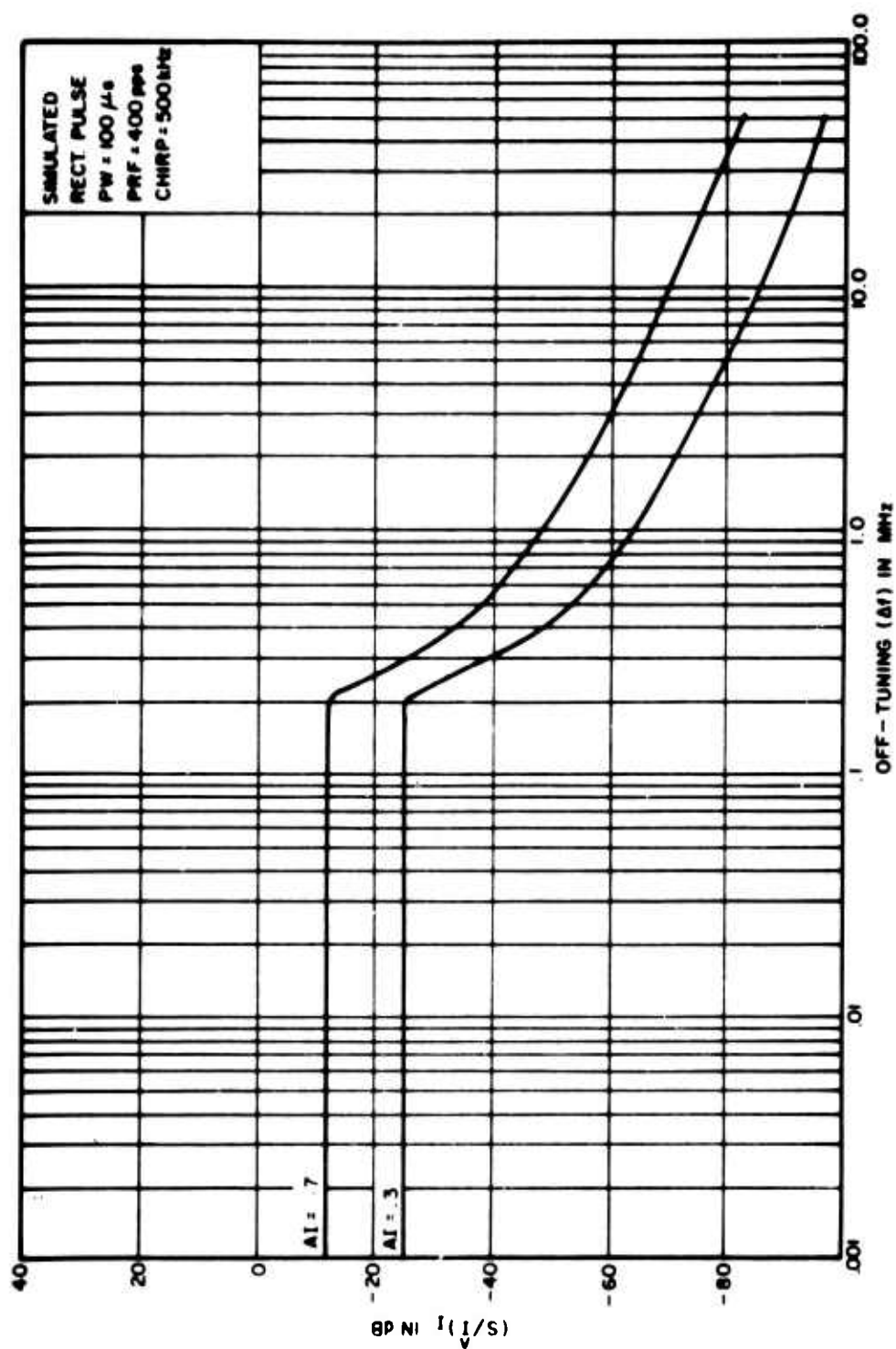


Figure 6-14. Input Signal to Peak Interference as a Function of Δf

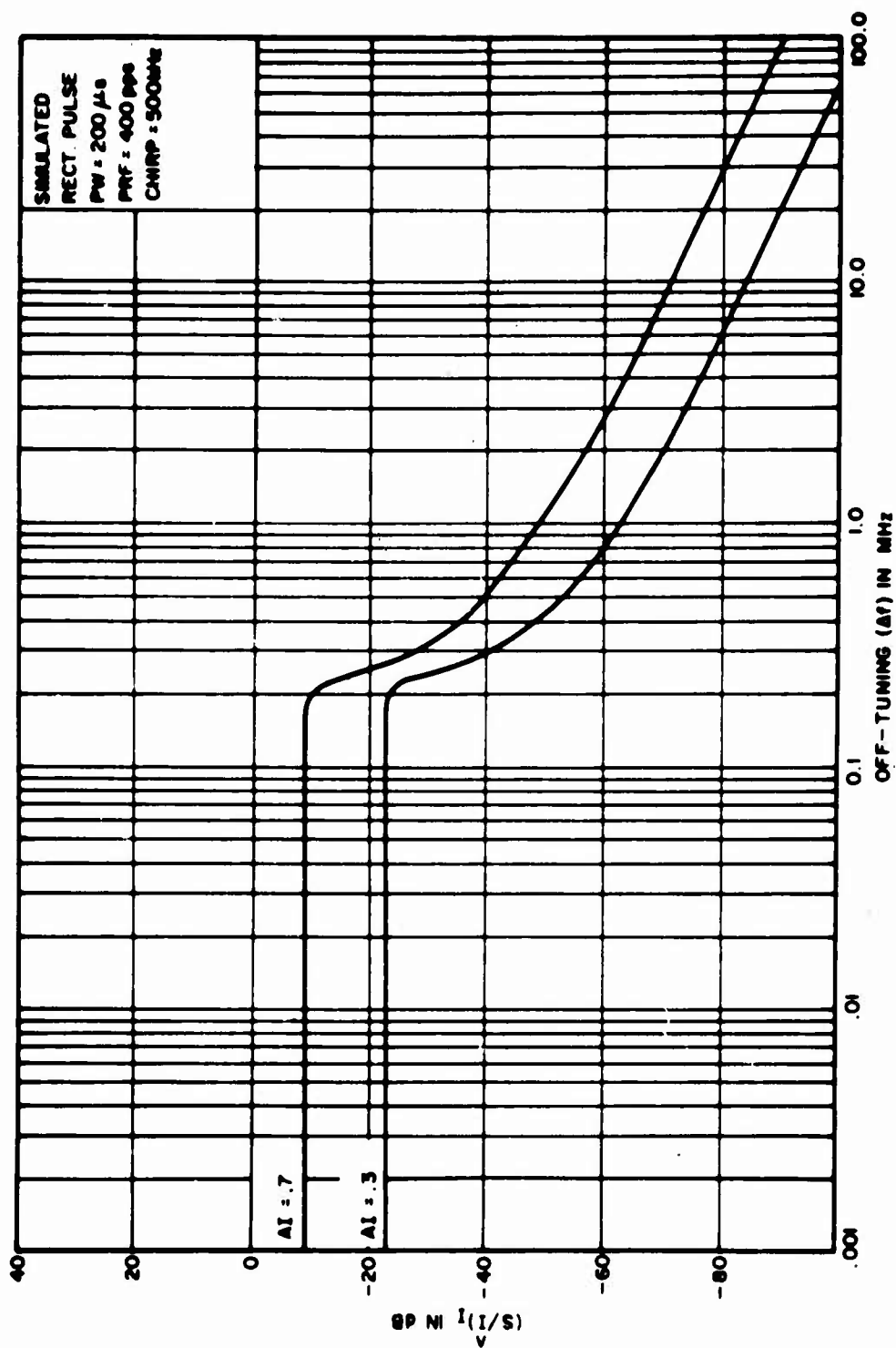
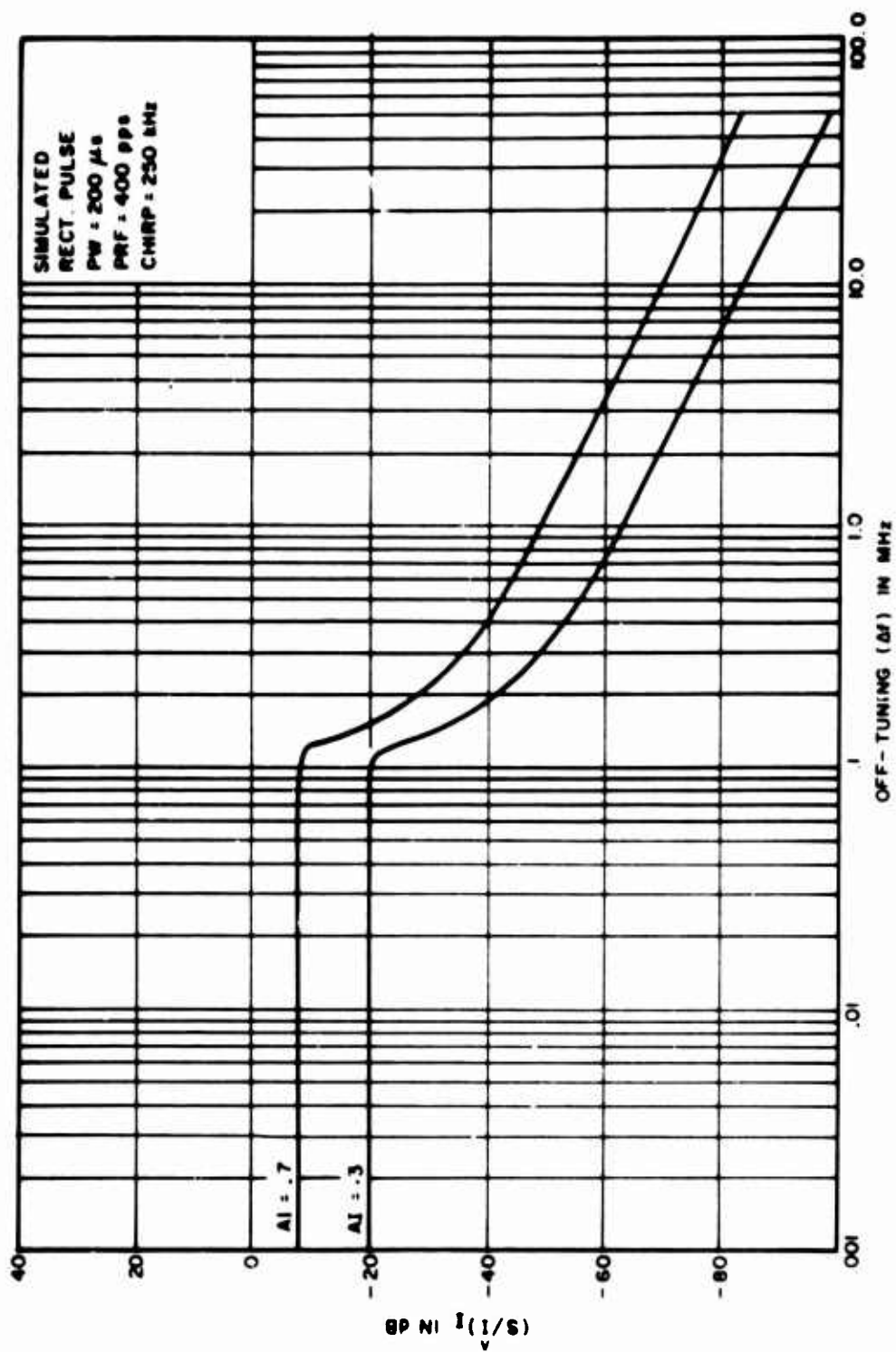


Figure 6-15. Input Signal to Peak Interference as a Function of Δf

Figure 6-16. Input Signal to Peak Interference as a Function of Δf

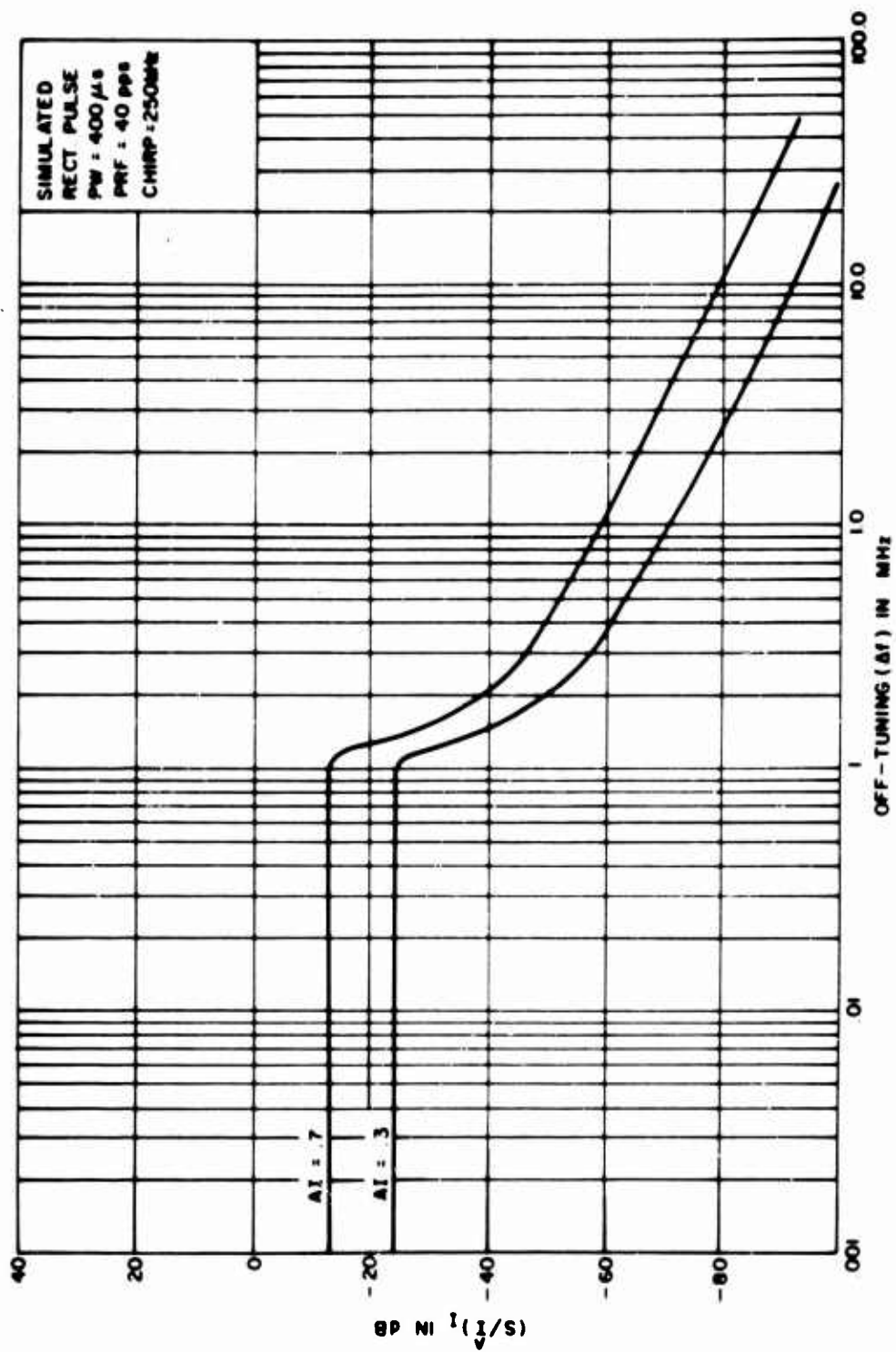


Figure 6-17. Input Signal to Peak Interference as a Function of Δf

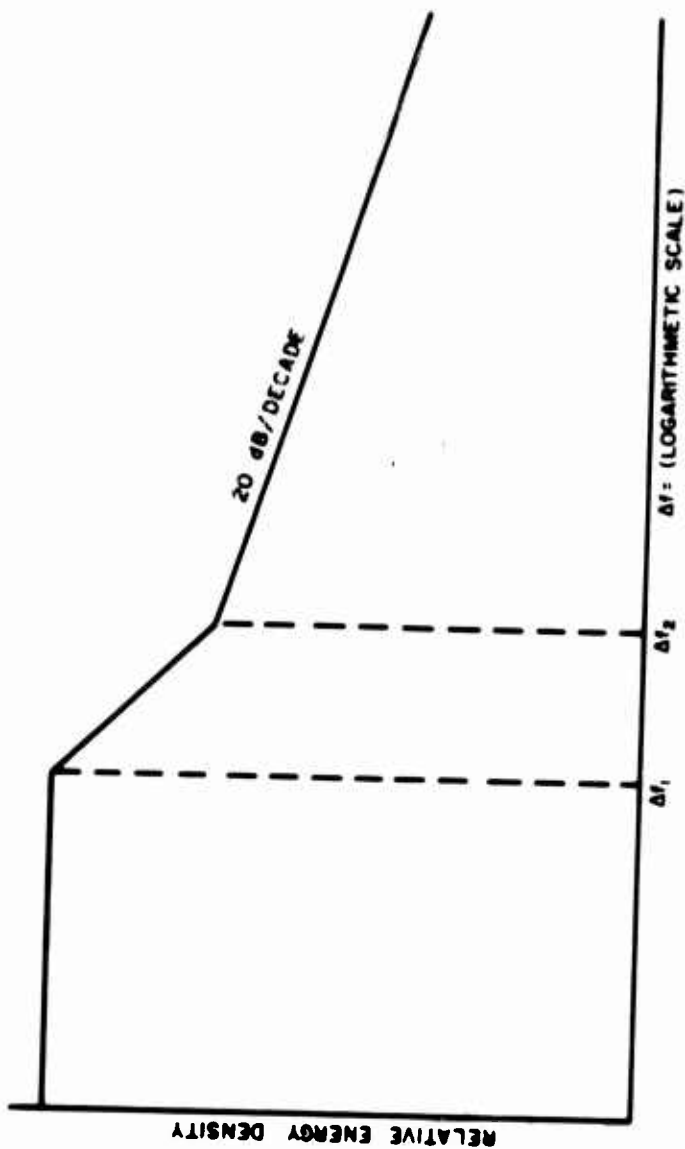


Figure 6-18. Envelope of Idealized Chirped Spectrum

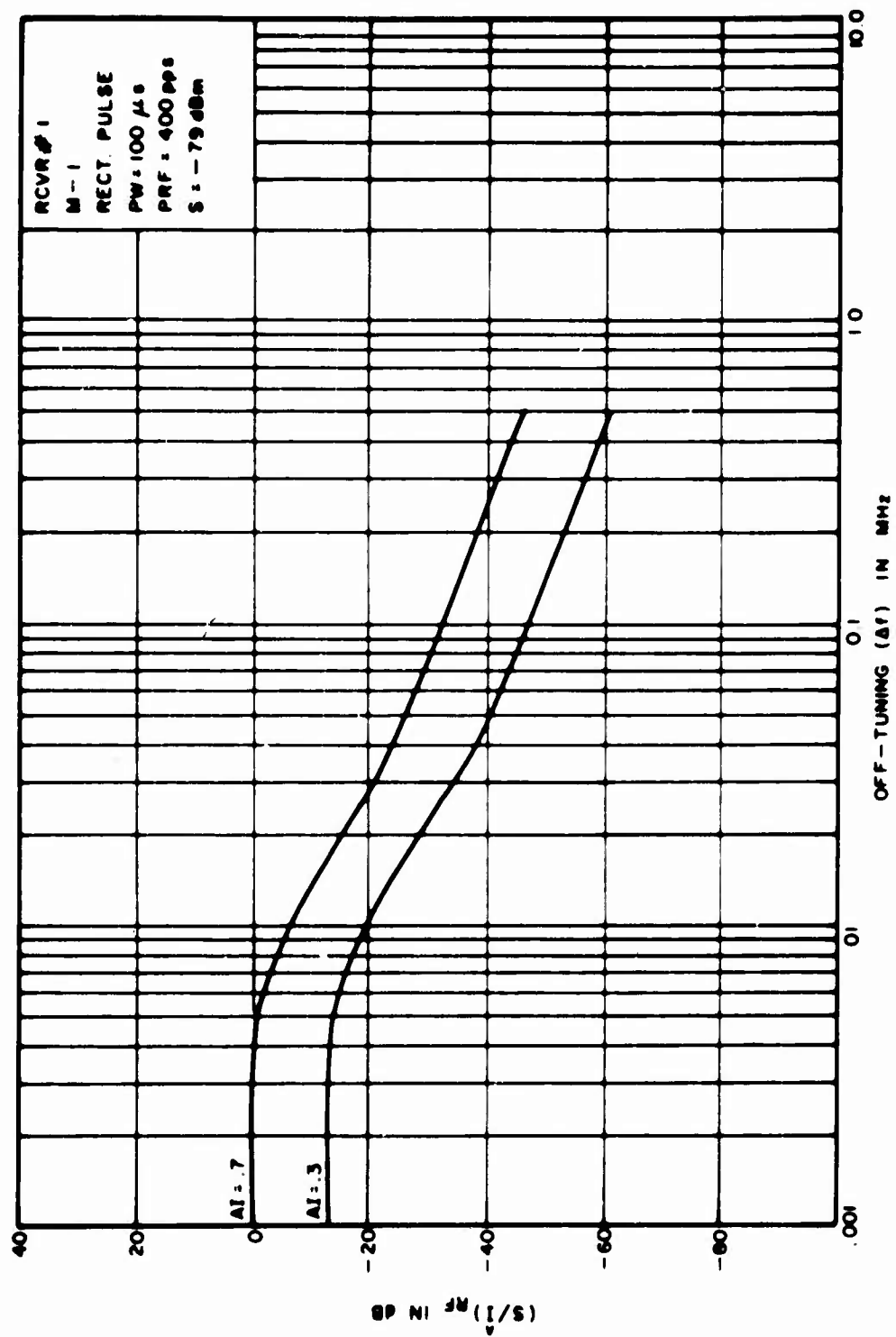


Figure 6-19. Input Signal to Peak Interference as a Function of Δf

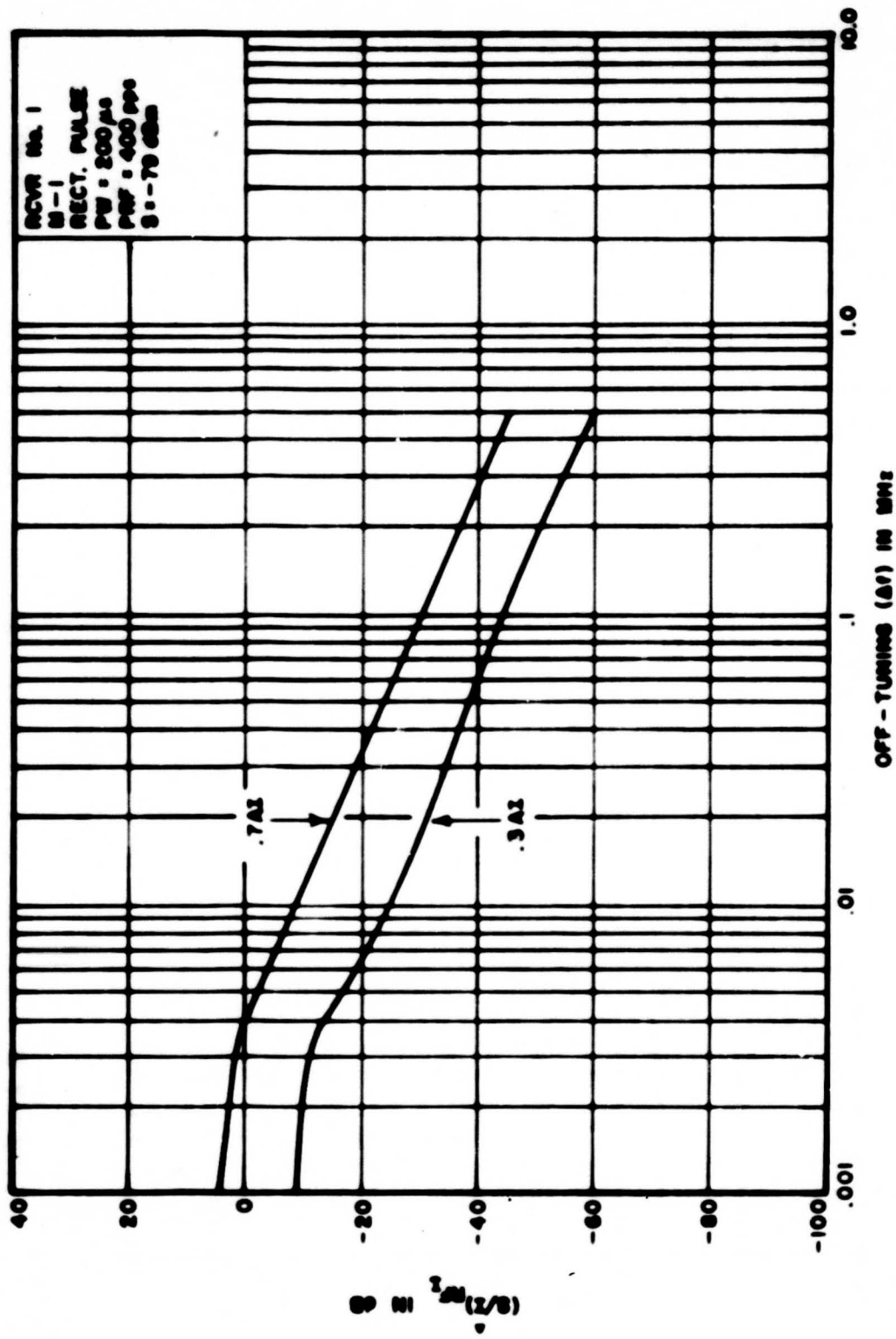


Figure 6-20. Input Signal to Peak Interference as a Function of Δf

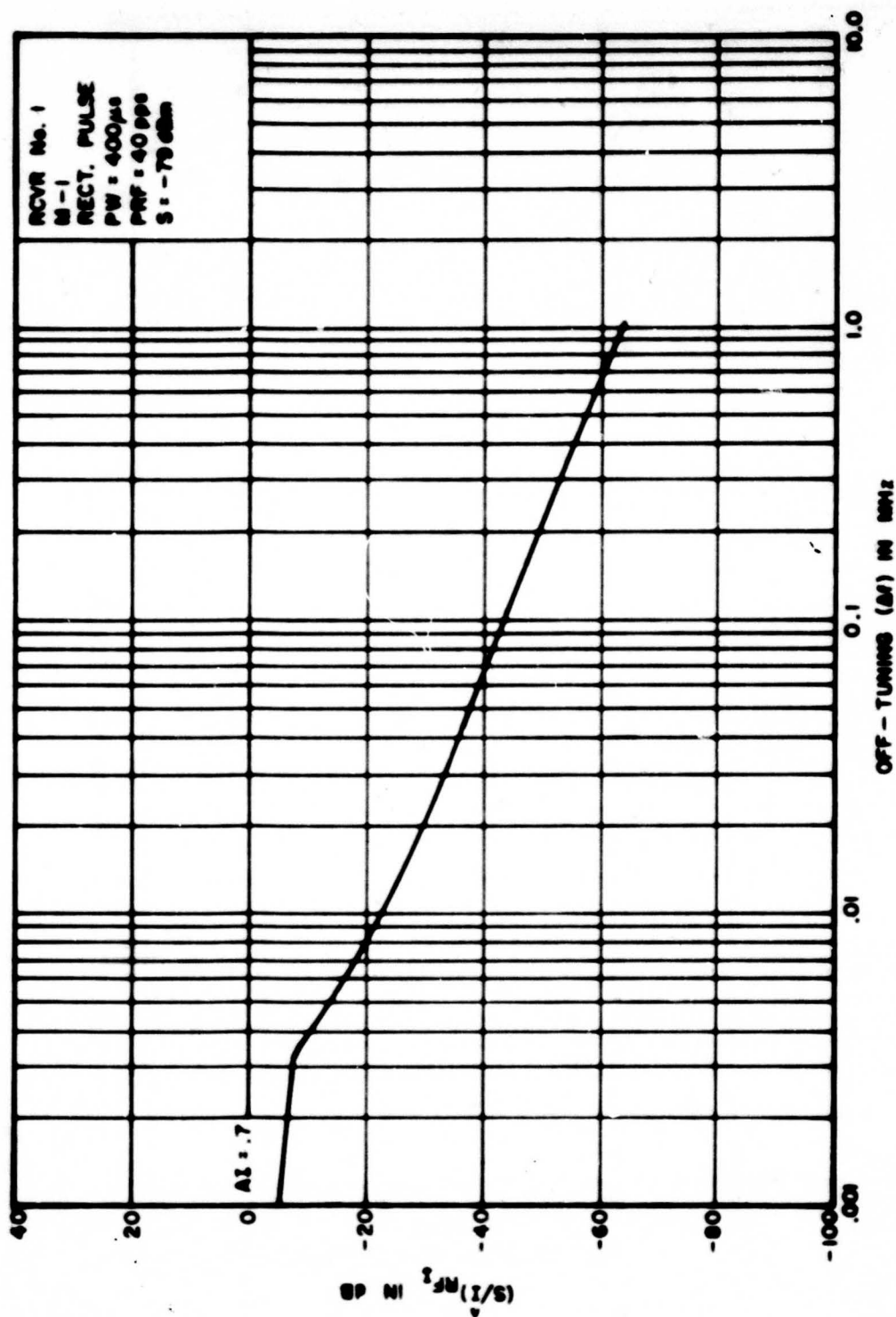


Figure 6-21. Input Signal to Peak Interference as a Function of Δf

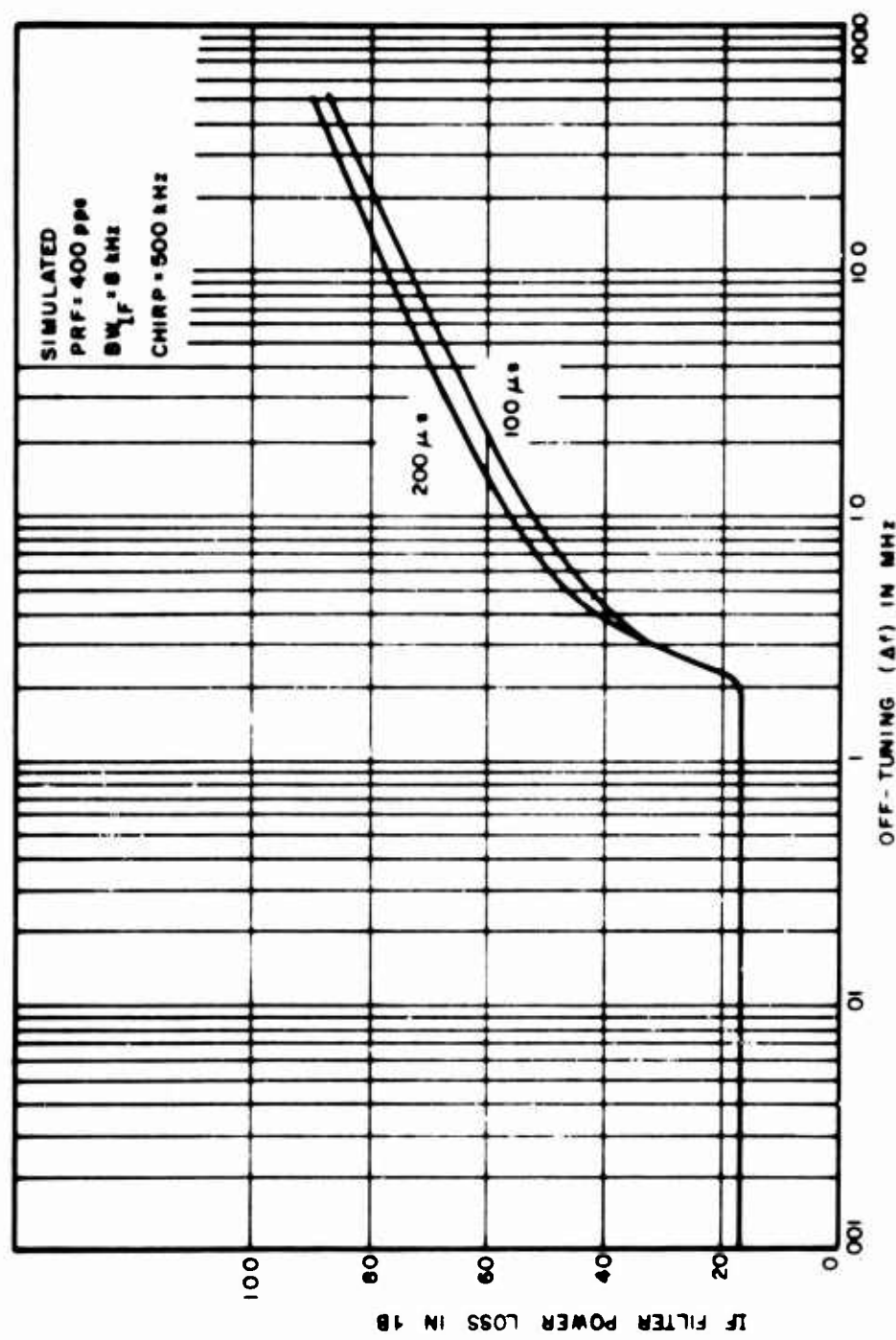


Figure 6-22. IF Filter Power Loss Transfer Function

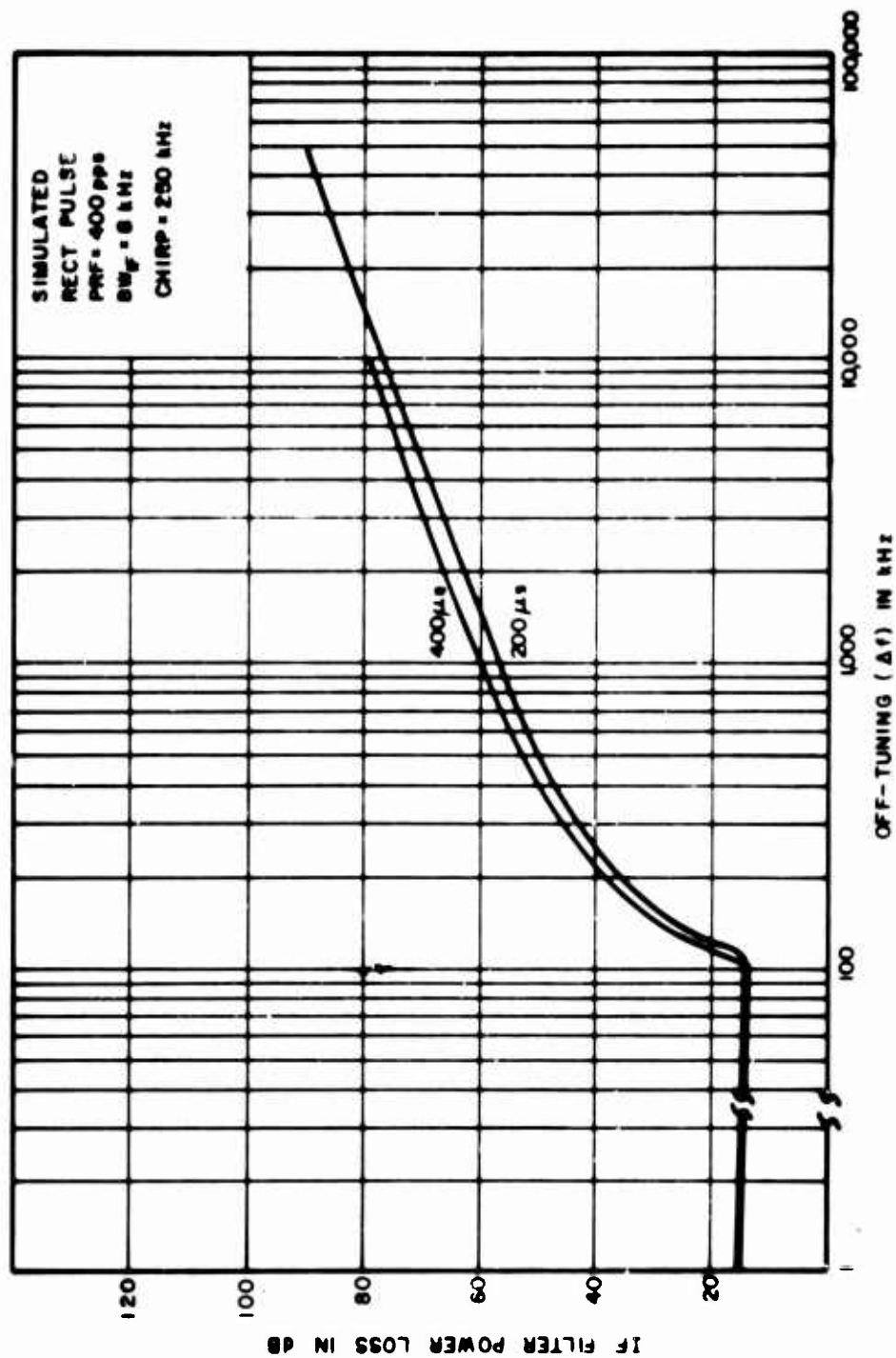


Figure 6-23. IF Filter Power Loss Transfer Function

TABLE 6-3
COMPARISON OF INBAND POWER FOR
CHIRPED AND NON-CHIRPED PULSES

Pulse Width	PRF (pps)	Δf (Chirp)	Δf (Non-chirp)	IF BW	AI	Chirp (MHz)	(S/I) RF (Chirp)	(S/I) RF (Non-chirp)	IF Filter Loss in dB (Chirp)	IF Filter Loss in dB (Non-chirp)	In Band S/I (Chirp)	In Band S/I (Non-chirp)	In Band Power Difference
100 μ s	400	0	0	8 kHz	.7	.5	-12	0	17	2.0	5.0	2.0	3.0
					.3		-25	-13	17	2.0	-8.0	-11.0	3.0
200 μ s	400	0	0	8 kHz	.7	.5	-9	4	17	.7	8.0	4.7	3.3
					.3		-23	-9	17	.7	-6.0	-8.3	2.3
200 μ s	400	0	0	8 kHz	.7	.25	-7.5	4	15	.7	7.5	4.7	2.8
					.3		-20	-9	15	.7	-6.0	-8.3	3.3
400 μ s	40	0	0	8 kHz	.7	.25	-13	-5	14	.3	1.0	-4.7	5.7
100 μ s	400	3 MHz	24 kHz	8 kHz	.7	.5	-60	20.5	63.5	24.0	3.5	3.5	0.0
					.3		-74	-34	63.5	24.0	-10.5	-10.0	-0.5
200 μ s	400	3 MHz	24 kHz	8 kHz	.7	.5	-60	-13	67	20.0	7.0	7.0	0.0
					.3		-74	-28	67	20.0	-7.0	-8.0	1.0
200 μ s	400	3 MHz	48 kHz	8 kHz	.7	.25	-60	-26	66	32.0	6.0	6.0	0.0
					.3		-73	-40	66	32.0	-7.0	-8.0	1.0
400 μ s	40	3 MHz	48 kHz	8 kHz	.7	.25	-69	-36	70	33.0	1.0	-2.0	3.0
100 μ s	400	30 MHz	240 kHz	8 kHz	.7	.5	-79	-42	83	44.0	4.0	2.0	2.0
					.3		-93	-56	83	44.0	-10.0	-12.0	2.8
250 μ s	400	30 MHz	240 kHz	8 kHz	.7	.5	-80	-36	86	40.5	6.0	5.5	-0.5
					.3		-94	-48	86	40.5	-7.0	-7.5	0.5
200 μ s	400	30 MHz	480 kHz	8 kHz	.7	.25	-80	-47	86	53.0	6.0	6.0	0.0
					.3		-94	-62	86	53.0	-8.0	-9.0	1.0
400 μ s	40	30 MHz	480 kHz	8 kHz	.7	.25	-89	-57	90	54.0	1.0	-2.0	3.0

Δf_c = off-tuning for chirped pulse

β_t = the total frequency deviation

For a 0.5 MHz chirp rate the equivalent Δf for a non-chirped pulse is given by $\Delta f_{NC} = 2 \times 10^{-6} f_m \Delta f_c$ and for a 250 kHz chirp rate the equivalent Δf for a non-chirped pulse is given by $\Delta f_{NC} = 4 \times 10^{-6} f_m \Delta f_c$. Using these results and the curves of Figures 6-13 through 6-22, the inband power was calculated for chirped and non-chirped pulses for various off-tune values. The data is tabulated in Table 6-2 and again shows that more inband interference power is required for the non-chirped pulse than for the chirped pulse to produce a given AI performance level for equivalent values of off-tuning. The average off-tune increase in interference power required for the non-chirped pulse is 1 dB.

In summary, the chirped pulse requires approximately 2 dB less inband interference power to produce the same system degradation effect as the non-chirped pulse. The inband (S/\hat{I}) ratio for a non-chirped pulse would then be 2 dB less than the inband (S/\hat{I}) ratio for an equivalent chirped pulse. This relationship provides a simplified method for modeling the effect of chirped pulses on an AM receiver.

DEGRADATION WITH OFF-TUNING

The following is a discussion of how degradation can be modeled as the pulsed interference is tuned from an on-tune case ($\Delta f = 0$), to a co-channel case ($\Delta f \leq B_{IF}$) and finally to a far adjacent channel case ($\Delta f \gg B_{IF}$).

Figures 6-24 through 6-31 show the AM degradation curves, with input (S/\hat{I}) versus Δf , for receiver No. 1 and non-chirped rectangular pulse interference. The curves show the RF input (S/\hat{I}) level which corresponds to the minimum threshold level and AI levels of .7 and .3 for various degrees of off-tuning (Δf). An examination of these figures show degradation trends which aid in predicting pulsed interference to AM receivers. The most noticeable trend is the 20 dB per decade fall-off of the minimum interference threshold, .7 AI and .3AI curves. This indicates that the interference level for the off-tuned pulsed interference is determined by the amount of interfering power within the IF passband since the envelope of the power spectrum for non-chirped rectangular pulses falls off at 20 dB per decade. An examination of other types of pulse spectrum revealed the same trend. Namely, if the pulse were a cosine squared pulse with a 60 dB/decade fall-off rate, the degradation curve would also fall-off at 60 dB/decade.

The slope of the degradation curve shown in Figure 6-31 is more than 20 dB per decade. The reason for this is that the measurement taken at 1.0 MHz occurs at a null in the

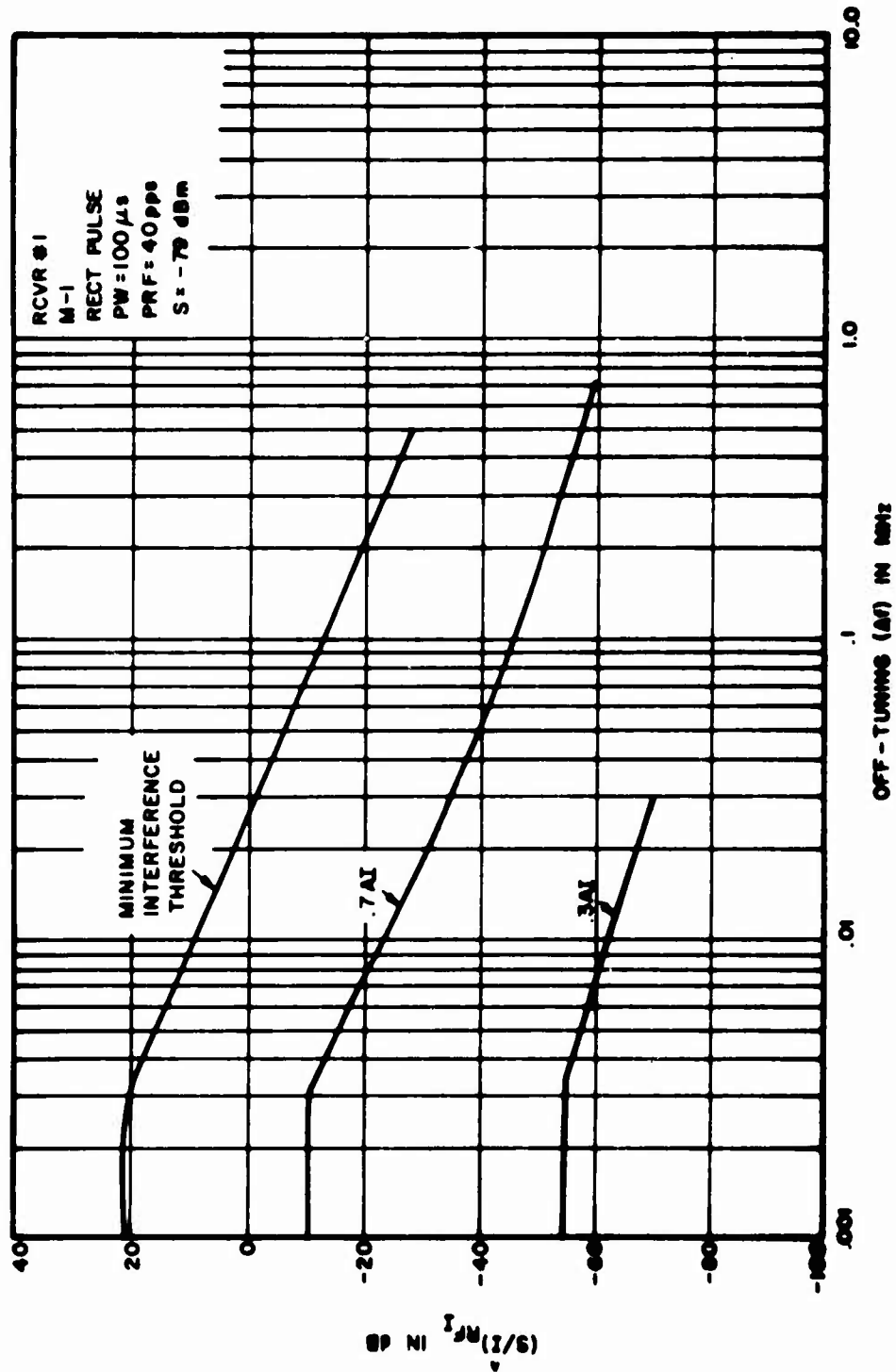


Figure 6-24. Input Signal to Peak Interference as a Function of Δf

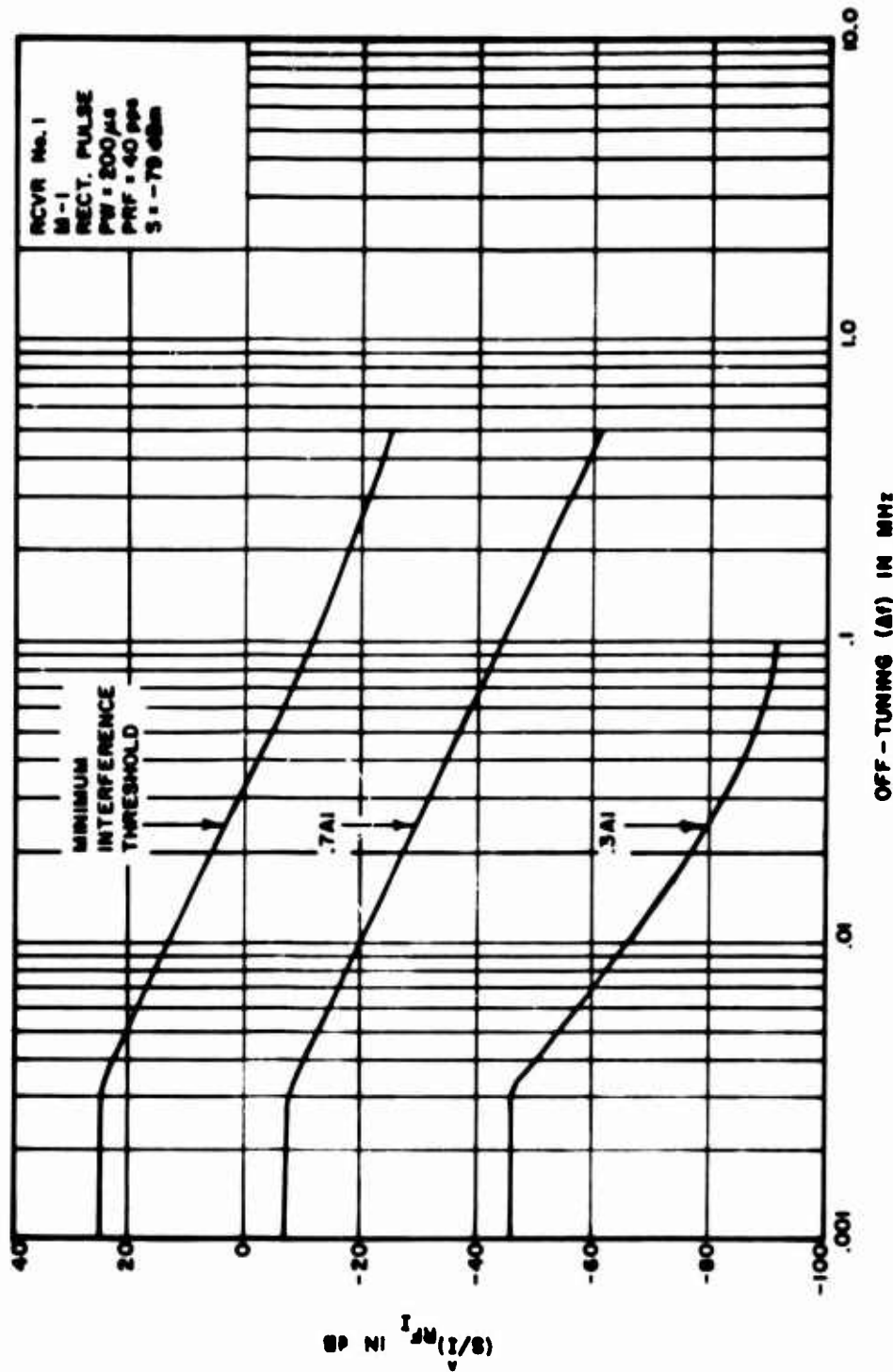


Figure 6.25. Input Signal to Peak Interference as a Function of Δf

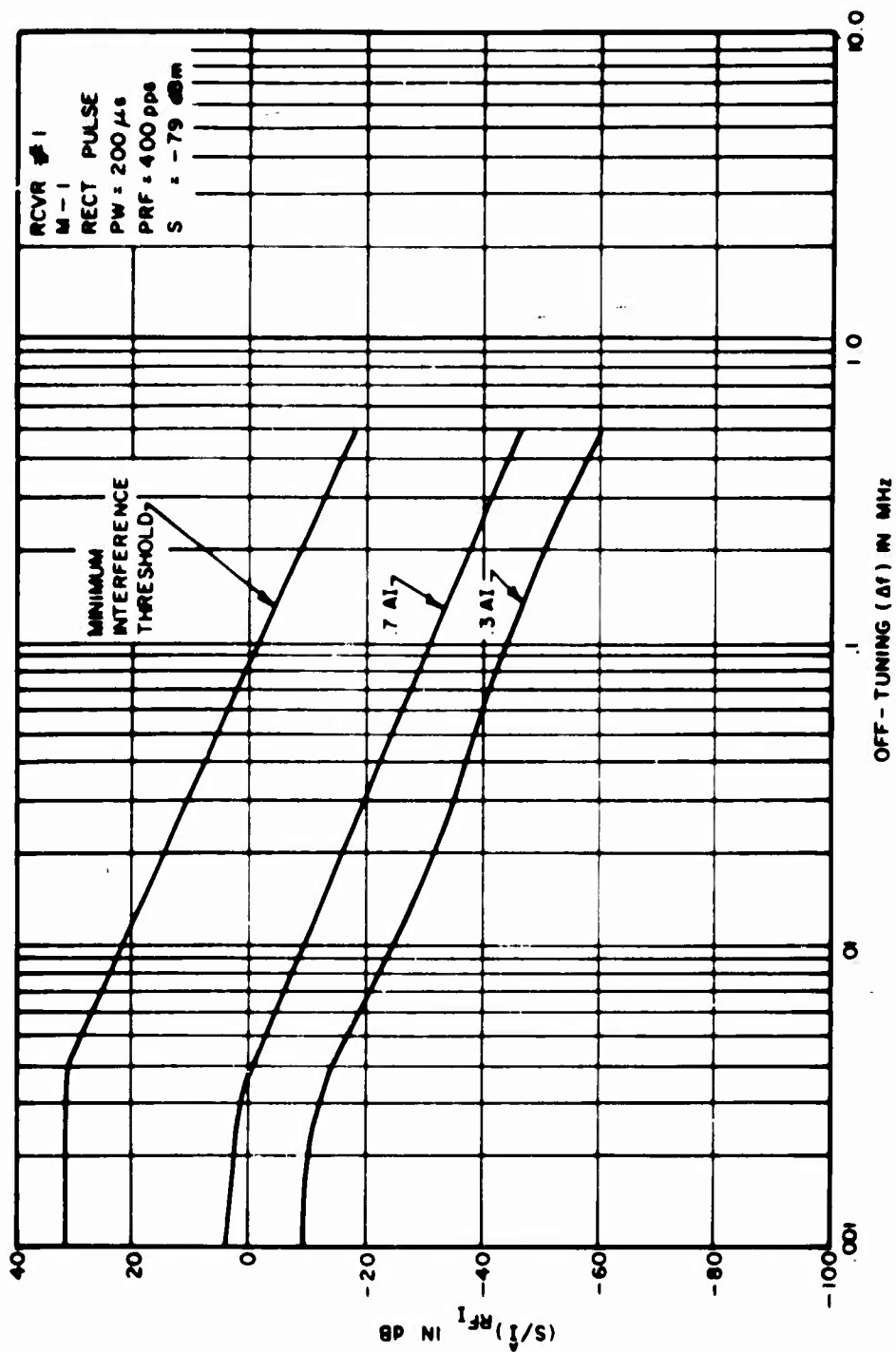


Figure 6-26. Input Signal to Peak Interference as a Function of Δf

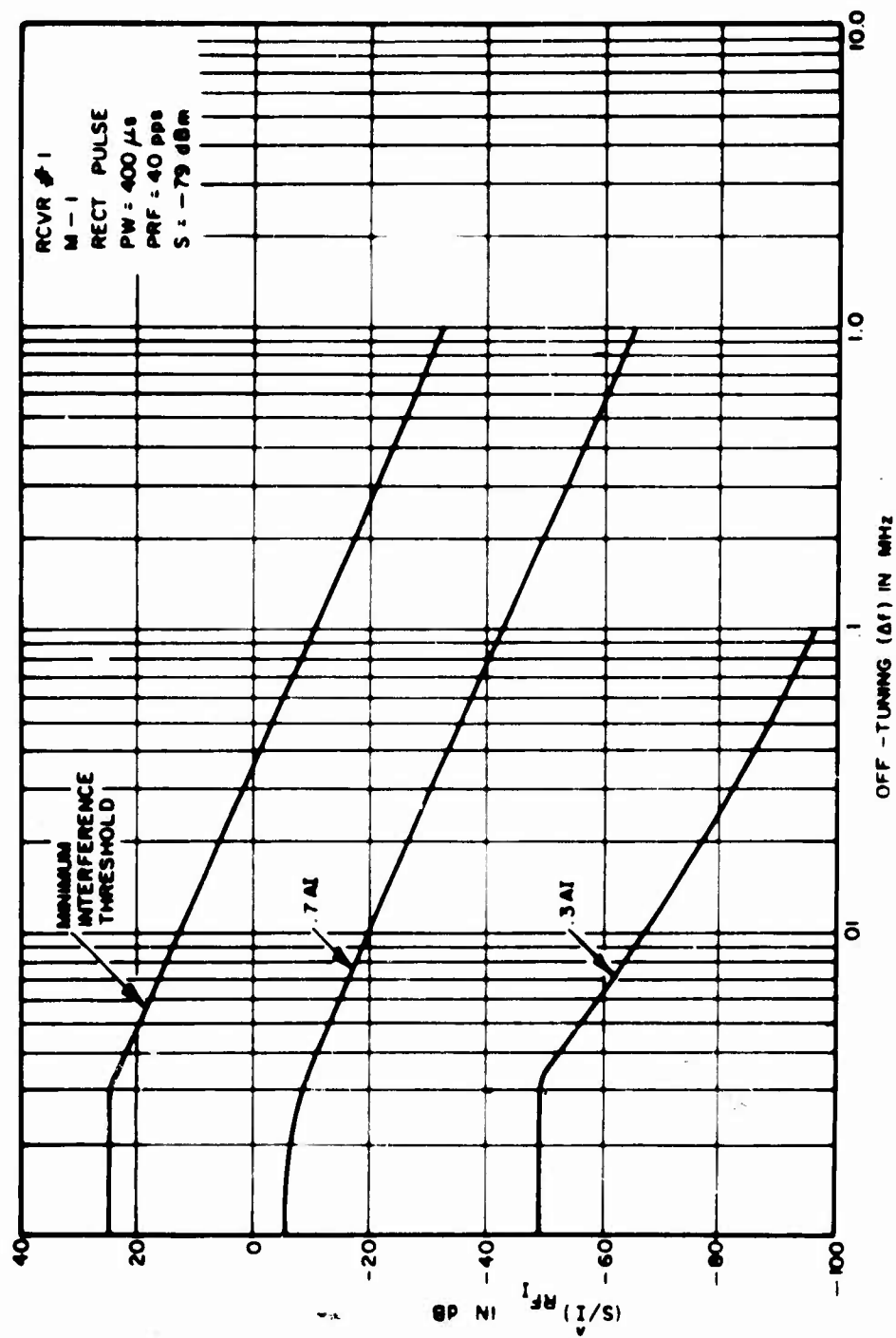


Figure 6 27. Input Signal to Peak Interference as a Function of Δf

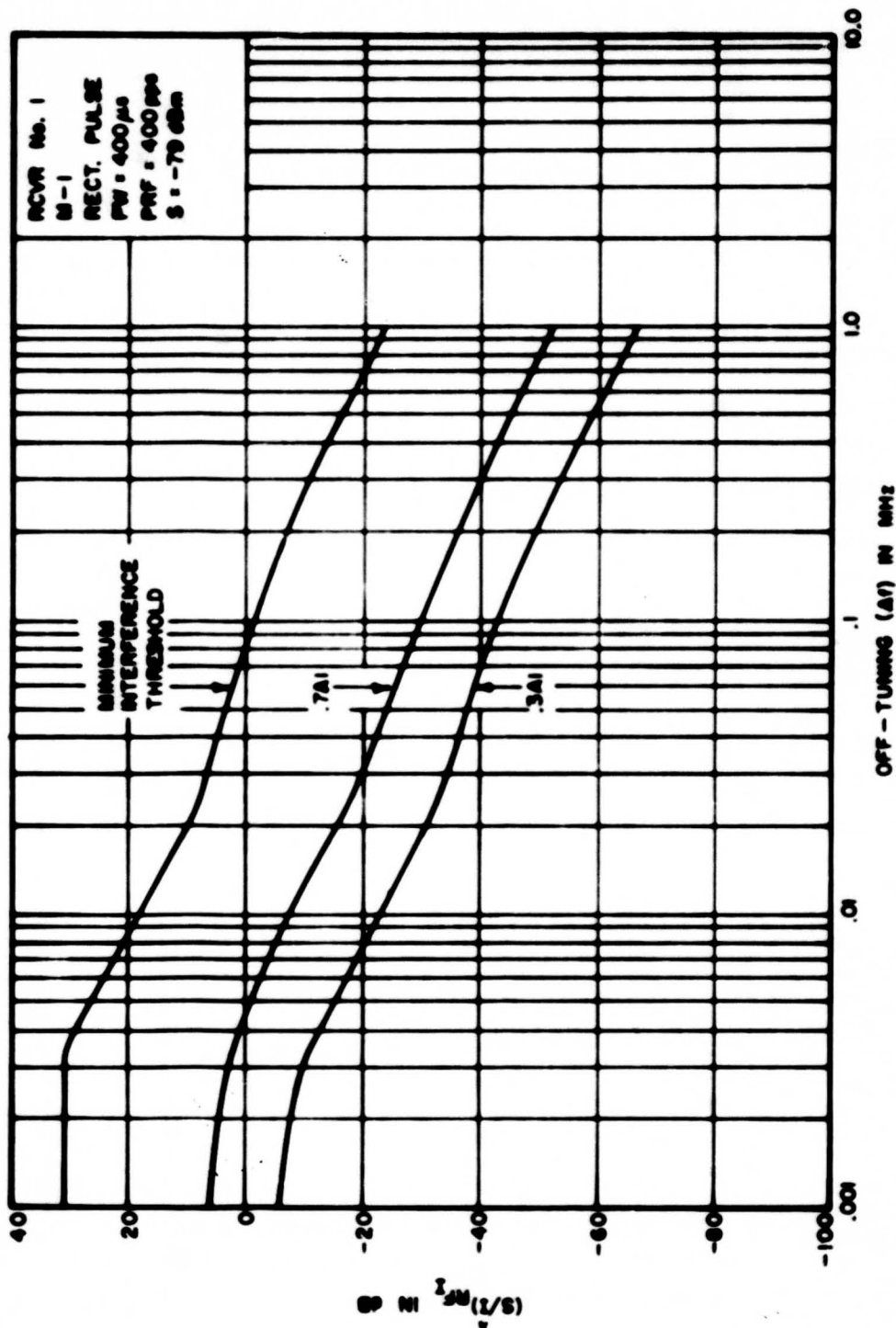
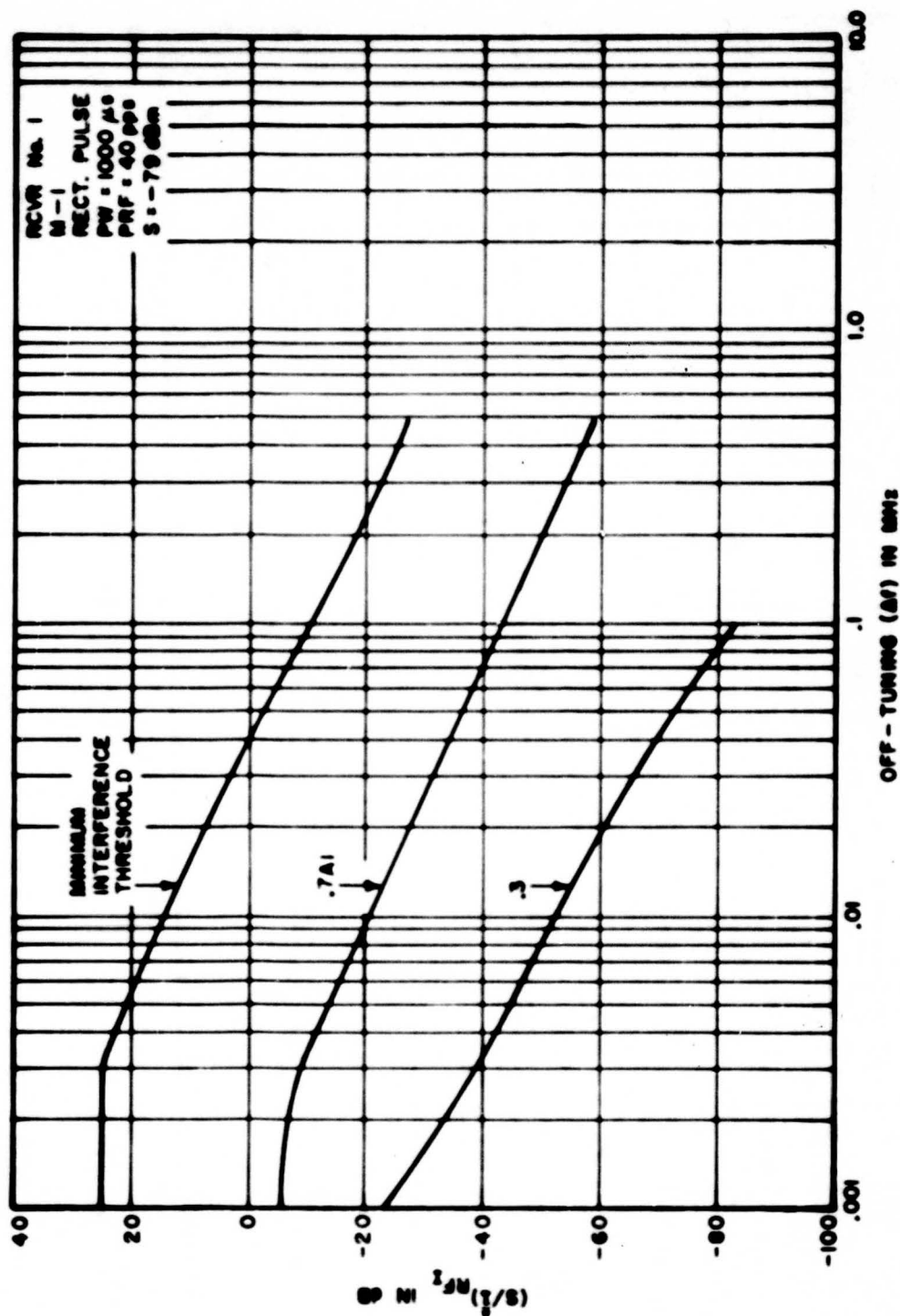


Figure 6-28. Input Signal to Peak Interference as a Function of Δf

Figure 6-29. Input Signal to Peak Interference as a Function of Δf

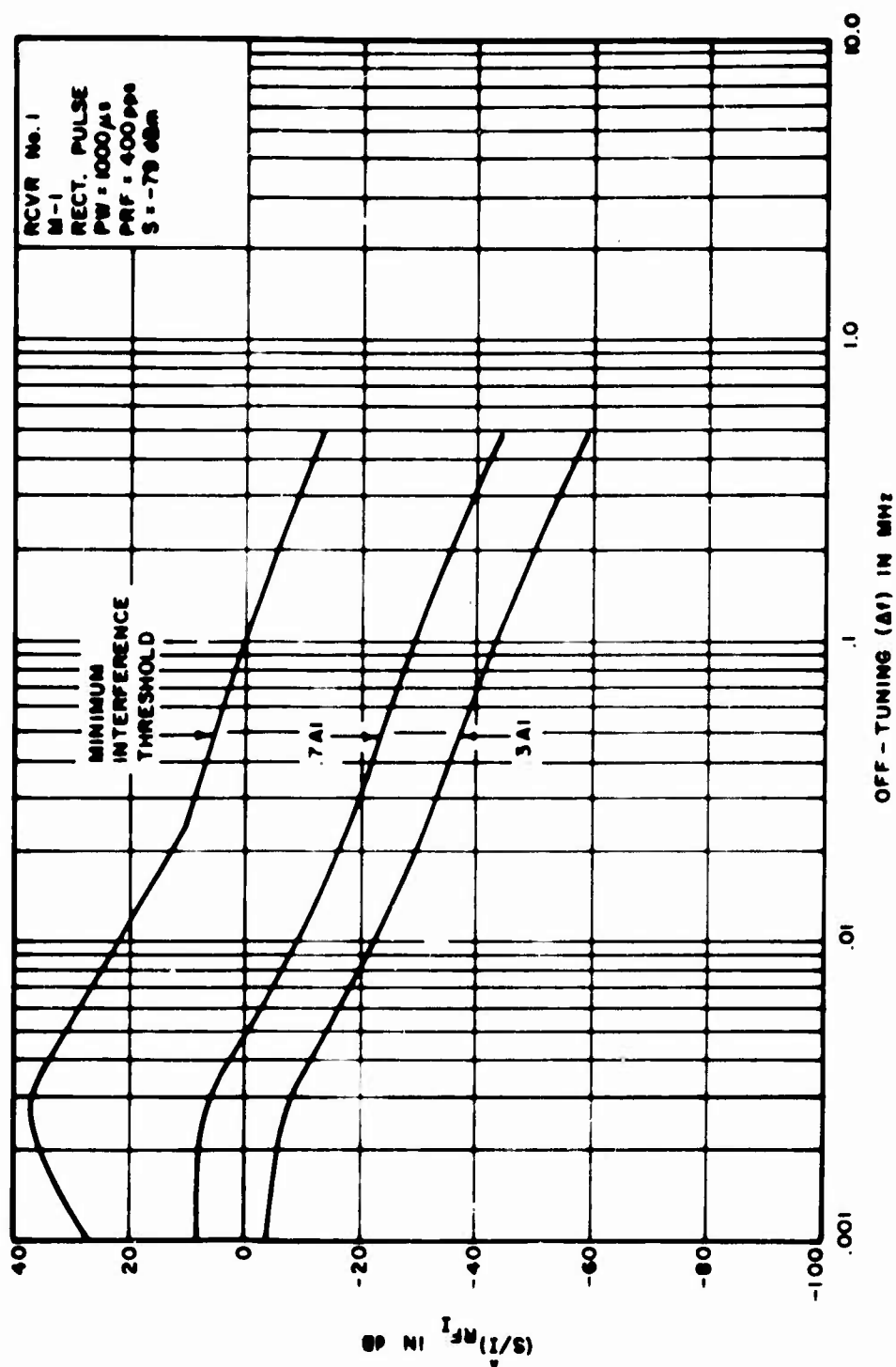


Figure 6-30. Input Signal to Peak Interference as a Function of Δf

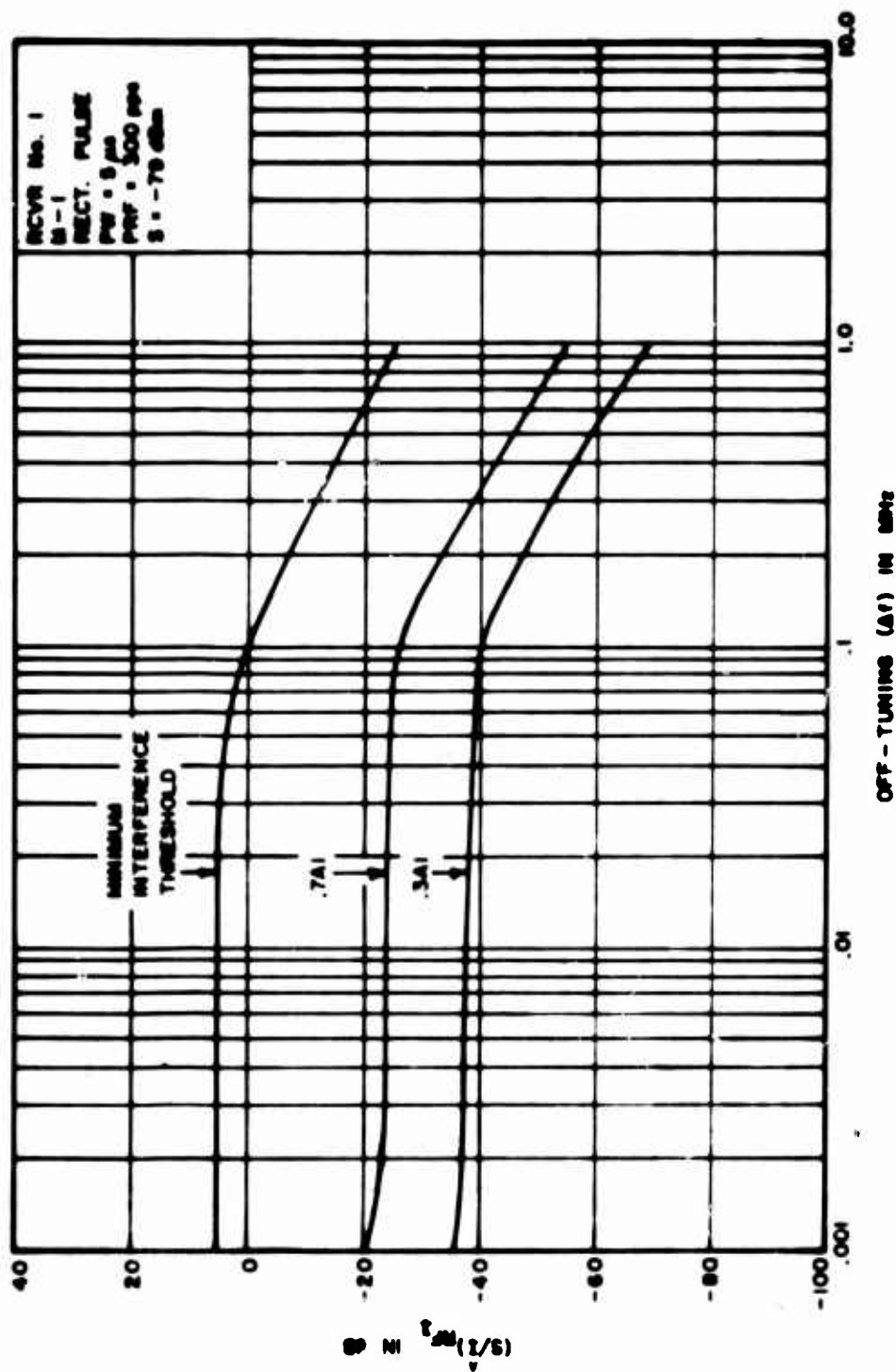


Figure 6-31. Input Signal to Peak Interference as a Function of Δf

pulse spectrum. This curve shows that when the frequency spacing between pulse spectrum nulls is greater than the IF bandwidth the degradation measurement will follow the exact shape of the interfering pulse spectrum rather than the envelope of the pulse spectrum. This also points out that the previous comments about the fall-off refer to the envelope of the spectrum and not a random occurrence of the nulls and peaks of the spectrum. The figures also show that the break point for the 20 dB per decade fall-off is a function of the pulse width of the interfering signal and the receiver IF bandwidth. If the pulse width of the interfering signal has a power spectrum with a mainlobe approximately equal to or narrower than the IF bandwidth, the break point will occur when the off-tuning is approximately one half the IF bandwidth. Figures 6-25 through 6-30 ($PW > 200 \mu\text{sec}$) indicate this trend. When the mainlobe of the interfering pulse spectrum is much greater than the IF bandwidth, the break point should theoretically occur when the off-tuning is $(1/\pi\tau)$.

In general, it appears that the off-tune pulse problem can be divided into three categories. These categories are:

1. Mainlobe much narrower than the IF bandwidth
2. Mainlobe approximately equal to the IF bandwidth
3. Mainlobe much wider than the IF bandwidth

Figures 6-32 through 6-36 show the AM degradation, input (S/\hat{I}) versus Δf for receiver No. 1, and chirped rectangular pulse interference. The figures show the RF input (S/\hat{I}) level which corresponds to the minimum threshold level and AI level of .7 for various degrees of off-tuning (Δf). The dotted lines show the theoretical envelope of the pulse spectrum. The measured data was not taken at a sufficient number of Δf 's to accurately define the minimum threshold and .7 AI levels as a function of Δf . However, the measured data shown in Figures 6-32 through 6-36 indicates that the RF input (S/\hat{I}) level, for minimum threshold level and .7 AI level falls off at the same rate as the envelope of the power spectrum of the interfering chirped pulse signal. This was also discussed in the previous section on chirped versus non-chirped pulses. Simulated off-tune degradation curves were given in Figures 6-14 through 6-17.

DEGRADATION WITH OUTPUT SIGNAL-TO-NOISE RATIO

The output (S/N) characteristics are a function of the particular receiver and the input desired signal level. The output (S/N) characteristics can affect the performance measured under similar input signal levels or input signal-to-noise ratios (for AM receivers having the same bandwidth characteristics). The output (S/N) characteristics also determine when the degradation becomes strictly a function of the input (S/\hat{I}) ratio rather than a function of interference and noise.

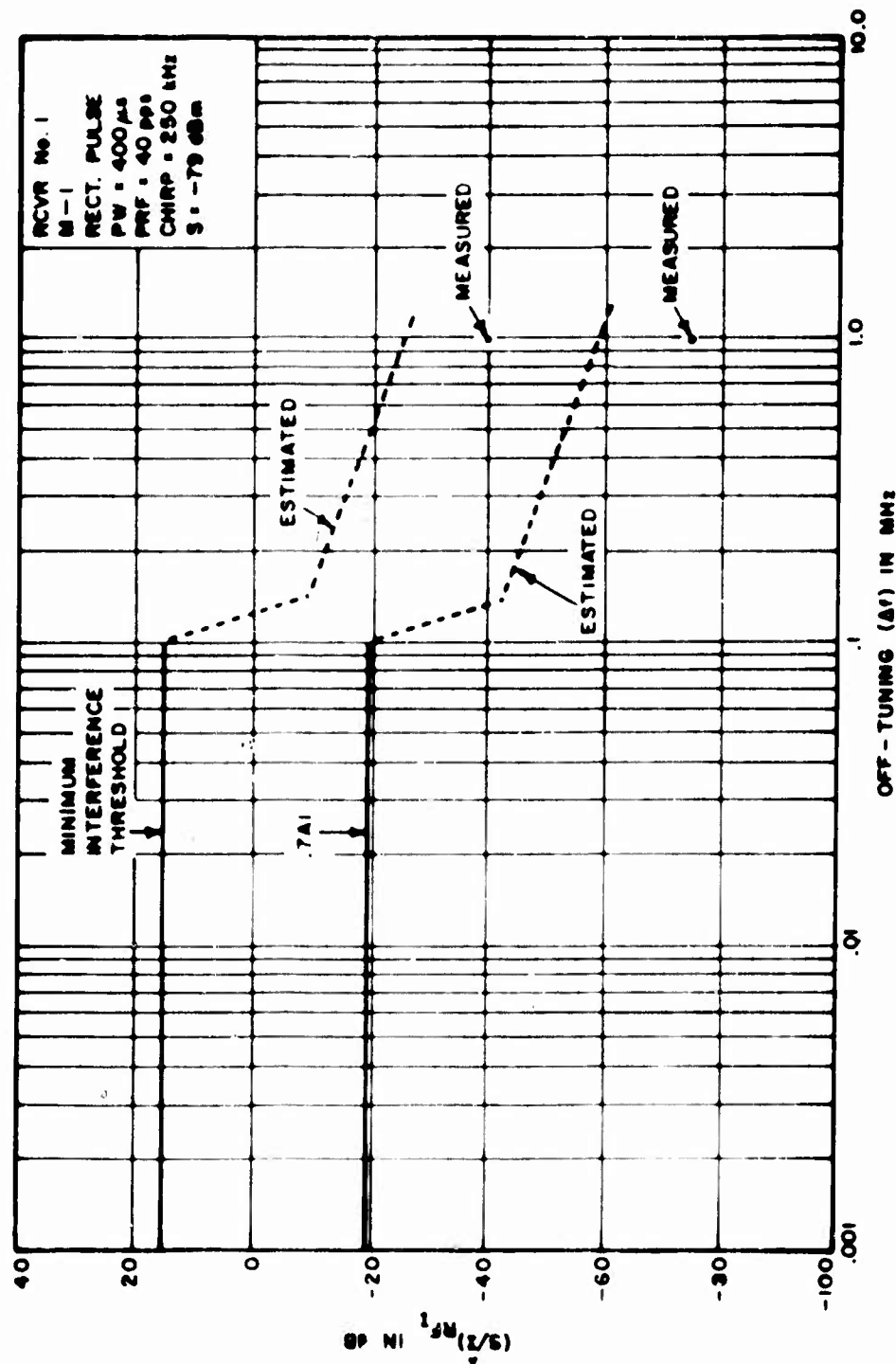


Figure 6-32. Input Signal to Peak Interference as a Function of Δf

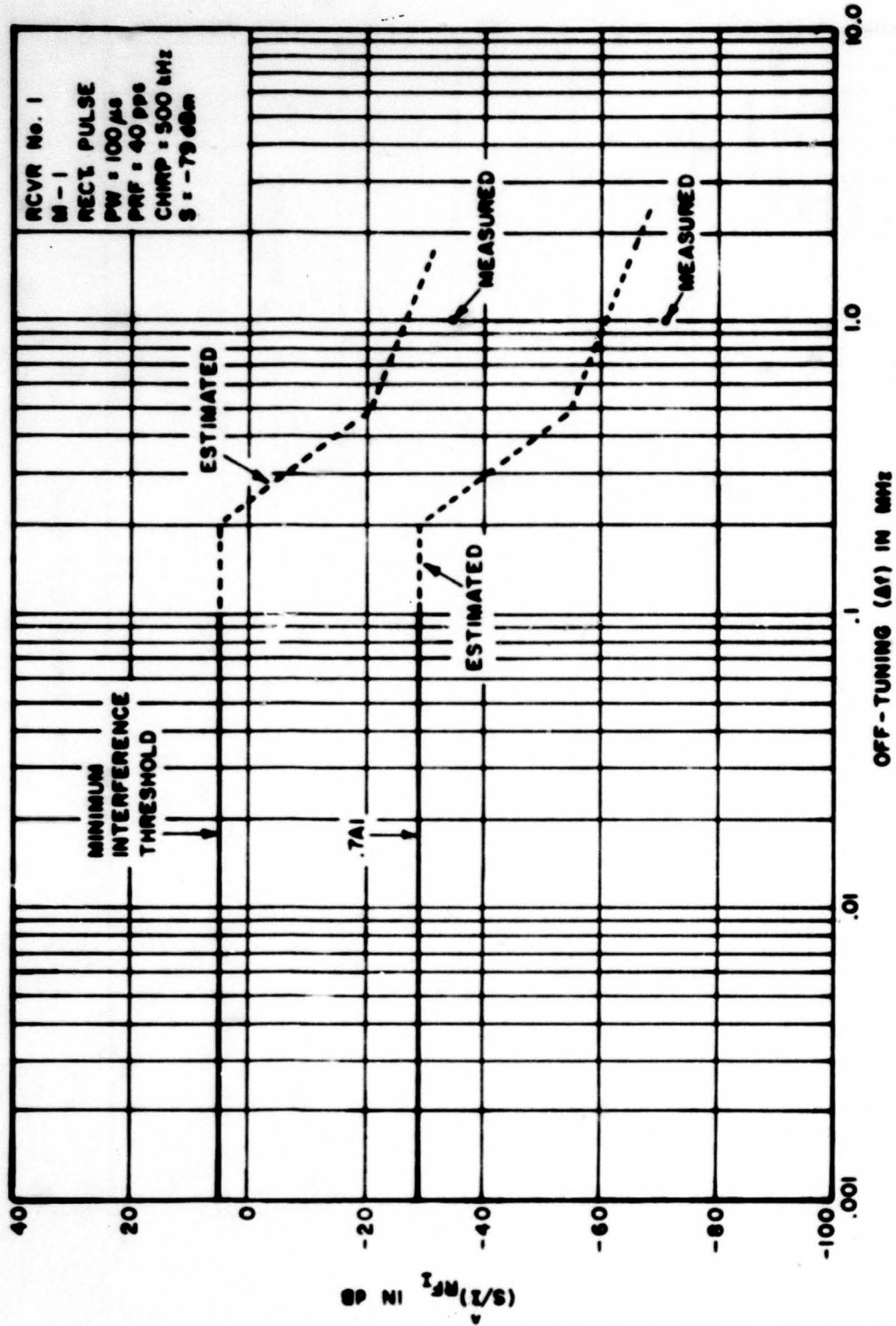
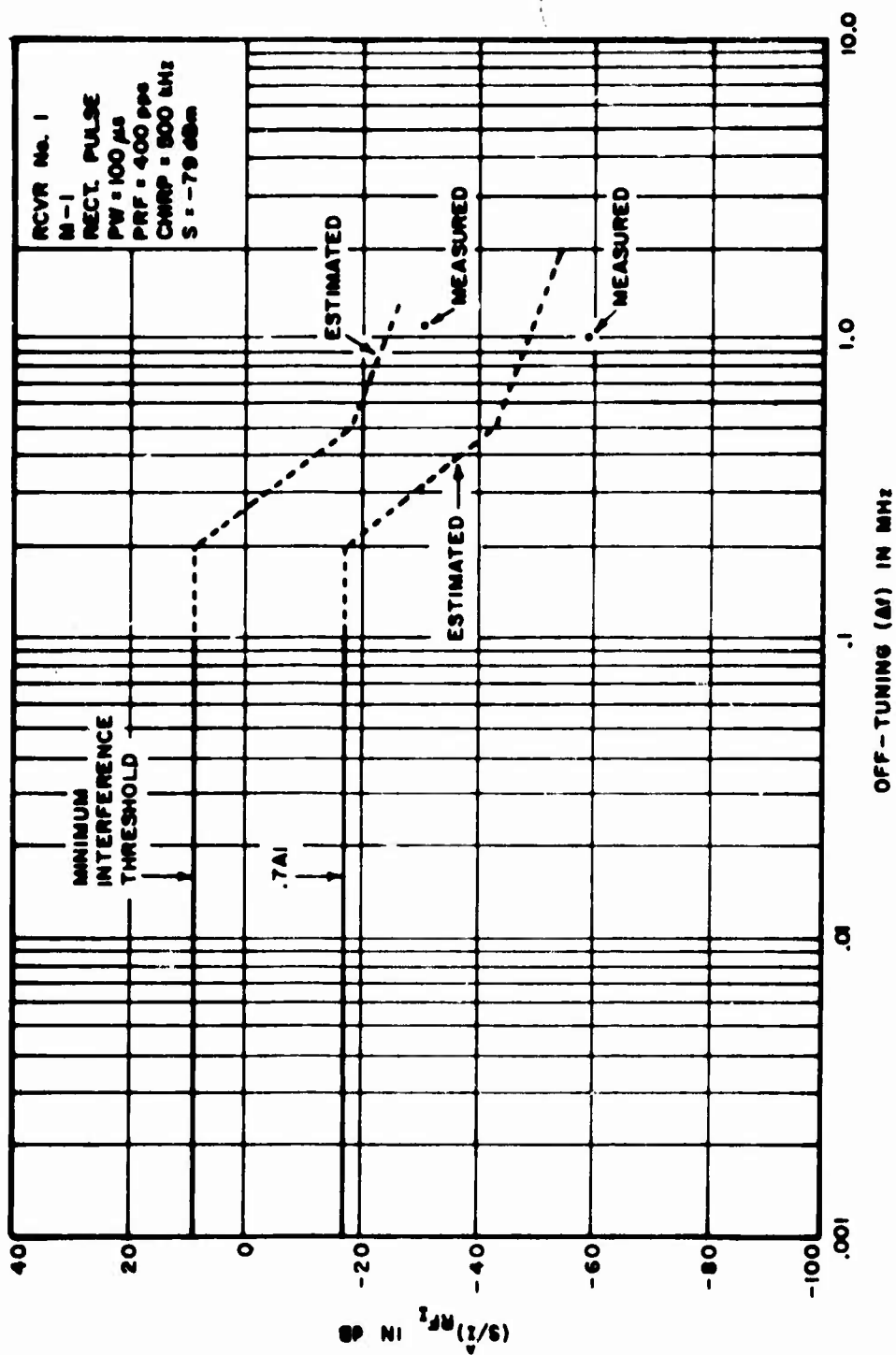


Figure 6-33. Input Signal to Peak Interference as a Function of Δf

Figure 6-34. Input Signal to Peak Interference as a Function of Δf

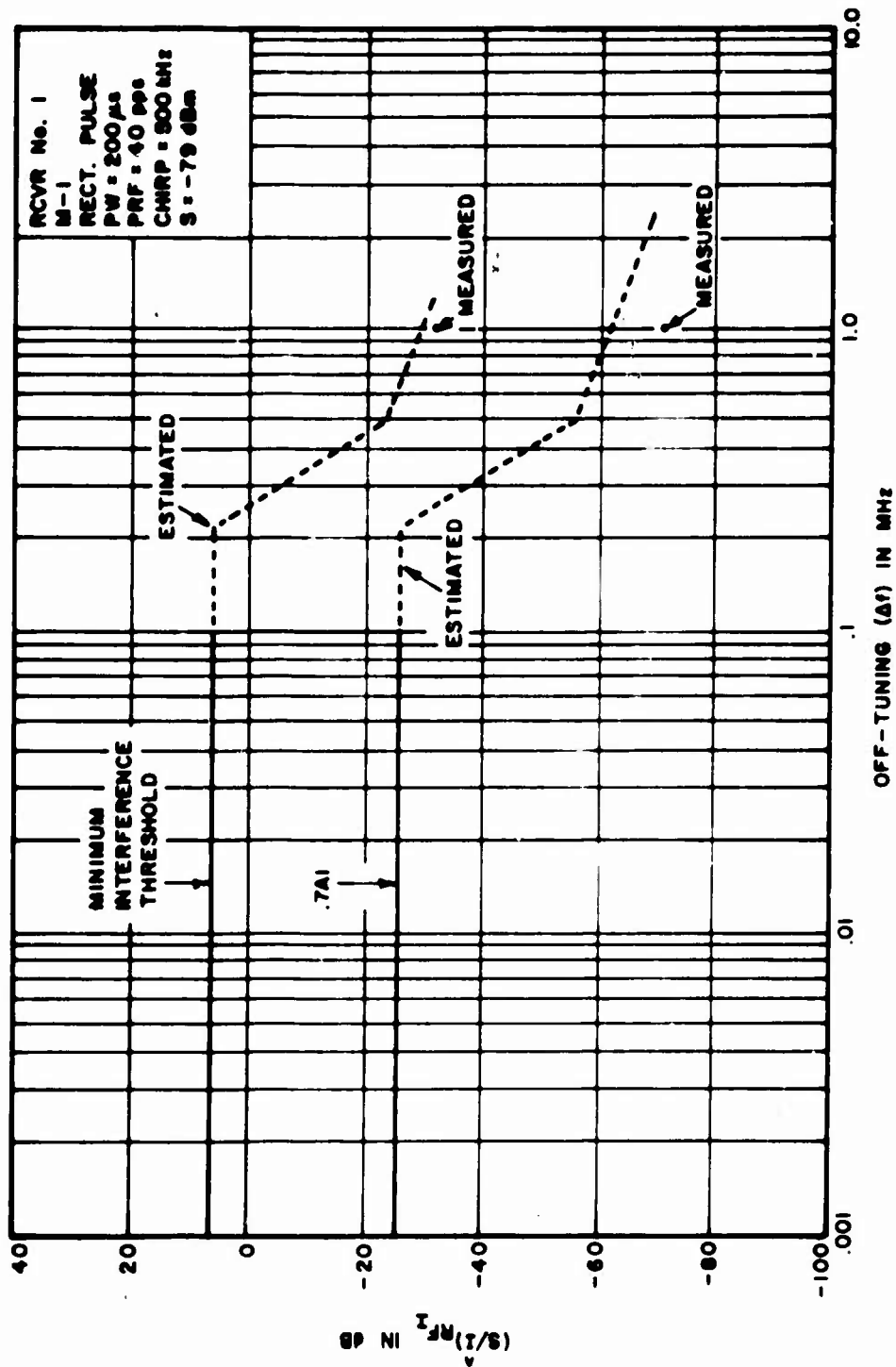


Figure 6-35. Input Signal to Peak Interference as a Function of Δf

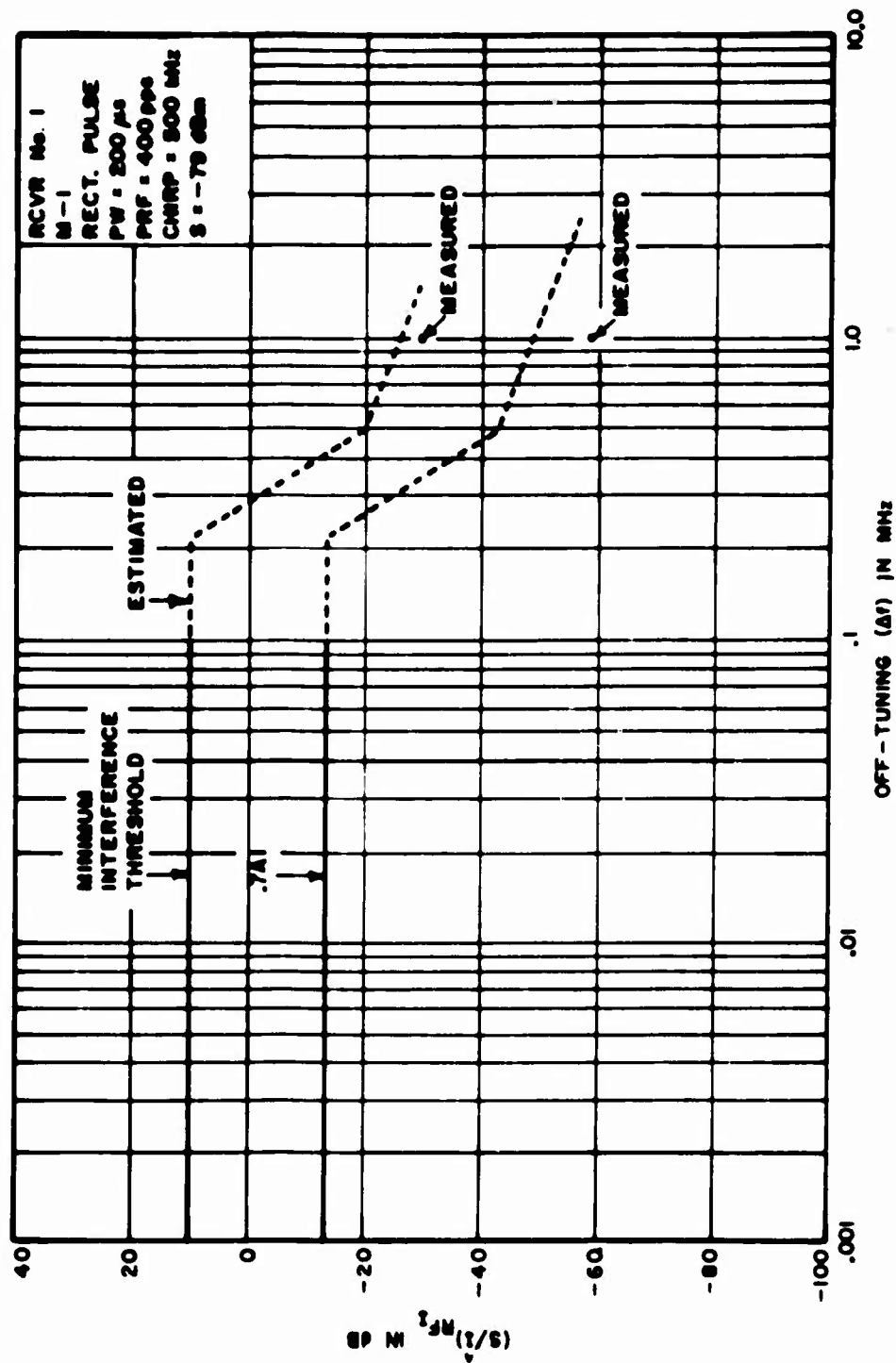


Figure 6-36. Input Signal to Peak Interference as a Function of Δ f

The primary indication of different performance degradation levels due to different receivers or the same receiver with different signal levels is given by the upper performance limit (UPL). The UPL is the highest performance level obtainable, without interference, for a given input signal level. This is the level that the performance (measured with interference) must be compared with to note the relative degradation in performance. The UPL is governed by the receiver output (S/N) level and is a function of the input desired signal level and the dynamic range characteristics.

Dynamic range characteristics are graphs of the output voltage level or the output (S/N) ratio as a function of the input signal level. Typical dynamic range curves showing the (S/N) or SINAD ratios for receiver No. 1 and No. 2 were given in Section 5, Figure 5-8. These curves show the audio signal plus noise plus distortion-to-noise plus distortion ratio (SINAD) as a function of varying input signal levels. Although these curves are similar to the dynamic range curves specified in MIL-STD-449(reference 10), there is actually considerable difference in that the MIL-STD-449(reference 10) curves only measure the total voltage and consequently give no indication of performance. The curves shown in Figure 5-8 indicate a power ratio which can be related to the performance of the system. The SINAD ratio very closely approximates the desired signal-to-noise plus distortion ratio for values greater than 10 dB.

The series of tests performed for this investigation specified that the input signal level should be adjusted to a level 30 dB above the 6 dB AM sensitivity criteria. This means, from an examination of Figure 5-8, that the input signal level for receiver No. 1 was adjusted to -79 dBm and No. 2 was adjusted to -72 dBm. This corresponds to output signal-to-noise plus distortion ratios of 26.5 and 20.0 dB, respectively.

These output ratios are actually less than the theoretical output ratios because of the nonlinear distortion generated within the receiver. The ideal signal-to-noise curves are also shown in Figure 5-8 and increase at a 1 to 1 ratio (i.e., a dB change on the input corresponds to a dB change on the output). These curves indicate that, ideally, output (S/N) ratio should have been 37 dB for the input signal level used in this investigation.

The difference between the UPL (S/N) of receiver No. 1 and No. 2 is 6.5 dB. This also means that, in general, the performance with interference present will be lower for receiver No. 2 than No. 1 for the input desired signal levels used in this investigation. However, this type of trend should be more apparent at low interference levels (high AI or threshold values) than at levels at which the peak interference is much larger than the noise level. At large negative (S/I) ratios the results should be independent of the S/N ratio. This general trend is "qualitatively" indicated by the difference between the same degradation levels for receiver No. 1 and No. 2 shown in Table 6-4. In this table, the (S/I) ratios for the same AI

TABLE 6-4
DIFFERENCE IN INPUT (S/\hat{I}) FOR RECEIVER
NO. 1 AND NO. 2

HIGH AI SCORES					
Pulse Width	PRF (pps)	AI	Receiver No. 1 (S/\hat{I}) in dB	Receiver No. 2 (S/\hat{I}) in dB	Δ
5 μ s	300	.89	12	0	12
100 μ s	80	.88	5	0	5
100 μ s	300	.85	7	0	7
200 μ s	40	.89	0	0	0
200 μ s	80	.87	5	0	5
400 μ s	40	.87	3	0	3
LOW AI SCORES				Δ Avg. = 5.3	
100 μ s	400	.79	4	0	4
200 μ s	400	.75	6	10	- 4
400 μ s	80	.80	3	9	- 6
400 μ s	400	.76	8	10	- 2
400 μ s	400	.67	6	0	6
1000 μ s	40	.80	- 1	0	- 1
1000 μ s	80	.81	4	10	- 6
1000 μ s	80	.73	1	0	1
1000 μ s	400	.76	10	10	0
Δ Avg. = -1					

score are averaged for different PW, PRF conditions. The results show that the average difference is -1 dB for the lower AI scores, while the difference is 5 dB for the higher AI scores. These results are somewhat qualitative since only a limited amount of data was available for comparison due to the audio limiter employed in receiver No. 2. This limited the data that could be used for comparison to (S/\hat{I}) values higher than the limit level of approximately -6 dB.

The degradation from the same receiver can also be different due to different output (S/N) ratios. This type of problem essentially divides into those associated with input signal levels below the knee of the dynamic range curve and those above the knee and below saturation. In the first case the performance is increasing with increasing output (S/N) ratio and is shown in Figure 6-37 for receiver No. 2. Input signal levels that are above the knee result in approximately the same $(S/N)_0$ levels and consequently should result in the same input (S/\hat{I}) levels for the same AI criteria. This is shown in Table 6-5 which summarizes the input (S/\hat{I}) ratios obtained with receiver No. 1 for the two signal levels at an AI criteria of .5. This shows an average difference of only 1.1 dB.

As previously discussed, the higher performance levels are greatly affected by the output (S/N) ratios. This, in particular, includes the threshold levels, averaged over all pulse widths, that were measured for this test. This can best be seen by examining Figure 6-38 which shows how the threshold is a function of the output signal to peak-to-peak interference and the output (S/N) ratio. These measurements essentially show that the threshold level changes by approximately 19 dB when the output (S/N) ratio changes from 10 to 40 dB. The 10 to 40 dB output (S/N) range represents the range over which most receivers operate. Figure 6-38 will be further discussed in the minimum interference threshold effects discussion.

In summary, the relationship of performance to the output (S/N) ratio has been discussed. It has been shown that performance is a function of the input (S/\hat{I}) ratio only for high input signal levels. This high level condition is represented by output (S/N) ratios above 10 dB. For low or sensitivity type input signal levels (i.e., output S/N ratios of approximately 6 dB) the interference problem becomes a function of both interference and noise. In this region the interference effects discussed in this report are partially hidden by the noise. In general, a comparison between the performance levels of two receivers should not be made without considering the input and the corresponding output (S/N) characteristics.

BASEBAND POWER RATIOS

The following is a discussion of the modeling trends obtained from an examination of

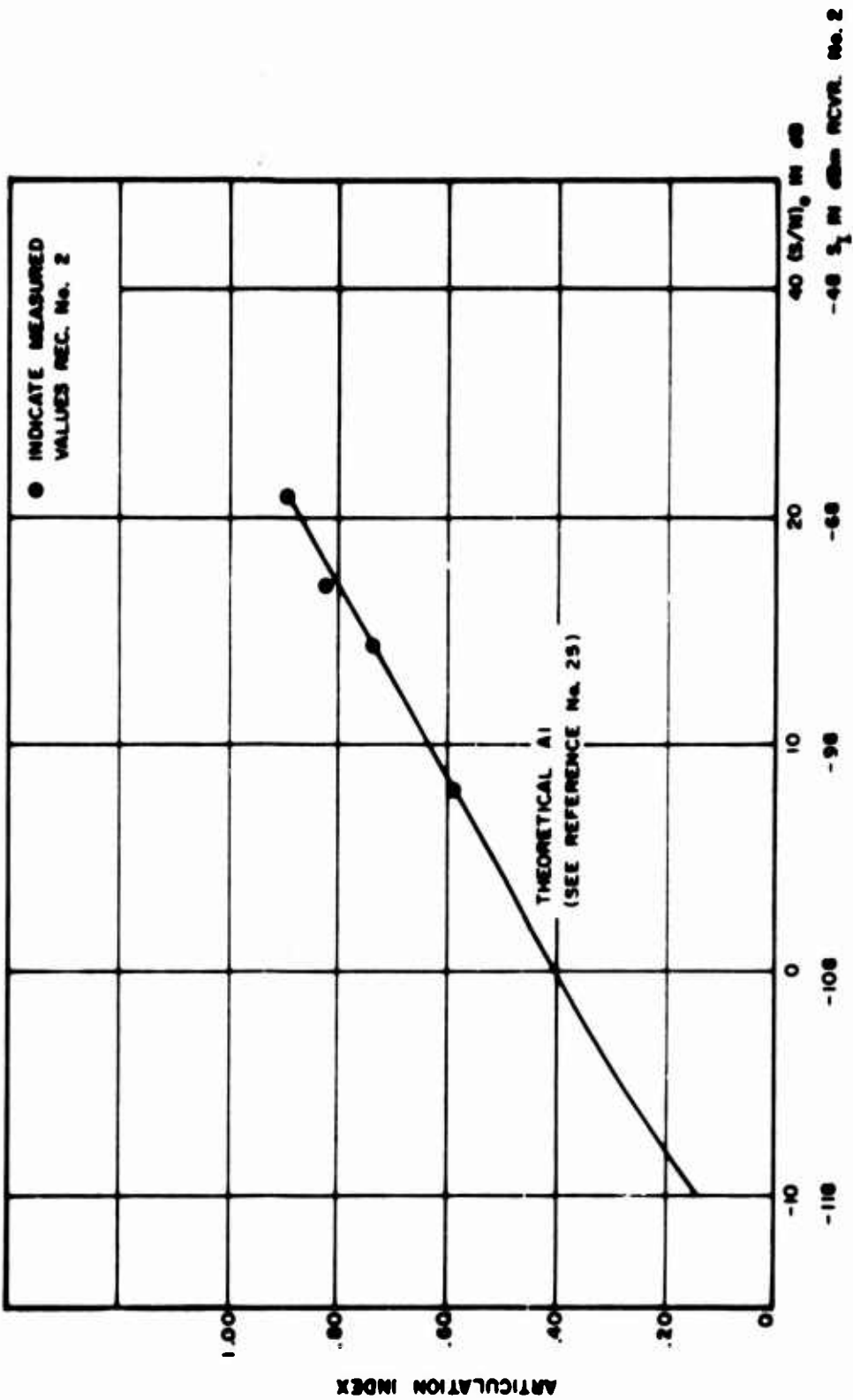


Figure 6-37. Articulation Index Versus Input Signal Level

TABLE 6-5

AVERAGE DIFFERENCE FOR
THE INPUT SIGNAL-TO-PEAK
INTERFERENCE RATIO FOR
TWO SIGNALS

AI	Pulse Width	PRF (pps)	Δf (kHz)	S = -79 dBm (S/I) in dB	S = -40 dBm (S/I) in dB	ΔS		
.5	100 μs	40	0	-20	-21	1		
			3	-18.5	-18	0.5		
			25	-43	-43	0		
			100	-58	-60	2		
		400	0	- 7	- 6.0	1		
			3	- 8	- 5.0	3		
			25	-25	-24	1		
			100	-41	-40	1		
		.5	400 μs	40	0	-12	-12	0
					100	-52	-50	2
				400	0	0	0.0	0
					100	-37	-36	1
.5	1000 μs	40	0	-12	-13	1		
			100	-51	-49	2		
		400	0	2.5	1.0	1.5		
			100	-37	-36	1		
		Δ Avg. = 1.1						

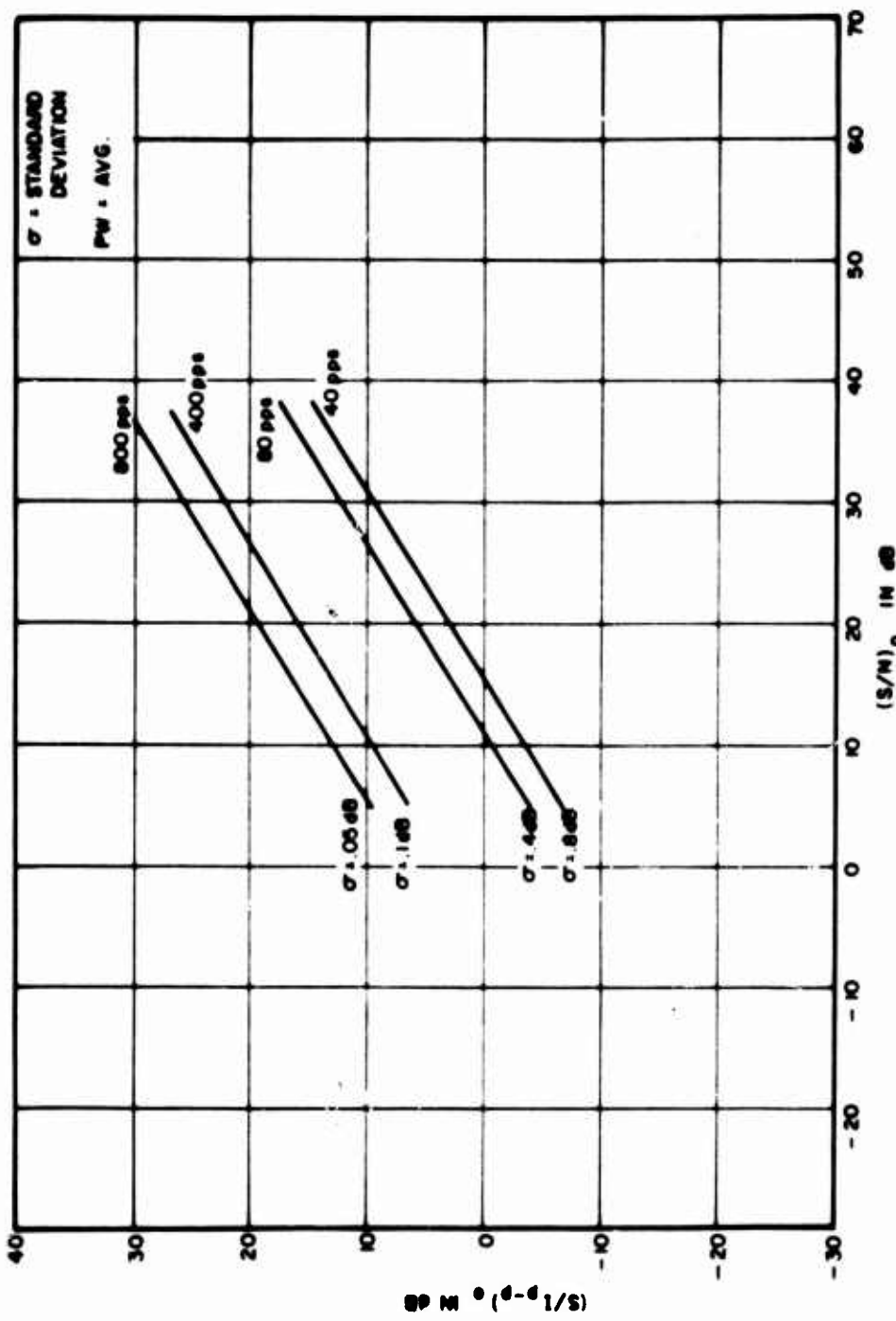


Figure 6-38. Average Audio Threshold as a Function of Signal to Noise

the baseband (audio) output power ratios. An examination of this data is important since baseband measurements are the easiest type of degradation measurement to make. If baseband power ratios can be simply associated with performance degradation, a number of future measurements and receiver modeling simplifications are feasible.

Baseband power ratio measurements (the ratio of two measured power quantities, e.g., signal-to-noise ratio) typically include the types shown in Table 6.6. The first three measurements in the "Measurement Ratio" column include those types typically obtained with a distortion analyzer. This method is not ideally suited to degradation measures since the degradation is proportional to the desired to undesired signal ratio. It is, therefore, desirable to convert this data to the format shown in column two.

The last measurement in the first column is essentially the measurement of signal to-peak output interference. This measurement is appropriate to this particular study because the interference is pulsed and consequently the output performance degradation may be related to the signal to peak interference. The presentation of the data is again more appropriate to degradation analysis in the signal to peak interference format rather than the signal plus peak interference to peak interference format. The peak interference could be measured in terms of a zero to peak or a peak to peak reading. Since the output pulse is not generally symmetrical (see Section 4 for a discussion of output pulse shapes) due to the ringing of the various filters in the receiver the peak to peak measurement was used. However, the zero-to-peak pulse power can be obtained approximately by reducing the interference peak-to-peak measurement by 3 dB. This corresponds to adding 3 dB to the signal-to-peak to peak interference ratio (i.e. $(S/I_{pp})_O \approx (S/I_{op})_O + 3 \text{ dB}$).

The two types of baseband measurements listed in Table 6.6 consist of RMS (average power) or peak voltage type measurements. An examination of AI in terms of the average output (S/\hat{I}) ratio led to no significant parameter trends. The output AI curve was, therefore, plotted for average PW, PRF and off-tuning and is shown in Figure 6-39 along with the variability ($\pm 1\sigma$ limits) in the measurements. This figure also shows the theoretical VIAS response curve with noise interference (reference 25). An examination of these curves indicates a close agreement between the pulsed interference and baseband noise measurements. This figure also implies that the AI score for pulse interference is uniquely related to the pulse input (S/\hat{I}) ratio.

An examination of AI in terms of the peak-to-peak output (S/\hat{I}) ratio indicated a significant PRF degradation trend. This is shown in Figure 6-40 along with the measured variability ($\pm 1\sigma$ limits) in which the PW and off-tuning parameters have been averaged. The 80 PRF curve in this figure is 22 dB more negative than the average output power ratio curve of Figure 6-39. The majority of this difference should be due to the duty cycle

TABLE 6-6
COMMON OUTPUT BASEBAND POWER MEASURES

Measurement Ratio	Degradation Ratio	Comments
1 $\left(\frac{S+N}{N} \right)_o$	$(S/N)_o$	Standard idealized output
2 $\left(\frac{S+N+D}{N+D} \right)_o$	$\left(\frac{S}{N+D} \right)_o$	(SINAD)
3 $\left(\frac{S+N+D+I}{N+D+I} \right)_o$	$\left(\frac{S}{N+D+I} \right)_o$	SINAD measurement technique applied to pulsed interference
4 $\left[\frac{S+N+D+I}{(N+D+I)_{p.p}} \right]_o$	$\left[\frac{S}{(N+D+I)_{p.p}} \right]_o$	Special measurement for peak type interference

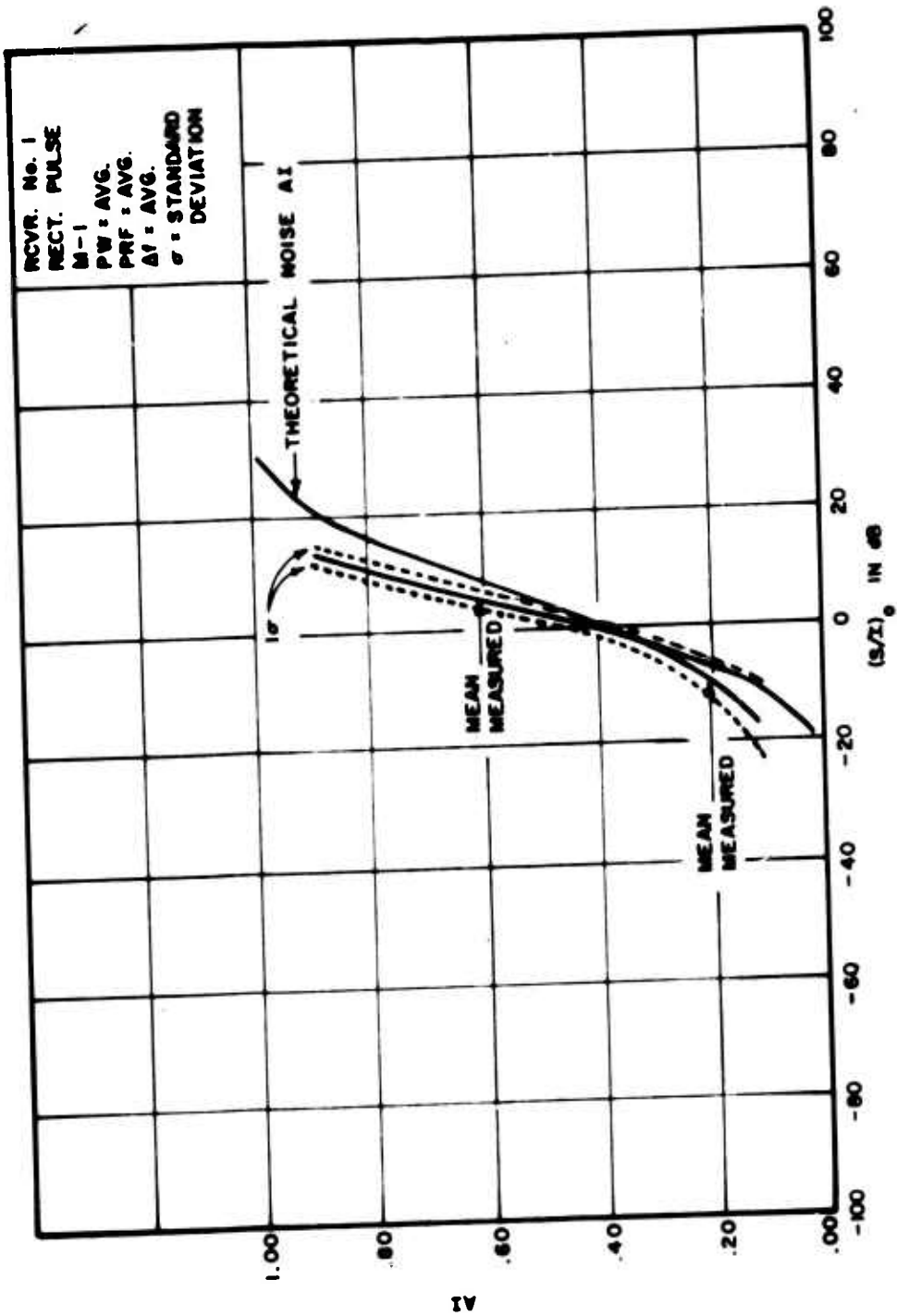


Figure 6-39. Mean Power Transfer Curves for Pulsed Interference to an AM Receiver

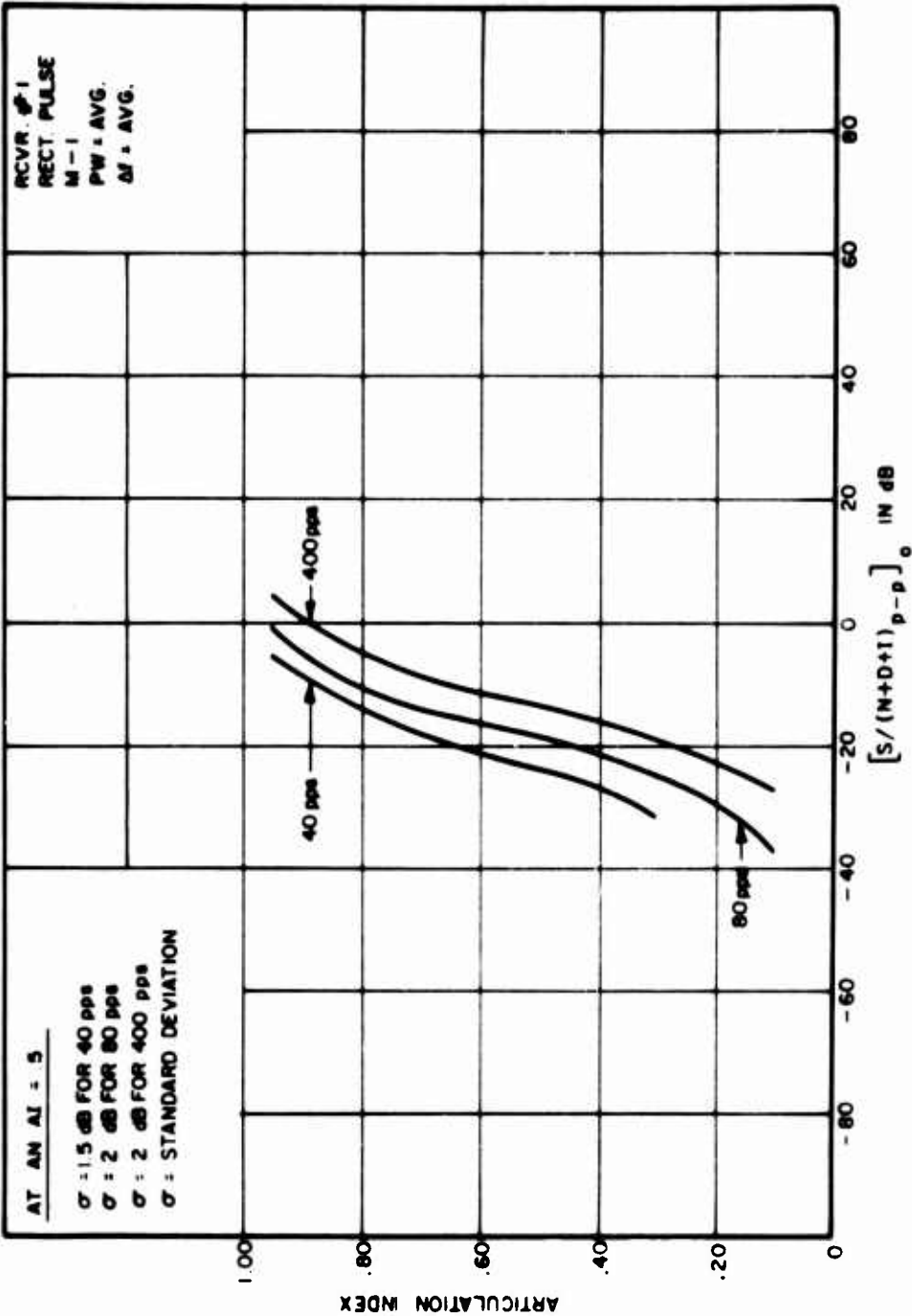


Figure 6-40. Mean Power Transfer Curves for Pulsed Interference to an AM Receiver

difference between the peak and average curves. The average duty cycle (on-tune and off-tune) for the 80 PRF pulsed curve was found to be 15 dB. In addition to this basic difference a peak-to-peak factor and the shape of the pulse should be taken into consideration. A further examination of this difference can be found in the discussion of audio threshold effects.

Figures 6-39 and 6-40 indicate that both peak and average output power ratios can be used for measurements and prediction purposes to simply obtain an estimate of a particular performance degradation criterion. As a particular example it is only necessary to measure a -14 dB output (S/I_{pp}) ratio for a 1 on tune and off-tune pulsed conditions with a PRF of 80 pps to maintain an AI score of .7.

It is also advantageous to be able to convert the output degradation curves that have been described, or other output degradation functions, to receiver input performance degradation criteria. This can be simply accomplished through the use of a transfer function that relates the input (S/I) power ratio to the output (S/I) power ratio. This process is symbolized in Figure 6-41. These transformations are complex (untractable) functions of the PW, PRF, detector and the filter characteristics. Both the average output and the peak output transfer curves were measured for the typical AM system (receiver no. 1) being considered and are given in Figures III 107 to III 161 of Appendix III. The average transfer curves were also simulated and are shown compared to the measured curves in Figures 6-42, 6-43 and 6-44. These curves again show a close agreement between the simulated and measured data which was previously discussed in the simulation section. Although the peak-to-peak curves were not simulated they could have been generated through the simulation process. The average or peak-to-peak transfer curves can be used with the appropriate degradation curves to relate the system output to the system input. These curves, in conjunction with the average AI curves, can be used to obtain a solution to the voice degradation problem. They can also be used with other types of output degradation criteria (i.e., such as the S/N corresponding to a particular error rate for a digital system) to obtain solutions for digital and analog systems.

In summary, it has been shown that either the peak to-peak or average output power ratios can be used for measurement or prediction purposes to determine output degradation criteria for voice systems. A number of power transfer functions that can be used in degradation calculations for voice, digital or analog systems have also been discussed.

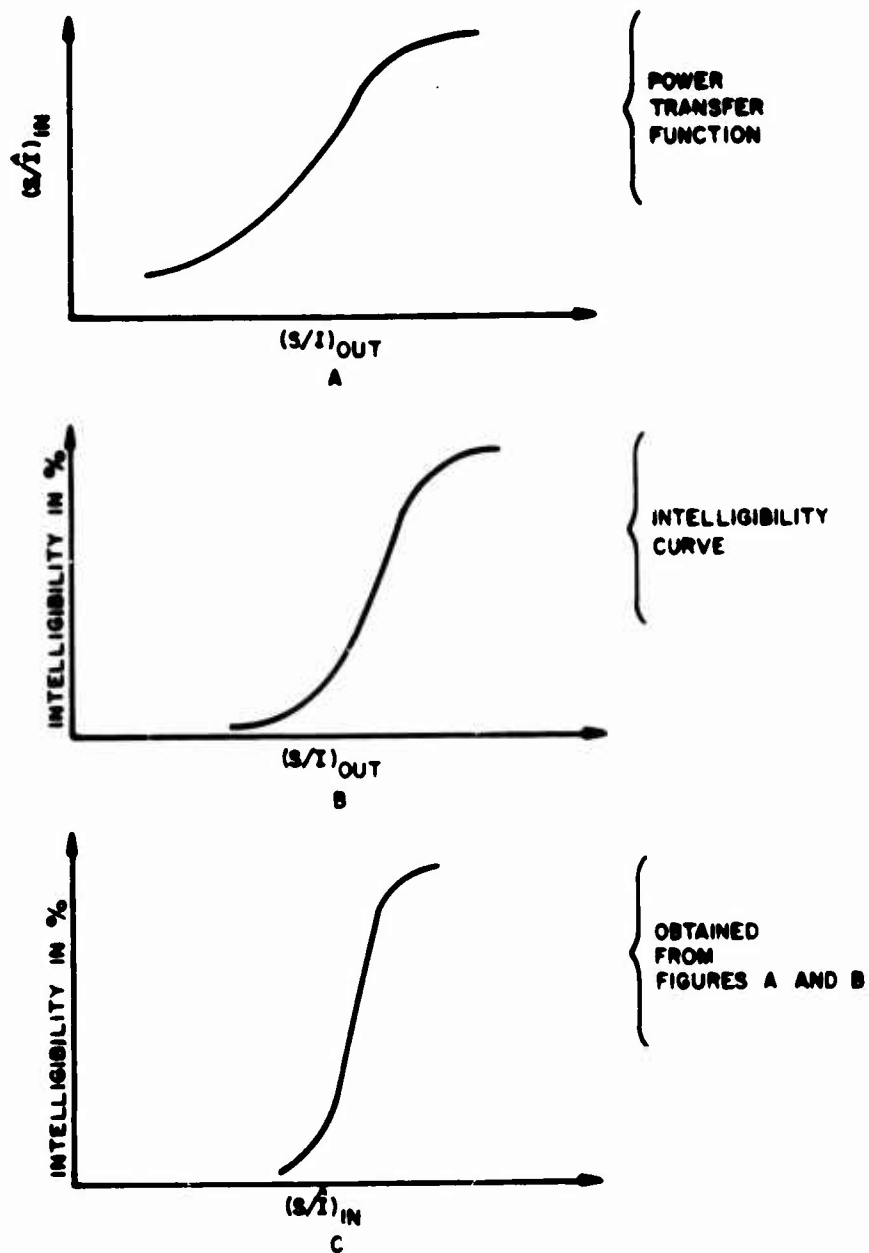


Figure 6-41. Synthesized Performance Degradation Procedure

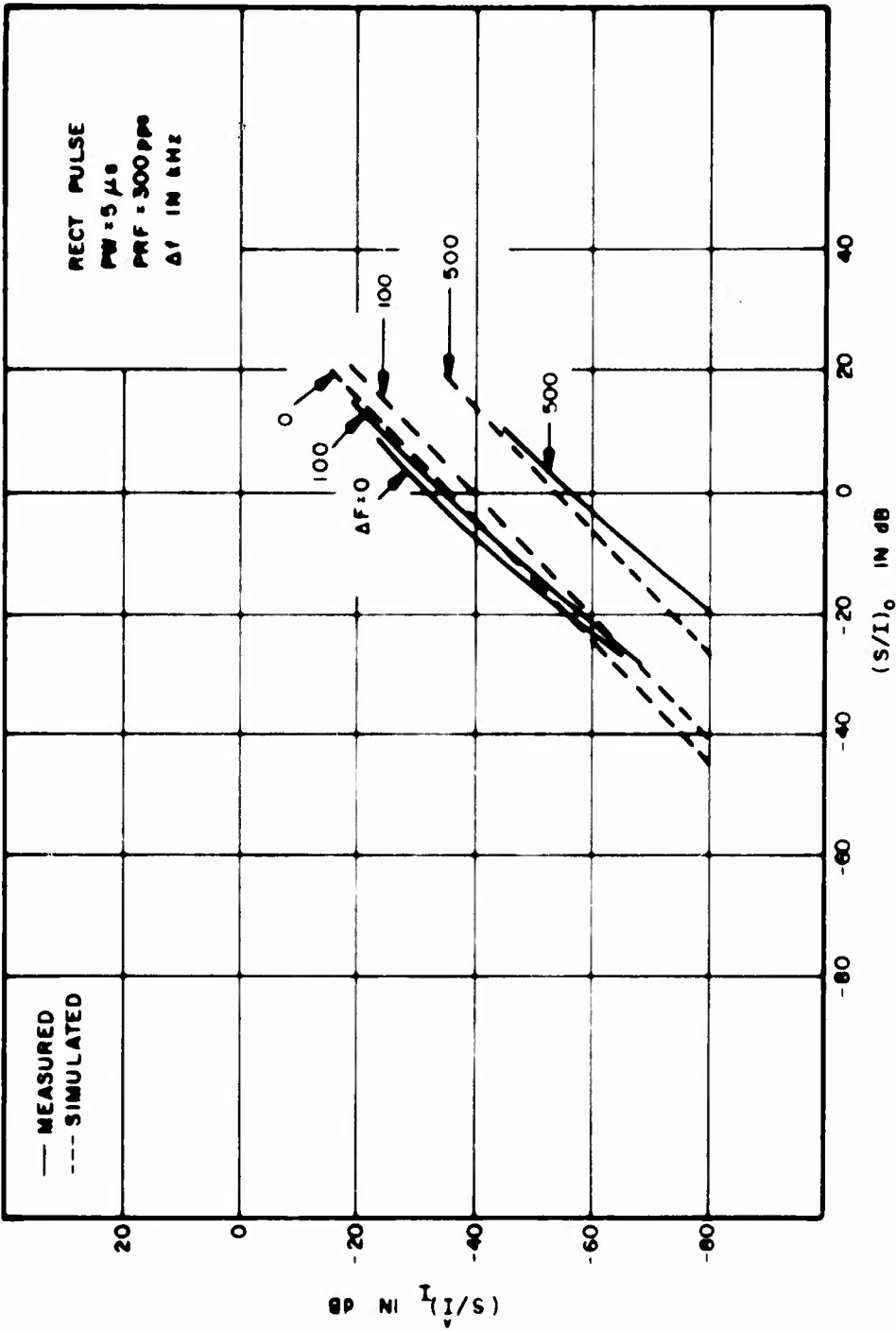


Figure 6.42. Power Transfer Curves for an AM Receiver

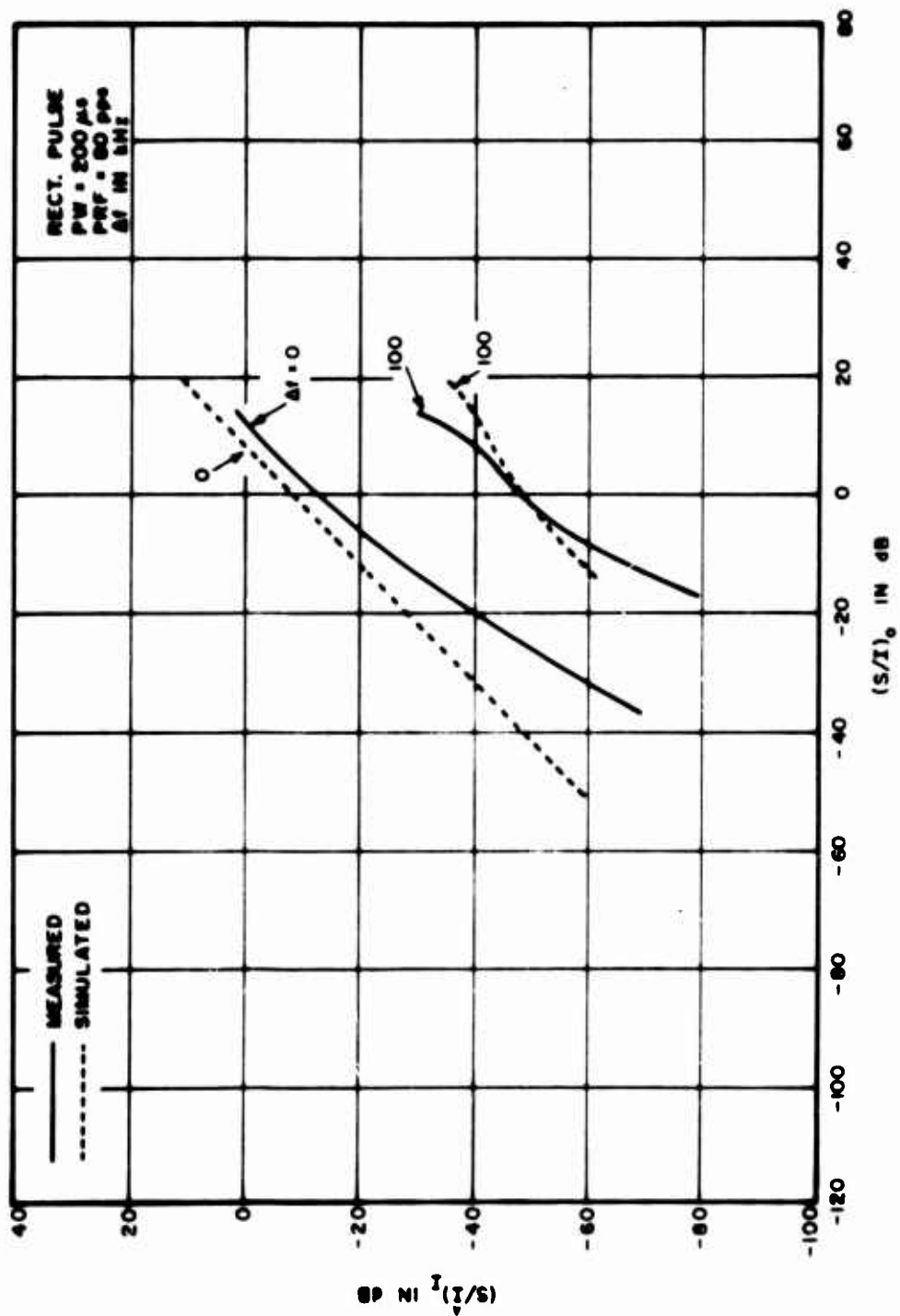


Figure 6-43. Power Transfer Curves for an AM Receiver

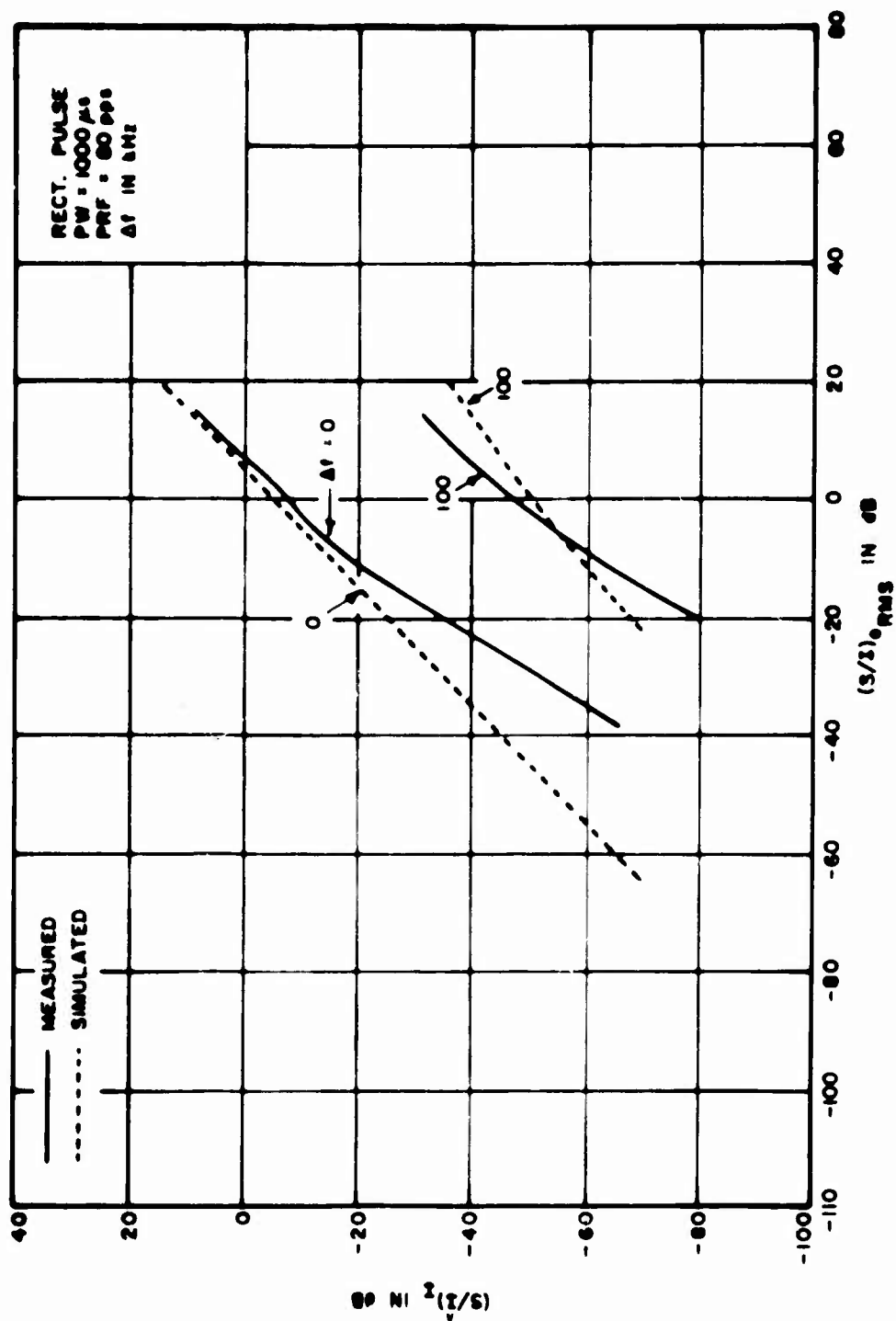


Figure 6-44 Power Transfer Curves for an AM Receiver

MINIMUM INTERFERENCE THRESHOLD DEGRADATION EFFECTS

Introduction

The following is a discussion of the modeling of minimum interference threshold effects. A minimum interference threshold is the level at which the interference is first observed. For the audio case this is the level at which the pulsed interference is first heard. This is an important degradation response to obtain since the input (S/\hat{I}) ratio or the peak input interference level obtained from this test is a conservative (or safe) criteria. In particular, the levels recorded for this test are just detectable under optimum listening conditions and would not necessarily be observed in less ideal situations. If the interference level can be kept less than the threshold, all pulse degradation problems can be avoided.

At the minimum interference threshold level there is no practical degradation in the intelligibility of a voice message from pulsed interference. This statement is not generally applicable to all types of desired and undesired signals.

The following threshold evaluation is divided into a discussion of overall receiver measurements and a discussion of a set of measurements performed entirely at baseband.

Receiver Threshold Measurements

Tables III-1 and III-2 summarize the minimum interference thresholds measured on receiver No. 1 for chirped and non-chirped, rectangular pulsed interference. Tables III-3 and III-4 show the minimum interference thresholds for receiver No. 2 with a chirped and non-chirped rectangular pulsed interference.

For the range of interfering signal parameters that were measured, Tables III-1 and III-3 indicate the following general trends for non-chirped interference:

1. For fixed PW and Δf , the required input (S/\hat{I}) generally becomes more positive as the PRF is increased.
2. For fixed PRF and Δf , the input (S/\hat{I}) becomes slightly more positive as the PW is increased.

Tables III-2 and III-4 show that trends 1 and 2, listed above, also apply for a constant chirp rate. Tables III-2 and III-4 also show that for the on-tune case ($\Delta f = 0$) the minimum interference level, (S/\hat{I}), becomes more negative as the chirp rate is increased. The reason for this is that the interfering power within the IF passband decreases as the chirp rate is increased.

Figure 6-45 shows input (S/\hat{I}) versus off-tuning for receiver No. 1. The data is plotted for an average PW (all PW's are averaged except the 5 μ sec pulses) and individual PRFs. This figure shows a log PRF trend for minimum interference thresholds. A similar PRF trend was previously noted for degradation in terms of AI (see the Degradation With Pulse Rate section).

Audio Threshold Measurements

The objective of this portion of the pulsed investigation was to obtain baseband degradation criteria that could be used with the simulation program to obtain an overall voice receiver modeling capability (in terms of thresholds and AI degradation). In order to obtain this type of information it is necessary to know how the thresholds vary with baseband power ratios (not receiver input ratios), since this is the normal output of the simulation model. Therefore, a second set of threshold measurements was made at the detector output. The measurements were made directly feeding the desired and interfering signals into the audio filter in order to accurately control the audio signal levels. The baseband signal level could not be accurately controlled when the desired and interfering signals were fed into the RF input because of the variability due to the measurement technique and the inherent receiver nonlinearities. The test was run as though an idealized detector output signal was available as the input to a baseband audio filter. The test procedure is described in Section 5 and is basically summarized in Figure 5-12 which shows the measurement block diagram. The basic difference between this test and the previous test is that idealized rectangular pulses from a pulse generator were used as inputs to the audio filter. The results of this test, averaged over three observers and PW's from 100 μ sec to 1,000 μ sec, are shown in Figure 6-38. This figure shows that the actual audio threshold is a function of the audio (S/N) and the output signal-to-peak interference $(S/\hat{I})_O$, or equivalently, the output peak interference-to-noise $(\hat{I}/N)_O$. From these figures the output signal-to-peak-to-peak interference $(S/I_{pp})_O$ in dB required for a minimum audio threshold is given by

$$(S/I_{pp})_O = 7 + .62 (S/N)_O - 12 \text{ Log } \frac{800}{\text{PRF}} \quad (6-6)$$

It is also true that

$$(I_{pp}/N)_O = (S/N)_O - (S/I_{pp})_O \quad (6-7)$$

so that the output $(I_{pp}/N)_O$ can be obtained.

This indicated the same result that was contained in the overall receiver measurements.

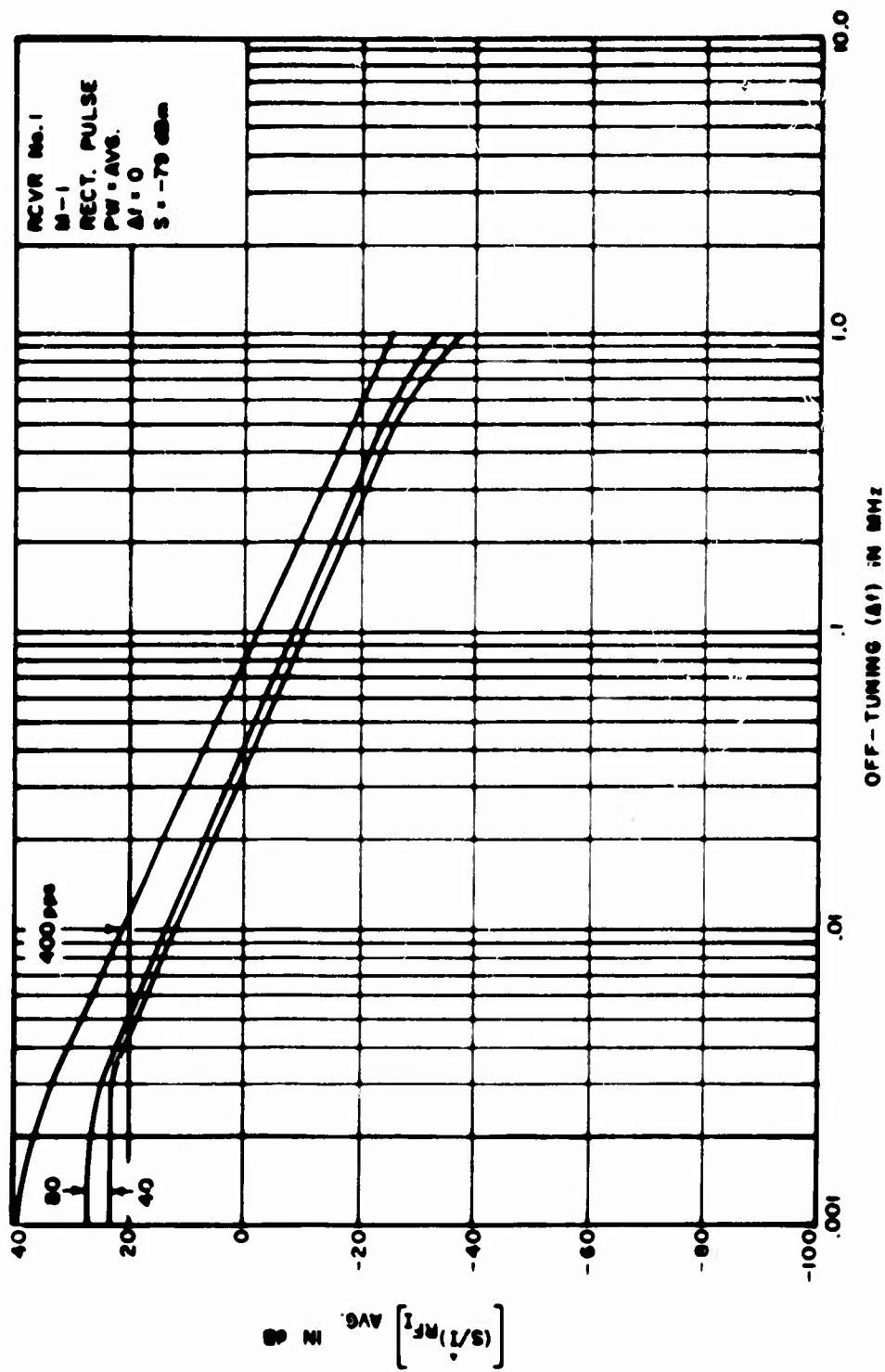


Figure 6-45. Average Threshold Input Signal to Peak Interference as a Function of Δf

The audio threshold model given by Equation (6-6) can be used, with the transfer function described in the simulation portion of Section 4, to obtain an automated threshold level. This threshold and the AI degradation model bracket the usable range of degradation from threshold to a loss of intelligibility.

AUDIO LIMITING

The following discusses the effect of an audio noise limiter in the receiver signal processing circuitry. This circuit is designed to limit peak noise signals that exceed a given voltage level in the audio circuits. Although the limit level is adjustable (within the receiver chassis), one level is present for all noise signals. The circuit also clips all interfering signals, especially pulsed interfering signals, that exceed the limit level. Ideally, the limit level is set to a point above the average signal level which does not affect the desired information intelligibility. The test results used 50% modulation for average signal levels with voice peaks representing approximately 100% modulation. Thus, a clipping level set for a signal-to-peak interference output ratio of -6 dB resulted in the pulse interference being limited at the peak voice levels. This result is shown in Figure 6-46 in which the input (S/I) versus the output (S/I_{pp}) is shown for receiver No. 2 with the limiter and receivers No. 1 and No. 2 without the limiter. Figures 6-47 and 6-48 show the audio output waveform with and without the limiter. Figure 6-46 shows the knee of the limiter curve to be above -7 dB for receiver No. 2. This figure also shows that by removing the limiter the linear range increased by almost 13 dB. This change is not as large or infinite as theoretically would be expected, due to AGC saturation effects (see Section 4). This also shows that, although the audio limiter clipped the pulsed interference and kept the performance degradation to a low level, the receiver would have saturated at only a 13 dB higher output level.

The performance degradation as measured by AI for receivers No. 2 and No. 1 (with and without limiting, respectively) is shown in Figure 6-49. This figure shows that the audio noise limiter decreases the effect of pulsed interference. As a particular example, this figure shows the receiver with the audio limiter can tolerate a 77 dB higher interference level than the receiver without the limiter for the same AI score of .6.

The same type of general trend can be found in Appendix III by an examination of the curves of receivers No. 1 and No. 2. This pattern can also be shown on a plot of the AI score (for the same input S/I ratios) of one receiver versus the other. Figure 6-50 compares the AI scores for three different PW and PRF combinations. This figure again shows that the receiver with the audio limiter is performing better in terms of AI than the other receiver.

The AI degradation measure is, however, only part of the solution to this problem. This measure has been primarily used in this report as a tractable measure of a decrease in

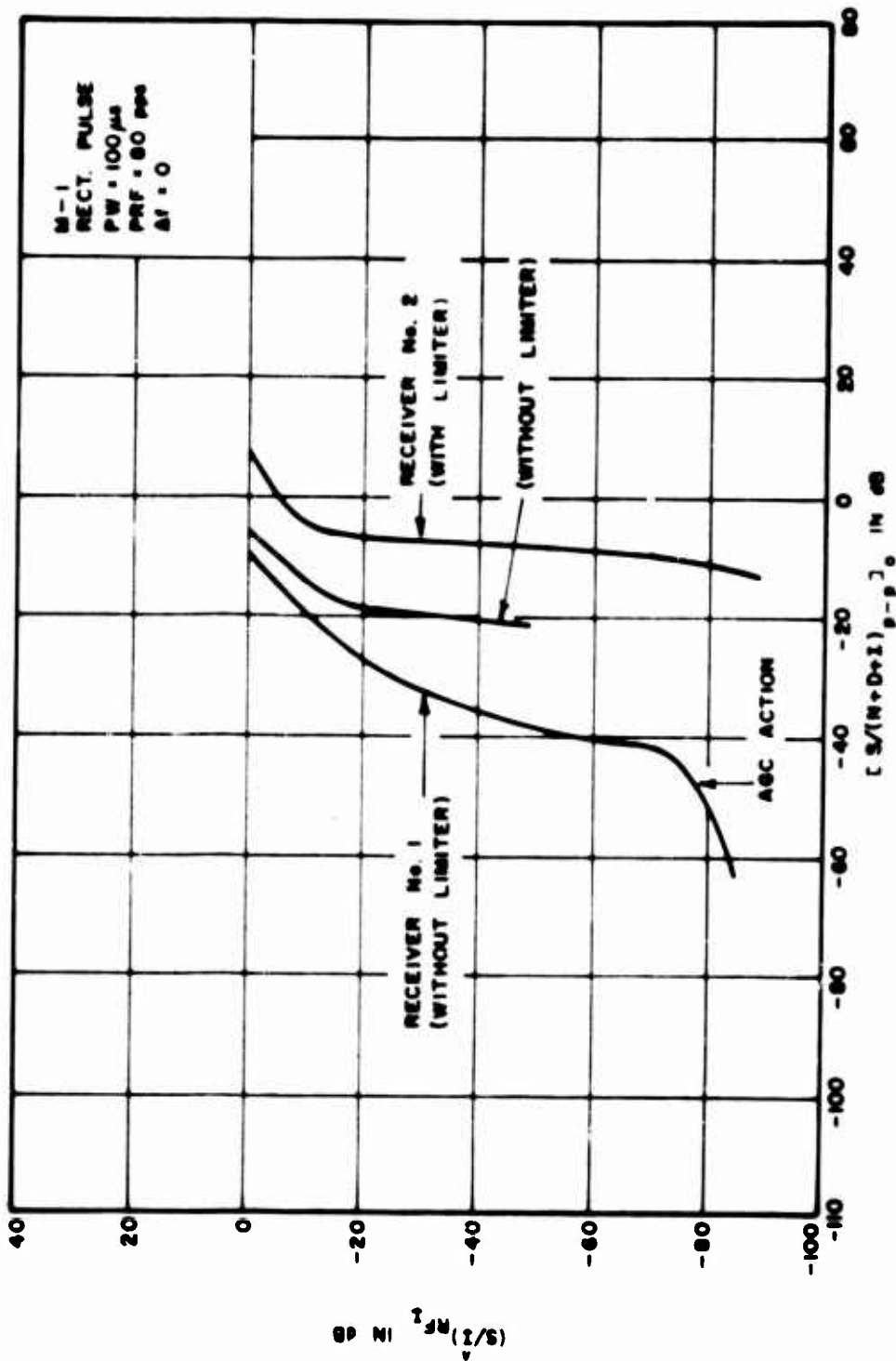
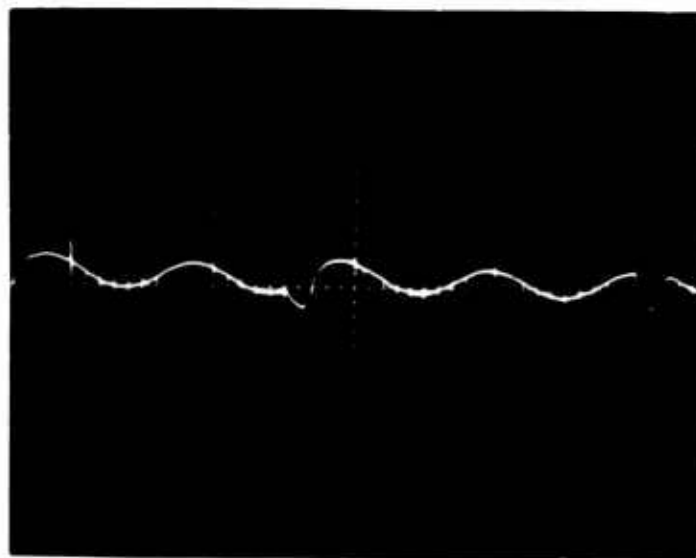


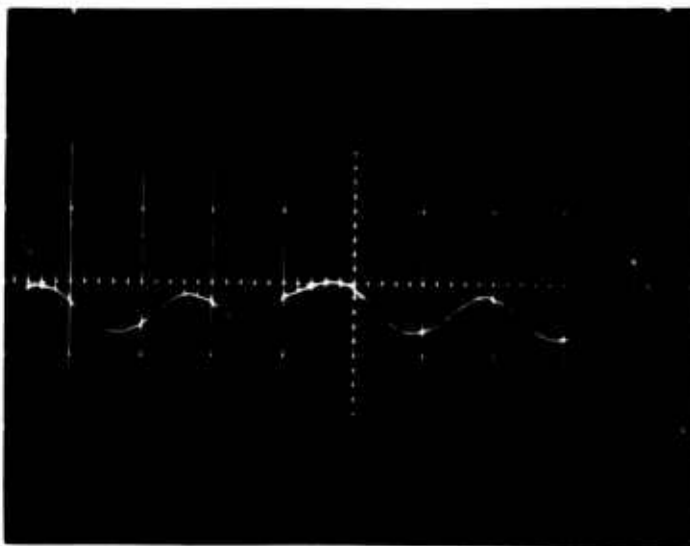
Figure 6-46. Power Transfer Loss to an AM Receiver



PW = 100 μ s
PRF = 400
(S/I)_{IN} = -25 dB
VERTICAL = 2.0 V/cm
SWEEP RATE = .5 μ s/cm

RECEIVER NO. 2

Figure 6-47. Audio Output with Limiter On



PW = 100 μ s
PRF = 400
(S/I)_{IN} = -25 dB
VERTICAL = 2.0 V/cm
SWEEP RATE = .5 ms/cm

RECEIVER NO. 2

Figure 6-48. Audio Output with Limiter Off

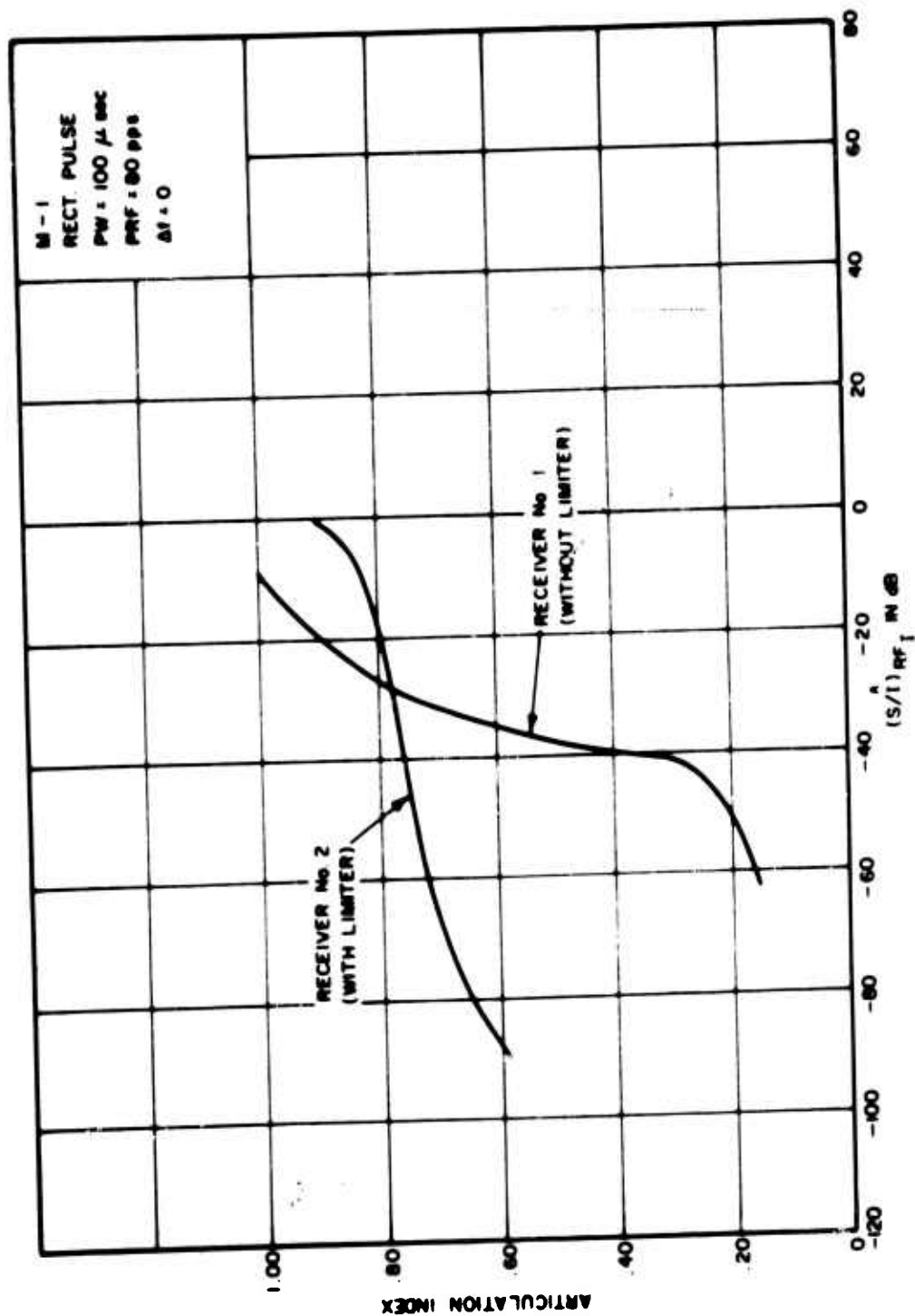


Figure 6.49. Articulation Index for Pulse Interference to an AM Receiver

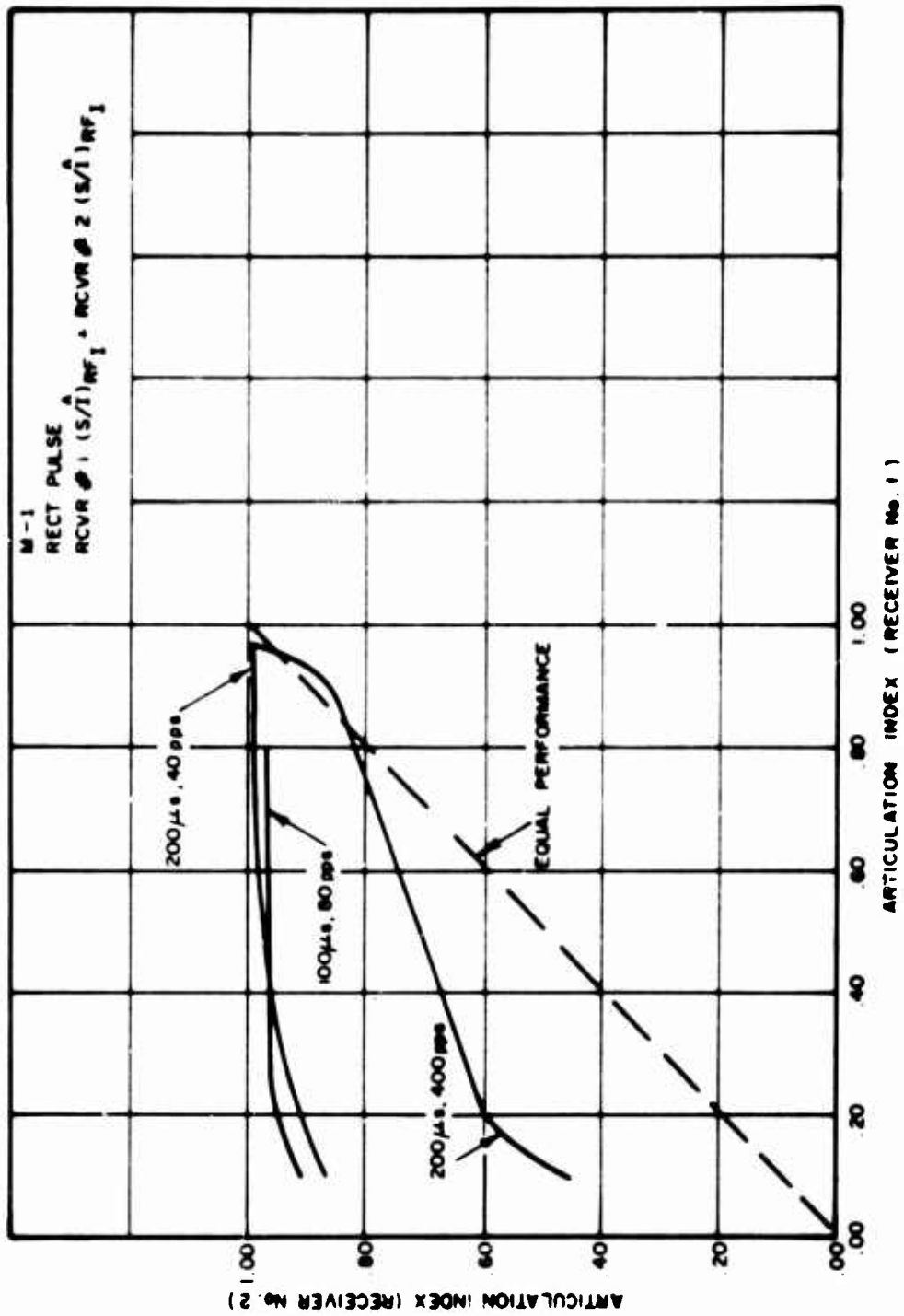


Figure 6-50. Articulation Index for RCVR 1 Versus Articulation Index for RCVR 2

intelligibility. The true picture of what is happening to intelligibility can only be obtained in terms of Articulation Score (AS).

Figure 6-51 shows the relationship between AS and AI for the two receivers averaged over the PW and PRF parameters used in this investigation. The curve for receiver No. 1 was previously discussed in the section on intelligibility.

This figure shows that, in terms of intelligibility, the two receivers are performing in a similar fashion. The performance of the receiver with the limiter is slightly better at high intelligibility levels, while the performance of the receiver without the limiter is somewhat better at lower intelligibility levels.

In summary, this section has shown that an audio noise limiter in an AM receiver improves the low AI scores in terms of the input (S/\hat{I}) ratios. (It can also be postulated that an RF or IF limiter with a similar clipping level would improve the performance by a similar amount.) The intelligibility, measured in terms of AS, was, however, maintained about the same with and without a limiter.

AGC AND AMPLIFIER SATURATION EFFECTS

The following is a discussion of the degradation effect of AGC action and amplifier saturation that occurs at low PRFs.

Figures III-13 through III-46 in Appendix III show the AM degradation curves for AI versus RF input (S/\hat{I}) ratio for receiver No. 1. The AM degradation curves for the non-chirped rectangular pulse interference at low PRFs (10, 40 and 80 pps) indicate the receiver becomes saturated at certain input (S/\hat{I}) levels. The saturation levels were obtained from the intersection of straight lines fit to the data. Table 6-7 summarizes the AI scores and the saturation levels measured for receiver No. 1 with a slow AGC response setting. As previously reported (see Section 4) using the fast or slow time constant had no effect on the measurements.

The average saturation level for a 40 pps rate was found to be -18 dB for an AI score of .41. The receiver becomes saturated because at low PRF rates the interference does not affect the DC level of the AGC bias line (see Section 4 for a discussion of AGC action). Since the AGC does not respond to these pulses and lower the overall gain of the receiver, the large interfering pulse (these cases are all for $\hat{I} \gg S$) overdrives an amplifier stage and is clipped or limited. Therefore, the interfering pulse is reduced with no additional degrading effect of the desired signal. This effect is important primarily in the intelligibility degradation region (i.e., $\hat{I} > S$) and not important in the minimum threshold degradation region (i.e., $S \gg \hat{I}$).

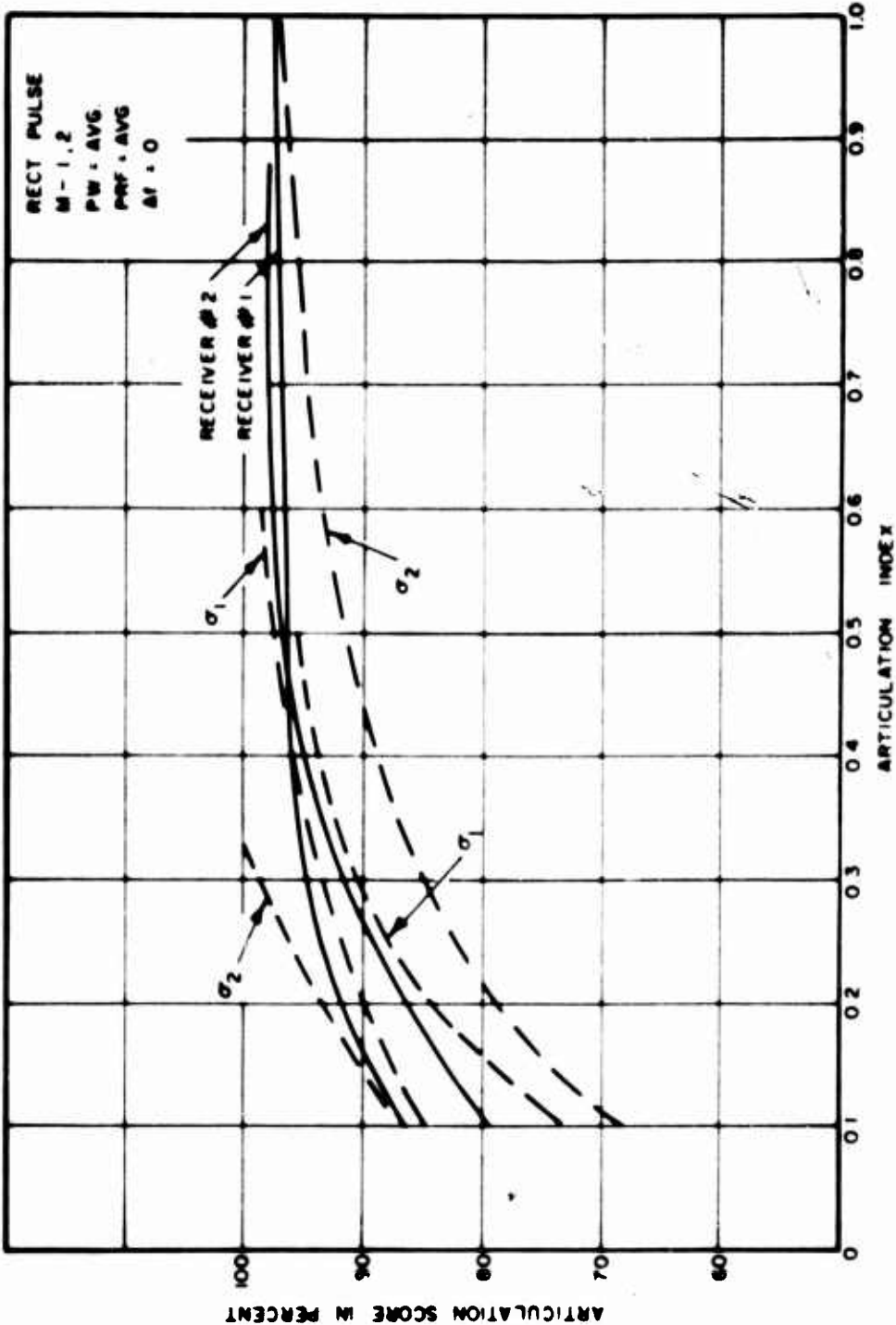


Figure 6-51. Articulation Score Versus Articulation Index for an AM Receiver

Saturation begins to affect the linear response for AI scores of approximately .3 and a PRF of 40 or lower. Figure 6-52 and Figure 6-53 compare the .3 AI off-tuned response for a PW of 200 μ sec and a PRF of 80 and 40, respectively. The first figure, obtained for an 80 pps rate, shows close agreement between the simulated output (obtained without an AGC model) and the measured data. The second figure, obtained for a 40 pps rate, shows considerable difference between the simulated output (without AGC) and the measured output with AGC.

A comparison of the non-chirped and chirped interference degradation curves shows the non-chirped pulse has a lower saturation level (this data is also summarized in Table 6-6) than the chirped pulse for a given PW, PRF and $(S/I)_{IN}$ level. The reason for this difference is the mainlobe of the chirped pulse interference spectrum is spread proportional to the chirp rate causing less interfering power in the IF passband.

The saturation levels for two different input signal levels (-79 dBm and -40 dBm) are also shown in Table 6-7. This shows that saturation level is independent of signal levels and can be completely described by the input (S/I) power ratio. This effect is due to the AGC action which has lowered the gain for the higher input signal level. The AGC is, however, still responding to the pulses in the same manner as it responded for the lower signal level.

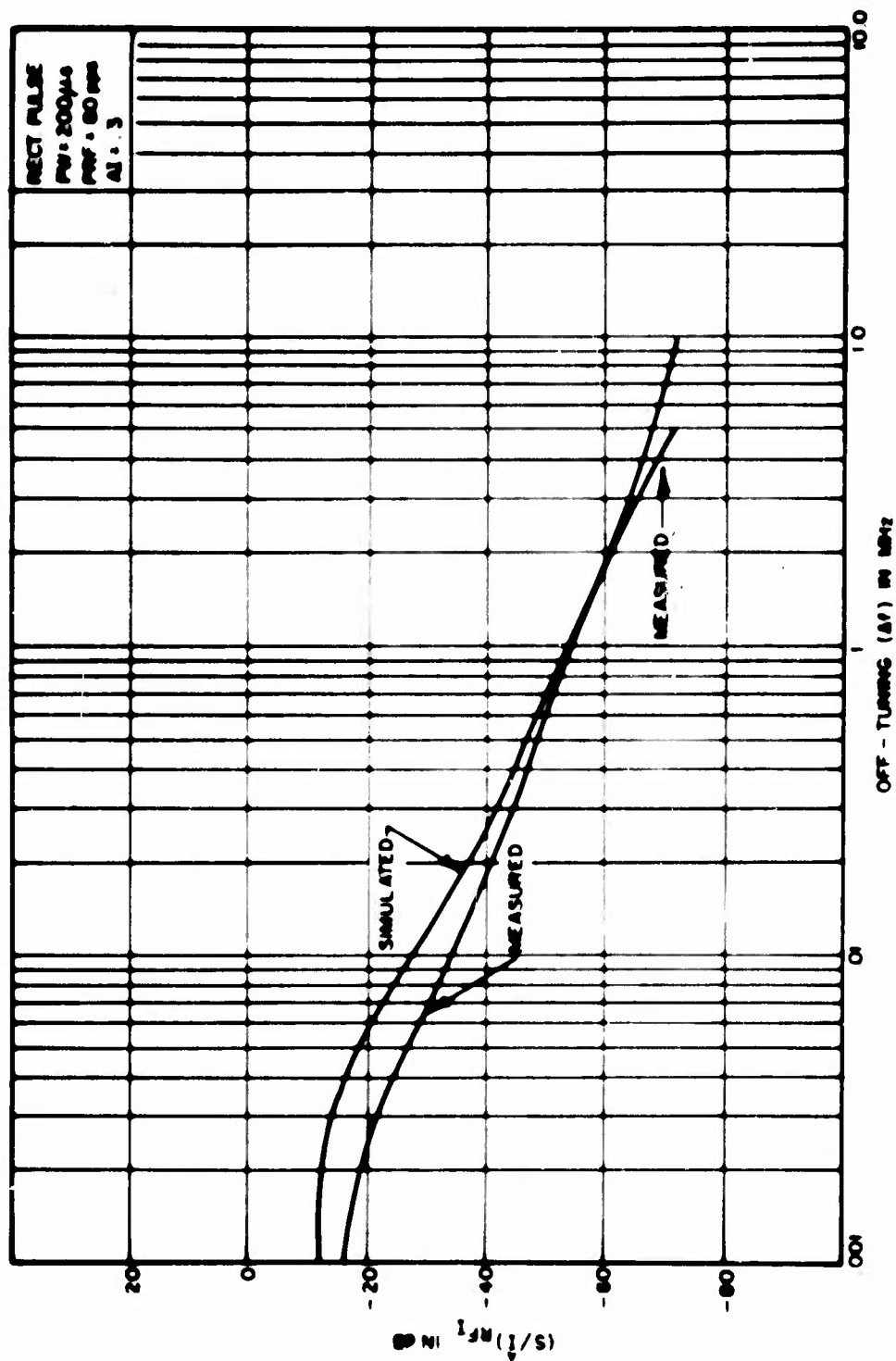


Figure 6-52 Input Signal to Peak Interference as a Function of Δf

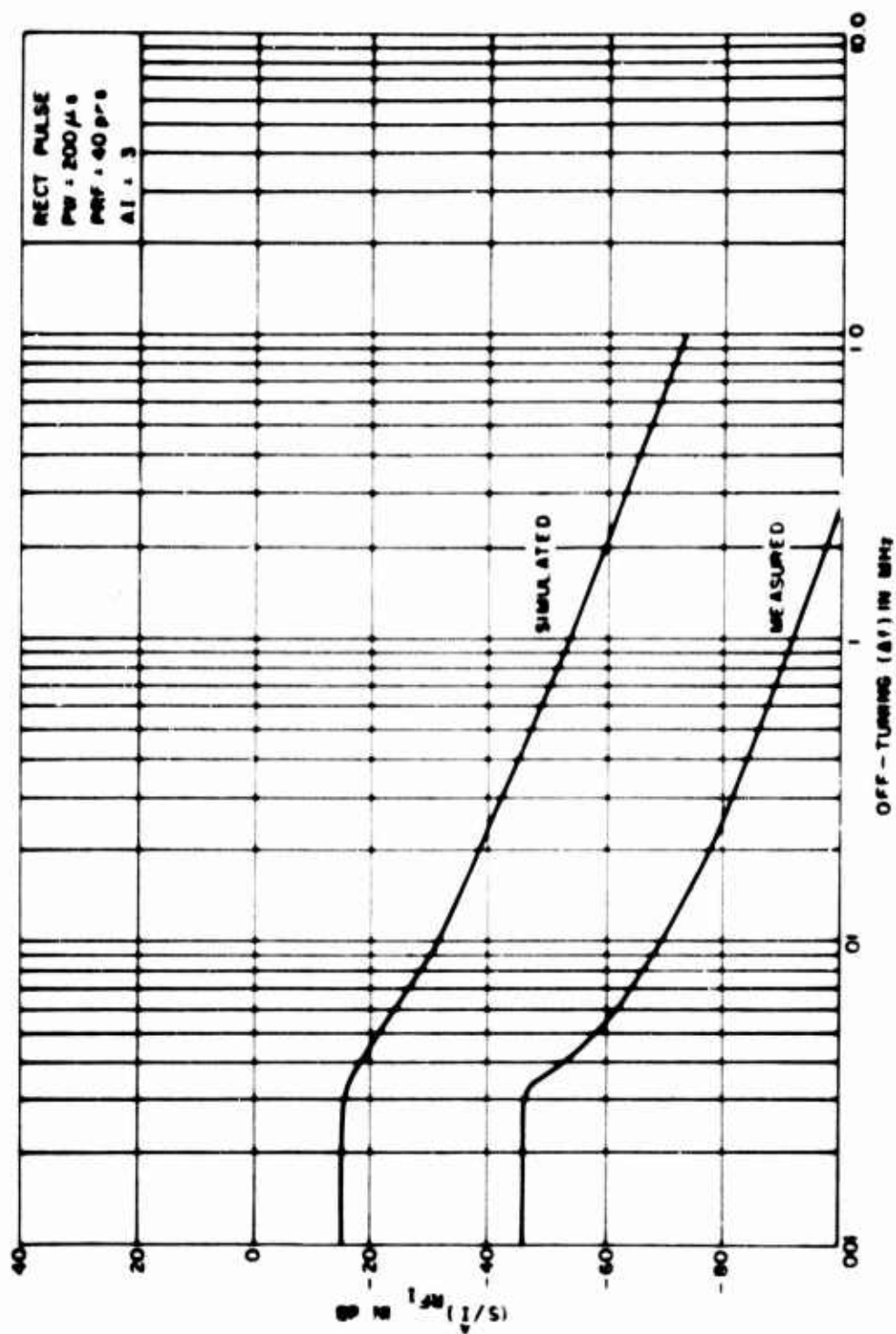


Figure 6-53 Input Signal to Peak Interference as a Function of Δf

TABLE 6-7
SATURATION BREAKPOINTS FOR AM
RECEIVER NO. 1

Figure Number	Signal (dBm)	Chirp (kHz)	Pulse Width	PRF (pps)	Δf (kHz)	Bk.Pt. (dB)	AI
4-14	-79		100 μs	40	0	-20	.49
4-15	-79		100 μs	80	0	-25	.21
4-18	-79		200 μs	40	0	-16	.49
4-19	-79		200 μs	80	0	-11	.48
4-21	-79		400 μs	10	0	-16	.82
4-22	-79		400 μs	40	0	-16	.39
4-23	-79		400 μs	80	0	-15	.21
4-25	-79		1000 μs	10	0	-15	.79
4-26	-79		1000 μs	40	0	-20	.28
4-27	-79		1000 μs	80	0	-13	.26
Average breakpoint for PRF = 10						-15.5	.805
Average breakpoint for PRF = 40						-18	.412
Average breakpoint for PRF = 80						-16	.29
4-29	-40		100 μs	10	0	-33	.82
4-30	-40		100 μs	40	0	-23	.46
4-32	-40		400 μs	10	0	-17	.84
4-33	-40		400 μs	40	0	-11	.51
4-35	-40		1000 μs	10	0	-15	.79
4-36	-40		1000 μs	40	0	-17	.39
Average breakpoint for PRF = 10						-22	.82
Average breakpoint for PRF = 40						-17	.45
4-41	-79	500	100 μs	40	0	-46	.41
4-42	-79	500	100 μs	80	0	-43	.20
4-44	-79	500	200 μs	40	0	-40	.40
4-45	-79	500	200 μs	80	0	-39	.18
Average breakpoint for PRF = 40						-43	.405
Average breakpoint for PRF = 80						-41	.19